Universität für Bodenkultur Wien

Department for Biotechnology

Name of Institute: Institute for Applied Microbiology (IAM)
Head of Institute: O.Univ.Prof. Hermann Katinger

Advisor: O.Univ.Prof. Hermann Katinger

TITLE OF DISSERTATION**: MYELIN PROTEIN MEDIATED INHIBITION OF OLIGODENDROCYTE DIFFERENTIATION**

Dissertation
for obtaining a doctorate degree
at the University of Natural Resources and Applied Life Sciences Vienna, Institute for Applied Microbiology (IAM)

Submitted by
Syed Yasir Ahmed, Max-Planck-Institute for Experimental Medicine, Göttingen, Germany

Vienna, August 2009

## Acknowledgements

I begin with by praising and thanking to Allah, who bestowed me with health, strength and knowledge all along the way to complete this study.

I am very indebted to my supervisor DDr. Mark Kotter for providing guidance and support whenever required. I appreciate all his contributions of time, ideas, and funding to make my Ph.D. experience productive and stimulating. I very much enjoyed his style of supervision.

I must express my gratitude to Prof. Hermann Katinger for supporting this thesis at the university. Many thanks to collaborators Prof. Friedrich Altmann, Vienna for help with chromatographic techniques and Dr. Wiebke Möbius, Gottingen for electron microscopy. I sincerely appreciate Prof. Klaus Nave, Director, Max Planck Institute of Experimental Medicine, for making all possible to work at the institute.

I also owe a debt of gratitude to my lab collogues Alexandra Bäer, Elisabeth Kähler and Matthias Hofer for their good support and help. Special thanks to all the people at the MaxPlanck Institute who supported me with their professional and efficient work.

I cannot finish without saying how grateful I am to family and friends for all their love and encouragement. Especially, for my parents who raised me with love and supported me in all my pursuits. Thank you

## Abstract (German)

Bei demyelinisierenden Krankheiten ist die Remyelinisierung des Zentralnervensystems (ZNS) von besonderer Wichtigkeit, um die saltatorische Erregungsleitung wiederherzustellen und Axone vor Degeneration zu schützen. Schlägt die Differenzierung von Oligodendrozyten-Vorläuferzellen (oligodendrocyte precursor cells, OPCs) zu Myelin-bildenden Oligodendrozyten fehl, trägt dies maßgeblich zur unvollständigen Regeneration der Myelinscheide bei. Ein potenzieller Inhibitor der Remyelinisierung sind Überreste von abgebautem Myelin. Unklar ist jedoch, welche molekularen Komponenten des Myelins die ZNS-Remyelinisierung beeinträchtigen. *Das Ziel der vorliegende Arbeit ist die Identifizierung der molekularen Myelin-Substrate, welche die Differenzierung von OPC nach dem Auftreten von Demyelinierung verhindern.* Den Mechanismus dieser inhibitorischen Moleküle zu verstehen, ist von großer Bedeutung die Genesung von Patienten mit demyelinisierenden Erkrankungen und anderen Verletzungen des ZNS zu unterstützen.

Myelin-assoziierte Inhibitoren (Myelin Associated Inhibitors, MAIs) verhindern nicht nur die Differenzierung von Oligodendrozyten, sondern regulieren auch die Expression von Nkx2.2 herunter. Basierend auf Proteinextraktion und -verdau konnte gezeigt werden, dass es sich bei MAIs um Proteine handelt und die Hemmung der OPC-Differenzierung charakteristisch für Myelin des ZNS ist. Um die inhibitorischen Proteine im Myelin zu identifizieren, wurden sowohl ein Screening- als auch ein Hypothesen-basierter Ansatz gewählt. Für das Screening-Verfahren wurde ein zweischrittiges Chromatographie-Aufreinigungsverfahren zur Anreicherung der inhibitorischen Myelinproteine entwickelt. Die aufgereinigte Proteinfraktion wurde anschließend mit 3D/BN/PAGE gefolgt von Massenspektrometrie analysiert. Der hypothesen-gesteuerte Ansatz basierte auf der Annahme, dass die maßgeblichen Myelinprotein, welche die Regeneration von Axonen inhibieren, auch die Differenzierung von OPCs verhindern. Während die hauptsächlichen Inhibitoren von axonalem Wachstum, MAG, Nogo und Omgp, keinen Einfluss auf OPC Aktivität zeigten, traten Ephrin 3 und Semaphorin 3A als Inhibitoren von OPC Differenzierung in Erscheinung.

Ephrin B3, ein bekanntes inhibitorisches Molekül für die Lenkung von axonalem Wachstum, wird in postnatalen Myelin-bildenden Oligodendrozyten exprimiert. Immuno-Elektronenmikroskopie Aufnahmen zeigten, dass Ephrin B3 ein integraler Teil der Myelinmembran ist. Der spezifische inhibitorische Effekt dieses Proteins auf OPC Differenzierung konnte in einer Vielzahl von Experimenten bestätigt werden, die zusätzlich zeigten, dass Ephrin B3 die Komplexität der Oligodendrozytenfortsätze verringert und dass RhoA als Mediator der inhibitorischen Effekte von Ephrin B3 agiert. Die Hemmung der Differenzierung von OPCs durch Ephrin B3 oder angereicherten Myelinmembran-Präparationen kann durch Maskierung des Epitops mittels Anti-Ephrin B3 Antikörper umgekehrt werden. Daraufhin wurde die Hypothese der Ephrin B3 vermittelten Inhibition der ZNS-Remyelinisierung in einem Remyelinisierungsmodell mit fokaler Gliatoxizität getestet. Zu diesem Zweck wurde eine fokale Demyelinisierung im kaudalen Kleinhirnschenkel induziert, gefolgt von einer Ephrin B3 Infusion. Remyelinisierung war in Tieren, welche eine stereotaktische Ephrin B3 Infusion erhielten, erheblich beeinträchtigt, während Kontroll-Läsionen vollständig remyelinisiert wurden. Molekulare Analyse der Läsionen hingegen

zeigte, dass Ephrin B3 nicht die Expression von Myelin-assoziierten Genen auf Transkriptionsebene verhindert.

Semaphorin 3A wird ebenfalls in OLCs exprimiert, lenkt das axonale Wachstum und übt chemorepulsive Effekte auf migrierende OPCs aus. Diese Dissertation beinhaltet Experimente, die zeigen, dass Sema 3A selektiv OPC Differenzierung inhibiert. Die Hypothese, dass Sema 3A ZNS-Remyelinisierung durch Hemmung der OPC Differenzierung inhibiert, wurde wie zuvor ausgeführt, *in vivo* getestet. Analyse der Läsionen offenbarte eine signifikante Beeinträchtigung der Remyelinisierung in Tieren, welche eine Sema 3A Infusion erhielten. *In situ* Hybridisierung für PLP zeigte, dass Sema 3A wichtige Entwicklungsschritte von OPCs hemmt.

Die vorliegende Dissertation beschreibt zwei wichtige regulatorische Moleküle, die durch Beeinflussung der OPC Differenzierung, die Dynamik der ZNS-Remyelinisierung steuern. Diese Ergebnisse bieten entscheidende Hinweise über die Abläufe, die zum Versagen der Remyelinisierung in demyelinisierenden Krankheiten führen und eröffnen neue Möglichkeiten für therapeutische Interventionen.

Keywords. Myelin-assoziierte Inhibitoren, Oligodendrozyten, Remyelinisierung, Ephrin B3, Semaphorin 3A

## Abstract (English)

Remyelination of the central nervous system (CNS) in demyelinating diseases is important to restore saltatory conduction and protect axons against degeneration. Failure of differentiation of oligodendrocyte precursor cell (OPC) into myelin forming oligodendrocytes contributes significantly to impaired myelin sheath regeneration in chronic demyelinating diseases. One of the potential inhibitors of remyelination is the presence myelin debris. However, the molecular components of myelin inhibiting CNS remyelination remain to be elucidated. *The aim of the present thesis was to identify the molecular substrates of myelin that inhibit OPC differentiation following demyelination*. Identifying and understanding the actions of these inhibitory molecules is important for promoting recovery in patients with demyelinating diseases and other types of CNS injury.

Myelin Associated Inhibitors (MAIs) not only inhibit differentiation of OPCs into mature oligodendrocytes *in vitro* but also downregulates Nkx2.2 expression. On the basis of protein extraction and digestion experiments it was demonstrated that MAIs are proteins and that OPC differentiation block is characteristic of CNS myelin. To identify the myelin inhibitory protein(s) a screening and a hypothesis driven approach was employed. For the screening approach the inhibitory myelin protein was enriched by developing a two step chromatographic separation protocol. The resulting protein fractions were then analyzed by 3D/BN/PAGE followed by mass spectrometry. The hypothesis driven approach was based on the assumption that major myelin inhibitors of axon regeneration also mediate the inhibitory effects on OPC differentiation. Whereas major MAI of axon outgrowth including MAG, Nogo, and OMgp did not show inhibitory activity on OPCs, Ephrin B3 and Semaphorin 3A emerged as inhibitors of OPC differentiation.

Ephrin-B3, a known inhibitory axon guidance molecule, is expressed in postnatal myelinating oligodendrocytes. Immuno-electron microscope analysis demonstrated that ephrin B3 is an integral part of myelin membranes. Its specific inhibitory effects on OPC differentiation were confirmed by a number of experiments that also demonstrated that ephrin B3 causes a reduction in process complexity in oligodendrocyte lineage cells and that RhoA mediates the inhibitory effect of ephrin B3 on the OPC differentiation process. The inhibitory effect of ephrin B3 and enriched myelin membrane preparation on OPC differentiation can be reversed by epitope masking using anti-ephrin B3 antibodies. Subsequently, the hypothesis was tested that ephrin B3 inhibit CNS remyelination using a focal gliotoxic model of remyelination. For this purpose a focal demyelination was induced at caudal cerebellar peduncle followed by infusion of Ephrin B3. Remyelination in animals, which received stereotactic infusions of ephrin B3 was severely impaired whereas control lesions were fully remyelinated. However, molecular analysis of the lesions showed that ephrin B3 was unable to stop expression of myelin genes on a transcriptional level.

Semaphorin 3A is also expressed on OLCs and acts as an axonal guidance cue that also exerts chemorepulsive effects on migrating OPCs. Experiments included in this thesis demonstrate that Sema 3A selectively inhibits OPC differentiation. The hypothesis that Sema 3A inhibits CNS remyelination by inhibiting the OPC differentiation process was tested in vivio as outlined above. Analysis of the lesions revealed a significant impairment of

remyelination in Sema 3A infused animals. *In situ* hybridization for PLP showed that Sema 3A inhibits the lineage progression of OPC.

The work in the present thesis identified two important molecules that regulate the dynamics of CNS remyelination by regulating OPC differentiation. The results provide critical clues to the process of remyelination failure in demyelinating disease and open new windows for therapeutic interventions.

Keywords. Myelin Associated Inhibitors, Oligodendrocytes, Remyelination, Ephrin B3, Semaphorin 3A

## Abbreviations

| | |
|---|---|
| ANOVA | analysis of variance |
| CCP | caudal cerebellar peduncle |
| CNS | central nervous system |
| DEPC | diethylpolycorbonate |
| DTT | dithiotreitol |
| EAE | experimental allergic encephalomyelitis |
| EB | ethidium bromide |
| FGF-2 | fibroblast growth factor-2 |
| HRP | horse radish peroxidase |
| ICAM-1 | intercellular adhesion molecule |
| IGF-β | insulin like growth factor-beta |
| IGF-1 | insuline like growth factor-1 |
| IPF | immune-privilege factor |
| MAI | myelin associated inhibitor |
| MAG | myelin associated glycoprotein |
| MARCKS | myristoylated, alanine-rich C-kinase substrate |
| MBP | myelin basic protein |
| MGC | mixed glial culture |
| mRNA | messenger ribonucleic acid |
| MPE | myelin protein extract |
| MS | multiple sclerosis |
| MOG | myelin oligodendrocyte glycoprotein |
| Msr-B | (macrophage) scavenger receptor-B |
| OPC | oligodendrocyte precursor cell |
| OLC | oligodendrocyte lineage cells |
| PBS | phosphate buffered saline |
| PCR | polymerase chain reaction |
| PDGF-A | platelet derived growth factor-A |
| PECAM | platelet/endothelial cell adhesion molecule |
| PFA | paraformaldehyde |
| PLP | proteo lipoprotein |
| PKC | protein kinase C |
| PLL | poly-l-lysine |
| PNS | peripheral nervous system |

| | |
|---|---|
| PSA-NCAM | polysialylated-neural cell adhesion molecule |
| Sema | semaphorin |
| SSC | standard saline citrate (buffer) |
| SVZ | subventricular zone |
| TGF-β | transforming growth factor-beta |
| TNF-α | tumour necrosis factor-alpha |

# Table of contents

# Chapter 1
# Literature review

# 1. Literature review

## 1.1 The Oligodendrocytes in CNS

Oligodendrocytes form the cellular compartment of brain and the spinal cord, responsible for the production of myelin (Southwood et al., 2004). Myelination is important for the normal functioning of the vertebrate CNS, as failure in conduction result in disrupted impulse condition and some time loss of neuron itself (Franklin and Ffrench-Constant, 2008). Oligodendrocytes are believed to be the direct ancestor of the oligodendrocyte precursor cells.

### 1.1.1 Oligodendrocyte precursors are formed in restricted regions of the CNS

Oligodendrocyte precursor cells (OPCs) are arguably the best-characterized precursors in the mammalian CNS, which make up around 5–8% of the glial cell population in the CNS(Dawson et al., 2000). In the rat forebrain the majority of oligodendroglial progenitors arise during late embryogenesis. These cells originate mainly from two types of precursors: the OPCs nestled in the SVZ in the brain and a group of Sox10/Olig1-positive cells in the ventral spinal cord (Liu et al., 2002; Stolt et al., 2006; Timsit et al., 1995).

The current view is that cortical oligodendrocytes in rodents are born from the cortical subventricular zone (SVZ) after birth; however, new evidence suggest that many forebrain oligodendrocyte progenitor cells (OPCs) are specified much earlier (between E9.5 and E13.5 in the mouse) in the ventricular zone of the ventral forebrain under the control of sonic hedgehog (*Shh*) and then migrate into the cortex (Ivanova et al., 2003) and that even caudal OPC can compensate loss of cortical oligodendrocytes (Kessaris et al., 2006).

Very dynamic combinations of transcription factors (TFs) are required for the OG specification. Olig2 is critical to OG specification in the spinal cord since (Lu et al., 2002). Sonic hedgehog (*Shh*) controls the expression of Olig1 and Olig2 in a concentration-dependent manner (Lu et al., 2000). Nkx2.2, Pax6, and Irx3 seems to be crucial in spatial aspects of OG specification since they determine the boundaries of the Olig2 motor neuron progenitor (pMN) domain (Briscoe et al., 2000).

### 1.1.2 Oligodendrocyte differentiation is controlled by multiple factors

OPCs after specification migrate and settle randomly along white matter and generate processes passing through the developmental stage that is characterized by distinct cell morphology and the expression of specific cell surface proteins. During early stages of oligodendrogenesis, $A_2B_5$+ oligodendrocyte precursor cells (OPCs) and O4+ pro-oligodendrocytes actively proliferate (Fok-Seang and Miller, 1994) and migrate(Noble et al., 1988). These precursor cells are dependent on the presence of PDGF for proliferation and can be identified on the basis of PDGF receptor-$\alpha$ expression (Baron et al., 2002; Barres et al., 1992) while surrounding neurons secrete PDGF (Ellison et al., 1996). Upon reaching their target OPCs start to express galactocerebroside (GalC)(Fok-Seang and Miller, 1994; Noble

et al., 1988) and myelin proteins like PLP, MBP, and MOG, which signal terminal differentiation into myelinating OG (Duchala et al., 1995). Once differentiation occurs, oligodendrocytes lose their ability to migrate. The final number of mature myelinating oligodendrocytes is determined by the proliferative rate of their progenitors and by programmed cell death occurring during development. Some evidence suggests that mature oligodendrocytes have a defined lifespan, albeit very long. The turnover time of mature oligodendrocyte was estimated to be 10–15 months in the rat (Imamoto et al., 1978). Furthermore, Oligodendrocyte progenitors continue to be born over life and proliferate after CNS injury (Horner et al., 2000).

Differentiation of oligodendrocyte precursors is regulated by growth factors PDGF (Yoo and Wrathall, 2007), NT-3 (Yan and Wood, 2000), BDNF (Du et al., 2003), CNTF (Marmur et al., 1998), bFGF (Wang et al., 2007), Notch signaling(Park and Appel, 2003) and chemokines (Kadi et al., 2006). The development of a mature oligodendrocyte in vivo is also regulated by axonal signals. Both soluble and cell mediated signals from adjacent axons are integrated into the developmental profile of oligodendrocyte precursors resulting in cell differentiation, up-regulation of myelin gene expression and formation of the myelin organelle. Candidates from axonally derived soluble factors include FGFs (Bansal et al., 1996; Qian et al., 1997) and thyroid hormone (Barres et al., 1994), while axonal cell surface molecules such as L1, MAG, NCAM and N-cadherin may regulate formation of the myelin sheath(Payne and Lemmon, 1993; Trapp, 1990).

Oligodendrocyte differentiation is also influenced by neuregulins that are expressed on many axons. Neuregulin exposure induces morphological changes in cultured oligodendrocytes (Vartanian et al., 1994). Furthermore, in the absence of the neuregulin receptor ErbB2, while many oligodendrocyte precursors develop, few of these cells mature and those that do fail to interact with axons and do not produce myelin (Park et al., 2001). Studies involving the transplantation of oligodendrocyte precursors derived from erbB3 mutant mice, the expression of dominant-negative ErbB receptor in oligodendrocytes, or the analysis of heterozygous nrg1 type III mutant mice (Roy et al., 2007; Schmucker et al., 2003; Sussman et al., 2005; Taveggia et al., 2008) suggest the proposal that NRG1 might affect CNS myelination. However recent finding demonstrated that overexpression of NRg1 leads to hypermyelination in the developing CNS but not during remyelination (Brinkmann et al., 2008) suggesting that remyelination in CNS takes place in a NRG1-independent fashion.

Differentiation oligodendrocytes are under the joint control of Olig1 and Olig2. Fore- and hindbrain regions of Olig1-deficient mice lack myelinating oligodendrocytes (Xin et al., 2005). Olig proteins induce the zinc finger protein Zfp488 in terminally differentiating oligodendrocytes (Wang et al., 2006). Expression of this transcription factor correlates with myelin gene expression in the spinal cord and its siRNA dependent downregulation leads to impairment of myelin gene expression. Sox 10 are another key player during terminal-differentiation. Sox10-deficient mice display a terminal differentiation defect (Stolt et al., 2002) that can at least be partly explained by its ability to directly induce expression from the regulatory regions of several myelin genes including the genes for MBP, PLP, MAG, connexin-32 (Cx32), and connexin-47 (Cx47; (Bondurand et al., 2001; Schlierf et al., 2006; Stolt et al., 2002). Three members of the homeodomain transcription factor family, Nkx2.2, Nkx6.1 and Nkx6.2, are expressed in differentiated OPCs (Nicolay et al., 2007). Nkx2.2 is not

essential for OPC formation, but is required for the progression of oligodendrocyte differentiation and maturation (Qi et al., 2001). Finally, two members of the Zinc-finger superfamily of transcription factors, Myt1 and YinYang1 (YY1), seem to play a role in the transition of OPC from cell cycle exit to differentiation (He et al., 2007; Nielsen et al., 2004). A recently identified gene model 98/myelin gene regulatory factor (MRF), as a transcriptional regulator required for OL maturation and CNS myelination. MRF is not detectably expressed by OPCs, neurons, or astrocytes and is upregulated strongly upon OL differentiation. In the absence of MRF, OPCs are able to withdraw from the cell cycle and differentiate into premyelinating OLs but are unable to mature, express the full complement of myelin genes, or myelinate and instead undergo apoptosis (Emery et al., 2009).

## 1.2 Demyelinating disease

Demyelination refers to the process where myelin is lost and can be subdivided into primary and secondary demyelination. Primary demyelination refers to the direct destruction of myelin sheaths with relative sparing of axons. Secondary demyelination occurs as a consequence of damage to neurons and axons. Central nervous system myelin and peripheral nervous system myelin are antigenically different (as befits the fact that CNS myelin derives from oligodendroglia and PNS myelin comes from Schwann cells). Therefore, some demyelinating disorders attack the central nervous system (the prototype is multiple sclerosis), while others affect the peripheral nervous system (the prototype being Guillain-Barre syndrome).

### 1.2.1 Demyelinating disorders of the central nervous system (CNS)

Demyelinating disorders of the central nervous system (CNS), remain among the most prominent and devastating diseases in contemporary neurology. In these diseases CNS demyelination is the consequence of a direct insult targeted at the oligodendrocyte, the cell that makes and maintains myelin sheaths. Demyelination in the CNS may arise because of genetic (such as in ALD), immune, viral such as HIV, toxic, environmental factors, and due to idiopathic causes. Regardless of its cause, demyelination impairs function and results in a conduction block. Depending on the disease different mechanisms may be involved in the process of demyelination. Neurotransmitters, especially glutamate, may exert a direct deleterious effect on oligodendrocytes and lead to demyelination (Steinman, 2000). Heat shock proteins may be involved (Brosnan and Raine, 1996), Matrix metalloproteinases (MMP) a group of zinc-dependent enzymes that can degrade extracellular matrix components have been implicated in demyelination (Yong et al., 1998). Finally, more than one mechanism may be present in the same disease or even in the same lesion (Ludwin, 1978).

Multiple sclerosis (MS) is the most common and best studied demyelinating disease of CNS that leads to severe neurological disability resulting from the interruption of myelinated tracts in the CNS (Hauser and Oksenberg, 2006). In most patients, the disease begins as an episodic disorder and evolves over time into a progressive one. Contemporary models of the pathogenesis of MS support the occurrence of two overlapping and connected effectors arms — inflammatory and neurodegenerative (Hauser, 2006). A general consensus is that multiple sclerosis begins with the formation of acute inflammatory lesions characterized by

breakdown of the blood-brain barrier (BBB). Such lesions are often clinically 'silent' and have been estimated to be about ten times more frequent than episodes of clinical worsening (Stone et al., 1995). Activated microglia may represent one of the initial steps in lesion development (Ponomarev et al., 2005), but the mechanisms contributing to microglial activation in multiple sclerosis are not known. The importance of axonal damage in multiple sclerosis is now well established; however, its cause is less well understood. The final pathway for axonal damage consists probably in the influx of calcium and subsequent mitochondrial collapse. One contributing factor is glutamate excitotoxicity; large amounts of glutamate can be produced by activated lymphocytes as well as by activated microglial cells (McFarland and Martin, 2007).

### 1.2.2 Experimental models of de- and remyelination

Experimental demyelination has been induced in the CNS of adult animals by a variety of means, including physical injury, toxic, immune-mediated, and viral-induced demyelination. Injection of myelinotoxic chemicals, such as lysolecithin (Gilson and Blakemore, 1993), cuprizone (Matsushima and Morell, 2001) or ethidium bromide (EB) (Woodruff and Franklin, 1999),or injection of anti-galactocerebroside antibodies combined with complement (Carroll et al., 1984) causes a focal , demyelinating lesion in the white matter of the CNS. In toxin-based models demyelination occurs as a consequence of the administration of the toxin and all subsequent events are associated with the regenerative response, which provides a useful means of separating demyelination from remyelination. To prevent host remyelination, focal X-irradiation of the lesion has been conducted to kill endogenous cells capable of reforming myelin. Widespread, disseminated demyelination has been achieved by providing cuprizone in the drinking water (Blakemore, 1974). Strains of Theiler's virus, a picornavirus, induce in susceptible mice strains a biphasic disease-an early acute disease resembling encephalomyelitis, followed by late chronic multifocal demyelinating disease (Oleszak et al., 2004; Pirko et al., 2004; Tsunoda and Fujinami, 1996). The A-59 and JHM strains of mouse hepatitis viruses also produce multifocal demyelination in mice (Sorensen et al., 1980; Woyciechowska et al., 1984).

## 1.3 Remyelination in the CNS

Remyelination , is the sponataneous repair in the central nervous system where new myelin sheaths are reinvested around the demyelinated axons. Remyelination is associated with functional recovery of remyelinated neurons (Jeffery and Blakemore, 1997), although the new myelin sheets are thinner and shorter than the original sheets that were lost (Blakemore, 1974). Remyelination in CNS is mainly mediated by oligodendrocytes and the process of remyelination can be better understood by dissecting it into two events which involve the recruitment of OPCs and their differentiation into mature myelin forming cells.

### 1.3.1 Cellular events of remyelination

The first step in the process of remyelination consists in the recruitment of OPCs to the demyelinated lesions (Franklin, 2002a). In response to injury, local OPCs undergo a switch from an essentially quiescent state to a regenerative phenotype and then migrate to be recruited to the area of demyelination. This phase of remyelination is called the *recruitment phase*.

In rodents, there are at least two known sources of remyelinating oligodendrocytes in the CNS: the first is the large pool of OPCs expressing the proteoglycan NG2 and/or PDGF-receptor alpha, the second comes from precursors in the adult subventricular zone (SVZ) (Menn et al., 2006; Zhao et al., 2008). Experimental evidence indicates that new myelin sheaths are made by oligodendrocyte precursor cells (OPCs) present throughout the adult CNS and not by oligodendrocytes that survive an episode of demyelination (Dawson et al., 2003; Watanabe et al., 2002). In response to demyelination, these cells proliferate and migrate, and rapidly fill the demyelinated area (Penderis et al., 2003; Sim et al., 2002b).

As the recruited OPCs differentiate into oligodendrocytes they must engage demyelinated axons and form new myelin sheaths. This second phase is called the *differentiation phase*. It encompasses three distinct steps: establishing contact with the axon that is to be remyelinated, expressing myelin genes and generating a myelin membrane, and finally wrapping and compacting the membrane to form the sheath.

Experimental data shows that macrophages also play a key role in the remyelinating process. Blockade of the macrophage function within the demyelinating lesion delay the recruitment and effectively impair differentiation of OPCs as well as subsequent remyelination (Kotter et al., 2001). Macrophages also help in removing the myelin debris that is generated during demyelination (Kotter et al., 2005). This is a critical step because CNS myelin contains proteins that inhibit OPC differentiation (Baer et al., 2009; Kotter et al., 2006; Syed et al., 2008). Astrocytes display a large diversity of properties and are known to produce a number of growth factors that promote OPC proliferation and differentiation (Ridet et al., 1997). It has been demonstrated that the presence of astrocytes in an area of demyelination has an inhibitory effect on the extent of oligodendrocyte remyelination achieved by OPCs (Blakemore et al., 2003). An absence of lymphocytes in the demyelinating areas leads to impaired remyelination (Bieber et al., 2003; Bieber et al., 2002), which points to the fact that lymphocytes also have an important role in the process of remyelination. The contribution of these diverse cell types reflects the complexity of the process involved in myelin regeneration. It is a plausible hypothesis that the different cell types appear in the lesions in an ordered fashion and that each type prepares the ground for the next step until oligodendrocytes can finally make myelin sheaths.

### 1.3.2 Molecular events in remyelination

Both the recruitment and differentiation phase of the remyelination are driven by distinct molecular events. Many OPC mitogens have been identified during development and so it is reasonable to hypothesize that similar molecules function during remyelination. Epidermal growth factor (EGF) and platelet-derived growth factor A (PDGFA) stimulate OPCs to divide and migrate during CNS development (Rogister et al., 1999). Experiments in transgenic mice have also revealed a role for these factors in remyelination. Indeed, mouse OPCs over expressing human EGF-R showed increased mitotic and migratory activity toward a corpus callosum lesion and this resulted in acceleration of remyelination and functional recovery (Aguirre et al., 2007). Transgenic mice overexpressing the human PDGF A gene and submitted to a cuprizone diet that caused chronic demyelination, showed enhanced remyelination and oligodendrocyte numbers after removal of the diet (Vana et al., 2007).

However, in another model of remyelination, over expression of PDGF-A did not show any beneficial effects on remyelination (Woodruff et al., 2004).

Some molecules have been shown to contribute to the regulation of differentiation. FGF plays a key part in inhibiting differentiation as well as in promoting recruitment, and it thereby regulates the transition from the recruitment to the differentiation phases (Armstrong et al., 2002; Zhou et al., 2006). Culture studies have confirmed the maturational effects of IGF-1 on both rat and human oligodendrocytes (Barres et al., 1993; McMorris and Dubois-Dalcq, 1988; Mozell and McMorris, 1991; Wilson et al., 2003). An absence of IGF-1 support, as demonstrated in IGF-1 null mice, instigates a strong reduction of myelin formation and axonal growth during early development, a mechanism that involves a decrease in myelin production (Ye et al., 2002).

The process of remyelination is not only controlled by the glial and neuronal derived growth factor but also by immune mediators. Specifically, the proinflammatory cytokines interleukin1β(IL1β) (Mason et al., 2001) and tumour necrosis factor α (TNFα) (Arnett et al., 2001), along with major histocompatibility complex class II(MHCII) molecules (Arnett et al., 2003), have all been implicated as mediators of remyelination in the cuprizone model of remyelination. On the other hand the anti-inflammatory cytokine interferonγ (IFNγ), inhibits remyelination (Lin et al., 2006). The observation that macrophage activation enhances myelination by transplanted OPCs in the myelin free retinal nerve fibre layer points to there being additional, unidentified regenerative factors that are produced by macrophages (Setzu et al., 2006).

Both rodent and MS white matter OPCs express Olig 2, Nkx2.2 and Myt1 transcription factors when recruited to demyelinating lesions (Fancy et al., 2004; Nait-Oumesmar et al., 2007; Sim et al., 2002a; Vana et al., 2007). Nkx2.2 and Olig2 expression can be used to distinguish activated OPCs that will give rise to remyelinating oligodendrocytes from quiescent OPC populations such as associated with remyelination failure (Kuhlmann et al., 2008a).

## 1.4 Remyelination failure

Given a framework in which remyelination involves distinct well defined phases of recruitment and differentiation, it is possible to identify the critical juncture at which arrest would lead to remyelination failure. This may occur due to an inadequate provision of the OPCs (recruitment failure) or via the failure of the recruited OPC to differentiate into myelin forming oligodendrocyte (differentiation failure).

### 1.4.1 Recruitment failure

The recruitment phase of myelin repair involves the proliferation and migration of the endogenous OPC to the demyelinating lesion. Failure of recruitment could stem either from insufficiency of endogenous remyelinating cells or from lack of environmental support for this process. In experimental focal demyelination, only a local progenitor cell pool reacts to injury by generating new oligodendrocytes and myelin (Keirstead et al., 1998). One potential cause for recruitment failure is the depletion of the OPC pool. Experimental studies have shown that repeated cycles of immune-mediated demyelination can result in chronically

demyelinated lesions (Linington et al., 1992). Similarly, long-term administration of cuprizone can result in remyelination failure caused by a lack of OPCs (Ludwin, 1978). On the other hand, a more recent study showed that impaired remyelination and depletion of oligodendrocyte progenitors does not occur following repeated episodes of ethidium-bromide induced focal demyelination in the rat central nervous system (Penderis et al., 2003). Age could be critical factor in the recruitment of the OPC's. The capacity for the recruitment of the OPC to demyelinating area was less in old animals as compared to that of young animals (Hinks and Franklin, 2000).

### 1.4.2 Differentiation Failure

The final step in the process of remyelination consists in the differentiation of OPCs into mature myelin forming oligodendrocytes. In some MS lesions, however, progenitor cells are abundantly present (Chang et al., 2000; Chang et al., 2002; Kuhlmann et al., 2008a; Wolswijk, 1998), but the remyelination fails because OPCs fails to undergo complete differentiation into functional oligodendrocytes (John et al., 2002) or because the axons are not permissive for remyelination (Charles et al., 2002). However, observation on retina shows that axons that have been demyelinated for long time are still capable of the myelination, supporting notion that the axonal changes resulting from the demyeliination are unlikely contribute for the remyelination failure (Franklin, 2002a). Hence, the presence of inhibitory factors and/or a lack of the stimuli required to differentiate the oligodendrocyte precursor cells into remyelinating oligodendrocytes contribute for remyelination failure (Foote and Blakemore, 2005; Kuhlmann et al., 2008a).

Several such differentiation inhibitors have been suggested to have roles including the PSA-NCAM (Charles et al., 2002), hyaluronan (Back et al., 2005), LINGO-1 (Mi et al., 2005), Bone morphogenetic proteins (BMPs) (Gomes et al., 2003), and Chondroitin sulfate proteoglycans (Larsen et al., 2003), Notch pathway (John et al., 2002), and myelin debris (Kotter et al., 2006).

Polysialic acid-neural cell adhesion molecule (PSA-NCAM) is re-expressed on demyelinated axons and may act to inhibit OPC attachment to axons (Chang et al., 2002). The expression of PSA-NCAM on axons has been suggested to inhibit the myelination program during development, and its removal facilitates myelination by oligodendrocytes (Charles et al., 2000). Therefore, even after the OPCs have been recruited and differentiated into mature oligodendrocytes, the challenge remains for these cells to make appropriate contacts and to receive accurate signals from the demyelinated axons in order to produce myelin. However, there is a report that in experimental CNS regeneration paradigms PSA promoted myelination (Papastefanaki et al., 2007). This indicates that a negative correlation between PSA-NCAM and myelination may be development-specific, and dependent on the context in which myelination occurs. PSA-NCAM is not the only cell adhesion molecule to be implicated as an axonal inhibitor of primary myelination. Neural adhesion molecule L1, have also been shown to be downregulated from axonal surface upon the onset of myelination. Furthermore, interfering with L1 prior to myelination onset inhibited myelination (Barbin et al., 2004).

The GAG hyaluronan is synthesized at the inner surface of cell membranes of reactive astrocytes and composed of repeating units of glucuronic acid and N-acetyl glycosamine.

Hyaluronan accumulates in demyelinating MS lesions and in the brain tissue of experimental autoimmune encephalomyelitis mice, an animal model to study MS pathology (Back et al., 2005). Back and co-workers demonstrated that the HMW form of hyaluronan inhibits the maturation of oligodendrocyte precursors into myelin-forming oligodendrocytes. These findings suggest that deposition of HMW hyaluronan in MS lesions may contribute to lesion progression by blocking the differentiation of oligodendrocyte precursor cells

LINGO-1 is selectively expressed in the CNS and is a component of the Nogo receptor complex, is a potent inhibitor of oligodendrocyte differentiation and myelination (Mi et al., 2005). It is a trans membrane protein that contains a leucine-rich repeat and an immunoglobulin domain. Both in vitro and in vivo, LINGO-1 inhibit myelination, and removal of LINGO-1 results in widespread precocious myelination (Mi et al., 2004; Mi et al., 2005). LINGO-1 is expressed on both axons and OPCs and is therefore ideally positioned to regulate interactions between premyelinating oligodendrocytes and their target axons (Lee et al., 2007; Mi et al., 2005). New reports reveal that inhibition of LINGO-1 enhances OL differentiation and remyelination following spinal hemisection and EAE (Ji et al., 2006; Mi et al., 2007).

Bone morphogenetic proteins (BMPs), members of the transforming growth factor super family of growth factor play important roles in the development of many cell types including CNS glial cells (Mabie et al., 1997). They have been shown to suppress oligodendrocyte differentiation in vitro (Yung et al., 2002) and in vivo (Gomes et al., 2003). Chondroitin sulfate proteoglycans (CSPG) are glial scar-associated extracellular matrix molecule. such as NG2 and proteoglycans with glycosaminoglycan (GAG) chains can often accumulate in lesions and be inhibitory to repair (Sherman and Back, 2008).

Notch receptor family members (Notch1–Notch4) are type 1 transmembrane proteins that, following ligand binding, are cleaved by a metalloproteinase and a γ-secretase, generating Notch intracellular domain (NICD), which then translocates to the nucleus where it acts as a second messenger to modulate expression of target genes (D'Souza et al., 2008). Depending upon the ligand involved in Notch1 activation, these target genes may either inhibit (via canonical signaling) or promote (via noncanonical signaling) differentiation and maturation of oligodendrocyte precursor cells (OPCs). Ligands belonging to the canonical pathway, such as Delta, Serate/Jagged, and Lag2 (DSL), transduce signals through the CSL/NICD/Mastermind (where CSL represents CBF1, Su[H], Lag1) signaling pathway, leading to transcriptional activation of the inhibitory genes hairy and enhancer of split 1 (*HES1*), *HES5,* and *HES7* as well as hairy and enhancer of split related with YRPW motif 1 (*HEY1*), *HEY2,* and *HEYL*, which block OPC maturation, resulting in maintenance of the OPC pool (D'Souza et al., 2008; Popko, 2003).

#### 1.4.2.1 Environmental regulators blocking OPC differentiation

Many local environmental factors also contribute for the differentiation process of the oligodendrocytes and remyelination. These include direct cellular interactions with astrocytes and/or microglia/macrophages, growth factors, cytokines, age and gender.

Oligodendrocytes were colocalised with astrocytes, microglia, and macrophages along the borders of ischemic lesions in the brain (Komitova et al., 2006; Mabuchi et al., 2000; Mandai et al., 1997) supporting hypothesis that presence of astrocytes and macrophages might be essential for Oligodendrocyte differentiation and remyelination. Astrogliosis is characteristic pathological feature of MS plaques. The expression of astrocyte-derived neuregulin was found to be reduced in active MS lesions and neuregulin has been suggested as candidate growth factor responsible for the poor remyelination in MS (Viehover et al., 2001). Furthermore, astrocytes in demyelinated lesions express Jagged1, while in remyelinated lesions Jagged1 expression was negligible (John et al., 2002). Jagged1 is the ligand for oligodendroglial Notch1 receptors, a pathway that inhibits oligodendrocyte differentiation and process outgrowth (John et al., 2002; Wang et al., 1998). Also, depletion of macrophages leads to impairment of the remyelinating process (Kotter et al., 2001). Changes in the behavior of phagocytic macrophages with aging is a key factor responsible for recruiting and activating the phagocytic macrophages as to facilitate remyelination (Zhao et al., 2006).

The pathological conditions at lesion site also induce local production of growth factor, cytokines and chemokines, many of which can have negatively influence OPC differentiation. FGF2 is another negative regulator of OPC differentiation and strong mitogen for postnatal rodent OPCs. In adult mouse CNS demyelinated by corona virus infection or exposed for a long time to cuprizone, FGF2 increases in the lesions, leading to chronic demyelination whereas FGF2-deficient mouse OPCs repopulate the lesions and remyelinate completely (Armstrong et al., 2006; Armstrong et al., 2002). These results show that deletion of FGF can create a permissive environment for OPC differentiation leading to endogenous remyelination. The pro-inflammatory cytokines TNFα and IFNγ cause reversible inhibition of OPC proliferation and differentiation (Agresti et al., 1996).

The young rats displayed better remyelination efficiency as compared with old rats (Sim et al., 2002b). However, reports using aged monkeys or rats reveal a significant increase in new OLs in older animals compared with younger ones (Peters and Sethares, 2004). Yet, this elevated basal level of OLs may not translate into improved repair following demyelination, as remyelination and growth factor up-regulation are significantly delayed and lower in older rodent brains following demyelination (Hinks and Franklin, 2000). The age dependent remyelination failure is attributed to be under the control of the epigenetic gene expression. Myelin gene expression is associated with recruitment of histone deacetylases (HDACs) to promoter regions of myelin genes in young mice brains. However in old animals the decrease in remyelination efficiency is associated with failure of recruitment of histone deacetylases (HDACs) paving way for transcriptional inhibitors leading to failure of myelin gene expression (Shen et al., 2008).

Gender appears to play major role in remyelination efficiency. Male rats displayed better remyelination efficiency as compared with females (Li et al., 2006). The better remyelination efficiency in males can be attributes to increased oligodendrocytes number, as the adult male rats had about 20–40% more OLCs than females (Cerghet et al., 2006). However, the white matter of female rats had a higher rate of oligodendrocyte generation coupled with a higher rate of oligodendrocyte death. Thus, in end the number of oligodendrocytes was less in female rat brains. Pregnancy also appears to play a role oligogenesis and remyelination. When EAE or chemical demyelination was induced in pregnant rats, the level of OL death

and demyelination is markedly lower than in non-pregnant rats, suggesting that factors associated with pregnancy drives toward OPC differentiation and remyelination survival (Gregg et al., 2007).

#### 1.4.2.2 Myelin associated inhibitors of OPC differentiation

Following injury the myelin is disrupted locally and degenerates leaving large amount of debris which needs to be cleared to pave the way for the remyelination. Myelin is a complex structure with peculiar lipid protein ration of 70:30. Robinson and Miller showed that the precursor cells in tissue culture when grown on myelin substrates were unable to differentiate and mature into oligodendrocytes. However on removal of myelin substrate the precursor cell differentiated into o4+ oligodendrocytes indicating that a component of myelin blocks differentiation of precursor cells in vitro. Furthermore, they demonstrated that differentiation block associated with myelin is restricted to CNS myelin and not with that of PNS (Robinson and Miller, 1999). Possibly these inhibitory myelin molecules are expressed on mature oligodendrocytes providing a feed-back inhibition for early precursor cells during development as to control the number of mature oligodendrocytes.

To test the effect of myelin substrate on remyelination, toxin induced experimental lesions were stereotactically supplemented with exogenous myelin membranes. In myelin treated animals at day 28, where the remyelination is complete in controls, most of the axons remain demyelinated except at the border of the lesion. qPCR based quantification of myelin basic protein in the lesion site revealed a profound inhibition of MBP expression. However, the number of precursor cells in the lesion site was identical in controls and the animals, in which myelin debris was added, indicating that failure of remyelination is due to impaired differentiation rather than insufficient recruitment of precursor cells (Kotter et al., 2006).

Recently two signaling cascades by which MAI inhibit OPC differentiation have been described (Baer et al., 2009). Myelin associated inhibitors induce an OPC differentiation block by modulating Fyn-RhoA-ROCK signaling as well as by activation of protein kinase C. Furthermore, by inhibition of the RhoA-ROCK-II and/or PKC signaling by siRNA-mediated and pharmacological inhibition the OPCs were able to overcome the differentiation block induced by myelin associated inhibitors invitro (Baer et al., 2009).

*The components in CNS myelin that inhibit OPC differentiation are still unknown. The main aim of the present thesis was identify potential candidate(s). For this purpose a screen based and hypothesis driven approach was employed, as summarized in chapter 3 and 4 of this thesis. Two potential candidates emerged from the hypothesis driven approach, namely ephrin B3 and semaphorin 3A. The following sections will review the relevant literature with respect to ephrin B3 and Sema 3A signaling.*

## 1.5 Ephrins

### 1.5.1 The Eph receptor and ephrin families

Ephs, the largest subfamily of receptor tyrosine kinases (RTKs) and ephrins can be divided into two classes on the basis of their structural features and binding affinities. A-subclass

ephrins (ephrin-A1 to ephrin-A5) are attached to the outer leaflet of the plasma membrane by a glycosylphosphatidylinositol (GPI) linkage. They bind to and activate the A-subclass Eph receptors (EphA1 to EphA8). The three B-subclass ephrins (ephrin-B1 to ephrin-B3) are attached to the plasma membrane by a single hydrophobic transmembrane domain and have a short, highly conserved cytoplasmic tail. They bind to and activate B-subclass Eph receptors (EphB1 to EphB6). With the exception of EphA4, which can bind both A- and B-subclass ephrins, there seems to be very limited crosstalk between the A and B subclasses. The Eph and ephrins, are vital to both developing and mature nervous systems.

In ephrins, the N-terminal receptor-binding domain (RBD) is structurally conserved, even between the A- and B-type ephrins but not with any other proteins (Himanen and Nikolov, 2003), and forms an eight stranded β-barrel with some structural similarities to plant phytocyanin and nodulin copper-binding proteins (Himanen et al., 2001). A stretch of ~40 disordered amino acids that are not involved in Eph/ephrin interactions (Himanen et al., 2004; Himanen et al., 2001), separates the RBD from the cell membrane (Toth et al., 2001). A-type ephrins harbors the recognition site for Eph contact-dependent cleavage by a disintegrin and metalloprotease (ADAM-10) (Hattori et al., 2000). In B-type ephrins, the transmembrane region connects to a highly conserved cytoplasmic domain containing a C-terminal PDZ (PSD-95 post-synaptic density protein, Discs large, Zona occludens tight junction protein) binding motif and five conserved tyrosine residues, three of which are critical for ephrin signalling.

Consistent with other types of RTKs, both A and B Eph class receptors contain a single transmembrane spanning domain. The extracellular region of the Eph receptor is glycosylated, and consists of a ligand binding domain containing immunoglobulin-like motifs, followed by a cysteine-rich domain and two fibronectin III-like repeats. The intracellular region consists of a juxtamembrane region, a single tyrosine kinase domain, and PDZ binding motif within the non-catalytic region of the COOH terminus (Bruckner et al., 1997; Torres et al., 1998). The kinase domain and juxtamembrane region contain tyrosine residues, and phosphorylation of these tyrosine residues creates docking sites for interactions with signaling proteins containing SH2/SH3 (Src-Homology-2/3) domains. The PDZ binding motif binds to PDZ domain-containing proteins, which are thought to serve as scaffolds for the assembly of multi-protein signaling complexes at the membrane.

It is, however, interesting to note that Ephs, the only family of RTKs dependent on oligomerisation for biological activity (Davis et al., 1994; Stein et al., 1998). Furthermore, ephs are also the only RTKs containing a SAM domain (Hubbard and Till, 2000). Thus known role of the SAM domain in mediating protein/protein interactions and homodimerisation observed at high local concentrations (Behlke et al., 2001), might suggest participation of this domain in the formation of active Eph signaling complexes (Stapleton et al., 1999). Functional analysis of the Eph–ephrin system is challenging for at least two reasons. First, Eph receptors can have overlapping functions in vertebrates, and loss of one receptor can be partially compensated for by another Eph receptor that has a similar expression pattern and ligand binding specificities. Second, an Eph receptor can also act as a ligand in the same way that an ephrin ligand can act as a receptor.

### 1.5.2 Eph-Ephrin bidirectional signaling

On cell–cell contact, these molecules transduce important signals bidirectionally into both the receptor-expressing cell and the ligand-expressing cell in what is known as ‘forward’ and ‘reverse’ signaling, respectively (Henkemeyer et al., 1996). In this way, the Eph receptors can also function as ligands and the ephrin ligands can also function as receptors. While most RTKs become activated by dimerization, the ephrin–Eph system additionally requires the formation of higher-order signaling clusters (Davis et al., 1994).

Unlike any receptor–ligand complex of known structure, the Ephs and ephrins appear to associate as a cyclic heterotetramer with 2:2 stoichiometry. This is consistent with studies demonstrating that Ephs and ephrins can associate as a 1:1 unit (Lackmann et al., 1997). Additionally, it is known that soluble ephrins must be artificially clustered to activate Ephs when added exogenously in vitro (Davis et al., 1994). In their recent study, Nikolov and co-workers defined the minimal stoichiometry of Ephs to ephrins that satisfied the previous biochemical data: a planar arrangement of RTK ligand-binding domains and RTK ligands, arranged with the C-termini perpendicular to the plane in opposite directions. Although this structure does not resemble any other RTK–ligand complex, this is not unexpected because, unlike diffusible RTK ligands, the ephrins are membrane-associated. The architecture of the complex, therefore, must accommodate ephrins and Ephs interacting between cell surfaces – hence the need for a planar structure.

#### 1.5.2.1 Forward signaling

‘Forward signaling’ in Ephrin-Eph interaction is defined when Ephrins act as the ligand and Ephs as the receptor. Eph receptors are known to signal through a number of different pathways and molecules, including small GTPases of the Rho and Ras family, focal adhesion kinase (FAK), the Jak/Stat pathway and the PI3K pathway (Lai et al., 2004; Miao et al., 2000). Small GTPases of the Rho family mediate the effect of Eph receptor activation on actin dynamics. Rho GTPases are activated by EphA receptors, and control cell shape and movement (Shamah et al., 2001). This GTPase activation is mediated by exchange factors and adaptor proteins such as ephexin and Crk respectively (Lawrenson et al., 2002; Shamah et al., 2001). EphB receptors can also activate Rho family GTPases, mediated through the exchange factors intersectin and kalirin (Irie and Yamaguchi, 2002; Penzes et al., 2003). This activation plays a role in elongation of actin filaments and morphogenesis and maturation of dendritic spines. In addition to Rho GTPases, Eph receptors can also regulate the activity of the Ras family of GTPases, including H-Ras and R-Ras (Miao et al., 2001; Zou et al., 1996). Activation of H-Ras leads to activation of the MAP kinase pathway, resulting in transcriptional regulation, proliferation, and cell migration. In contrast to EphA activation of Rho GTPases, the majority of Eph receptors negatively regulate the Ras-MAP kinase pathway (Miao et al., 2001). EphB receptors can also negatively regulate the R-Ras-MAP kinase pathway, resulting in a reduction in integrin-mediated adhesion (Zou et al., 1996). EphA receptors have also been demonstrated to regulate the Jak/Stat pathway, whereas EphB receptors promote proliferation via activation of the PI3 kinase pathway (Lai et al., 2004). FAK is important in mediating Eph receptors and integrin signaling (Miao et al., 2002).

#### 1.5.2.2 Reverse signaling

Studies demonstrated that the extracellular domain of EphB receptors can induce tyrosine phosphorylation of ephrinB ligands (Holland et al., 1996). A number of proteins have been identified which contain SH2 or PDZ domains, which bind to the phosphorylated ephrin ligand and transmit the signal (Cowan and Henkemeyer, 2001; Lu et al., 2001). The adaptor protein, Grb4, contains an SH2 domain and is known to link ephrinB activity to cell morphology (Cowan and Henkemeyer, 2001). The mechanisms of reverse signaling of ephrinA ligands are less understood, but are thought to be the result of ephrinA clustering and recruitment of regulatory proteins (Davy et al., 1999).

### 1.5.3 Eph and ephrins in CNS

Ephs and ephrins are expressed in many cell types and regions in normal adult CNS. In the white matter, Ephs and ephrins are mainly expressed on astrocytes in contact with blood vessels or closely associated with the pial surface. They are also expressed on neuronal populations in the grey matter (Bundesen et al., 2003; Martone et al., 1997; Olivieri and Miescher, 1999). EphrinA5, ephrinB2 and ephrinB3 are expressed by migrating OPCs in the optic nerve (Prestoz et al., 2004). Benson et al., have recently reported ephrin-B3 expression on myelinated oligodendrocytes in vivo (Benson et al., 2005).

In the developing nervous system, repulsive interactions are required between Eph receptors and their ligands in diverse areas, including anterior commissure formation (Henkemeyer et al., 1996; Orioli et al., 1996), spinal cord motor neuron pathway selection (Wang and Anderson, 1997) and neural crest cell migration (Krull et al., 1997; Wang and Anderson, 1997). The A-class Ephs and ephrins are involved in establishing the nasal–temporal (N-T)/ anterior–posterior (A-P) axis during retinocollicular mapping. Analysis of the B-class Ephs and ephrins has revealed a role for these molecules in specifying the dorsal–entral(D-V)/ lateral–medial (L-M) axis. Studies in chick and mouse have revealed low to high gradients of EphBs (B2, B3 and B4) expressed along the D-V axis of the retina (Birgbauer et al., 2000; Connor et al., 1998; Henkemeyer et al., 1996), whereas ephrin-B1 is expressed in a low–high L-M gradient in the chick tectum (Braisted et al., 1997) and mouse SC (Hindges et al., 2002).

All ephrin-B ligands (ephrin-B1–B3) are expressed in the lateral floor plate boundary region of the spinal cord. At the interface between the floor plate and the ventral funiculus, a receptor for these ligands, EphB1, is highly expressed in those axonal segments that have crossed the ventral midline (Imondi et al., 2000). In the developing hindbrain, EphA4, EphB2 and EphB3 are expressed in rhombomeres r3/r5, whereas ephrin-B1, ephrin-B2 and ephrin-B3 are expressed in r2/r4/r6 (Xu and Wilkinson, 1997). Expression of a truncated EphA4 receptor leads to the presence of r3/r5 cells in r2/r4/r6 areas, suggesting that this receptor might regulate the identity of cells or restrict arrangement between segments (Xu et al., 1995), possibly by affecting cellular de-adhesion and repulsive migration.

It appears that Eph receptors and their ligands may play an important role in the underlying maintenance of neuronal connections in the CNS, such as synapse formation and regulation of synaptic function and plasticity (Murai and Pasquale, 2002; Olivieri and Miescher, 1999;

Takasu et al., 2002) including hippocampal plasticity (Murai et al., 2003) and spinal cord pain processing (Battaglia et al., 2003). Ephs and their ephrins are expressed in the subventricular zone (SVZ) of the lateral ventricle and in the rostral migratory stream (RMS), which constitutes an ongoing neurogenic pathway in the adult mammalian CNS. Eph/ephrin interactions in these regions have been linked to the control of cell numbers in this pathway and have been shown to influence both proliferation (Holmberg et al., 2005) as well as apoptosis (Ricard et al., 2006). Ephrin-B3 knockout mice have increased numbers of proliferating cells in the SVZ and RMS with a reduction in the numbers of neuroblasts reaching the olfactory bulb due to elevated levels of apoptosis. These effects were shown to be mediated by the extracellular domain of ephrin-B3; however, the Eph receptors responsible could not be identified (Ricard et al., 2006). Inactivation of the EphA4 or ephrin-B3 genes in knockout mice results in specific defects in the corticospinal tract (CST), with axons inappropriately crossing the midline. These mice exhibit locomotor abnormalities and have no reciprocal movement in their hind limbs, resulting in a hopping gait (Dottori et al., 1998; Kullander et al., 2001). EphA4 knockout mice also have anterior commissure defects (Dottori et al., 1998).

The research described above suggests that reverse signaling through ephrin-As and -Bs may regulate proliferation in discrete cell types and in different ways, whereas forward signaling through the EphAs appears to be pro-apoptotic. The widespread expression of the Eph/ephrin family by the progenitor cells of many different organs (Batlle et al., 2002; Ramalho-Santos et al., 2002; Tumbar et al., 2004) indicate a conserved role for these molecules in the control of stem cell niche outputs during tissue homeostasis.

### 1.5.4 Eph and ephrins in the adult CNS after injury and disease

Expression of Eph/ephrins in the adult brain may result in additional effects that are not present during development. It has been shown that ephrins are inhibitory and repulsive for the axonal growth of many different neuronal populations (Gao et al., 1998; Kullander et al., 2001; Monschau et al., 1997; Wahl et al., 2000; Wang and Anderson, 1997; Yue et al., 1999). For example, clustered ephrin-A5-Fc inhibits neurite outgrowth of the EphA4 receptor-positive ventral spinal cord neurons derived from mouse embryos (Yue et al., 1999). Similar results were demonstrated for retinal ganglion cells in response to ephrin-A5 (Wahl et al., 2000) and for cortical neurons in response to ephrin-B3 (Benson et al., 2005; Kullander et al., 2001). compared to wild-type neurons, neurite outgrowth of EphA4 knockout neurons on EphA4 knockout astrocytes was further increased, indicating that EphA4 expressed on the neurons also inhibited neurite outgrowth in response to ephrins (Goldshmit et al., 2004).

After SCI in adult rats, EphA3, A4, A6 and A8 receptors are upregulated in the ventrolateral white matter at the injury site on both astrocytes and oligodendrocytes and in grey matter ventral motor neurons (Willson et al., 2002). Expression of EphB3 has also been shown on astrocytes at the injury site in the adult rat spinal cord after a complete transection (Willson et al., 2003) or contusion (Miranda et al., 1999). It was proposed that such expression of EphB3 on astrocytes may inhibit regrowth of axons (Miranda et al., 1999). Astrocytes have also been shown to express ephrin-B2, but rather than being involved in axonal repulsion, in this case such expression appears to be involved in interactions with meningeal fibroblasts at the spinal cord lesion site (Bundesen et al., 2003). In EphA4 knockout mice, there was a dramatic decrease in astrogliosis and glial scar formation after spinal cord injury, whereas

EphA4 expression was upregulated on astrocytes by 4 days in wild-type mice (Goldshmit et al., 2004). In the neuroinflammatory disease, multiple sclerosis (MS), Ephs and ephrins have been shown to be upregulated on reactive astrocytes in demyelinated areas.Ephrin-A1, ephrin-A3 and EphA1 were detected in more than 90% of the human samples, whereas ephrin-A2, EphA3, Eph-A4 and Eph-A7 were detected in 20–90% of the samples (Sobel, 2005). It has been proposed that B-class Ephs and ephrins may play a role in the phagocytosis of axon debris following hippocampal injury. Several different members of the Eph and ephrin family are upregulated in the hippocampus following injury (Wang et al., 2005a; Wang et al., 2003), with the up regulation of ephrin-B1 and EphB receptors on astrocytes in the stratumlacunosum-moleculare and outer molecular layer at time points corresponding to astrocytes clearing of debris at the lesion site (Bechmann and Nitsch, 1997; Wang et al., 2005b).It is not clear at present whether expression, upregulation and activation of the Eph/ephrin molecules leads to a cascade of events regulating the inflammatory response after injury. However, it is evident that, in general, Eph/ephrin expression and activation may be inhibitory for neuronal regeneration and remyelination after injury, possibly by multiple mechanisms.

Several major questions still need to be addressed with respect to the Eph receptors and ephrins. Are ephrins and Eph receptors positioned to mediate neuro-glial signaling or are they colocalized on the same surface at compact myelin or central synapses as they are at the neuromuscular junction? Do coexpressed Eph receptors and ephrins sort to different subcellular compartments or plasma membrane subdomains? Can receptors, such as EphA4, simultaneously engage both glial and neural ephrins? Undoubtedly, knowing the precise location of Eph receptors and ephrins will help advance our understanding of the actions of these proteins and their mode of engagement in mature neurons and oligodendrocytes in context of remyelination.

## 1.6 Semaphorins

Semaphorins are secreted, transmembrane, and GPI-linked proteins, defined by cysteine-rich semaphorin protein domains that have important roles in a variety of tissues. Genes encoding semaphorins have been highly conserved in evolution, from invertebrates to humans. Humans have 20 semaphorins, *Drosophila* has five, and two are known from DNA viruses; semaphorins are also found in nematodes and crustaceans but not in non-animals. The expression of semaphorins has been described most fully in the nervous system, but they are also present in most, or perhaps all, other tissues. Functionally, semaphorins were initially characterized for their importance in the development of the nervous system and in axonal guidance. More recently, they have been found to be important for the formation and functioning of the cardiovascular, endocrine, gastrointestinal, hepatic, immune, musculoskeletal, renal, reproductive, and respiratory systems (Kruger et al., 2005; Kumanogoh and Kikutani, 2003; Pasterkamp and Verhaagen, 2006; Yazdani and Terman, 2006). A common theme in the mechanisms of semaphorin function is that they alter the cytoskeleton and the organization of actin filaments and the microtubule network.

### 1.6.1 Semaphorin-neuropilin-plexin superfamily

Semaphorins are grouped into eight classes on the basis of phylogenetic tree analyses and the presence of additional protein motifs. The semaphorins found in invertebrates are

grouped in classes 1 and 2; classes 3–7 are vertebrate semaphorins; and the final group is encoded by viruses. Individual proteins are designated by a letter code — for example, Sema3A and Sema4D. All semaphorins contain a conserved ~400 aminoacid 'Sema' domain (1999; Gherardi et al., 2004). These effects occur primarily through binding of semaphorins to their receptors, although transmembrane semaphorins also serve as receptors themselves. The best characterized receptors for mediating semaphorin signaling are members of the neuropilin and plexin families of transmembrane proteins. Plexins, in particular, are thought to control many of the functional effects of semaphorins; the molecular mechanisms of semaphorin signaling are still poorly understood, however. The semaphorins range in size from 400 to 1000 amino acids, depending on what other domains. They have in addition to the Sema domain and a PSI (plexins, semaphorins and integrins) domain. C-terminal to the Sema and PSI domains, a single IMMUNOGLOBULIN LIKE DOMAIN is found in semaphoring classes 2, 3, 4 and 7, whereas class 5 semaphorins have seven THROMBOSPONDIN domains. Proteins in semaphorin classes 1, 4, 5, 6 and 7 are membrane-associated, whereas those in classes 2 and 3 and the viral semaphorins are secreted. Of the transmembrane semaphorins, class 6 proteins have the largest intracellular domains by far (~400 amino acids), all of which contain proline-rich motifs. Class 4 semaphorins frequently have PDZ-DOMAIN binding motifs at their C termini (1999).

Plexins are the predominant family of semaphorin receptors and are grouped into four categories (A–D) on the basis of overall homology. Individual proteins are named according to a number code — for example, Plexin-A1 or Plexin-B1. There are four A-type, three B-type, one C-type and one D-type, in addition to the two plexins that are found in invertebrate species. The plexins are a homogeneous family of proteins, which, when first identified, were shown to function in cell adhesion (Kruger et al., 2005; Tamagnone and Comoglio, 2000). Like semaphorins, Sema domains are characteristic of plexins. Additionally, following the Sema domain, plexins have three PSI domains and three IPT (Ig-like, plexins and transcription factors) domains in their extracellular domains. Plexins can function as both ligand-binding receptors and as signalling receptors for semaphorins. Most plexin–semaphorin interactions are mediated through the Sema domains of both proteins, except for class 3 semaphorins, which, with one exception, require neuropilins as essential semaphoring binding co-receptors to signal through class A plexins. Neuropilins are transmembrane proteins of ~900 amino acids 16 with short intracellular domains that lack intrinsic enzymatic activity. They function as the ligand-binding partner in co-receptor complexes for both plexins and vascular endothelial growth factor receptors (VEGFRs) (Cheng et al., 2001; Suto et al., 2005; Swiercz et al., 2002; Takahashi et al., 1999; Tamagnone et al., 1999; Yaron et al., 2005; Yoshida et al., 2006).

### 1.6.2 Semaphorin signaling

Although individual elements of semaphorin signaling cascades have been identified, it is at present unclear how they interact and how they couple to the cytoskeleton. Membrane-bound and secreted semaphorins are likely to trigger analogous signaling pathways through plexins. However, transmembrane semaphorins might in addition transduce intracellular signals themselves through their small cytoplasmic domain; an analogous 'bidirectional' signalling is well known for ephrins. In general, the cytoplasmic domains of transmembrane semaphorins are divergent, even within the same subclass, which might account for reports of their association with diverse signal transducers, such as kinases and phosphatases (Billard et al., 2000; Eckhardt et al., 1997).

The first protein shown to act as effectors of semaphoring signaling was the collapsing response mediator protein (CRMP), which is required for Sema3A-induced growth cone collapse in DRG neurons in vitro (Goshima et al., 1995). The other proteins required for the Sema3A-induced growth cone collapse are Rho family GTPase Rac-1 (Jin and Strittmatter, 1997; Kuhn et al., 1999). Eicosanoids, signaling molecules derived from fatty acids such as arachidonic acid, also participate in Sema3Ainduced growth cone collapse. Treatment of DRG neurons with Sema3A stimulates eicosanoid synthesis, whereas an inhibitor of lipoxygenase blocks Sema3A-mediated growth cone collapse (Mikule et al., 2002).

Zanata et al., showed that, the interaction of Rnd1 with PlexA1 triggers signaling by PlexA1 and results in cytoskeletal collapse, binding of RhoD has the opposite effect and blocks PlexA1 activity. Transfection of RhoD into Sema3A-sensitive neurons prevents response to Sema3A (Zanata et al., 2002). The authors propose that the recruitment of Rnd1 is an essential step in the initiation of cytoskeletal collapse by PlexA1. In contrast to the observations made on the binding of the Rho GTPases RhoA and Rac to PlexB, RhoD binds to a site in PlexA1 that is identical or overlapping with that of Rnd1(Vikis et al., 2000), suggesting that modulatory mechanisms of Rho GTPase activities might differ between PlexA and PlexB proteins. Mikule et al 2002 demonstrate that Sema3A treatment of dorsal root ganglia growth cones stimulates the synthesis of 12(S)-hydroxyeicosatetraenoic acid and that generation of this eicosanoid is necessary for growth cone collapse and detachment following reduction of growth cone adhesion sites (Mikule et al., 2002).

### 1.6.3 Role of semaphorins in the adult nervous system

Semaphorins are best known for their roles in the nervous system. They have been implicated in many processes of neuronal development, including axon guidance, axonal fasciculation, dendritic guidance, and neuronal migration, as well as in the plasticity and neural regeneration of adult nervous system (de Wit and Verhaagen, 2003).

In order to address the function of semaphorins in vivo, a number of studies have analyzed the effects of semaphorin and semaphorin receptor gene deletions on nervous system development, with the main focus on class 3 semaphorin signaling. Several general themes arise from these studies. First, the deletion of semaphorin and semaphorin receptor genes often results in severe defasciculation of peripheral nerves. Second, the effects on CNS development in these null mutants are subtler. Targeting errors are most pronounced in the olfactory system and the hippocampus. Third, although neuropilins can bind most or all class 3 semaphorins, the phenotypes from Sema3A and NP-1 knockout mice are similar, as are the phenotypes of Sema3F and NP-2 mutant mice. Fourth, some of the null mutant lines display severe abnormalities in the development of non-neuronal tissues, especially the cardiovascular system.

Sema 3A has been expressed both in neuronal and glial cells. A CNS defect originally reported in Sema3A null mutants was an abnormal orientation of processes of cortical layer 5 neurons (Behar et al., 1996). Besides defects in the orientation of processes of cortical

neurons, minor targeting errors of entorhinal axons occur in the CNS of Sema3A null mutants (Pozas et al., 2001).Whereas most axons in the PNS of Sema3A knockouts terminate near their appropriate targets (Schwarting et al., 2000). Loss of Sema3C function results in severe cardiovascular abnormalities, but cranial nerve projections are apparently normal in Sema3C null mutants (Feiner et al., 2001). Null mutants have been generated for three membrane-bound semaphorins: Sema4D (CD100), Sema6A and Sema7A. Sema4D-deficient mice display defects in the immune system, but gross macroscopic and histological examination showed no obvious defects in nervous system development (Shi et al., 2000). Sema6A null mice on the other hand do have abnormalities in the CNS. Disruption of the Sema6A gene in thalamocortical neurons, which normally express Sema6A, results in an abnormal ventral projection of their axons. This suggests that Sema6A might act as a receptor in these neurons. loss of the membrane-attached Sema7A results in impaired growth of the lateral olfactory tract (Pasterkamp et al., 2003).

### 1.6.4 Semaphorins in the injured nervous system

Semaphorins released by nonneuronal cells or injured neurons may interfere with regenerative axon growth or participate in scar formation and neovascularization of the lesion. A recent post-mortem study explored the expression of Sema3A and Sema 3F in brains of individuals suffering from MS and controls (Williams et al., 2007). While adult control brain white matter as well as chronic MS lesions did not show any evidence of Sema3A/F expression, an up-regulation of Sema transcripts in active MS lesions was detected. The main cellular source for Sema3A/3Fwere astrocytes and microglia, although expression by cells expressing olig2, which belong to the oligodendroglial lineage, was also noted. Furthermore, an up-regulation of the Sema receptors neuropilin-1 and 2 was detected in oligodendroglial (and other lineage) cells which was restricted to cells at the plaque and periplaque area but absent in normal appearing white matter. This suggests that in the context of demyelination OPCs become reactive to Sema mediated guidance clues. Interestingly, an up-regulation of Sema transcripts in cortical neurons independent of the presence of cortical demyelination was also noted. Finally, evidence of an early expression of Sema3A/F specific to experimentally induced demyelinating lesions was reported (Williams et al., 2007). However, the exact role of these semaphorins is during the course of MS remains to be elucidated.

It has been shown that Sema3A and NRP1 expression is increased and sustained in ischemic brain territories (Hou et al., 2008). The inhibition of Sema3A/ NRP1 signaling would be beneficial for patients because this abnormal expression is supposed to prevent new neurons from entering the infarct area. Similarly to ischemic brain, the abnormal expression of Sema3A is observed following spinal cord injury (Hashimoto et al., 2004). The inhibitory Sema3A signals delivered by the glial scar are considered to contribute to the establishment of a non-permissive environment preventing nerve regeneration. Strikingly, the therapeutic potential of semaphorin inhibitors in this context has been recently proved in a study showing a functional recovery in rats treated with a Sema3A inhibitor after a spinal cord transection (Kaneko et al., 2006).

The presence of semaphorins in the visual system may have significant implication during optic nerve regeneration. Sema5A, which is expressed by oligodendrocytes, is also able to repel RGC axons and it has been proposed that this expression may contribute to the lack of optic nerve regeneration after axotomy (Goldberg et al., 2004)}. Sema3A is over expressed in the cerebellum of schizophrenic patients (Eastwood et al., 2003). This abnormal over expression is associated with down regulation of genes involved in synaptic formation and maintenance. Another intriguing issue is certainly the accumulation and abnormal expression of Sema3F in the brain of patients with Alzheimer's disease (Hirsch et al., 1999).

## 1.7 Conclusion

Proliferative precursor cells of the oligodendrocyte lineage which emerge out of the germinal zones develop into mature oligodendrocytes produce the multilamellar myelin sheath, around axons allowing for saltatory conduction. When demyelination takes place, the OPCs attempt to restore lost myelin sheaths in a spontaneous regenerative process called remyelination. In many cases the remyelination is incomplete and it often fails (Franklin and Ffrench-Constant, 2008; Franklin, 2002b).

An increasing number of studies have demonstrated that in chronic MS lesions OPCs are more vulnerable during the differentiation phase than during the recruitment phase and in theses lesions premyelinating oligodendrocytes fail to differentiate and remyelinate (Chang et al., 2002; Kuhlmann et al., 2008b; Wolswijk, 1998). One possible explanation is the persistence of differentiation inhibitors in chronic lesions. Several such differentiation inhibitors have been suggested to have roles including the Notch pathway (John et al., 2002), PSA-NCAM (Charles et al., 2002), hyaluronan (Back et al., 2005), LINGO-1 (Mi et al., 2005) and myelin debris (Kotter et al., 2006).

Myelin inhibition of OPC differentiation in vitro (Robinson and Miller, 1999), suggests that the removal of myelin debris may be critically to allow OPCs to differentiate and remyelinate. This was confirmed in a recent experiment, which demonstrated that the addition of myelin debris to a lesion that would normally undergo rapid and complete remyelination results in a substantial inhibition of this process. (Kotter et al., 2006). This study identified myelin as an inhibitor of OPC differentiation. An important question therefore is which are the specific components in myelin that inhibit OPC differentiation.

*The aim of the present thesis was to identify and characterize the molecules in myelin, which mediate the differentiation block in OPCs. For this purpose two approaches were employed. Chapter 4 describes a candidate approach based on the hypothesis that known myelin associated inhibitors of neurite outgrowth also mediate inhibitory effect on OPC differentiation. In chapter 4 a screening based approach was used as to reduce the complexity of inhibitory substrate using column chromatographic techniques followed by substrate identification based on mass spectrometry. From the results of the hypothesis based approach, Ephrin B3 and Sema 3A emerged as candidates mediating inhibitory effects on OPC differentiation. Whereas Ephrin B3 is an integral myelin protein exclusively expressed by oligodendrocytes, Sema 3A is more regarded as a glial scar associated molecule expressed by both glial cells and neurons. However, I found that Oligodendrocyte*

*also express Sema3A at various stages of development. Chapter 5 tests the hypothesis that Ephrin B3 is a potent and selective inhibitor of OPC differentiation. These studies formed the basis for the subsequent chapter 6 where the hypothesis was tested that the presence of Ephrin B3 is inhibits CNS remyelination. Similarly, in chapter 7 the hypothesis that Sema3A is a potent and selective inhibitor of OPC differentiation was tested and the results were translated into an in vivo model of CNS remyelination*

# Chapter 2
# Materials and Methods

# 2. Material and Methods

## 2.1 Cell culture

### 2.1.1 Preparation of mixed glial cultures

Primary cultures of mixed glial cells were isolated from P0-P2 neonatal Sprague-Dawley rat forebrains following a standard protocol (McCarthy and de Vellis, 1980). Following extraction, the cerebral cortices of postnatal day 0-2 Sprague-Dawley rats were stripped free of the meninges. Hemispheres were pooled in groups of six and each incubated in 1ml of digestion solution for 30 minutes in a standard CO2 incubator (37°C, 7.5% CO2). Following incubation, the cortices were homogenized by carefully pipetting up and down two to three times. Digestion was stopped by addition of 9ml D-MEM supplemented with 10% FCS. Subsequently, the homogenates were pelleted for 10 minutes/1500rpm, the supernatant removed and the pellets re-suspended with 1ml D-MEM. Finally, the cells were plated at a density of 1,5 brains per T75 tissue culture flask, which had been pre-coated with Poly-L-Lysine-hydrobromide for 30 minutes at 37°C followed by three washes with dH2O, and cultured at 37°C/7.5% $CO_2$. The cell culture medium was changed every three days. After about a week the cells separate into two layers: a basal monolayer consisting of fibroblasts and astrocytes, and a top layer formed by oligodendrocyte precursor cells and microglia.

### 2.1.2 Preparation of highly enriched OPC cultures

10 to 14 days following preparation of the MGCs, the loosely attached microglia were removed by placing the flasks on an incubated orbital shaker at 260 revs/minute, 37°C for one hour. The supernatant containing the detached microglia cells was removed and 8ml fresh medium was added. Shaking was continued for 24 hours at 260 revs/minute at 37°C to detach OPCs. Alternatively, OPCs can be dislodged manually by a series (2-3) of manual shakes and brief inspection under an inverted microscope to make sure all cells have been detached. Subsequently, microglial contaminants were removed by differential adhesion: the supernatant was incubated in non-tissue culture Petri dishes (60cm) for 10 minutes at 37°C. While OPCs remain in solution the highly adhesive microglia cells attach to the plastic and thus can be separated. The highly enriched OPC suspension is then centrifuged for 10 minutes at 1500rpm and the pellet re-suspended in Sato's medium (see below) and plated on tissue culture flasks or 8-well chamber slides pre-coated with Poly-L-Lysine-Hydrobromide as outlined above. To keep OPCs proliferating Sato's medium was supplemented with PDGF-AA and FGF (both at 10ng/ml). To induce differentiation, 0,5% heat inactivated FCS was added to the medium (no PDGF-AA or FGF). The purity of each culture was monitored following OPC purification by immunocytochemistry and only cultures with >94% purity were used. In the cultures minor contaminations of microglia that can be detected by isolectin staining and which amount to 4-5% of the cells as well as by astrocytes (detectable by GFAP) and fibroblasts with distinct morphology, which account for about 1-2% of the cells were present.

## 2.2 Preparation of substrates

### 2.2.1 Myelin Preparation

Adult rat brains were homogenized in 20 volumes of ice cold 0.32M sucrose solution using an UltraTurrax T18 basic (IKA) for 2 minutes. After the homogenization step the sucrose solution was diluted to 0.25M. The ultracentrifugation tubes (Beckman) were washed with EtOH and the homogenized samples were transferred into the prewashed tubes. After centrifugation at 55,000xg (Sorvall Ultracentrifuge*;* DuPont, Combi, OTD) for 10 minutes at +4°C the pellet was resuspended in 14ml 0.88M sucrose solution and carefully overlaid with 14ml 0.25M sucrose solution following a centrifugation step 100,000xg for 60 minutes at +4°C. The white interface was collected and washed with 30ml dH2O following a centrifugation step at 55,000xg for 10 minutes at +4°C. Afterwards the supernatant was taken off and the pellet was resuspended in 10ml dH2O and an incubation step for 60 minutes on ice was performed for an osmotic shock. One more centrifugation step was performed at 55,000xg for 10 minutes on +4°C following a repeat of the flotation step performed with 0.88M and 0.25M sucrose. The interface was collected and washed twice with 30ml dH2O and pelleted at 55,000xg. Finally the pellet was stored at -80°C until further usage.

### 2.2.2 Myelin protein extraction

The myelin pellet was dissolved in 10% Octyl-β-D-Glucopyranoside to final 1%, 0.5M Phosphate Buffer to final 0,2M, 1M Na2SO4 to final 0,1M and 0,5M EDTA to final 1mM and incubated on a heating block at 23°C for 2 hours. The suspension was ultra centrifuged (Sorvall Ultracentrifuge*;* DuPont, Combi, OTD) at 100,000xg for 30 minutes at room temperature. After centrifugation the supernatant was collected and the protein concentration estimated with BCA standard method. Myelin protein extracts were stored either at -20°C till further usage.

### 2.2.3 Plating of substrates

40µg of myelin protein extract was plated onto Poly-L-Lysine-Hydrobromide (SIGMA-ALDRICH) precoated cell culture dishes over night. After coating with myelin protein extract the dishes were washed twice with dH2O and the OPCs were plated onto the dishes at a density of $2x10^4$ cells for 8-well chamber slides or $3x10^5$ cells for 6-well plates.

### 2.2.4 Preparation of Nogo-A, Nogo-A D20, MAG, OMgp, GAP-43, Netrin, Ephrin B3, Brevican and Sema 3A

Nogo-A–transfected Chinese hamster ovary cells were kindly provided by Professor Martin E. Schwab. Cells were grown and selected with 250 mg/ml Zeocin (Invitrogen) until they reached confluence. After being rigorously washed with phosphate-buffered saline, they were lysed with lysis buffer, and recombinant proteins were purified over a Ni2+-NTA column (Qiagen) according to the manufacturer's protocol. Successful purification of Nogo-A was confirmed by Western blot analysis using Nogo-A monoclonal antibody 11C7 kindly provided by Professor Martin E. Schwab. Bacterial Nogo-A D20 constructs were expressed in

*Escherichia coli* and purified as described elsewhere (Oertle et al., 2003). In brief, after growing in selective medium, the bacteria were lysed in lysis buffer and the supernatant was purified using the $Co^{2+}$- Talon Metal Affinity Resin (Clontech). Similarly, OMgp was purified from constructs kindly provided by Dr. Zingang He as well as obtained from a commercial source. Purified MAG, OMgP, GAP-43, Netrin, Ephrin B3, Brevican and Sema 3A were obtained from a commercial source and diluted based on manufactures instruction.

### 2.2.5 Clustering of Ephrin B3

The ephrin B3 was dissolved in PBS at a concentration of 100µg/ml. The anti-human Fc-IgG (1mg/ml) was mixed with dissolved ephrin B3 in a ratio of 1:10 and allowed to incubate for 2hours at room temperature. Following 2 hour, the dilution were made according to required concetrations

### 2.2.6 Protein precipitation of MPE

Enriched myelin proteins were precipitated with either a highly acidic organic solvent-based commercial kit (ProteoExtract Protein Precipitation Kit, Calbiochem) according to the manufacturer's instructions or a standard ammonium acetate–methanol precipitation. After overnight incubation at 14°C, precipitated protein pellets were washed extensively, and subsequently the proteins were incubated with either proteinase K (Sigma) or lipase (Sigma) for 1 hour at 37°C. The efficiency of digestion was confirmed by means of SDS-PAGE before the substrate was tested in our assay.

## 2.3 Chromatography

### 2.3.1 Cationic chromatography (CM Colum)

About 50 ml of the MPE (~1 mg/ml) were filtered through a 0.22 m Millipore membrane filter. The filtrate was desalted and concentrated using Amicon ultrafiltration cell (Millipore, Billerica, MA, USA; membrane diameter 44.5mm; cut off 10 000 Da) with 50mM sodiumacetate (pH4). This step was repeated three times to ensure that the sample was maximally desalted. The concentrated and desalted lysate was subsequently loaded on a CM column (Econo-Pac CM cartridges, 1 ml, Biorad, Hercules, CA, USA). Column chromatography was performed using an FPLC System with a built in detector (Pharmacia Fine Chemicals, GE Healthcare, Bucks. UK). The injection volume was 10 ml; 50mM sodium acetate buffer containing 1% octlyglucoside (mobile phase A) was used as washing buffer and 1M NaCl containing1% octylglucoside (mobile phase B) was used as elution buffer. The following chromatographic gradients were applied: 0% B for 15 min, 0–70% B, hold with 70% B for 10 min followed by a wash with A for 10 min. The flow rate used was 2 ml/min, the fraction size 1 ml/min and sensitivity of the detector was 1U at a wavelength of 280 nm. The non-binding fractions and the binding fractions were pooled together separately and assessed for inhibitory activity on OPC differentiation using the in vitro substrate assay outlined above. Repeat experiments demonstrated that the inhibitory effects on OPC differentiation were associated with the nonbinding fraction of the CM column.

### 2.3.2 Anionic chromatography(High Q Colum)

To further eliminate proteins with non-inhibitory activity, the inhibitory non-binding fraction was concentrated and the buffer exchanged to a 0.1M Tris–Cl buffer containing 1% octlylglucoside (pH 8). The concentrate was subsequently loaded on an anion exchange EconoPac High Q cartridge (1 ml; Bio-Rad) and coupled to the FPLC system (GE Healthcare UK Ltd, Little Chalfont, Buckinghamshire, UK). 0.1M Tris–Cl containing 1% octylglucoside was used as washing buffer (Mobile phase A). The binding fraction was eluted using 1M NaCl in 0.1M Tris–Cl containing 1% octylglucoside (Mobile Phase B).The injection volume was 10 ml. The reaction conditions were as follows:0% B in 5 min and 0–100% B in 10 min, 100% B for 10 min and washing with A for 5 min. The flow rate was maintained at 2 ml/min at25_C. The detection wavelength was 280nm and sensitivity set at 1U.The resulting binding and non-binding fractions were again pooled separately. When tested for their inhibitory effects the inhibitory activity was associated with the binding fraction. The pooled binding fractions were further concentrated and the buffer exchanged to a buffer composed of 250mM 6-aminocaproic acid, 25mM Bis–Tris,pH 7.0 using Amicon ultra centrifugal filter devices.

## 2.4 Proteomic analysis

### 2.4.1 One dimensional electrophoresis: Blue native PAGE

60 ml of purified inhibitory myelin protein fractions (~2 mg/ml) was added to 10 ml of G250 solution [5% (w/v) Coomassie G250 in10mM 6-aminocaproic acid] and loaded onto the gel. BN-PAGE (Wittig et al., 2006) was performed in a PROTEAN II xi Cell (BioRad, Germany) using a 4% stacking and a 5–13% separating gel. The gel buffer contained 250mM 6-aminocaproic acid, 25mM Bis-Tris, pH 7.0; the cathode buffer 50mM Tricine, 15mM Bis-Tris, 0.05% (w/v) Coomassie G250, pH 7.0; and the anode buffer 50mM Bis-Tris, pH 7.0. For electrophoresis, the voltage was set to 70V for 2 h, and was increased to 250V (10 mA/gel) until the dye front reached the bottom of the gel. BN-PAGE gels were cut into small pieces of ~1–3 cm depending on the intensity of protein bands for the BN/SDS/SDS–PAGE three dimensional electrophoresis (3DE).

### 2.4.2 Three dimensional electrophoresis: BN/SDS/SDS–PAGE

The experimental procedures and advantages of BN/SDS/SDS–PAGE (3DE) are summarized in Kang et al. (2008). Briefly, 1–3 cm gel pieces from BN-PAGE were soaked for 2 h in a solution of 1% (w/v) SDS and1% (v/v) 2-mercaptoethanol. Gel pieces were then rinsed twice with SDS–PAGE electrophoresis buffer [25mM Tris–HCl, 192mM glycine and 0.1% (w/v) SDS; pH 8.3], then the gel pieces were placed onto the wells. 2DE-SDS–PAGE was performed in PROTEAN II xi Cell using a 4% stacking and a 6–13% separating gel for BN/SDS–PAGE (2DE).Electrophoresis was carried out at $25^0$C with an initial current of 70 V (during the first hour). The voltage was then set to 100V for the next 12 h (overnight), and increased to 200V until the bromophenol blue marker moved 17 cm from the top of separation gel. 2DE gels were cut again into lanes and gel strips from each lane were soaked for 20 min in a solution of 1% (w/v) SDS and 1% (v/v) 2-mercaptoethanol. Gel strips were then rinsed twice with SDS–PAGE electrophoresis buffer (25mM Tris–HCl, 192mM glycine and 0.1%(w/v) SDS; pH 8.3), and were placed onto the wells of another gel (3DE).

SDS–PAGE was performed in PROTEAN II xi Cell using a 4% stacking and a 7.5–17% separating gel. Electrophoresis was carried out at $25^0$C with an initial current of 70V (during the first hour). Then, the voltage was set to 100V for the next 12 h(overnight), and increased to 200V until the dye front reached the bottom of the gel. Colloidal Coomassie blue staining was used for visualization.

### 2.4.3 Trypsin In gel digestion

The gel pieces of interest were cut into small pieces to increase surface and collected in a 0.6 ml tube. They were initially washed with 50mM ammonium bicarbonate and then twice with 50% 50mM ammonium bicarbonate/50% acetonitrile for 30 min with occasional vortexing. The washing solution was discarded at the end of each step. 100 microlitre of 100% acetonitrile was added to each tube to cover the gel piece followed by incubation for at least 5 min. The gel pieces were dried completely in a Speedvac Concentrator 5301 (Eppendorf, Germany). Cysteines were reduced with a10mM dithiothreitol solution in 0.1M ammonium bicarbonate pH 8.6 for 60 min at $56^0$C. The same volume of a 55mM solution of iodoacetamide in 0.1M ammonium bicarbonate buffer pH 8.6 was added and incubated in darkness for 45 min at $25^0$C to alkylate cysteine residues. The reduction/alkylation solutions were replaced by 50mM ammonium bicarbonate buffer for 10 min. Gel pieces were washed and dried in acetonitrile followed by Speedvac concentration. The dried gel pieces were re-swollen with 12.5 ng/ml trypsin (Promega, WI, USA) solution buffered in 25mM ammonium bicarbonate. They were incubated for 16 h (overnight) at $37^o$C. Supernatants were transferred to new 0.6 ml tubes, and gel pieces were extracted again with 50 ml of 0.5% formic acid/20% acetonitrile for 15 min in a sonication bath. This step was performed twice. Samples in extraction buffer were pooled in a 0.6 ml tube and evaporated in a Speedvac. The volume was reduced to ~10 ml and 10 ml water was added.

### 2.4.4 Nano –HPLC-ESI-Q-TOF-mass spectrometry

LC-ESI-MS/MS analyses were carried out with the UltiMate 3000 system (Dionex Corporation, Sunnyvale, CA, USA) interfaced to the QSTAR Pulsar mass spectrometer (Applied Biosystems, Foster City, CA,USA). A nano flow HPLC equipped with a reversed phase PepMap C-18 analytic column (75 mm_150mm) was used. Chromatography was performed using a mixture of two solutions, A (0.1% formic acid in water) and B (80% acetonitrile/0.85% formic acid in water), with a flow rate of 300 nl/min. First a linear gradient between 4% and 60% B was run over 45 min, then 90% B was used for 5 min and 0% B for 25 min. Peptide spectra were recorded over the mass range of m/z 350–1300, and MS/MS spectra were recorded under information dependent data acquisition (IDA) over the mass range of m/z 50–1300. One peptide spectrum was recorded followed by three MS/MS spectra on the QSTAR Pulsar instrument; the accumulation time was 1 s for peptide spectra and 2 s for MS/MS spectra. The collision energy was set automatically according to the mass and charge state of the peptides chosen for fragmentation. Doubly or triply charged peptides were chosen for MS/MS experiments due to their good fragmentation characteristics. MS/MS spectra were interpreted by the MASCOT software (mascot.dll 1.6b21; Matrix Science, London, UK) in Analyst QS 1.1 (Applied Biosystems). Searches were done by using the MASCOT 2.1 (Matrix Science, London, UK) against Swissprot 53.3 and MSDB 20051115 database for protein identification. Searching parameters were set as follows: enzyme selected as trypsin with a maximum of two missing cleavage sites, species limited to mouse, a mass tolerance of 500 ppm for peptide tolerance, 0.2 Da for MS/MS tolerance, fixed

modification of carbamidomethyl (C) and variable modification of methionine oxidation and phosphorylation (Tyr, Thr and Ser).

### 2.5 Preparation of liver membrane fraction

For isolation of liver membrane fractions, 0.85M and 1.23M sucrose in 2.5mM Tris/HCl was prepared as above. The liver of a young adult Sprague-Dawley rat was extracted and homogenised in 0.85M sucrose (using an Ultra-Turrax). The homogenate was layered onto a 1.23M sucrose solution. After centrifugation (100,000g, 4°C, 1h) the interface was collected and washed in $dH_2O$ (55,000g, 4°C, 10min). Finally, the pellet was resuspended in an equal volume of 1xPBS.

### 2.6 Neutralization assay

Neutralization assay assess the ability of antibody to inhibit or neutralize the toxic effect of the substrate and to rescue cells in culture. The Myelin protein extract was coated on the precoated poly-L-lysine slides. The ephrin B3 antibody ( Abcam and R&D ) was diluted in SATOS's differentiation medium to a final concentration of 5µg/ml and 10µg/ml. It was added on top of the coated MPE and incubated for 2 hour at room temperature. Later the antibody was removed and slides were washed with PBS. The OPC were then plated on top of it at a density of 2x104 cells/ well. Similarly the ephrin B3 antibody was diluted in SATO's differentiation medium at required concentration and was incubated on the percolated ephrin B3 in 8 well chamber slides at room temperature for 2 hours. Later the wells were washed with PBS then OPC were plated above it.

### 2.7 Processes retraction assay

The OPC's were plated and differentiated as outlined in 2.1.2. Following today of differentiation the medium was replace with differentiation medium contain preclutered ephrin B3-FcIgG at a concentration of 10µg/ml. after 24 hours cells were fixed by 4%PFA .

### 2.8 Immunocytochemistry

The pooled OPCs harvested as outlined above were seeded at the same density of 20000 cells per well into polylysine (PLL)-coated 8-well chamber slides (Nunc). Cells were differentiated for 48 hours and subsequently fixed with 4% paraformaldehyde in PBS, permeabilised and blocked with 0.3% Triton X-100 and 10% NGS. To assess the differentiation state of OPCs the cells were incubated with O4 antibody (1:100*;* Chemicon) or *Nkx2.2* antibody (1:50*;* Developmental Studies Hybdridoma Bank, University of Iowa), A2B5(1:100, Chemicon), MARCKS(1:100,Sigma), MBP(1:100, Sigma) and Ephrin B3(1:200, R&D) for 1 hour in the presence of 0.1% Triton X- 100 and 2% NGS, washed, and incubated for another 1 hour with the appropriate fluorescent secondary antibody (Cy3-conjugated antibody 1:100*;* Jackson Immuno Research*;* Cy2-conjugated antibody 1:100*;* Jackson Immuno research) and the nuclei were stained using Hoechst stain solution (SIGMA-ALDRICH) (Robinson and Miller, 1999). It is important to note that permeabilisation of cells results in a punctate representation of the extracellular antigen O4 (Reynolds and Weiss, 1993; Syed et al., 2008). Under a fluorescent microscope using a triple-filter the percentage of O4-positive cells in relation to >100 DAPI-stained nuclei in randomly selected eye fields for

each experimental condition was determined. To establish the purity of the OPC cultures immunocytochemistry for A2B5 (1:100*;* Chemicon) was performed according to the same principles and the percentage of A2B5+ cells to >100 DAPI-stained nuclei in randomly selected eye fields was determined. Only cell cultures with >94% A2B5-pos. cells were used for this thesis. To assess the morphological phenotype of OPCs, A2B5+-cells were categorized according to the following criteria: stage I: mono/bipolar*;* stage II: multipolar, primary branched*;* stage III: multipolar, secondary branched*;* stage IV: secondary branched cells with membranous processes.

## 2.9 Immunohistochemistry

### 2.9.1 Chromogenic Immunohistochemistry

Frozen slides were preincubated in water for 5 min and another 5 min in Citrate buffer. 300 ml Citrate buffer were boiled in a micro oven. Slides were transferred to hot Citrate buffer and heated for 10 min at max. 600 Watt. Attention was given to not boiling the buffer, because tissue loss was observed during strong boiling processes. Slides were cooled down at room temperature for app. 20 min. Afterwards slides were prechilled in 0.05 M Trisbuffer containing 2% milk powder for 5 min. Washing and antibody conjugating steps were done using the Coverplate System™ (Thermo). Endogenous peroxidase was inhibited with 100 µl 1.5% H2O2 in MeOH, slides were rinsed with Trisbuffer (+ 2% milk powder). Blocking of unspecific background stain was accomplished by applying 100 µl Protein Block Serum-Free ready-to-use (DAKO). Primary antibody (rabbit-anti-EphrinB3, Abcam; goat-anti-Semaphorin3A, R&D Systems) was diluted 1:100 in Dako Antibody Diluent (DAKO) and slides were incubated with 100 µl either at 4°C overnight or for 2 hours at room temperature. Slides were then washed with Trisbuffer (+2% milk powder) and the DAKO-LSAB kit was used for secondary antibody conjugation according to manufacturer's instructions. Visualization was obtained using DAB (DAKO) for 10 minutes on each slide. Slides were counterstained in Haematoxilin and mounted with Eukitt.

### 2.9.2 Fluorescent Immunohistochemistry

Frozen slides were prechilled for 30 min with 0.05M Trisbuffer, then blocked for 30 min with Protein Block Serum-Free ready-to-use (DAKO) and incubated with 100 µl primary antibody (1:100 in PBS/BSA) for 2 hours at room temperature. After two washing steps for 5 min each with Trisbuffer, the slides were incubated with secondary antibody (for EphrinB3: Cy™3 goat anti-rabbit (Dianova) 1:100 in PBS/BSA, for Semaphorin3A: Cy™3 donkey anti-goat (Dianova) 1:100 in PBS/BSA) for 2 hours at room temperature. Slides were washed three times for 5 minutes with Trisbuffer and mounted with Aqua-mount.

## 2.10 Confocal laserscan microscopy

The harvested OPCs were plated onto 8-well chamber slides at a density of 20000 cells per well and allowed to differentiate for 48 hours before fixation with 4% paraformaldehyde in PBS. Staining was performed according to the same principles as outlined above. To assess the cellular localization of phosphorylated MARCKS cells were incubated with p-MARCKS antibody (SIGMA-ALDRICH*;* 1:100) and the appropriate second antibody (Cy3-conjugated antibody 1:100*;* Jackson Immuno Research) for one hour at room temperature. For an

internal control OPCs were stained with A2B5 antibody (1:100*;* Chemicon) and the appropriate second antibody (Cy2-conjugated antibody 1:100*;* Jackson Immuno Research) after p-MARCKS staining. After embedding (VECTASHIELD Mounting Medium with DAPI, Vector Laboratories H-1200) the slides were scanned with a Zeiss LSM 510 motorized confocal laser scan microscope (Carl Zeiss, Jena, Germany) equipped with an argon-ion laser source (488 nm excitation) and two Helium Neon lasers (543 and 633nm excitation). To eliminate "bleed-through" from either channel, an appropriate combination of excitation and barrier filters (bandpass filter 505-530nm and long pass filters 560nm and 650nm) was used. Parameters were set constant at 63x/1.0 for magnification and the Pinhole was set at 100µM.

### 2.11 TUNEL assay

Fragmented DNA was detected by incorporation of biotinylated nucleotides at the 3'-OH DNA ends using Terminal Deoxynucleotidyl Transferase recombinant (rTdT) enzyme according to the manufacturer's instruction (Promega). Stained cells were visualized by light microscopy and the percentage of apoptotic nuclei was determined using an Olympus IX 51 microscope.

### 2.12 RhoA GTPase activity assay

For the detection of active RhoA, OPCs were lysed (125mM HEPES, pH 7.5, 750mM NaCl, 5% Igepal CA-630, 50mM MgCl2, 5mM EDTA, 10% Glycerol, 25mM NaF, 1mM Na3VO4) according to the manufactures instructions (Upstate) and active GTP-Rho was precipitated by the use of beads specific for the GST-binding domain (RBD) of rhotekin (Upstate). After removing cell debris the lysates were incubated with Rho Assay Reagent Slurry which specifically binds Rho-GTP and not Rho-GDP (30 min, 4°C). Beads were then washed with Mg2+ Lysis/Wash Buffer and bound material was eluted with 25µl 2x Laemmli sample buffer, boiled for 5 min, resolved by SDS-PAGE and immunoblotted using mouse anti-RhoA antibody (3µg/ml, Upstate). Peroxidase-conjugated anti-mouse IgGs (Amersham Biosciences, 1:5000) were used as secondary antibodies. Immunoreactive proteins were visualized using ECLTM detection system (Amersham Biosciences).

### 2.13 Reverse Transcriptase-Polymerase Chain Reaction (RT-PCR)

Total RNA of OPCs grown on PLL control was harvested after the cells were differentiated for 3 days using RNeasy Mini Kit (Qiagen, Hilden, Germany) according to the manufacturer's instruction. First strand cDNA synthesis kit for RT–PCR (Roche Applied Science, Vienna, Austria) was used for reverse transcription of 500 ng RNA (each sample) according to the manufacturer's instructions.

The second-round PCR was performed using GoTaq DNA polymerase (Promega), as described in the product information but with the following final reagent concentrations: deoxynucleoside triphosphates, 200 nM (each); primers, 0.27 picoM (each); and polymerase, 0.4U/µl. Touchdown PCR protocol was used (Don et al., 1991). This is achieved by using a temperature gradient in the first few cycles (in our instance, nine cycles) using Biometra T3000 Thermocycler. This is then followed by a conventional PCR amplification for the remaining number of cycles. After incubation at 94 ◦C for 5 min, a temperature gradient was carried out for the nine cycles (94 ◦C for 30s, 65 ◦C for 35 s, 72 ◦C for 50 s), whereby the annealing temperature was decreased 1 ◦C every cycle. This was then followed by a further

30 cycles of 94 ◦C for 30 s, 56 ◦C for 35 s, and 72 ◦C for 30 s. The PCR was terminated with an extension phase at 72 ◦C for 7 min.

**Table 1: List of primers used for RT-PCR**

| Gene name | Primers | Amplicon size |
|---|---|---|
| **Ephrin-A1** | F: 5-atcccaagttccgagaggagg<br>R: 5-ctccttgcccaaggtgaaaggc | 251 |
| **Ephrin-A2** | F:5-ctataccgtggaggtgagca<br>R:5-caggtgctccaaccctccac | 300 |
| **Ephrin-A3** | F: 5-tcgccttcttcctcatgacg<br>R: 5-ctgagcactgcctttatagcc | 274 |
| **Ephrin-A4** | F:5-gagctgggcttcaacgatta<br>R:5-tgacttggaaggtgtgcttg | 550 |
| **Ephrin-A5** | F: 5-aacggaccgctgaagttctcgg<br>R: 5-tttgtgccgcgttctctccgcg | 273 |
| **Ephrin-B1** | F: 5-agctgcttgcagcactgtgc<br>R: 5-ctcatgcttgccatcagagtc | 350 |
| **Ephrin-B2** | F: 5-accgctaaggactgcagacag<br>R: 5-gtccaagtggggatctcctag | 319 |
| **Ephrin B3** | F:5- gacacaggttttcggggtacagct<br>R:5- gagcctgtctactggaactcggc | 455 |
| **EphA1** | F: 5-ttgccaactttgaccctagg<br>R: 5-cttaaatccttgaatactgcag | 247 |
| **EphA2** | F: 5-cccgagtgtccattcggctac<br>R: 5-tcacttggtctttgagtcccag | 244 |
| **EphA3** | F: 5-ggagttacgggattgtactctg<br>R: 5-tggcaatggtgtcacaggagc | 389 |
| **Eph A4** | F:5-agcgcttcatcagagagagcc<br>R:5-ggtccgggctagggttatact | 889 |
| **EphB1** | F: 5-aagccccctacctcaaagttg<br>R: 5-caccatccactctccatctcc | 352 |
| **EphB3** | F: 5-gtagggtcaggtggggataag<br>R: 5-gacagcaccaagggtaggcag | 217 |

| | | |
|---|---|---|
| **EphB4** | F: 5-cacccagcagcttgatcctg<br>R: 5-accaggaccacacccacaac | 299 |
| **GADPH** | F:5-ctacatggtctacatgttccagta<br>R:5- tgatggcatggactgtggtcat | 450 |

## 2.14 Immuno precipitation

Ephrin-B3 proteins were immunoprecipitated from inhibitory chromatographic fraction and the cell lysate with anti-ephrin-B3 antibody (R&D) and protein A/G Plus-agarose (Santa Cruz Biotechnology., Inc) beads and eluted with SDS sample buffer. The boiled samples were separated on 12% SDS-polyacrylamide gels (Invitrogen) and transferred to PVDF membrane using an Xcell II Blot Module (Invitrogen). After blocking with 5% skim milk in phosphate-buffered saline (PBS) with 0.1% Tween 20 for 1 h, the membranes were probed with anti-ephrin B3 antibody (Abcam). Bound antibodies were visualized by enhanced chemiluminescence (Amersham Biosciences) using horseradish peroxidase-conjugated antibodies.

## 2.15 Surgical procedures

### 2.15.1.1 Creation of demyelinating lesions in caudal cerebellar peduncle.

All experiments were conducted in accordance with animal welfare regulations of the German animal protection law, the state of Lower Saxony (Niedersächsisches Landesamt für Verbraucherschutz und Lebensmittelsicherheit, Oldenburg) and MaxPlanck Institute for Experimental Medicine guidelines, Göttingen, Germany (animal license number: RKO_033/2008).

#### 2.15.1.1.2 Anaesthesia

Young Female SD rats 8-10 weeks (in 180-200 g weight range) were used. Animals were anesthetized using Ketamine (75 mg/kg) and Xylazine (10 mg/kg). Corneal desiccation was prevented by covering the eyes with Aureomycin Ophthalmic Ointment. The effect of anesthesia was assessed by pinching the legs. When animal when did not respond to pinch was then taken to the surgery.

#### 2.15.1.1.2 Surgical procedure for lesion induction

Following induction of surgical anesthesia, the rat head was shaved using the shaver and it was positioned on a small animal stereotaxic instrument. The surgical site was disinfected with a solution of 5% chlorhexidine gluconate (Hibitane, Medical Health Care, SSL International Plc, Oldham) and a midline skin incision was made over the surface of the skull with a scalpel blade. The underlying connective tissue was scraped away to expose the bregma, which was used as the reference point for stereotaxic measurements. Stereotaxic coordinates relative to the bregma were determined for the different age groups by the

injection of 0.05µl Evans Blue into dead rats. The brains were removed from the skull using small animal rongeurs and the hindbrain portion rapidly frozen by immersion in isopentane at approximately -30°C. Each individual brain was then mounted onto a cryostat chuck and sectioned using a cryostat (Bright Instrument Company Ltd), from rostral to caudal and observations made on the location of the Evans Blue relative to the caudal cerebellar peduncle. For the young female rats in the weight range 180 to 220g used the stereotaxic coordinates were generally 10.4mm caudal, ±2.6mm lateral and 7.07mm ventral to the bregma. Demyelination was induced bilaterally by stereotaxic injection of EB into the CCP with modifications to the method detailed previously (Woodruff and Franklin, 1999). Using the determined stereotaxic co-ordinates a Minicraft hand-drill (Roto Zip UK Ltd, Spennymoor, County Durham, UK) and dental burr were used to create a craniotomy over the site of injection. A 10µl Hamilton syringe (SGE [UK] Ltd, Milton Keynes, UK) with a cone-tipped needle was loaded with sterile filtered EB (0.01%)and lowered into the cerebellum, taking care that residual bone fragments did not cause any deviation of the needle. Injection of EB or saline was performed at a rate of 1µl per minute*;* the majority of lesions had a total volume of 4µl injected over four minutes. Irrespective of the volume injected, following completion of the injection the needle was left in place for further 4 minutes, after which it was carefully removed. The skin incision was closed using 1.5 metric braided silk thread (4/0 Mersilk, Ethicon Ltd, Edinburgh, UK).

#### 2.15.1.1.3 Sterotactic placement of cannaule

For continuous local delivery of proteins into the demyelinated lesion, a 30 gauge modified mouse osmotic pump connector cannula with dummy wire (tubing length of 6.1 mm below the cannula pedestal, Plastics One Inc., USA,) was placed stereotactically relative to the bregma, held in a modified clamp, immediately following injection of EB, and attached to the skull using cyanoacrylate gel adhesive (Loctite 454, Loctite, USA).

### 2.15.1.2 Post-operative care

The rat was then placed in an individual cage under a heat lamp and kept under observation until fully recovered from the anesthetic. They were given 5 ml of saline with 0.1ml batryil (10mg/ml). Post-operatively the rats were monitored for the development of adverse clinical signs. Although a few rats demonstrated a head-tilt of varying severity, these symptoms were usually mild, did not cause the rats visible distress, did not interfere with feeding or drinking and in most cases resolved within a couple of days of the surgery.

### 2.15.1.3 Infusion of Ephrin B3 and Sema 3A

Sema3A (R&D Systems; 50 µg/ml in PBS) was administered by an osmotic pump (0.5 µl/h, Alzet Osmotic Pumps, 2002, ALZA Corporation, USA), that was implanted and connected 10 days after induction of demyelination. Infusion lasts for 14 days. EphrinB3, applied as ephrinB3-Fc ligand (R&D Systems, 200 µg/ml in PBS), was pre-clustered for 2 hours at room temperature with mouse anti-human Fc antibody (Chemicon International, Inc.) in a ratio of ephrinB3-Fc : anti-human Fc 10:1. Clustered ephrinB3-Fc ligand administration took place in the same manner as administration of Sema3A. As a control served the Fc fragment (20 µg/ml). Animals were sacrificed 28 days after lesion induction, respectively after 10 days

those animals where no protein infusion was administered. For statistical significance the minimal group size was n = 5, including 5% drop-out.

## 2.16 Tissue collection

### 2.16.1 Tissue collection for Light microcopy and RNA-probe-based *in situ* hybridisation

To prepare tissue suitable for light microscopy and *in situ* hybridisation, rats were killed under anaesthesia by perfusion with 4% paraformaldehyde (PFA) in PBS via the left ventricle. Apart from using 4% PFA, the perfusion was performed as detailed under tissue processing for histological analysis of lesions. The spinal cords and brains were removed as previously outlined, taking care to avoid RNAse contamination by cleaning all instruments and work surfaces with 97% ethanol. The tissue was post-fixed in 4% PFA and was processed as outlined in 2.17.1.

### 2.16.2 Tissue collection for resins

Rats were killed under anaesthesia by perfusion with 4% gluteraldehyde in phosphate buffer via the left ventricle. The perfusion pressure was provided by a 1.5m column of perfusate. Deep anaesthesia was induced using halothane and maintained by the injection of a high dose of pentobarbitone sodium (Sagatal, Merial Animal Health Ltd, Harlow, UK). The rats were pinned on a corkboard in dorsal recumbency and the thoracic wall reflected to expose the heart. The pericardium was removed and a small incision made through the left ventricle, through which a cannula was introduced. The cannula was secured in place using a clamp, a large incision was made in the right atrium to create an outflow for the perfusate and the perfusion started. Each rat was perfused for 10 minutes, requiring approximately 400 to 500ml of perfusate. The brains were removed from the skull using small animal rongeurs. The brains were then post-fixed for at least 24-hours in 4% gluteraldehyde in phosphate buffer. Tissue blocks encompassing the caudal cerebellar peduncle were cut as detailed previously (Woodruff and Franklin, 1999). While maintaining their correct orientation and sequence, blocks were processed through osmium tetroxide, dehydrated and embedded in TAAB resin (TAAB Laboratories, Aldermaston, Berkshire, UK). One micrometer sections were cut and stained with methylene blue and Azur-II (appendix 10.3).

## 2.17 Tissue processing

### 2.17.1 Tissue processing for Light microcopy and RNA-probe-based *in situ* hybridisation

The extracted brain tissue was post-fixed for 2 hours in 4% paraformaldehyde and cryoprotected for 24-hours at 4°C in 30% sucrose in diethyl pyrocarbonate (DEPC, Sigma-Aldrich) - treated phosphate buffer. Following cryoprotection the tissue was rapidly frozen in isopentane maintained at -30°C and stored at -70°C. Using a cryostat, sections (brain sections: 15µm, 3 sections per slide) were cut at -20°C and thaw mounted onto polysine slides (VWR). Sections were air dried and then placesd in plastic slide boxes and stored at -70°C until required for *in situ* hybridisation.

### 2.17.2 Tissue processing for resins

The tissue blocks of perfused animals outlined in 2.15.2 were arranged in order and post-fixed in osmium tetroxide at 4°C for overnight. Subsequently, the tissue was dehydrated for 15min in 70% and 95% ethanol, washed three times for 10min in 100% ethanol, and then immersed into propylene oxide (BDH Merck Ltd) twice for 15min. In continuation of the protocol, tissue was placed in equal parts propylene oxide and TAAB resin (TAAB Laboratories Equipment Ltd) for 3h, then in TAAB resin only for two 6-12h incubations. The resin embedded blocks were arranged in order in plastic wells, polymerised for 24-48h at 60°C, allowed to cool and, finally, semi thin (1µm) sections were cut for light microscopy using an ultracut microtome with diatome diamond knives. The sections were collected onto distilled water on pre-cleaned plain glass slides (VWR), flattened by exposing to chloroform and dried on hot plate (60°C). The dry sections were stained with methylene blue and azur-II by putting dye above them and heating it for 30 seconds at 60°C. Then they were rinsed with distilled water and tap water and dried on the mentioned hot plate (60°C) leaving them ready for light microscope analysis. On drying they were mounted with eukit. Details of the solutions used are provided in appendix 10.2.

## 2.18 Analysis

### 2.18.1 Light microscopic assessment of remyelination

A semi-quantitative scoring system for determining the relative proportions of axons that are remyelinated by oligodendrocytes or Schwann cells or remain demyelinated has been previously used to assess both spontaneous (Franklin and Gilson, 1996; Gilson and Blakemore, 1993; McKay et al., 1998) and transplant mediated remyelination (Blakemore and Crang, 1989; Franklin and Barnett, 1991) of gliotoxic lesions in the spinal cord. Results obtained using this scoring system are similar to those obtained by counting the absolute numbers of demyelinated and remyelinated axons by electron microscopy (McKay et al., 1998), indicating that this is a reliable method for quantifying remyelination. In order to evaluate the extent of remyelination of the lesions, sections were scanned with kappa camera using a leica microscope at 40X and images were combined using Hugin software. On the basis of this method, qualitative ranking of the lesions was conducted in a blindfold manner with the best remyelinated lesion receiving the highest rank value.

### 2.18.2 *In situ* hybridisation using RNA probes

To confirm the presence of lesions slides were stained with eriochrome cyanine, which stains myelin, and differentiated in 5% iron alum. Finally the samples were dehydrated and then mounted in Eukit (BDH Laboratory Supplies) for light microscopy. Lesions were identified on digital images of eriochrome cyanine stained sections at 4x magnification using a zeiss microscope and the lesion area was determined using Image J which calculates the area following a manual outline of the lesion border.

For *in situ* hybridization only specimens which displayed the biggest lesion area were taken. Representative slides for *in situ* hybridization with *Nkx2.2*, PDGFR-α, PLP, MOG and MsrB

RNA probes were selected based on eriochrome cyanine staining (see appendix 10.3) of adjacent slides, and allowed to thaw for at least 30 minutes in a fume hood. The labelled probes (kindly donated by Dr. Chao Zhao, Department of Clinical Veterinary Medicine, University of Cambridge) were diluted 1:750 (PDGFR-α, MOG and PLP), 1:600 (*Nkx2.2* and MsrB) in hybridization buffer (appendix 10.2) and denatured for 5 minutes at 75°C. 150µl of the diluted probe was added to each slide, covered with a sterile glass cover slip and hybridized overnight at 65°C in a sealed hybridization chamber wetted with 1x SSC containing 50% Formamide. The following day stringency washes were performed in glass Coplin jars using a water bath to remove excess unbound and non-specifically bound probe: three times in wash buffer (1× SSC, 50% Formamide, 0.1% Tween-20) at 65°C for 30 minutes each, followed by two washes in MABT (appendix 10.2) at room temperature for 30 minutes. The sections were then incubated with approximately 300µl of blocking solution (appendix 10.2) for at least 1 hour at room temperature in a humidified chamber. The blocking solution was then poured off and replaced with fresh blocking solution containing the anti-digoxigenin AP-conjugated antibody (Fab fragments, Boehringer), diluted 1:1500. Slides were incubated with the primary antibody at 4°C overnight in a humidified chamber. The following day the slides were washed 5 times for 10 minutes in MABTat room temperature and then twice for 10 minutes in prestaining buffer (appendix 10.22). The substrate used for the AP-conjugated reaction was a combination of nitroblue tetrazolium salt (NBT, Boehringer) and 5-bromo-4-chloro-indoyl-phosphate (BCIP, Boehringer) that produces a blue precipitate. The slides were incubated in staining buffer (appendix 2) in the dark at 37°C for the color reaction. The slides were incubated until a strong signal could be detected in normal white matter using a dissecting microscope, but before any significant background staining was observed. Sections were then rinsed in distilled water for 10 minutes.

Lesions were identified on digital images of eriochrome cyanine-stained sections, and the lesion area was determined using a public domain program (Image J 1.43c; free download on http://rsb.info.nih.gov/ij/). The same program was used to determine the number of PDGFR-α+, Nkx2.2+, MsrB+, PLP+ and MOG+ cells within the lesions on digitised adjacent sections. Only lesions with a size > 0.4mm$^2$ were included in the analysis. OPC density was calculated as the ratio of cell numbers per lesion area. All statistical calculations were done using Graph Pad Prism (Graph Pad software).

### 2.19 Electron Microscopy

Ultrathin sections of 50 nm were cut using Leica Ultracut S ultramicrotome (Leica) with help of diatome diamond knife. Sections were air dried and stained with aqueous 4% uranylacetate followed by lead citrate. The sections were viewed in an electron microscope (Leo EM912AB; Zeiss), and images were taken using on-axis 2048 x 2048 charge-coupled device camera (Proscan; Schering).

### 2.20 Statistics

For all studies at least 3 independent experiments (n as detailed in results) were conducted and statistically assessed using Graph Pad Prism software (Graph Pad, San Diego, CA). The strategies which were employed for the different data sets were chosen according to their

requirements and are detailed in each experimental chapter. In short to test the concentration dependent inhibition of OPC differentiation on MPE and the neutralizing experiments and *in situ* hybridization one way ANOVA followed by Dunett's Multiple Comparison test was used. For all statistical significance the value of $P<0.05$ is set.

# Chapter 3

# Inhibition of oligodendrocyte precursor cell differentiation by myelin-associated proteins

## 3.1 Introduction

The regeneration of myelin sheaths is increasingly recognized as an important therapeutic strategy for easing the devastating consequences of a variety of neurological disorders associated with injury to oligodendrocytes, including multiple sclerosis, spinal cord injury and stroke. Remyelination in the CNS is mediated by a population of stem/precursor cells that traditionally have been referred to as “oligodendrocyte precursor cells” (OPCs). Numerous studies have demonstrated that white matter injury is, in principle, conducive to repair by the endogenous OPC population or by transplantation of exogenous OPCs (Blakemore, 1974; Franklin and Blakemore, 1997). For unknown reasons, however, in human disease, myelin repair—commonly referred to as “remyelination”—is often disturbed and may become arrested at the step of OPC differentiation, leaving lesions containing oligodendrocyte lineage cells demyelinated and vulnerable to progressive axonal degeneration (Chang et al., 2002; Franklin and Blakemore, 1997; Wolswijk, 1998). Remyelination can restore function and saltatory signal conduction (Jeffery and Blakemore, 1997). As myelin sheaths also play an important role in axonal support (Edgar et al., 2004; Ferguson et al., 1997; Lappe-Siefke et al., 2003) demyelinated axons are more vulnerable to injury. One explanation for the failure of remyelination is the presence of inhibitors that accumulate in lesions as a consequence of the degeneration of myelin sheaths(Kotter et al., 2006), because inhibitors in myelin (MAIs) are able to prevent the differentiation of OPCs into mature oligodendrocytes (Kotter et al., 2006; Robinson and Miller, 1999) increasing the presence of OPCs may not be sufficient for promoting repair. The molecular substrate responsible for the myelin-mediated differentiation block in OPCs is unknown. Myelin is formed by a complex aggregation of predominantly lipid and protein compounds. To design strategies for promoting myelin repair, it is crucial to understand the inhibitory substrate within lesions.

In the present study I sought to determine the nature of the inhibitory molecules by assessing OPC differentiation in the presence of myelin substrates that were submitted to various biochemical precipitation and digestion steps and found that proteins enriched in white-matter preparations are potent inhibitors of OPC differentiation. The results also demonstrate that MAIs induce a down regulation of Nkx2.2 expression, an important transcription factor for OPC differentiation. Finally, to identify the potential MAIs responsible for the OPC differentiation block I followed an approach based on the hypothesis that MAI which are inhibitory for axon regeneration are responsible for the OPC differentiation block.

## 3.2 Materials and Methods

The materials and methods used for this chapter have been summarized in chapter 2

## 3.3 Results

### 3.3.1 Myelin inhibits OPC differentiation in vitro

To establish an in vitro assay for assessing the effects of myelin on OPC differentiation I adapted an approach previously reported by Robinson and Miller and plated neonatal OPCs on myelin substrates produced by incubation of myelin preparations on poly-L-lysine covered

culture dishes (Robinson and Miller, 1999). The differentiation of oligodendrocyte lineage cells (OLCs) in vitro is characterized by distinct morphological and immunological features. Antibodies against O4 identify late OPCs by reacting with a sulphated glycolipid antigen named POA (Proligodendrocyte Antigen), while the same antibody also recognizes terminally differentiated OLCs by reacting with sulphated galactosylcerebroside (Bansal et al., 1989). The differentiation block mediated by presence of myelin is manifested as a reduction in O4-expression by OPCs (Fig.1; n=3; p = 0.004, one-way ANOVA, Dunnet test PLL vs 6.5µg, 65µg, 650mg; P<0.05).

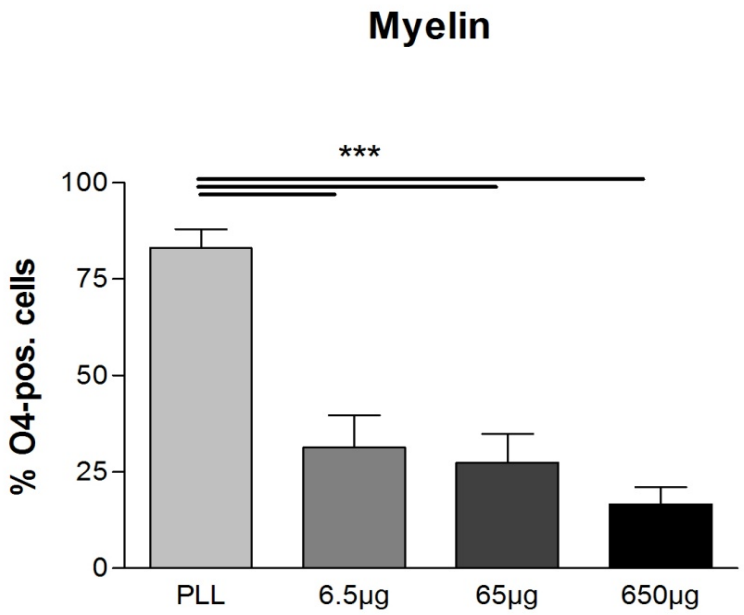


**Fig 1. Graph illustrating the concentration-dependent differentiation block induced by myelin in OPCs.**

### 3.2.2 Inhibitory activity is restricted to CNS myelin

To determine if the inhibitory activity of myelin exist in both PNS and CNS using protocol as described in chapter 2, OPCs were cultured on substrates generated from pig CNS and PNS myelin (Fig. 2). The results demonstrate that the inhibitory activity is more restricted to the CNS myelin. Although application of density gradient–based separation protocols to whole brain extracts effectively enriches for myelin membranes (Norton and Poduslo, 1973; Taylor et al., 2004; Vanrobaeys et al., 2005) the preparations thus obtained may well contain contaminants of cell membranes from other cell populakktions present in the CNS. To further specify the inhibitory molecules I took advantage of the distinct morphology of the brain that is characterized by white matter, which is mainly formed by myelin sheaths and axonal membranes, and gray matter, which is enriched with neuronal cell bodies. To evaluate whether the inhibitory molecules are more associated with CNS white matter or CNS gray matter, OPCs were plated onto extracts prepared from pig white and gray matter using the same protocol. The results show that the peak of activity seems to lie within CNS white matter and that membrane preparations derived from CNS gray matter may be less inhibitory (Fig. 2b). The results also indicate that the inhibitory substrate is conserved across species and not restricted to rodent CNS preparations.

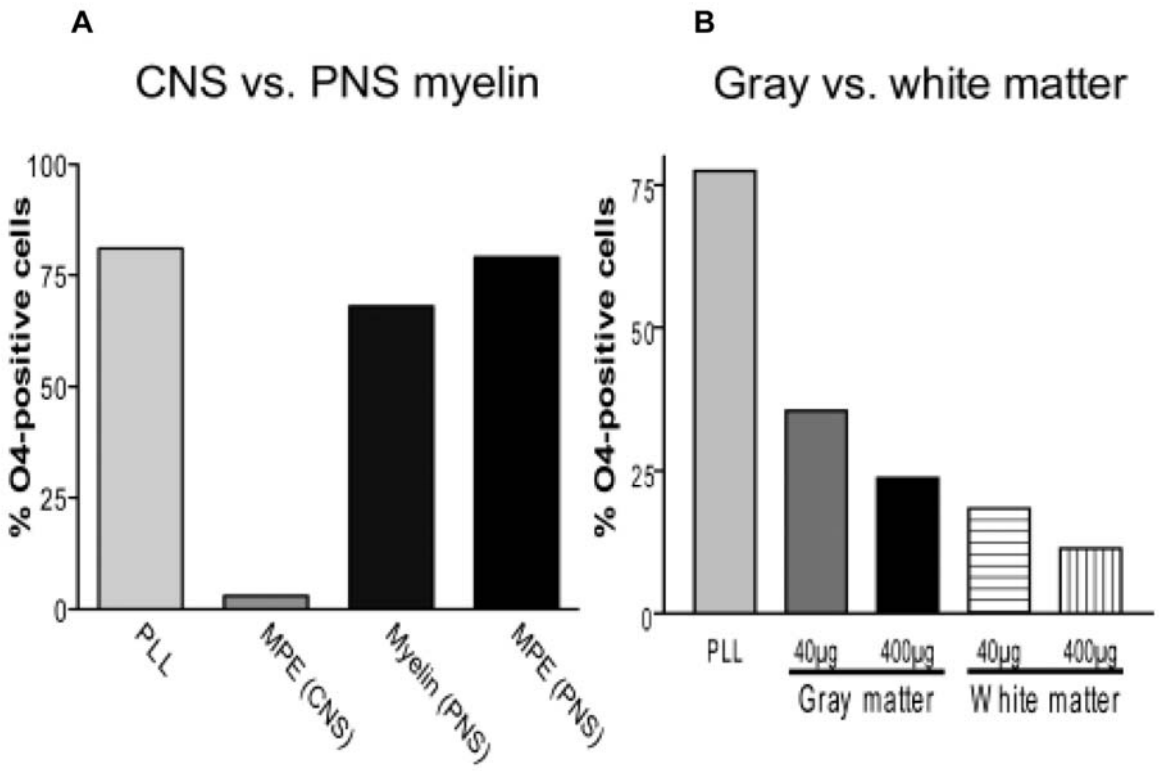


Fig.2 Graphs illustrating that MAIs are restricted to CNS myelin and are more associated with CNS white matter. A: Peripheral myelin did not affect OPC differentiation B: The OPCs plated onto membrane substrates prepared from CNS gray matter were less inhibited than cells plated onto membrane preparations from CNS white matter. All substrates were prepared at 40 µg/cm2;OPCs were incubated for 48 hours in differentiation medium.

### 3.2.3 Soluble myelin molecules inhibit OPC differentiation

Myelin membrane preparations comprise a complex mixture of lipids and proteins, some of which are myelin specific. As a first step in characterizing the substrate responsible for inhibiting OPC differentiation, I set out to investigate whether the inhibitory molecules can be solubilized from crude myelin membrane preparations by the use of detergents. I tested a number of different detergents and found that MPEs prepared with octyl-n-glucoside are able to induce an inhibition of OPC differentiation comparable to that of crude myelin membrane preparations. Oligodendrocyte precursor cells plated on MPE and cultured in differentiation medium for 48 hours displayed a concentration- dependent down regulation of O4 immunoreactivity (Fig. 3; $p=0.001$, one-way ANOVA; Dunnett's Multiple Comparison Test; PLL vs 4µg/40µg/200µg $P<0.05$).

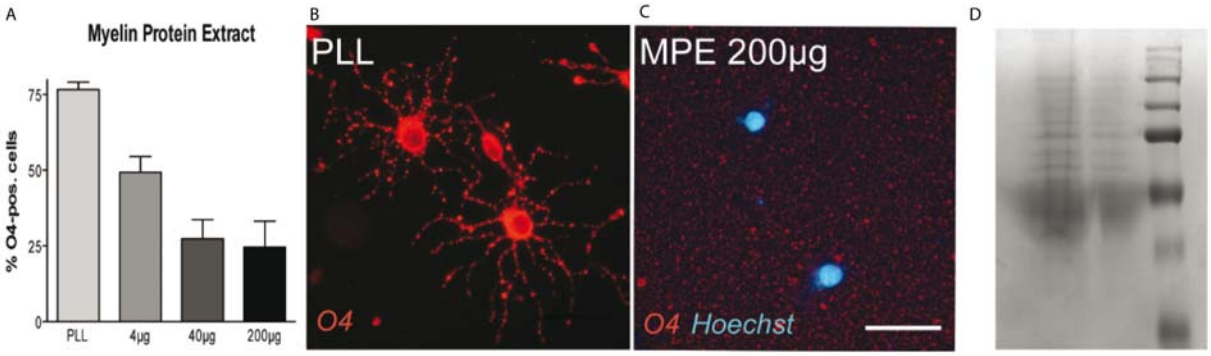


Fig 3 Graph (A), photomicrographs (B and C), and SDS-PAGE (D) illustrating the concentration-dependent differentiation block induced by MPEs in OPCs. A: Myelin protein extract induced a concentration-dependent downregulation of O4 expression after 48 hours' incubation in differentiation medium. Values are the means from 3 experiments. B: The OPCs on PLL control substrate demonstrated O4 immunoreactivity after 48 hours in differentiation medium. C: The O4 expression of OPCs plated on 200 µg myelin proteins was strongly suppressed. Cells are indicated by Hoechst nuclear stain. D: Coomassie-stained SDS-PAGE showed proteins extracted from myelin preparations with octyl-n-glucoside. Bar = 30 mm.

### 2.2.4 Myelin associated inhibitors down regulate Nkx2.2

An important regulator of OPC differentiation is the homeodomain transcription factor Nkx2.2. Previous in vivo study demonstrated that failure of remyelination mediated by the addition of myelin membranes is associated with decreased Nkx2.2 expression (Kotter et al., 2006). To test whether the in vitro system it holds true, I assessed Nkx2.2 immunoreactivity on OPCs plated on myelin membrane preparations. Similar to the situation in vivo, MAIs induced a downregulation of Nkx2.2 in vitro (Fig.4; p = 0.0036, one-way ANOVA).

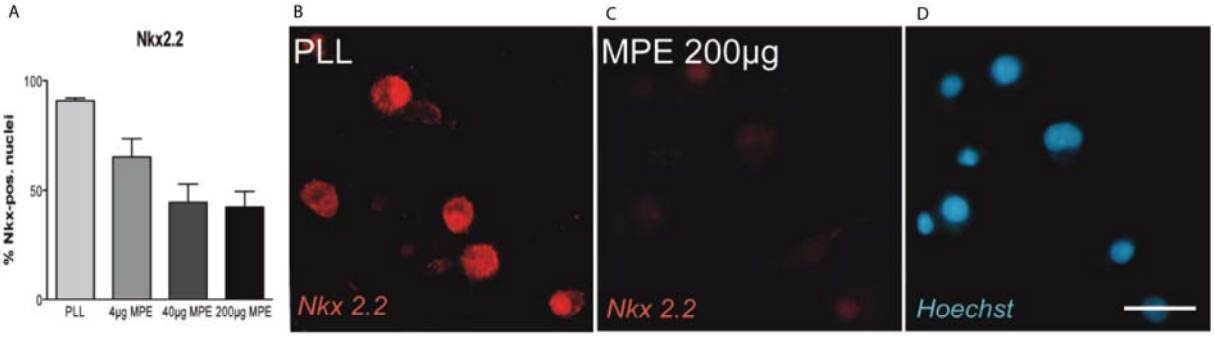


FIgure 4. Graph (A) and photomicrographs (B– D) illustrating that the presence of MAIs mediates changes in transcriptional regulation in OPCs. A: The Nkx2.2 immunoreactivity was downregulated in a concentration-dependent manner when OPCs were plated on myelin membrane preparations. Values shown are the means from 3 experiments. B: The OPCs were NKx2.2-positive after 48 hours of differentiation on PLL control substrates. C: Expression of Nkx2.2 was suppressed in OPCs grown on MPE after 48 hours. D: The same cells as in panel C stained with Hoechst. Bar = 30 µm.

### 3.2.5 Myelin associated Inhibitors are proteins in nature

In a next step to remove lipids, salts, and small-molecule contaminants, MPE was submitted to 2 different protein precipitation steps: 1) a generic highly acidic organic solvent–based protocol (MPE-p[A]), and 2) an ammonium acetate/methanol–based protocol (MPE-p[B]). Subsequently the inhibitory activity was assessed. Neither treatment affected the inhibitory nature of the MPE, suggesting that the

remaining protein was likely to be the source of the inhibition (Fig. 5). The notion that the inhibitory activity is associated with myelin protein was confirmed by an experiment in which the MPE precipitates thus prepared were subsequently treated with proteinase K, an enzyme that specifically disintegrates and destroys proteins. Treatment with proteinase K resulted in a loss of inhibitory activity; when MPE was incubated with lipase to destroy lipid components, however, the inhibitory activity remained unaltered.

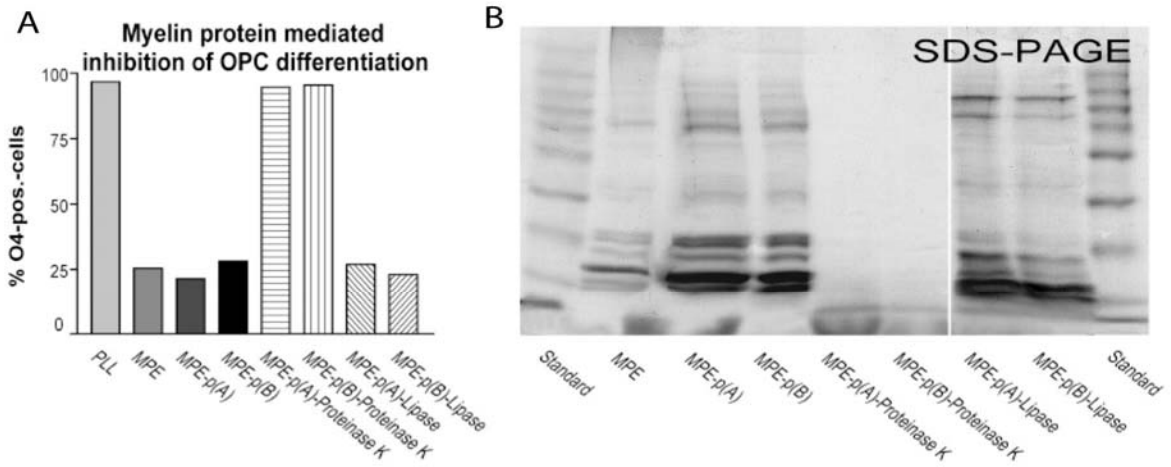


Fig 5. Graph (A) and SDS-PAGE (B) illustrating that the inhibitory effects are associated with the protein component of myelin membrane preparations. All substrates were prepared with 40 µg protein/cm2; OPCs cultured in differentiation medium for 48 hours.

### 3.2.6 Major myelin associated molecule doesn't exert OPC differentiation block

Myelin sheaths are characterized by a complex proteome (Taylor et al., 2004; Vanrobaeys et al., 2005) containing several regeneration-inhibiting factors. The best-studied myelin proteins exerting inhibitory effects on CNS regenerative processes are that inhibiting axon regeneration (Filbin, 2003). These include Nogo-A,(Chen et al., 2000), MAG (McKerracher et al., 1994) and OMgp (Kottis et al., 2002) which all bind the same axon receptor—NgR (Domeniconi et al., 2002; Fournier et al., 2001). NgR has not been detected on OPCs, and its importance is uncertain, as several myelin inhibitory molecules transduce inhibitory signals from myelin to axons independent of this receptor (Oertle et al., 2003; Schweigreiter et al., 2004), However, two other important coreceptors of inhibitory myelin proteins, LINGO-1 and p75NTR (Wang et al., 2002a; Wong et al., 2002) are expressed on OPCs (Petratos et al., 2004). Given these similarities, I sought to determine whether Nogo-A, MAG, and OMgp also control the inhibition of OPC differentiation. To test whether the inhibitory effect of myelin is mediated by Nogo-A, I plated primary rat OPCs on purified total Nogo-A and Nogo-A D20, the main inhibitory domain of Nogo-A, expressed and purified from transduced bacteria or stably transfected Chinese hamster ovary cells (Petratos et al., 2004). Similarly, OPCs were plated onto substrates prepared with purified MAG (Cai et al., 2002) and OMgp (Wang et al., 2002b), which are both potent inhibitors of axonal outgrowth. The results demonstrated that none of the proteins tested negatively affected OPC differentiation. Thus, the proteins in myelin that inhibit OPC differentiation differ from the most prominent inhibitors of axon regeneration (Fig. 6).

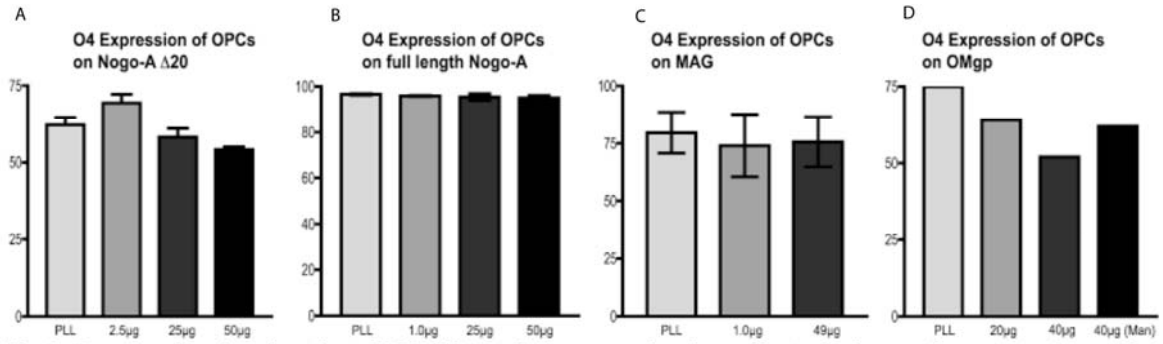


Fig 6. Bar graphs showing that OPC differentiation remained unaffected when cells were cultured for 48 hours in differentiation medium on Nogo-A D20 (A), full-length Nogo-A (B), MAG (C), and OMgp (D). Values are the means from 3 experiments. Man = manual, signifying that the protein was purified from constructs.

### 3.4 Discussion

The suppression of oligodendrocyte progenitor differentiation by myelin components may contribute to the lack of remyelination observed in experimental demyelination (Kotter et al., 2006). Since, myelin molecules blocking OPC differentiation remain unknown. The key aim of the present study was to examine the substrate that controls the myelin mediated OPC differentiation block.

The results obtained in the present study emphasize the importance of environmental factors that are able to influence CNS repair. While the importance of these factors has been recognized with respect to axon regeneration for some time, the results specifically point to the fact that increasing the number of cells capable of repairing myelin sheaths by transplanting exogenous or promoting the recruitment of endogenous stem/precursor cells may not be sufficient to enhance remyelination. Instead, to be able to therapeutically promote myelin repair it may be necessary to identify the proteins responsible for the inhibitory effects on OPC differentiation and to acquire an understanding of the molecular mechanisms that mediate the differentiation block.

Based on findings, a number of strategies could be employed to detect the proteins in myelin that mediate inhibitory effects. As the proteome of myelin membrane preparations has been investigated in several studies (Taylor et al., 2004; Vanrobaeys et al., 2005) a promising approach consists of the use of biochemical separation techniques combined with subsequent mass spectrometry–based identification of protein species.

# Chapter 4.
# Biochemical and proteomic approaches to characterize Myelin Associated Inhibitors (MAIs) of oligodendrocyte precursor cell differentiation

## 4.1 Introduction

One explanation for the failure of remyelination in disease is the presence of inhibitors that accumulate in lesions as a consequence of the degeneration of myelin sheaths and prevent the differentiation of OPCs (Kotter et al., 2006). The molecular substrate responsible for the myelin-mediated differentiation block in OPCs is unknown. Myelin is a physiologically active, highly polarized membrane that allows for dramatic savings in space, time and energy. Biochemically, myelin is defined as the lightweight membranous material accumulating at the interface between 0.32 and 0.85 M sucrose after sequential ultracentrifugation combined with osmotic shocks (Larocca and Norton, 2007; Norton and Poduslo, 1973). The molecular composition of myelin differs from other plasma membranes in that it contains 70–75% of its dry weight as lipid, unusually high compared to other eukaryotic plasma membranes. Also, its molar ratio of lipids with approximately 2:2:1:1 for cholesterol /phospholipid /galactolipid /plasmalogen (Morell and Jurevics, 1996; Norton and Poduslo, 1973) distinguishes myelin from other cellular membranes.

The most commonly used protocol for myelin isolation starts from brain homogenate contained in 0.32 M sucrose as the top layer, “spinning-down” myelin to accumulate at the interface with the bottom 0.85 M sucrose layer. One valuable modification is “floating-up” of myelin starting from brain homogenate contained in a more concentrated sucrose solution as the bottom layer (0.85, 1.2, 1.44, or 2 M). During ultracentrifugation, myelin also accumulates at the interface between the upper 0.85 and 0.32 M sucrose layers, while other fractions of interest assemble at higher sucrose concentrations. This method allows the simultaneous isolation of other brain fractions such as rough microsomes (Colman et al., 1982) or axogliosomes(Huang et al., 2005; Roth et al., 2003). The protein fraction of myelin is dominated by a few major proteins including myelin basic protein (MBP), proteolipid protein (PLP), and its alternatively spliced isoforms (DM-20), which account for most of the protein content (~30%and ~50%, respectively). Recently, with the availability of large scale preptide and lipid identification based on mass spectrometry, our understanding has advanced as complexity has become apparent. Myelin consists mainly of membrane proteins and basic proteins, two classes of proteins rarely represented on a 2D gel. The dynamic range of the technique is limited, which makes the analysis of low abundant proteins difficult. Some of these important shortcomings can be overcome by fractionating the myelin protein using chromatography coupled to MS detection.

In the previous chapter it was established that proteins in myelin induce inhibitory effects on OPC differentiation. To identify the proteins in myelin that are responsible for the inhibition I adopted two different approaches. First, a candidate approach in which known myelin associated inhibitors of regeneration where tested for their effects on OPC differentiation, and second, an iterative process based on chromatographic separation of inhibitory protein fractions was used. In order to reduce the number of potential candidates the inhibitory protein fractions were pooled and were sub-fractioned using chromatographic principle. The inhibitory proteins were separated using the Blue native-PAGE which is specifically tailored to resolve the membrane proteins. The inhibitory protein fraction was then identified using the Nano-HPLC-ESI-Q-TOF mass spectrometry.

## 4.2 Materials and Methods

The materials and methods used in this section are described in chapter 2.

## 4.3 Results

### 4.3.1 Candidate protein approach

To identify the inhibitory proteins that mediate the OPC differentiation block I adopted a candidate protein approach. A number of proteins that have been demonstrated to exert inhibitory effects on axon regeneration or having role in axon-glia interaction were taken into consideration (see table 2)

**Table 2. The cellular component and biological function of the candidate protein taken to test its role in OPC differentiation**

| Protein | Cellular distribution | Biological function |
|---|---|---|
| ***Growth associated protein-43*** | Cell junction<br>Cell membrane<br>Cell projection<br>Membrane<br>Synapse | This protein is associated with nerve growth. Implicated in axonal growth, synaptic remodeling, and secretion of both catecholamines and neuropeptide (Benowitz and Routtenberg, 1997; Oestreicher et al., 1997; Skene, 1989). |
| ***Bervican*** | Extracellular matrix<br>Membrane<br>Secreted | It is one of the most abundant proteoglycans in normal brain(Yamaguchi, 2000). Brevican contribute to the non-permissive environment of CNS regeneration and promotes CNS regeneration in Brevican deficient mice following rhizotomy (Quaglia et al., 2008) |
| ***Netrin-1*** | Extracellular matrix<br>Secreted | One of the major neuronal guidance cues (Serafini et al., 1994). It can provide both attractive and repulsive cues to neurons, depending on the receptors present and cellular context. In the adult, Netrin1 is likely involved in axon regeneration in peripheral nerves(Kappler et al., 2000; Madison et al., 2000). |
| ***Myelin Oligodendrocyte Glycoprotein*** | Membrane | Described as a target antigen for the autoimmune demyelination response(Lebar et al., 1986). Its presence on the outermost lamellae of mature |

| | | |
|---|---|---|
| | | CNS myelin and its late appearance during myelinogenesis suggest that it contributes to myelin maturation or maintenance (Amor et al., 1994; Genain et al., 1999). |
| ***Ephrin B3*** | Membrane | Ephrin-B3 acts as a midline repellent in postnatal mice(Yokoyama et al., 2001) induced reverse signaling is required for anterior commissure formation (Cowan et al., 2004; Henkemeyer et al., 1996). Has shown to inhbit neurite outgrowth (Benson et al., 2005) |
| ***Semaphorin 3A*** | Secreted | Act as axonal guidance cues in the developing nervous system (Chisholm and Tessier-Lavigne, 1999). It acts as a repellent for growth cones of DRG neurons (Luo et al., 1993) |

OPCs were placed on substrates made from the following proteins. Growth associated protein-43 (GAP-43) is a nervous tissue-specific cytoplasmic protein that can be attached to the cell membrane and is a major protein kinase C (PKC) substrate and is considered to play a negative regulatory role in neurite formation, regeneration, and plasticity (Apel et al., 1991; Spencer et al., 1992). Brevican is an axon growth-inhibitory CSPG (Yamada et al., 1997) isolated from CNS myelin (Niederost et al., 1999). A surface-bound GPI-linked isoform of Brevican is expressed in oligodendrocytes (Seidenbecher et al., 1998; Seidenbecher et al., 1995). Netrins are not only involved in axon guidance, exerting negative cues on growing axons?, but also play a central role in the migration of neurons, glial oligodendrocyte precursors and mesodermal cells during embryogenesis (Alcantara et al., 2000; Hamasaki et al., 2001; Tsai et al., 2003). Myelin Oligodendrocyte Glycoprotein (MOG) is a glycoprotein believed to be important in the process of myelination of axons in the central nervous system (CNS). It is a target antigen that leads to autoimmune-mediated demyelination. Ephrin B3 is expressed by myelinating oligodendrocytes and is the myelin associated inhibitor of neurite outgrowth (Benson et al., 2005). Finally, Sema 3A is secreted by fibroblasts and neurons and binds to a membrane-bound nonsignaling co-Rc, NP-1 (Kolodkin et al., 1997). The ECM-bound Sema 3A is thought to interact with NP-1/Plex A1 expressed on growth cones of axotomized neurons invading the developing scar, arresting regeneration (Pasterkamp et al., 2001; Pasterkamp et al., 1999; Pasterkamp and Verhaagen, 2001).Assessment of O4 immunogeneity was unable to detect differences between OPCs plated on the GAP-43, Brevican, Netrin-1, and MOG and OPCs plated on control substrates (fig7). However, when OPCs were grown in the presence of Ephrin B3, a potent inhibitory effect on OPC differentiation was found (fig 8). Similarly, OPCs plated on Sema 3A substrates failed to differentiate into an O4 positive stage (fig 8).

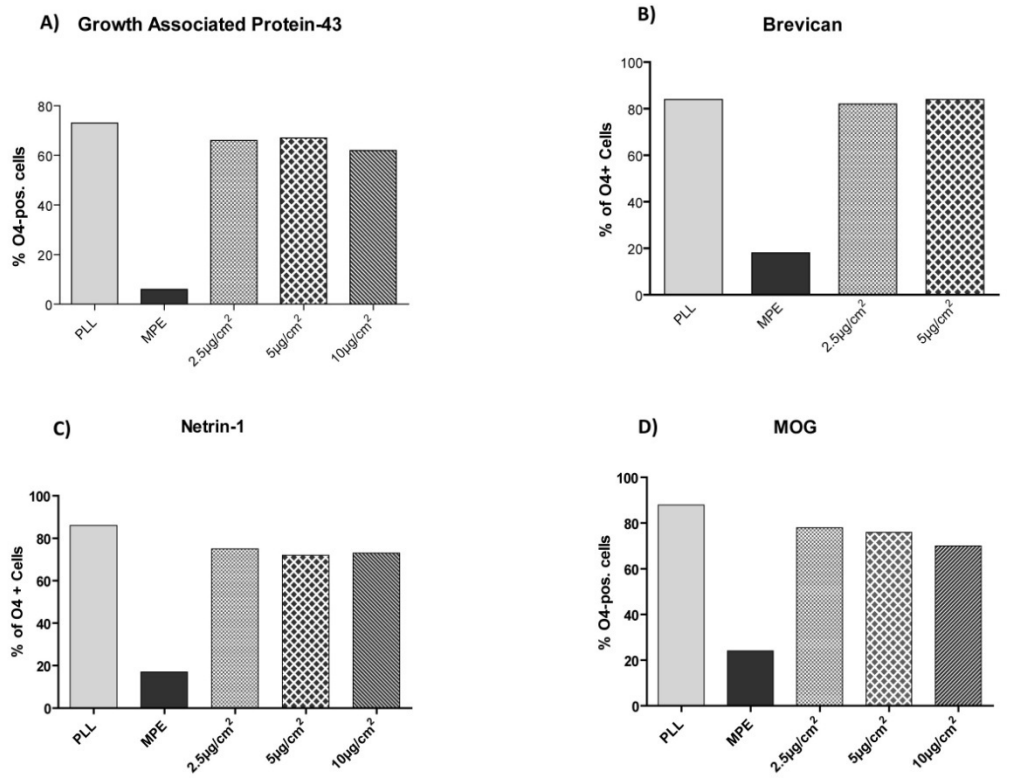


Fig 7 Bar graphs showing that OPC differentiation remained unaffected when cells were cultured for 48 hours in differentiation medium on Growth associated protein-43(a), Bervican (b), Netrin-1(c), MOG (d)

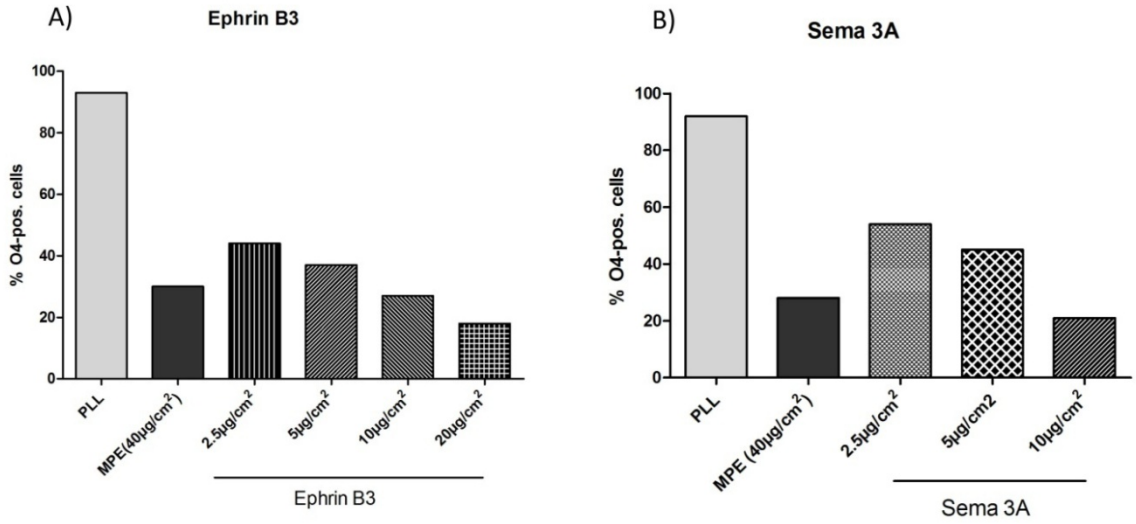


Fig 8.Bar graphs showing that OPC differentiation is arrested when cells were cultured for 48 hours in differentiation medium on Ephrin B3 (a), Sema 3A (b)

### 4.3.2 Inhibitory myelin proteins are acidic in nature

In the biochemical based approach to identify inhibitory proteins responsible for the differentiation failure of OPCs, an iterative approach based on chromatographic separation followed by proteomic analysis was applied. For this purpose careful sample preparations are the prerequisites for a successful analysis (Boguski and McIntosh, 2003). Myelin was prepared from brains of female Sprague dawley rats (180-300g) according to the protocol established by Norton and Poduslo (Norton and Poduslo, 1973). Subsequently, the proteins

were extracted by incubating myelin membrane in buffer contain 1% n-octyl glucoside at 25$^{o}$C for two hours in a shaker (Aveldano et al., 1991).

In a first step myelin enriched protein fractions obtained by biochemical separation were tested for heat stability. For this purpose MPE was heated to temperatures ranging from 40$^{O}$C to 80$^{O}$C. This leads to precipitation of the proteins. The supernatant was subsequently tested following separation from the precipitated protein by centrifugation in the tissue culture assay. A heat-dependent loss of function was observed by subsequent testing of the fractions on the OPC in vitro assay. (Fig 9A)

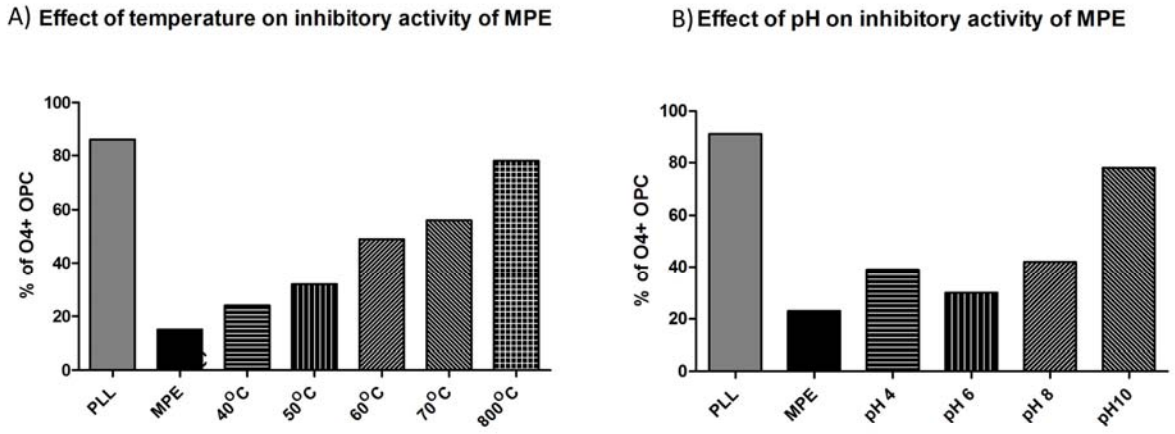


**Fig 9. Effect of temperature and pH on inhibitory activity of MPE.** A) Bar graph illustrating that MPE retains its inhibitory activity till 50 C. B) Bar graph showing that optimal pH for the inhibitory activity of the MPE is in the range of pH 4-8

To assess the pH range in which the MAI exert their inhibitory effects the pH of buffer containing MPE was changed from pH 4 until 10. The increases in pH lead to the precipitation of some proteins, which were removed by centrifugation. Subsequently, the supernatants were again tested by plating OPCs on the substrates prepared as outlined in chapter 2. Myelin associated inhibitors were active in pH ranging from pH 4-8, which indicates that the inhibitory proteins are acidic in nature. (Fig 9 B).

### 4.3.3 Inhibitory myelin proteins can be enriched by chromatographic fractionation

#### 4.3.3.1 Inhibitory protein can be enriched into distinct fraction using gel exclusion chromatography

To identify potential candidates a column-chromatography fractionation protocol was developed together with Prof. Friedrich Altmann, University of Natural Resources and Applied Life Sciences, Vienna. For a start with a one step chromatography was conducted as to see if the inhibitory protein can be fractionated into distinct fractions. The MPE was concentrated and then fractionated using Sephadex-300 gel exclusion column. The eluates obtained were tested for inhibitory activity by the in vitro differentiation assay. This demonstrated that the myelin inhibitory protein is associated with distinct fractions. Visualization of the proteins by separating the fractions on gel showed a reduction in the complexity of the fractions confirming the validity of the chosen approach.

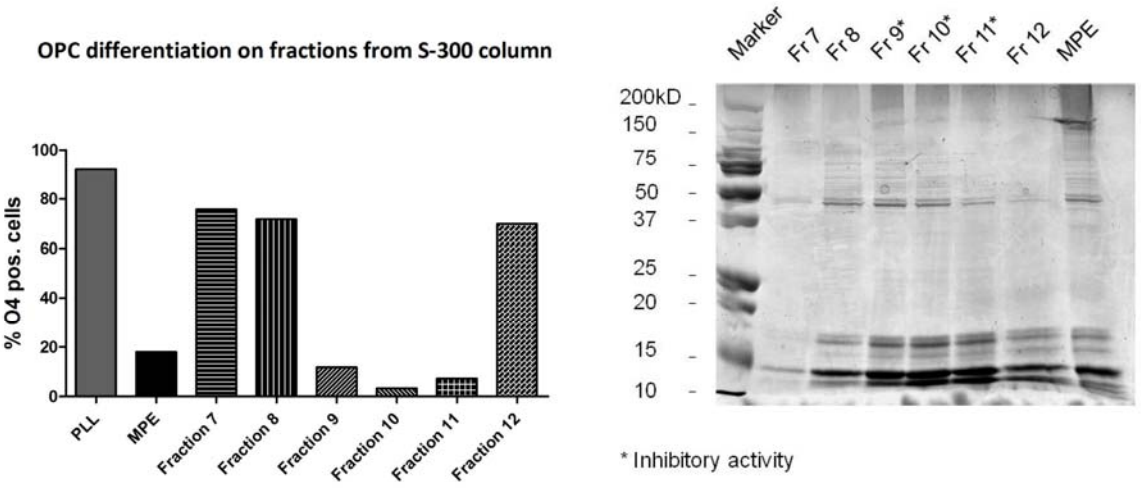


Fig 10. Bar graph illustrating that inhibitory protein can be enriched into distinct fraction following S-300 gel exclusion chromatography. SDS-PAGE demonstrating the reduction in complexity of protein bands following the gel exclusion chromatography.

#### 4.3.3.2 Inhibitory protein of myelin can be further enriched by ionic gel chromatography

After successful enrichment of inhibitory protein into distinct fraction using gel exclusion chromatography, it was planned to further enrich the protein using additional steps. To explore the possibility of enriching inhibitory protein based on ionic principles, an ionic column-chromatography fractionation was developed. Following concentration of MPE using Millipore ultra filtration cells, a buffer exchange was performed with 50mM sodium acetate pH4 containing 1% octlyl glucoside at 4$^{o}$C. After ensuring that the pH of the sample was set to pH 4, the MPE was subjected to a CM-column. The CM column is a weak cationic prepacked column. The non-binding fractions were collected at rate of 2ml/min. The binding fraction was recovered by desorption using the sodium acetate buffer containing 1% NaCl with 1% octyl glucoside. The binding and non-binding fractions were pooled separately and the resulting fractions were tested for their effects on OPC differentiation. This showed that the inhibitory activity was contained in the non-binding fraction. Inhibitory fractions from several runs were pooled and concentrated and the buffer exchanged using the 0.1M Tris–Cl buffer containing 1% octylglucoside (pH 8). After setting the pH of the buffer to pH 8 the sample was submitted to a second purification step using an anion exchange column (HighQ). The eluates obtained were tested in the same manner and the final inhibitory fraction was used for proteomic analysis.

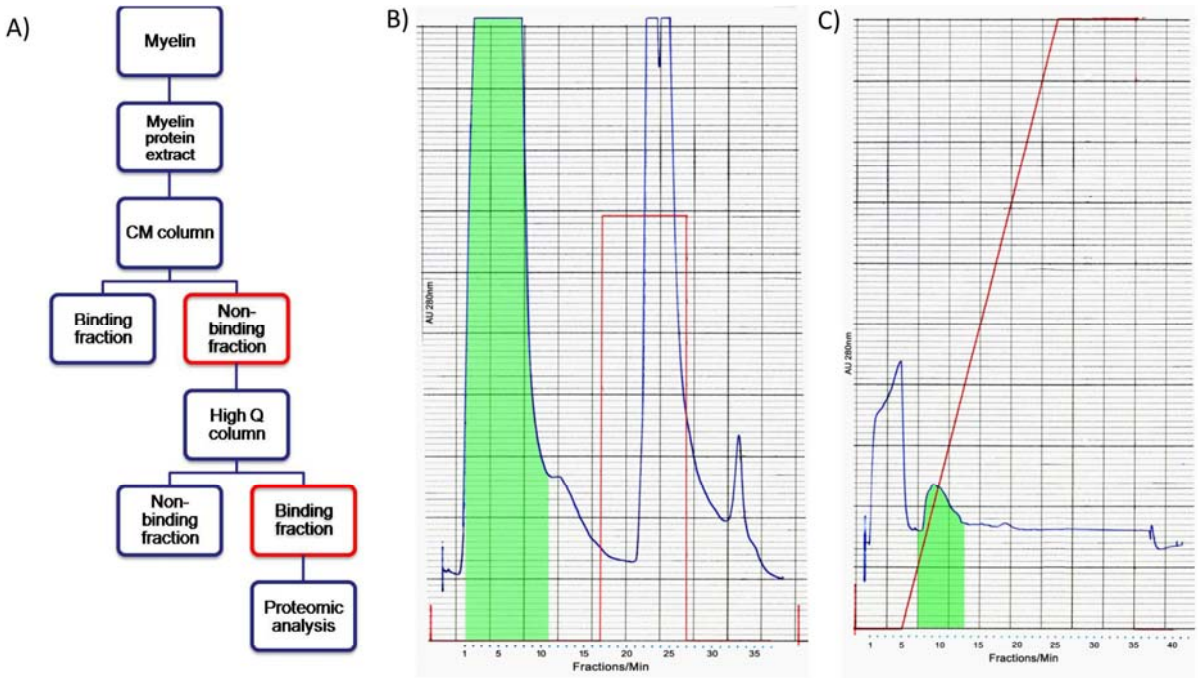


Fig 11. a) Flow chart presenting experimental design of proteomic analysis of myelin inhibitory protein of OPC differentiation
b) Chromatogram of the CM column. The green column corresponds the region where Inhibitory activity is localized
c) Chromatogram of the High Qcolumn. The green column corresponds the region where Inhibitory activity is localized

### 4.3.4 Proteomic analysis of the enriched myelin inhibitory proteins

To identify the protein species after enrichment using ionic principles, the inhibitory fraction were separated using a 3D gel-based separation protocol (BN-SDS) specifically tailored for identification of membrane-bound proteins (Kang et al., 2008). The protein spots on the 12 resulting gels were picked, digested and analyzed on a nano-HPLC-ESI-QTOF mass spectrometer. The protein identification using nano-HPLC-ESI-QTOF mass spectrometer was kindly conducted by Mr. Sung Kang, Department of Pediatrics, Medical university of Vienna, Vienna. The proteins identified are presented in Table 2 according to their annotation to the spots picked. To confirm the presence of selected protein species Western blots was done for selected proteins on fractions generated as outlined above (data not shown). The results provide a list of potential candidates that may be responsible for the inhibitory effect on OPC differentiation and illustrate the complexity of the myelin proteome, which becomes specifically apparent when highly abundant protein species are removed by column-chromatography based separation techniques.

**Table 3. Identified protein list from BN/SDS/SDS–PAGE (3DE) of purified inhibitory myelin protein fraction after two step purification.**

| Protein Name | Swiss-Prot ID | NCBI Acc. No[a] | Molecular weight (Theroy) | No. of TMD[b] | Total ion-score | No. of matched peptides (MS/MS) | Sequence coverage (%) | Spot No. |
|---|---|---|---|---|---|---|---|---|
| **Known myelin proteins** | | | | | | | | |
| Myelin-associated glycoprotein precursor | P07722 | gi\|12668509 | 69353 | 1 | 294 | 8 | 21 | 18 |
| Myelin basic protein S | P02688 | gi\|17378709 | 21546 | 0 | 36 | 1 | 5 | 131 |
| Myelin-oligodendrocyte glycoprotein precursor | Q63345 | gi\|2497314 | 27882 | 2 | 112 | 3 | 13 | 77 |
| Myelin proteolipid protein | P60203 | gi\|41019153 | 30077 | 4 | 124 | 3 | 18 | 3 |
| **Membrane proteins** | | | | | | | | |
| Abhydrolase domain-containing protein 6 | Q5XI64 | gi\|81883706 | 38312 | 1 | 155 | 4 | 13 | 89 |
| Acyl-CoA-binding domain-containing protein 5 | A0FKI7 | gi\|123797828 | 56782 | 1 | 59 | 1 | 4 | 58 |
| Basigin precursor | P26453 | gi\|51704207 | 42436 | 1 | 89 | 2 | 5 | 117 |
| Brain acid soluble protein 1 | Q05175 | gi\|730110 | 21790 | 0 | 321 | 10 | 41 | 17 |
| CD9 antigen | P40241 | gi\|729088 | 25215 | 4 | 239 | 7 | 32 | 2 |
| CD63 antigen | P28648 | gi\|113331 | 25699 | 4 | 79 | 2 | 11 | 101 |
| CD81 antigen | Q62745 | gi\|11131474 | 25889 | 4 | 211 | 5 | 16 | 4 |
| CD82 antigen | O70352 | gi\|9296930 | 29487 | 4 | 45 | 2 | 10 | 21 |
| CD151 antigen | Q9QZA6 | gi\|11131479 | 28355 | 4 | 160 | 4 | 20 | 51 |
| CD166 antigen precursor | O35112 | gi\|47605356 | 21635 | 1 | 194 | 6 | 29 | 74 |
| Cell adhesion molecule 2 precursor | Q1WIM2 | gi\|150438865 | 47528 | 1 | 194 | 4 | 11 | 53 |
| Cell adhesion molecule 4 precursor | Q1WIM1 | gi\|123778954 | 42781 | 1 | 193 | 6 | 15 | 28 |
| Cell cycle exit and neuronal differentiation protein 1 | Q5FVI4 | gi\|81882797 | 15043 | 1 | 88 | 3 | 23 | 44 |
| Choline transporter-like protein 1 | Q8VII6 | gi\|73918925 | 73092 | 10 | 61 | 3 | 4 | 27 |
| Clathrin coat assembly protein AP180 | Q05140 | gi\|2492686 | 93519 | 0 | 96 | 3 | 3 | 92 |
| Claudin-11 | Q99P82 | gi\|20532024 | 22046 | 4 | 189 | 6 | 37 | 45 |
| Disks large-associated protein 2 | P97837 | gi\|71153508 | 118978 | 0 | 164 | 6 | 8 | 34 |
| DnaJ homolog subfamily C member 5 | P60905 | gi\|46397406 | 22101 | 0 | 42 | 2 | 11 | 50 |
| Ectonucleotide pyrophosphatase/pho | P84039 | gi\|108862048 | 54290 | 1 | 164 | 5 | 12 | 71 |

| | | | | | | | | |
|---|---|---|---|---|---|---|---|---|
| sphodiesterase family member 5 precursor | | | | | | | | |
| Embigin precursor | O88775 | gi\|61223483 | 37005 | 1 | 176 | 5 | 23 | 72 |
| Erythropoietin receptor precursor | Q07303 | gi\|729431 | 55500 | 1 | 88 | 4 | 6 | 94 |
| FXYD domain-containing ion transport regulator 6 precursor | Q91XV6 | gi\|20138106 | 10388 | 1 | 229 | 7 | 26 | 63 |
| FXYD domain-containing ion transport regulator 7 | P59649 | gi\|30315809 | 8487 | 1 | 38 | 1 | 19 | 5 |
| Golgin subfamily A member 2 | Q62839 | gi\|6226622 | 111428 | 0 | 106 | 3 | 4 | 14 |
| Junctional adhesion molecule C precursor | Q68FQ2 | gi\|83286894 | 34783 | 1 | 168 | 5 | 16 | 38 |
| Leukocyte surface antigen CD47 precursor | P97829 | gi\|76364105 | 32995 | 5 | 69 | 3 | 14 | 33 |
| Limbic system-associated membrane protein precursor | Q62813 | gi\|2497324 | 37324 | 0 | 144 | 2 | 7 | 26 |
| Lysosome-associated membrane glycoprotein 1 precursor | P14562 | gi\|126378 | 43969 | 1 | 225 | 5 | 11 | 16 |
| Lysosome-associated membrane glycoprotein 2 precursor | P17046 | gi\|126382 | 45591 | 1 | 203 | 6 | 17 | 136 |
| Lysosome membrane protein 2 | P27615 | gi\|126291 | 54091 | 2 | 268 | 12 | 33 | 22 |
| Major prion protein precursor | P13852 | gi\|2507236 | 27804 | 0 | 33 | 1 | 7 | 49 |
| Membrane transport protein XK | Q5GH61 | gi\|77417634 | 51050 | 10 | 133 | 4 | 10 | 23 |
| Metabotropic glutamate receptor 4 precursor | P31423 | gi\|400255 | 101819 | 7 | 39 | 2 | 1 | 121 |
| Myosin-9 | Q62812 | gi\|13431671 | 226338 | 0 | 108 | 4 | 2 | 102 |
| Neural cell adhesion molecule 1, 140 kDa isoform precursor | P13596 | gi\|127859 | 94658 | 1 | 203 | 5 | 6 | 115 |
| Neurofilament medium polypeptide | P12839 | gi\|128150 | 95791 | 0 | 110 | 4 | 6 | 128 |
| Neuromodulin | P07936 | gi\|128102 | 23603 | 0 | 116 | 3 | 14 | 110 |
| Neuroplastin precursor | P97546 | gi\|81870588 | 31292 | 1 | 278 | 7 | 36 | 19 |
| Neurotrimin precursor | Q62718 | gi\|2497325 | 37998 | 0 | 44 | 2 | 7 | 39 |
| Nicastrin precursor | Q8CGU6 | gi\|37081094 | 78400 | 1 | 332 | 12 | 32 | 15 |
| Neuritin precursor | O08957 | gi\|81882120 | 15289 | 0 | 103 | 3 | 10 | 66 |
| Nuclear envelope pore membrane protein POM 121 | P52591 | gi\|1709213 | 120785 | 1 | 226 | 5 | 4 | 80 |
| Opioid-binding protein/cell adhesion molecule precursor | P32736 | gi\|1352640 | 38068 | 0 | 138 | 3 | 11 | 25 |
| Phosphatidylethanolamine-binding protein 1 | P31044 | gi\|400734 | 20801 | 0 | 154 | 5 | 21 | 62 |
| Phospholemman precursor | O08589 | gi\|22654268 | 10365 | 1 | 100 | 3 | 19 | 60 |
| Prostaglandin-H2 D-isomerase precursor | P22057 | gi\|1346697 | 21301 | 0 | 201 | 4 | 16 | 137 |

| | | | | | | | | |
|---|---|---|---|---|---|---|---|---|
| Protocadherin Fat 2 precursor | O88277 | gi\|22095688 | 480654 | 1 | 119 | 3 | 6 | 57 |
| Sodium channel protein type 9 subunit alpha | O08562 | gi\|55976160 | 226039 | 24 | 144 | 5 | 2 | 83 |
| Sodium channel subunit beta-2 precursor | P54900 | gi\|1705870 | 24145 | 1 | 121 | 4 | 19 | 36 |
| Sodium/potassium-transporting ATPase subunit beta-1 | P07340 | gi\|114395 | 35202 | 1 | 88 | 3 | 7 | 56 |
| Synaptosomal-associated protein 23 | O70377 | gi\|41017815 | 23235 | 0 | 79 | 2 | 9 | 65 |
| Synaptosomal-associated protein 25 | P60881 | gi\|46397720 | 23315 | 0 | 144 | 3 | 8 | 67 |
| Syntaxin-1B | P61265 | gi\|47117736 | 33245 | 1 | 188 | 6 | 17 | 64 |
| Tetraspanin-2 | Q9JJW1 | gi\|23396887 | 24190 | 4 | 63 | 2 | 8 | 29 |
| Thioredoxin domain-containing protein C5orf14 homolog | Q5BJT4 | gi\|81882519 | 37928 | 1 | 205 | 5 | 8 | 107 |
| Tyrosine-protein phosphatase non-receptor type substrate 1 precursor | P97710 | gi\|29427383 | 55691 | 1 | 105 | 4 | 10 | 122 |
| Thy-1 membrane glycoprotein precursor | P01830 | gi\|135832 | 18172 | 0 | 99 | 3 | 11 | 130 |
| Voltage-dependent anion-selective channel protein 2 | P81155 | gi\|46397780 | 31746 | 0 | 133 | 5 | 14 | 37 |
| 2',3'-cyclic-nucleotide 30-phosphodiesterase | P13233 | gi\|51338709 | 47268 | 0 | 319 | 6 | 13 | 7 |
| **Cytoplasmic proteins** | | | | | | | | |
| Amphiphysin | O08838 | gi\|14916529 | 74878 | 0 | 118 | 3 | 5 | 114 |
| Branched-chain-amino-acid aminotransferase, cytosolic | P54690 | gi\|1705438 | 46046 | 0 | 226 | 7 | 24 | 98 |
| Calmodulin | P62161 | gi\|49037408 | 16838 | 0 | 125 | 3 | 16 | 111 |
| Coiled-coil domain-containing protein 93 | Q5BJT7 | gi\|81882521 | 72636 | 0 | 152 | 4 | 6 | 104 |
| COP9 signalosome complex subunit 1 | P97834 | gi\|2494624 | 53428 | 0 | 108 | 4 | 9 | 24 |
| ERC protein 2 | Q8K3M6 | gi\|51701368 | 110618 | 0 | 98 | 2 | 3 | 42 |
| FKBP12-rapamycin complex-associated protein | P42346 | gi\|1169736 | 288794 | 0 | 68 | 2 | 1 | 87 |
| Glial fibrillary acidic protein | P47819 | gi\|115311597 | 49957 | 0 | 113 | 3 | 10 | 31 |
| Glutathione transferase omega-1 | Q9Z339 | gi\|12585231 | 27669 | 0 | 113 | 3 | 9 | 106 |
| Heat shock cognate 71 kDa protein | P63018 | gi\|51702273 | 70871 | 0 | 271 | 5 | 6 | 135 |
| Huntingtin | P51111 | gi\|1708162 | 343762 | 0 | 101 | 3 | 1 | 91 |
| Hypoxanthine-guanine phosphoribosyltransferase | P27605 | gi\|123501 | 24477 | 0 | 32 | 1 | 4 | 124 |
| Junction plakoglobin | Q6P0K8 | gi\|818850 | 81801 | 0 | 105 | 4 | 5 | 41 |

| | | | | | | | | |
|---|---|---|---|---|---|---|---|---|
| | | 83 | | | | | | |
| LAMA-like protein 2 precursor | Q4QQW8 | gi\|146324959 | 65456 | 0 | 201 | 5 | 9 | 90 |
| Myc box-dependent-interacting protein 1 | O08839 | gi\|14916534 | 64533 | 0 | 229 | 8 | 12 | 113 |
| NAD-dependent deacetylase sirtuin-2 | Q5RJQ4 | gi\|81883338 | 39319 | 0 | 91 | 2 | 5 | 109 |
| Neurocalcin-delta | Q5PQN0 | gi\|81909955 | 22245 | 0 | 126 | 4 | 20 | 61 |
| Neuron-specific calcium-binding protein hippocalcin | P84076 | gi\|51317364 | 22427 | 0 | 98 | 4 | 23 | 59 |
| glycosyltransferase GLT28D1 | Q5I0K7 | gi\|81883003 | 18329 | 0 | 62 | 2 | 7 | 69 |
| Phenylalanyl-tRNA synthetase alpha chain | Q505J8 | gi\|81887353 | 57720 | 0 | 88 | 2 | 5 | 118 |
| Phosphatidylinositol 4,5-bisphosphate 5-phosphatase A | Q9JMC1 | gi\|30315961 | 107208 | 0 | 97 | 4 | 3 | 88 |
| Protein kinase C and casein kinase substrate in neurons protein 1 | Q9Z0W5 | gi\|22256946 | 50449 | 0 | 114 | 5 | 14 | 116 |
| Protein S100-A3 | P62819 | gi\|51338664 | 11747 | 0 | 52 | 1 | 14 | 12 |
| Protein S100-A6 | P05964 | gi\|46397773 | 10035 | 0 | 89 | 2 | 28 | 11 |
| Protein S100-B | P04631 | gi\|134139 | 10744 | 0 | 93 | 13 | 18 | 68 |
| Superoxide dismutase [Cu-Zn] | P07632 | gi\|134625 | 15912 | 0 | 106 | 2 | 13 | 55 |
| Thioredoxin | P11232 | gi\|135776 | 11673 | 0 | 135 | 4 | 24 | 1 |
| Tropomyosin alpha-1 chain | P04692 | gi\|92090646 | 32681 | 0 | 88 | 2 | 6 | 76 |
| Tropomyosin alpha-3 chain | Q63610 | gi\|148840439 | 29007 | 0 | 76 | 2 | 7 | 75 |
| Ubiquitin carboxyl-terminal hydrolase 19 | Q6J1Y9 | gi\|81863791 | 150302 | 0 | 119 | 6 | 3 | 99 |
| UDP-glucose:glycoprotein glucosyltransferase 1 precursor | Q9JLA3 | gi\|68052986 | 174049 | 0 | 157 | 3 | 2 | 81 |
| Visinin-like protein 1 | P62762 | gi\|51338688 | 22142 | 0 | 213 | 6 | 31 | 78 |
| 14-3-3 protein zeta/delta | P63102 | gi\|52000883 | 27771 | 0 | 228 | 7 | 28 | 54 |

## Nuclear proteins

| | | | | | | | | |
|---|---|---|---|---|---|---|---|---|
| Calpain-5 | Q8R4C0 | gi\|28376969 | 73065 | 0 | 155 | 5 | 10 | 96 |
| Cell division cycle 5-related protein | O08837 | gi\|73619939 | 92218 | 0 | 33 | 3 | 3 | 79 |
| DNA repair protein RAD50 | Q9JIL8 | gi\|60392975 | 153784 | 0 | 223 | 5 | 3 | 125 |
| Histone H2B type 1 | Q00715 | gi\|399856 | 13990 | 0 | 123 | 2 | 21 | 8 |
| Histone H2B type 1-A | Q00729 | gi\|399855 | 14225 | 0 | 109 | 2 | 26 | 9 |
| Histone H3.1 | Q6LED0 | gi\|81863898 | 15404 | 0 | 49 | 1 | 8 | 13 |
| Histone H4 | P62804 | gi\|51317315 | 11367 | 0 | 102 | 3 | 34 | 10 |
| La-related protein 7 | Q5XI01 | gi\|134034153 | 64949 | 0 | 32 | 3 | 10 | 129 |
| RING finger protein 181 | Q6AXU4 | gi\|81891326 | 19288 | 0 | 34 | 2 | 9 | 119 |
| Small ubiquitin-related modifier 2 precursor | P61959 | gi\|48429128 | 10871 | 0 | 76 | 3 | 13 | 108 |

| | | | | | | | | |
|---|---|---|---|---|---|---|---|---|
| Structural maintenance of chromosomes protein 3 | P97690 | gi\|29336525 | 138448 | 0 | 149 | 4 | 3 | 82 |
| UV excision repair protein RAD23 homolog B | Q4KMA2 | gi\|123789085 | 43497 | 0 | 133 | 4 | 7 | 112 |
| Vimentin | P31000 | gi\|401365 | 53733 | 0 | 251 | 6 | 14 | 103 |
| Zinc finger CCCH type antiviral protein 1 | Q8K3Y6 | gi\|47117346 | 86771 | 0 | 100 | 4 | 7 | 84 |
| **Secreted proteins** | | | | | | | | |
| Alpha-1-antiproteinase precursor | P17475 | gi\|112889 | 46136 | 0 | 164 | 5 | 19 | 97 |
| Apolipoprotein D precursor | P23593 | gi\|114035 | 21635 | 0 | 162 | 5 | 19 | 97 |
| C-reactive protein precursor | P48199 | gi\|1345834 | 25468 | 0 | 65 | 3 | 17 | 20 |
| Serine protease inhibitor A3K precursor | P05545 | gi\|266407 | 46562 | 0 | 211 | 6 | 16 | 85 |
| Serine protease inhibitor A3L precursor | P05544 | gi\|2507387 x | 46277 | 0 | 206 | 5 | 16 | 86 |
| Sulfated glycoprotein 1 precursor | P10960 | gi\|134219 | 61124 | 0 | 264 | 5 | 10 | 6 |
| Transthyretin precursor | P02767 | gi\|136467 | 15720 | 0 | 76 | 2 | 10 | 134 |
| **Extracellular proteins** | | | | | | | | |
| Annexin A8 | Q4FZU6 | gi\|123792388 | 36706 | 0 | 151 | 4 | 15 | 52 |
| Hemoglobin subunit alpha-1/2 | P01946 | gi\|122477 | 15329 | 0 | 255 | 7 | 39 | 48 |
| Hemoglobin subunit beta-1 | P02091 | gi\|122514 | 16083 | 0 | 245 | 8 | 36 | 46 |
| **Lysosomal proteins** | | | | | | | | |
| Cathepsin D precursor | P24268 | gi\|115720 | 44681 | 0 | 126 | 5 | 16 | 32 |
| Deoxyribonuclease-2-beta precursor | Q9QZK9 | gi\|46395574 | 40472 | 0 | 83 | 3 | 7 | 100 |
| Dipeptidyl-peptidase 2 precursor | Q9EPB1 | gi\|13626317 | 55114 | 0 | 83 | 3 | 6 | 70 |
| N-acetylgalactosamine-6-sulfatase precursor | Q32KJ6 | gi\|123779981 | 58302 | 0 | 94 | 3 | 6 | 93 |
| Palmitoyl-protein thioesterase 1 precursor | P45479 | gi\|1172592 | 34455 | 0 | 154 | 3 | 8 | 35 |
| Prenylcysteine oxidase precursor | Q99ML5 | gi\|62286984 | 56288 | 0 | 164 | 3 | 9 | 123 |

| | | | | | | | | |
|---|---|---|---|---|---|---|---|---|
| **Mitochondrial protein** | | | | | | | | |
| Apoptosis-inducing factor 1, mitochondrial precursor | Q9JM53 | gi\|13431757 | 66723 | 0 | 35 | 1 | 2 | 120 |
| **Unknown protein** | | | | | | | | |
| Putative uncharacterized protein ENST00000281581 homolog | Q5PQJ9 | gi\|117940141 | 96777 | 0 | 185 | 4 | 3 | 126 |

a NCBI accession number (Acc. No.) is referred in website (http://www.ncbi.nlm.nih.gov/sites/entrez). b Theoretical number of transmembrane domain (TMD) was calculated in website (http://www.expasy.org)

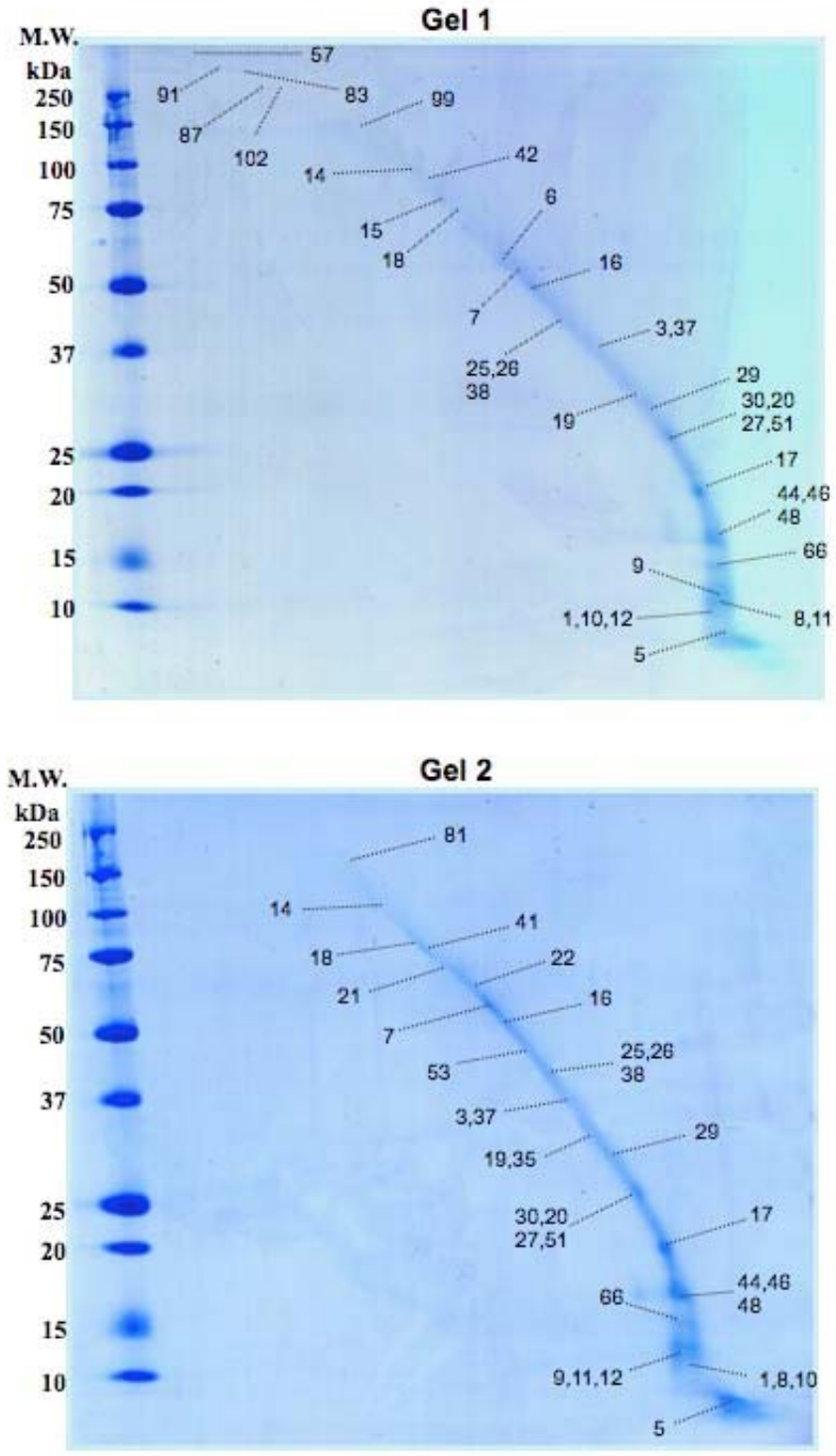
Gel 1
M.W.
kDa
250
150
100
75
50
37
25
20
15
10
57
91
83
99
87
102
14
42
6
15
18
16
7
3,37
25,26
38
29
19
30,20
27,51
17
44,46
48
66
9
1,10,12
8,11
5
Gel 2
M.W.
kDa
250
150
100
75
50
37
25
20
15
10
81
14
41
18
22
21
16
7
53
25,26
38
3,37
29
19,35
30,20
27,51
17
44,46
48
66
9,11,12
1,8,10
5

**Fig. 12a**

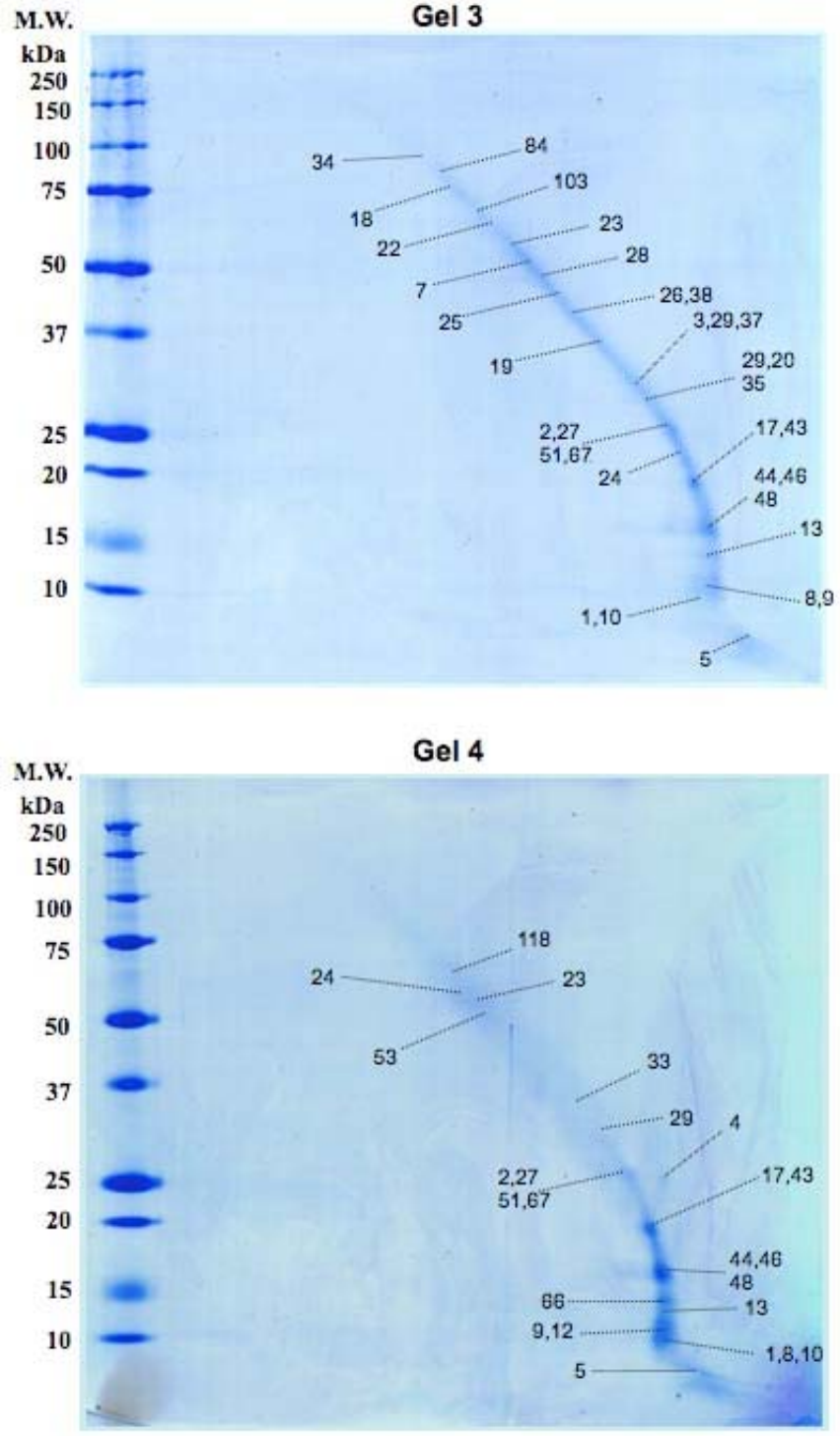
Gel 3
M.W.
kDa
250
150
100
75
50
37
25
20
15
10
34
84
18
103
22
23
7
28
25
26,38
3,29,37
19
29,20
35
2,27
51,67
17,43
24
44,46
48
13
1,10
8,9
5
Gel 4
M.W.
kDa
250
150
100
75
50
37
25
20
15
10
118
24
23
53
33
29
4
2,27
51,67
17,43
44,46
48
66
13
9,12
1,8,10
5

**Fig. 12b**

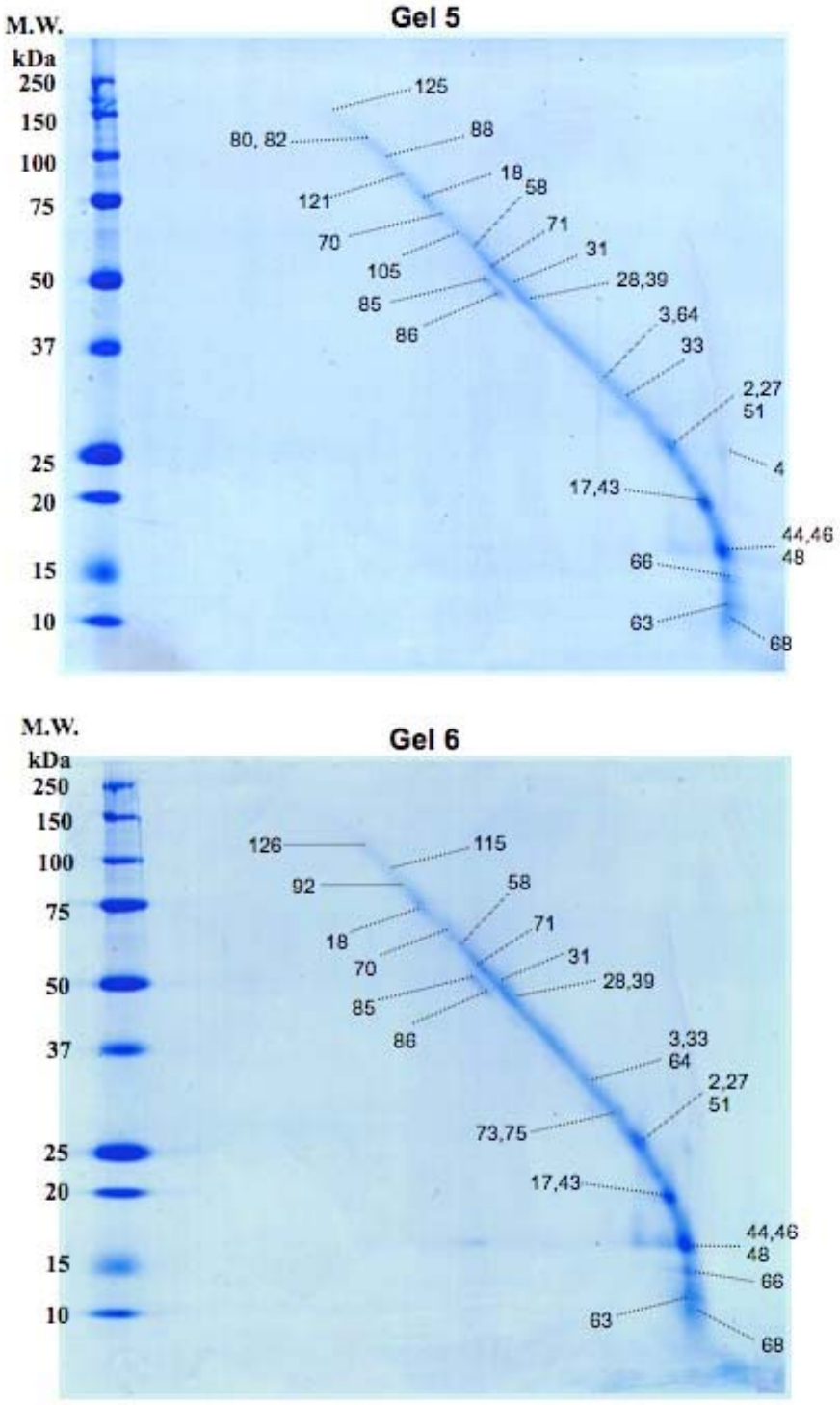
Gel 5
M.W.
kDa
250
150
100
75
50
37
25
20
15
10
125
80, 82
88
121
18
58
70
71
105
31
85
28,39
86
3,64
33
2,27
51
4
17,43
44,46
48
66
63
68
Gel 6
M.W.
kDa
250
150
100
75
50
37
25
20
15
10
126
115
92
58
18
71
70
31
85
28,39
86
3,33
64
2,27
51
73,75
17,43
44,46
48
66
63
68

**Fig. 12c**

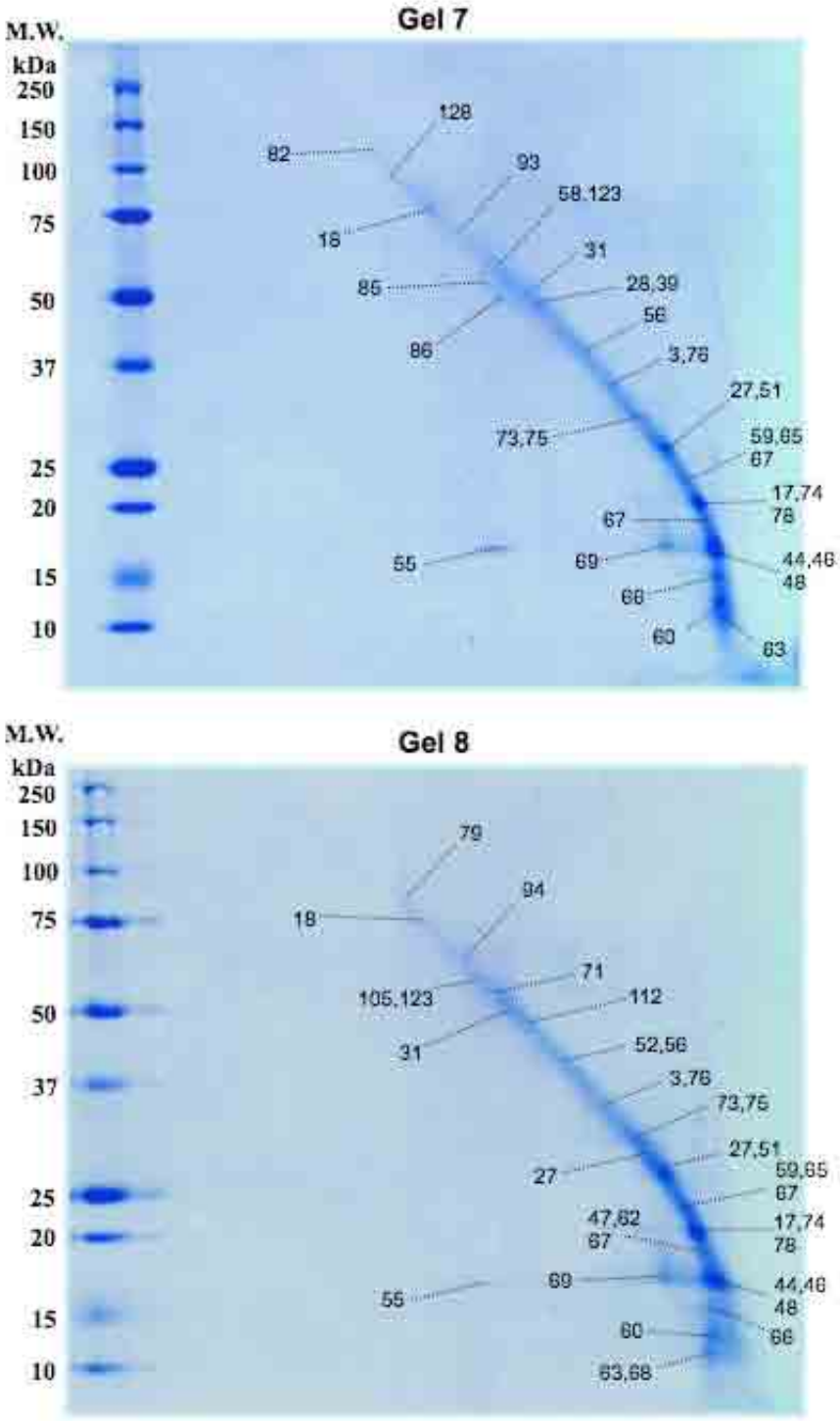
Gel 7
M.W.
kDa
250
150
100
75
50
37
25
20
15
10
128
82
93
58,123
18
31
85
28,39
56
86
3,76
27,51
73,75
59,65
67
17,74
78
67
55
69
44,46
48
66
60
63
Gel 8
M.W.
kDa
250
150
100
75
50
37
25
20
15
10
79
94
18
71
105,123
112
31
52,56
3,76
73,75
27,51
27
59,65
67
47,62
67
17,74
78
69
44,46
48
55
60
66
63,68

**Fig. 12d**

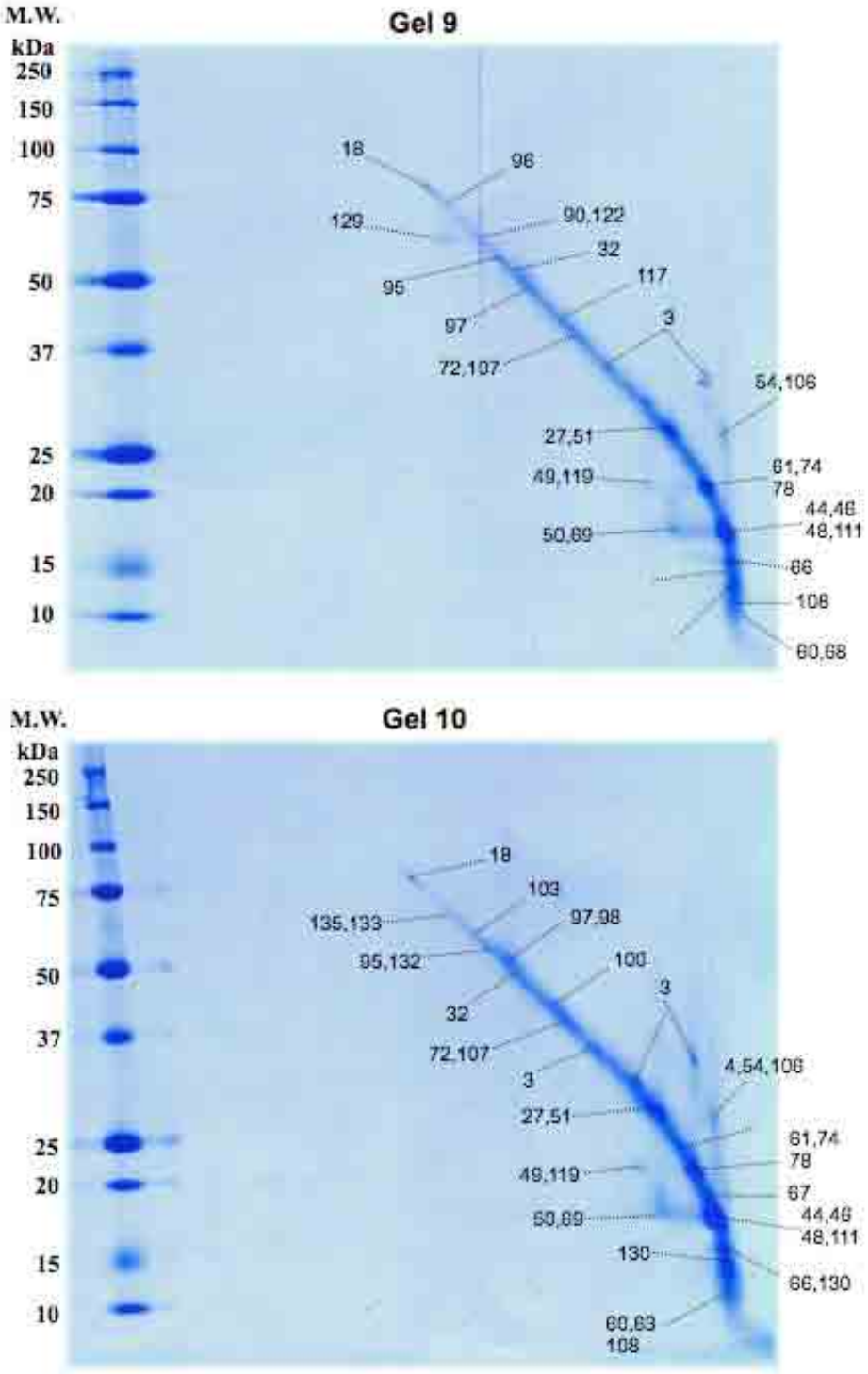
M.W.
kDa
250
150
100
75
50
37
25
20
15
10
Gel 9
18
96
129
90,122
32
95
117
97
3
72,107
54,106
27,51
61,74
49,119
78
44,46
48,111
50,69
66
108
60,68
M.W.
kDa
250
150
100
75
50
37
25
20
15
10
Gel 10
18
103
135,133
97,98
95,132
100
3
32
72,107
3
4,54,106
27,51
61,74
78
49,119
67
44,46
50,69
48,111
130
66,130
60,63
108

**Fig. 12e**

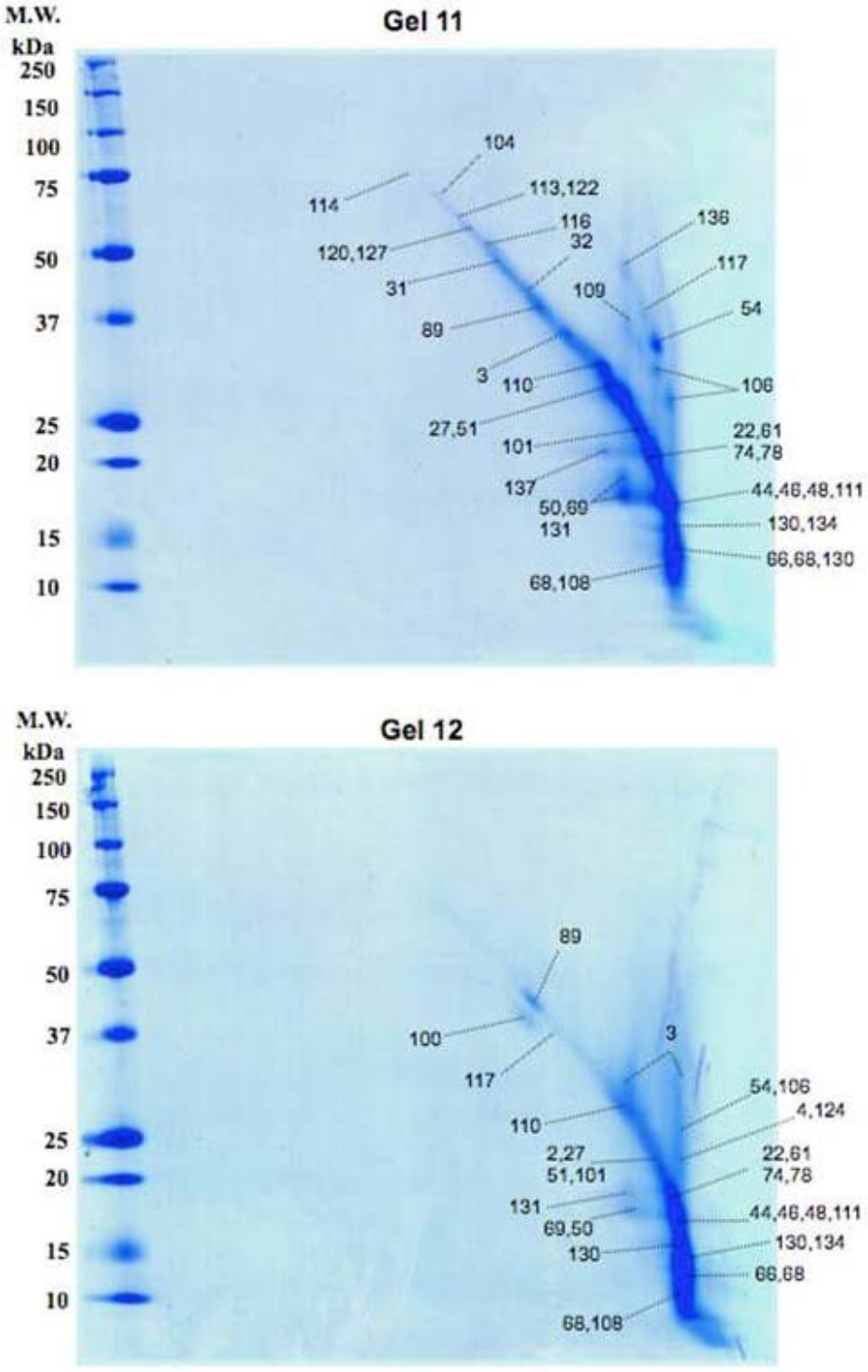


**Fig 12f, Fig 12 (a-f) Photo of the 3-D SDS gel depicting the protein spots**

### 4.3.5 Biological relevance of the identified proteins

A Venn diagram comparing the number of identified proteins in our proteomic approaches and those of the previous myelin proteomics study illustrate that our approach only identified 18 out of 137 proteins which were previously identified (Taylor and Pfeiffer, 2003; Taylor et al., 2004; Vanrobaeys et al., 2005; Werner et al., 2007).

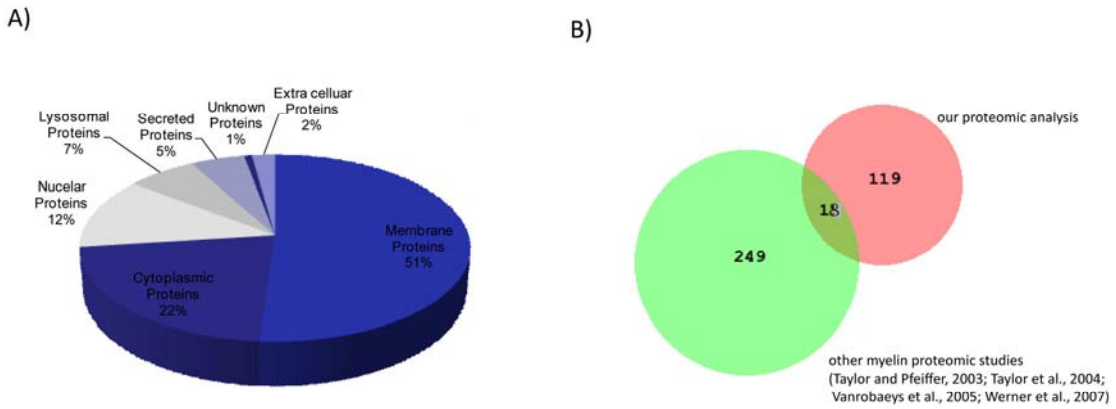


Fig 13. A) Pie chart depicting percentage of the functional categories of identified inhibitory myelin proteins of OPC differentiation B) Venn diagram showing the amount of overlap of identified protein compared to previous myelin proteomics studies.

As expected the major classes of proteins identified in this study were made of membrane bound proteins (51%). Among these Basigin, Embigin, Metabotropic glutamate receptor 4, Syntaxin-1B, Tetraspanin-2 wee found. Embigin and basigin are highly glycosylated transmembrane glycoproteins with two immunoglobulin domains and form a subgroup in the immunoglobulin superfamily. Both of them have been implicated in regulation of cell architecture and cell–cell recognition (Curtin et al., 2005; Fadool and Linser, 1993), act in signaling (Guo et al., 1997; Tang et al., 2006), and act as a chaperone for transmembrane proteins (Kirk et al., 2000). By analogy to other mammalian cell surface glycoproteins, and in particular to the CD44 transmembrane protein family (Ponta et al., 2003), Basign and Embigin may be essential for establishment of transmembrane complexes and for organization of cell structure and signal transduction cascades. Glutamatergic neurotransmission is involved in most aspects of normal brain function and can be perturbed in many neuropathologic conditions. The metabotropic glutamate receptors are a family of G protein-coupled receptors, Glutamatergic neurotransmission is involved in most aspects of normal brain function and can be perturbed in many neuropathologic conditions. The metabotropic glutamate receptors are a family of G protein-coupled receptors. Syntaxins are a family of membrane integrated Q-SNARE proteins participating in exocytosis (Bennett et al., 1993). Tetraspanins are a family of membrane proteins found in all multicellular eukaryotes. Generally, tetraspanins are often thought to act as scaffolding proteins, anchoring multiple proteins to one area of the cell membrane (Hemler, 2005). They are found in CNS and PNS and are involved in the formation of compact myelin in the PNS (Ishibashi et al., 2004).

Among the cytoplasmic proteins identified are Huntingtin and Visinin-like protein-1. The huntingtin protein is required for normal development before birth (Nasir et al., 1995). It is expressed in many tissues in the body, with the highest levels of expression seen in the brain. It is essential for development, and absence of huntingtin is lethal in mice (Nasir et al., 1995). The protein has no sequence homology with other proteins and is highly expressed in

neurons and testes in humans and rodents (Cattaneo et al., 2005). It has been experimentally demonstrated that Huntingtin acts as a transcription factor in up regulating the expression of Brain Derived Neurotrophic Factor (BDNF) (Zuccato et al., 2001). Visinin-like protein-1 (VILIP-1) belongs to a family of neuronal $Ca^{2+}$ sensor (NCS) proteins, which are conserved from yeast to human (Braunewell and Gundelfinger, 1999). The NCS proteins are reported to have a variety of biological functions. These include involvement in the modulation of voltage-gated $Ca^{2+}$ and A-type $K^{+}$ channels (An et al., 2000), transcriptional repression(Carrion et al., 1999), kinase modulation (Hendricks et al., 1999) and neurotransmitter release (Rajebhosale et al., 2003). The identification of all these myelin proteins in a single analysis offers among possibilities for comparative studies in white matter disorders.

### 4.3.6 Ephrin B3 can be detected in enriched inhibitory chromatographic fractions

The presence of ephrin B3 and Sema 3A was not detected in the protein list. To assess whether this is due to limitations of the approach I conducted an immuno precipitation on the enriched inhibitory protein fractions. The result showed that ephrin B3 was present at the end of the two step purification.

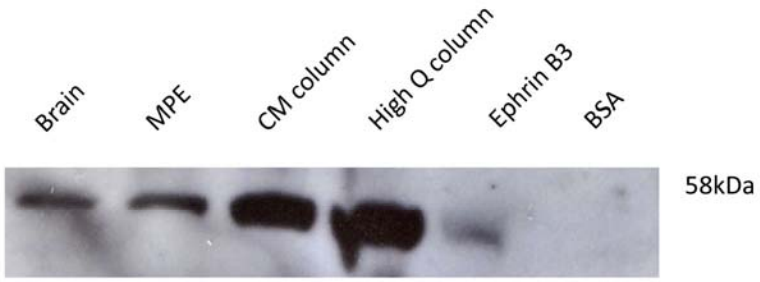


Fig 14. Immunoprecipitation for the ephrin B3 from the chromatographic fraction after two step purification revealed the presence of ephrin B3. Recombinant ephrin B3 served as positive control and BSA was used as negative control

Similarly, an immuoprecipation for Sema 3A was conducted. However, the presence of Sema was not detected. This may be related to fact that Sema 3A is a secreted protein and not a membrane bound protein.

## 4.4 Discussion

The results obtained in the candidate approach indicate that although OPC differentiation and axon outgrowth may have some regulatory mechanisms in common, important differences exist between the two. From the molecules tested only Ephrin B3 and Sema 3A were able to down-regulate O4 immunogeneity in OPCs. As down-regulation of O4 could also be caused by increased cell death or proliferation, further experiments are needed before the conclusion can be drawn that the differentiation of OPCs was inhibited by the presence of Ephrin B3 and Sema 3A. These have been conducted and summarized in chapter 5 and 7. The biological function of the present finding remains to be elucidated.

Similarly, the role of EphrinB3 and Sema3A for the process in CNS remyelination needs to be evaluated.

In this study, we developed a biochemical and proteomic protocol to reduce the complexity of the protein mixture contained in myelin, which served as a basis to identify potential candidates responsible for the myelin differentiation block. The profile of inhibitory fractions obtained following CM-High Q separation candidate proteins was assessed using 3D, Blue native PAGE followed by Q-TOF that is specifically tailored for the study of membrane-bound proteins that has not been previously used for the analysis of the myelin proteome. With the criteria we applied this resulted in a list of 137 myelin proteins—out which only 19 of which were previously identified using a proteomic approach. The detection of so many previously unidentified proteins in myelin can be explained in part by the biochemical separation process, which removes many of the most abundant proteins and is particularly suitable for detection of membrane-bound proteins. This study provides a unique snapshot illustrating the complexity of myelin proteome and show that different ways of proteome analysis is a method with the power to develop important new insights into pathogenic mechanisms in the demyelination.

Sema 3A and ephrin B3 were not included in the protein list derived from mass spectrometric analysis. While an absence of sema in the fractions was confirmed by immunoprecipitation, the lack of ephrin B3 must be caused by limitations of the proteomic approach. Identification depends very much on the sample preparation used before the proteomic procedure and ephrin B3 either could have been lost during the process of sample separation and preparation. Alternatively, it remained undetected because of restrictions inherent to the mass spectrometer.

While it is possible that ephrin B3 is the only substrate that accounts for the inhibition of OPC differentiation by myelin, at the same time other proteins that have been detected by the proteomic approach need to be evaluated. In a first step the exact localization of some of the identified proteins in our proteomic analyses should be further examined using techniques like immunogold electron microscopy and immunofluorescence microscopy. Additional experiments will be needed to establish the role of the identified proteins on OPC differentiation. As the list is still very long further work will focus on adding additional purification steps to further reduce the complexity of the final fractions.

# Chapter 5

# Ephrin B3 is a myelin associate inhibitor of OPC differentiation

## 5.1 Introduction

Remyelination of the CNS is important to protect axons against degeneration and restoration of clinical function (Duncan et al., 2009). Failure of the remyelination, as occurs in genetic leucodystrophies and cerebral palsy, or destruction of myelin, as occurs in multiple sclerosis, produces mental and physical disability. Oligodendrocyte precursor cells (OPCs) preserved in or around demyelinated lesions of MS often fail to differentiate into mature oligodendrocytes and consequently remyelinate axons (Chang et al., 2002; Wolswijk, 1998). Assuming that the preserved OPCs are naive and have no intrinsic dysfunction inhibiting their differentiation, remyelination failure may be due to an excess of inhibitory extracellular signals that blocks differentiation or a deficit in signals promoting differentiation. Hyaluronan, high-molecular-mass polysaccharide produced by astrocytes prevents the maturation process of oligodendrocytes (Back et al., 2005). PSA-NCAM abnormally expressed on demyelinated axons(Charles et al., 2002), LINGO-1 expressed on astrocytes and macrophages (Mi et al., 2005; Satoh et al., 2007), and myelin debris (Kotter et al., 2006) may also inhibit the differentiation of OPCs.

In chapter 4, a candidate approach was used to identify potential myelin associated inhibitors of OPC differentiation. One of the molecules identified, which displayed inhibitory effects on OPCs was Ephrin B3. Ephrins are membrane bound interesting guidance molecules in that they cannot function at a distance, but only through direct contact between cells and/or their processes (Davis et al., 1994). Upon cell–cell contact, ephrins and their Eph receptors activate bidirectional signals that are transduced in both cells, and each molecule can be considered to function as a ligand capable of sending non-cell-autonomous signals to adjacent cells and as receptors capable of transducing cell-autonomous signals into their own cell (Holland et al., 1996). Ephrin B3 has been identified as myelin-based inhibitor of neurite outgrowth (Benson et al., 2005). Upregulation of Eph receptors has been demonstrated in both astrocytes and neurons following spinal cord injury in the rat (Miranda et al., 1999; Willson et al., 2002). These results point towards potential roles of Eph/ephrins in neural regeneration. However, studies of Eph/ephrin expression and their roles in remyelination are lacking.

In the present chapter the expression of ephrin B3 at different stages of oligodendrocyte development was established. Subsequently, the hypothesis that ephrin B3 is a myelin associated protein mediating an OPC differentiation block was tested. Finally, possible mechanism by which ephrin B3 mediates inhibitory effects on OPC were investigated. The results demonstrate that ephrin B3 is a potent myelin associated inhibitor of OPC differentiation whose inhibitory effect can be reversed by antibody-mediated neutralization. Furthermore, a role of RhoA in mediating the effect of ephrin B3 on OPC differentiation block was established.

## 5.2 Materials and Methods

The materials and methods employed in this chapter have been summarized in chapter 2.

## 5.3 Results

### 5.3.1 Ephrin B3 is expressed in the CNS white matter and is located in compact myelin

To establish the presence of ephrin B3 in the CNS at protein level immuno-precipitation followed immunoblotting was conducted on total brain lysates and protein extract prepared from biochemical separated myelin membranes. The blots showed a clear band at ~ 58 kDa confirming the presence of ephrin B3 in the brain and in CNS myelin (fig 15 b). The presence of ephrin B3 in the brain was further confirmed on a transcriptional level by RT-PCR (fig 15 A). To assess the expression pattern of ephrin B3 immunohistochemistry was perfomed. The pattern revealed suggests that ephrin B3 is expressed mainly in the region of cotex, hippocampus and amygdala. This is in agreement with previous studies, which reported that ephrin B3 in the neonatal brain (Takemoto et al., 2002). To further specify the location of ephrin B3 in myelin, immuno gold electromicroscopy was conducted. The pattern detected indicates that ephrin B3 is an integral membrane component of myelin sheaths. However, there are some caveats as the signal detected was quite weak. This could result from the presence of limited amounts of the ephrin B3 in compact myelin or due to the poor quality polyclonal antibody that was used.

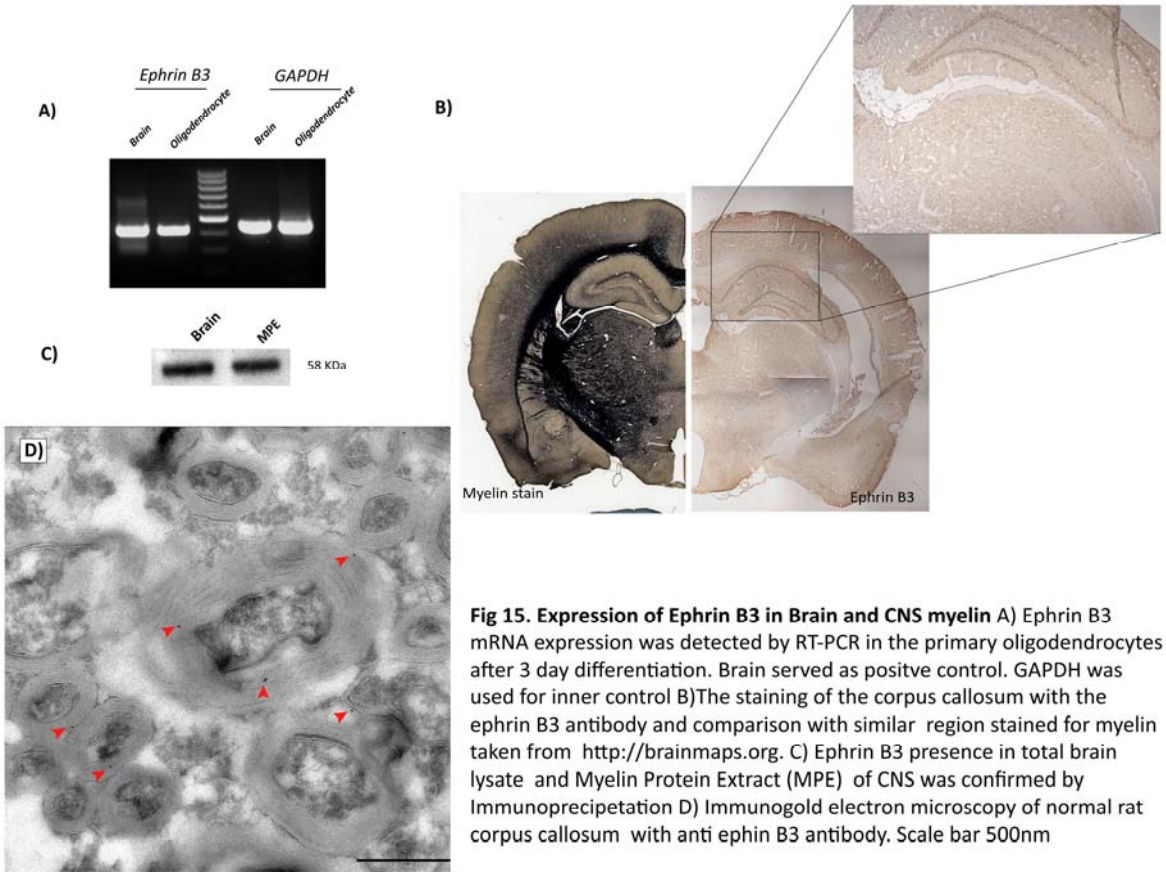


**Fig 15. Expression of Ephrin B3 in Brain and CNS myelin** A) Ephrin B3 mRNA expression was detected by RT-PCR in the primary oligodendrocytes after 3 day differentiation. Brain served as positve control. GAPDH was used for inner control B)The staining of the corpus callosum with the ephrin B3 antibody and comparison with similar region stained for myelin taken from http://brainmaps.org. C) Ephrin B3 presence in total brain lysate and Myelin Protein Extract (MPE) of CNS was confirmed by Immunoprecipetation D) Immunogold electron microscopy of normal rat corpus callosum with anti ephin B3 antibody. Scale bar 500nm

### 5.3.2 Oligodendrocytes express different classes of ephrins and eph receptors

To systematically establish the expression of the individual members of the ephrin/eph signalling family in oligodendrocytes RT-PCR for 7 Eph receptors and 8 ephrins was conducted following 3 days culture in differentiation medium. Whole brain was taken as internal control. The results demonstrate that mRNAs of ephrin-A1, -A3, -A4, -A5, -B1,-B2,-B3 are all expressed in the adult rat brain and especially in oligodendrocytes. Surprisingly, ephrin A2 was not detected using a variety of previously published primer sets. Potential explanations for this finding include a lack of primers efficiency or a lack of ephrin A2 expression in the adult brain. The main aim of our experiments was to establish the expression of ephs, which may act as the receptor for ephrin B3 in oligodendrocytes. In OPCs EphA4 and EphB3 both of which are high affinity receptors for ephrin B3 are strongly expressed, whereas EphB4 receptor is present in the brain but absent in oligodendrocytes. These expression profile need to be validated at a immunohistochemical level, however, this was beyond the scope of present study.

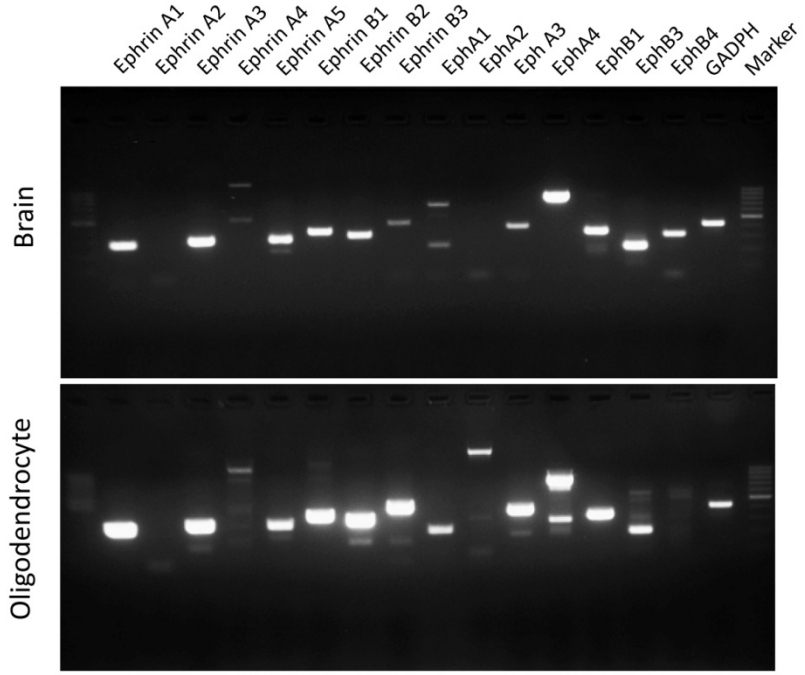


**Fig 16. Expression of ephrins and Eph receptors in OPCs cultured in differentiation medium for 3 days.**

### 5.3.3 Ephrin B3 is dynamically regulated in cultured oligodendrocytes

To evaluate the expression profile of ephrin B3 along the oligodendrocyte lineage immunolabling was conducted. The results demonstrate that although ephrin B3 can be detected at all stages, its expression increases as OPCs differentiate. To confirm this observation immunoprecipitations with anti-ephrin B3 (R&D) followed by immunoblots with anti-ephrin B3 (Abcam) was conducted on cell lysates collected at different stages of the oligodendrocyte lineage. This approach was used, as straight Western blotting was

inconsistent. The result demonstrates a dynamic increase in the amount of the protein as the OPCs differentiate. This could reflect an increased expression or stem from an increase in the cell volume/size.

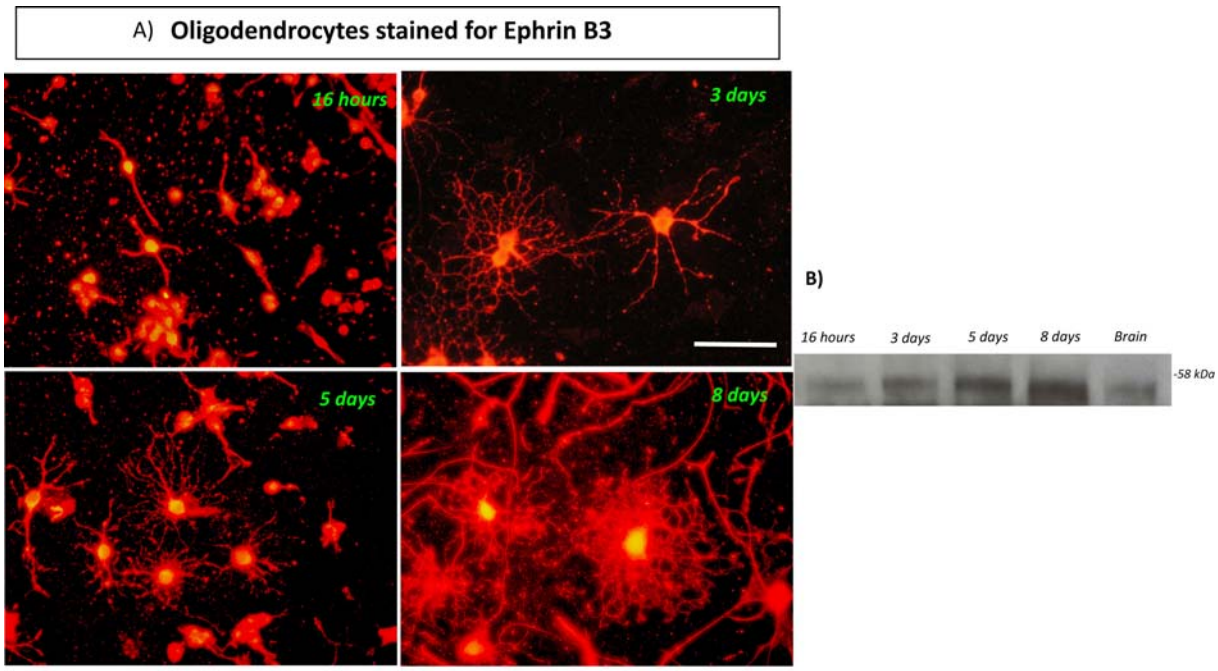


**Fig 17. Expression of of Ephrin B3 in Oligodendrocyte** A) Ephrin B3 was detected in OPCs directly following purification and increased in expression as the cells differentiated. scale bar 30µm B) The dynamic increase in the expression of Ephrin B3 was confirmed by immunoprecipitation of cell lysates generated at various stages of OPC differentiation

### 5.3.4 The Ephrin B3-mediated differentiation block in OPCs is associated with down-regulation of Nkx2.2 expression

The experiments described in chapter 3 indicated that OPCs down-regulate O4 expression in the presence of ephrin B3. This was confirmed by three repeat experiments in which OPCs plated on ephrin B3 were cultured in differentiation medium for 2 days followed by assessment of immunoreactivity for O4. The results demonstrate a significantly decreased O4 expression in presence of ephrin B3 (Fig 18 A; n=3;p ≤0.001, one-way ANOVA). Tunnel and proliferation assay demonstrated that the differentiation block is selective and not caused by cell death or an increase in proliferation (Fig 18B; n=3; p=0, 6622; one way ANOVA).

Nk2.2 is a homodomain transcription factor that plays a crucial role in the process of OPC differentiation (Qi et al., 2001). Furthermore, it was recently shown that OPCs show decreased Nkx2.2 expression in the presence of MAI (Baer et al., 2009). To investigate whether differentiation inhibition of OPCs by ephrin B3 is also associated with decreased Nkx2.2 expression OPCs were placed on ephrin B3 and cultured for 3 days in differentiation medium. The result showed a significant down-regulation of Nkx2.2 in the presence of ephrin B3 (Fig 18 C; p ≤0.0001, one-way ANOVA; Dunnett's post tests PLL versus MPE and ephrin B3 (10µg/ml): P<0.05).

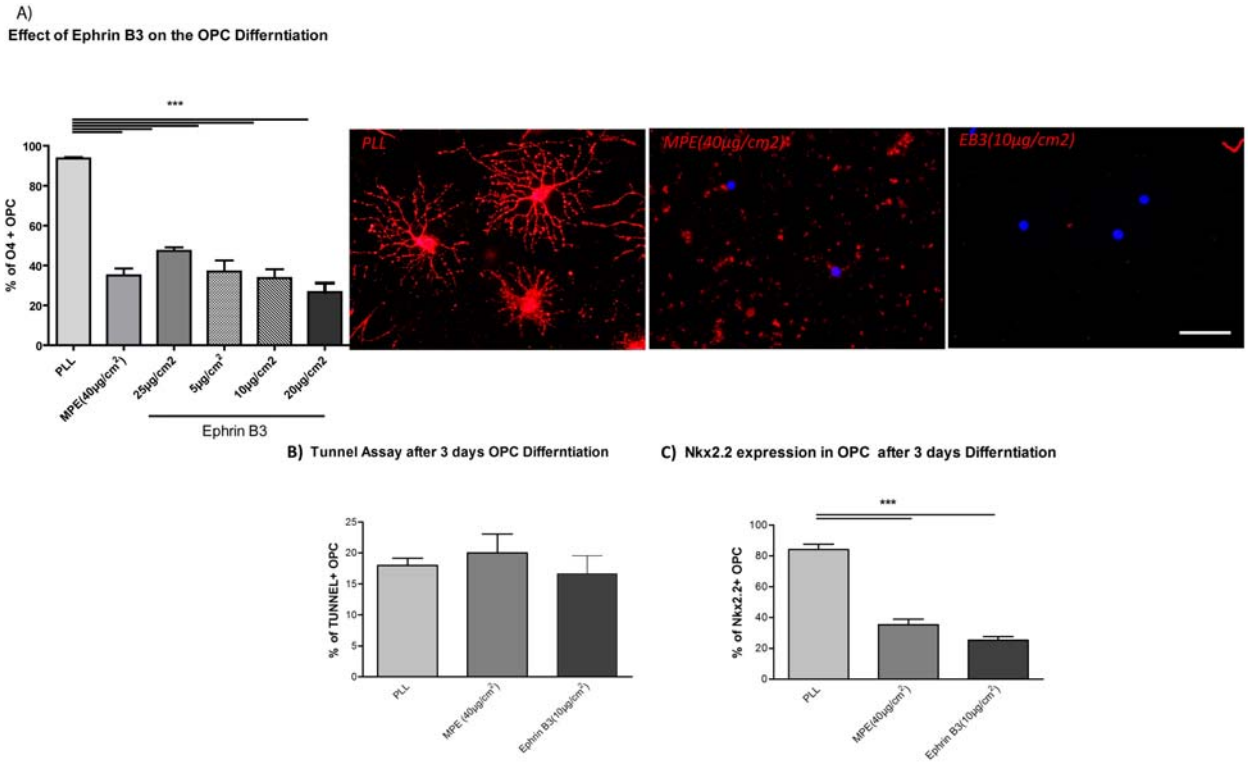


**Fig 18. Ephrin B3 inhibits OPC differentiation** a) Graph and photomicrograph illustrating the concentration-dependent differentiation block by MPE and ephrin B3 in OPCs. The OPCs on PLL control substrate demonstrated O4 immunoreactivity after 48 hours in differentiation medium. The O4 expression of OPCs plated on myelin proteins and ephrin B3 was strongly suppressed. Cells are indicated by Hoechst nuclear stain. Scale bar 30µm b) Bar graphs showing that OPC differentiation block by MPE and ephrin B3 are selective and not because of death of cells c) The bar graph showing Nkx2.2 immunoreactivity down regulation in OPCs in presence of myelin protein extract and ephrin B3.

### 5.3.5 Clustering of Ephrin B3 with Fc-IgG induces robust inhibitory response on OPC differentiation

Ephrin receptors belong to the family of receptor tyrosine kinases. A specific feature of eph receptors is their increased sensitivity to soluble ephrin proteins, which are fused to the Fc domain of human IgG, with *anti-Human IgG-Fc,* when presented in clusters (Davis et al., 1994; Lackmann et al., 1998; Stein et al., 1998). Although it must be noted that in vitro, rising ephrin surface densities also result in dose-dependently increased Eph phosphorylation (Huynh-Do et al., 1999; Lackmann et al., 1998). To investigate whether ephrin B3 presented in clusters increases the inhibitory effects on OPC differentiation, ephrin B3-fc was preclustered with Fc-IgG and ephrin B3 alone were added to the differentiation medium. As expected, the results showed an increased response of OPCs to pre-clustered Ephrin B3 as compared to ephrin B3 alones (Fig 19; $p \leq 0.0001$, one-way ANOVA; Dunnett's Multiple Comparison Test PLL vs EPHB3 (1/5/10µg/ml) and EPHB3+Fc-IgG (1/5/10µg/ml) ; $P<0.05$).

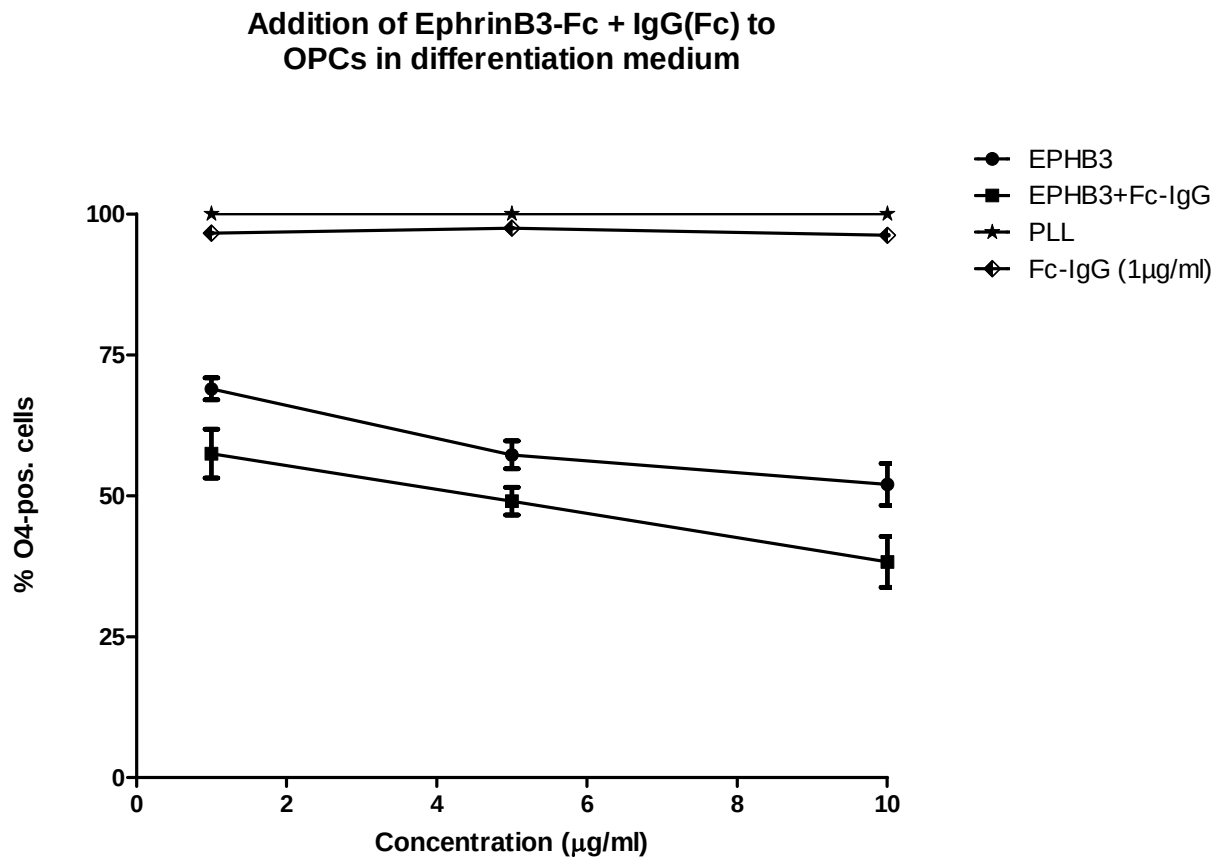


**Fig 19. Pre-clustering of the ephrin B3 with Fc-IgG increases the inhibitory effects on OPC differentiation**

### 5.3.6 The presence of ephrin B3 impairs processs formation in OPCs

The effects of MAI on OPCs are not limited to down-regulation of markers of differentiation but also include a reduction of process complexity (Baer et al., 2009). The next question I therefore asked was whether ephrin B3 had an effect on process formation in OPCs. For this purpose OPCs were cultured for 2d in differentiation medium containing ephrin B3 or preclustered-ephrin B3 and subsequently stained for A2B5. Cells were assessed on the basis of the following 4 stages. Stage I: monopolar/bipolar cels, Stage II: primary brnaches, Stage III: secondary branches, Stage IV: membranous processes. After 2d in differentiation medium the majority of oligodendrocytes in control medium displayed secondary and tertiary branches and a certain percentage even formed myelin sheet like structures. OPCs cultured in the presence of pre-clustered ephrin B3 displayed a strong reduction of process complexity as most of the cells displayed monopolar or bipolar morphology. Addition of non-clustered ephrin-B3 resulted in an intermediate phenotype (Fig 21).

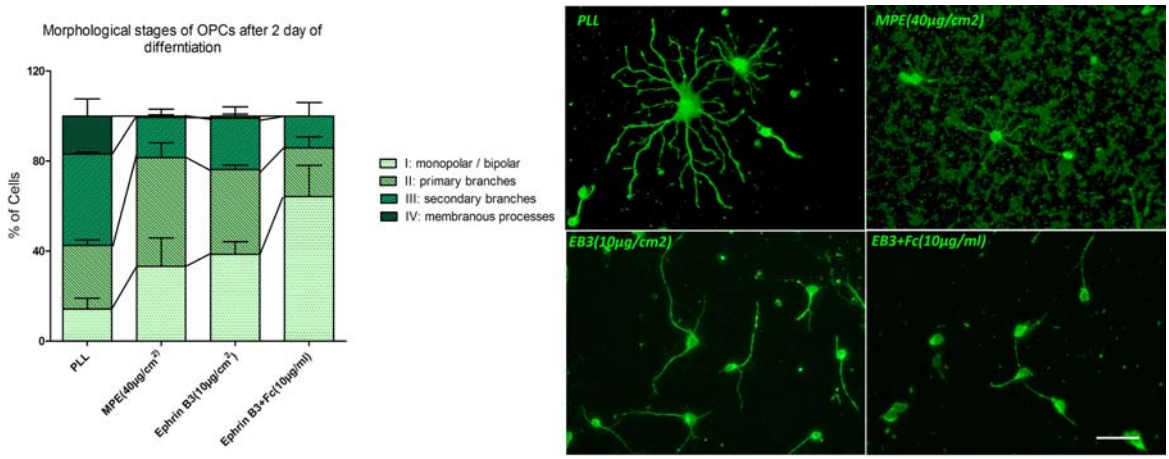


Fig 20. Oligodendrocyte exhibit distinct morphology in contact with ephrin B3. Oligodendrocyte plated on Poly-L-Lysine coated slides are differentiated and most of them have secondary and tertiary branches. Most of the OG plated on myelin protein extract had primary branches. The brances of oligodendrocytes plated on ephrin B3 shows long extended primary branches. Majority of the OG when treated with eprhin B3+Fc in differentiation medium shows the monopolar/bipolar structure scale bar 30µm

### 5.3.7 Ephrin B3 also inhbits OPC lineage progression at later stages

As has been mentioned earlier, an early event in OPC differentiation is the expression of O4. When ephrin B3 is presented to OPCs directly following purification, a decrease in O4 immunogeneity has been established. To investigate whether ephrin B3 is also able to revert OPCs to earlier stages of the lineage when presented at a point when O4 expression is well established, ephrin B3 preclustered with Fc-IgG was added to the OLCs following differentiation for 2 days. 24 hours later the cells were fixed and immunostained for MBP and O4. MBP, a structural component of myelin sheats is considered a late stage differentiation marker. The results demonstrate that while addition of ephrin B3 at later stages had little or no effects on the expression of O4, MBP immunoreactivity was significantly down-regulated. Furthermore, ephrin B3 treatment seemed to be associated with a reduction of the complexity of OPC processes; in this regard further studies are required, which were beyond the scope of the present thesis. In conclusion, ephrin B3 is able to exert inhibitory effects at different stages of OPC differentiation and may lead to non-myelinating O4-positive OPCs that resemble those that have been observed in non-myelinated MS lesions (Wolswijk, 1998, 2002).

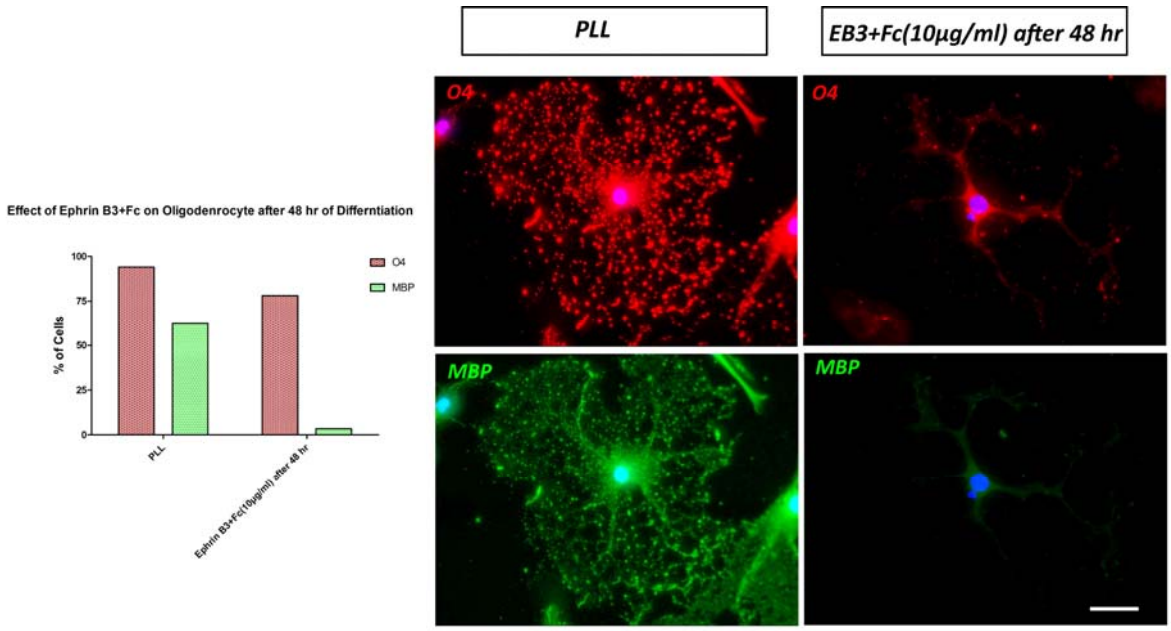


**Fig 21. Ephrin B3 inhbits OPC lineage progression.** The bar graph illustrate that late presentation of preclustered ephrin-B3 reduces MBP expression without significantly affecting O4 immuno-reactivity. The photomicrogrpah displaying the morphology of late stage OPCs on control and after addition of the clustered ephrin B3. Scale bar 30µm

### 5.3.8 The inhibitory effects of ephrin B3 can be neutralized by antibody-mediated epitope masking

I next investigated whether masking ephrin B3 epitopes is able to reverse the inhibitory effects on OPC differentiation. For this purpose ephrin B3 substrates were incubated with two commercially available antibodies (Abcam and R &D system) One of the antibodies (Abcam) was directed against amino acids 135-341 of recombinant human ephrin B3 expressed in E.coli. The other antibody (R&D system) recognizes an antigen corresponding to amino acid 1-224, which is the extracellular domain of the human ephrin B3.

Incubation of ephrin B3 substrates with the antibodies for 2 hours prior to cell plating was able to partially neutralise the inhibitory effects of ephrin B3 on OPC differentiation (fig 22; $p \leq 0.0001$, one-way ANOVA, Dunnett's Multiple Comparison Test Ephrin B3(10µg/cm2) vs PLL,Abcam(10µg/ml),R&D(10µg/ml),A+R(5µg+5µg)/ml,A+R(5µg+5µg)/ml, A+R (10µg+10µg) /ml ;$p<0.05$) whereas incubation with unspecific mouse IgG antibody had no loss effect.

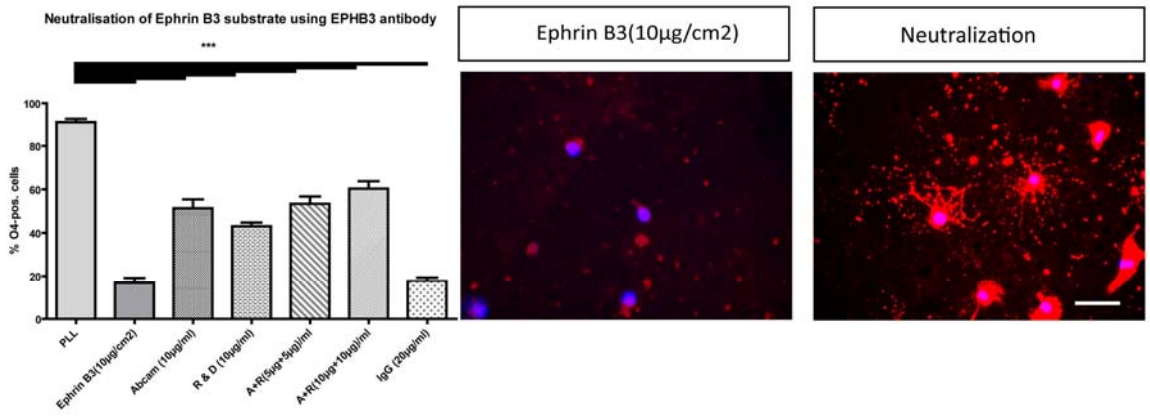


**Fig 22. Inhibitory effects of ephrin B3 can be neutralized by epitope masking with ephrin B3 antibody.** Bar graph illustrating that inhibitory activity of ephrin B3 can be reversed by masking substrate with anti-eprhin B3 antibody. Photomicrograph displaying the morphology of oligodendrocytes before and after neutralization. Scale bar 30µm.

### 5.3.9 Inhibitory effect of myelin protein extract (MPE) can be neutralized by masking MPE with ephrin B3 antibody

To establish the importance of ephrin B3 with respect to the OPC differentiation block induced by myelin (Baer et al., 2009; Kotter et al., 2006) ephrin B3 epitopes were masked in substrates prepared from total myelin proteins extracts. Assessment of O4 immunohistochemistry on OPCs cultured on the substrates for 2 days demonstrated that incubation with anti-ephrin B3 antibodies is able to promote OPC differentiation in the presence of MAI and that by using a combination of both antibodies OPC differentiation was restored to levels of control OPCs (fig 23; $p \leq 0.0001$, one-way ANOVA, Dunnett's Multiple Comparison Test ; MPE( 40µg/cm2) vs PLL, Abcam (10µg/ml), R & D (10µg/ml), A+R(5µg+5µg)/ml, A+R(5µg+5µg)/ml, A+R(10µg+10µg)/ml;$p<0.05$). This indicates that ephrin B3 plays a major role in the myelin mediated differentiation block in OPCs.

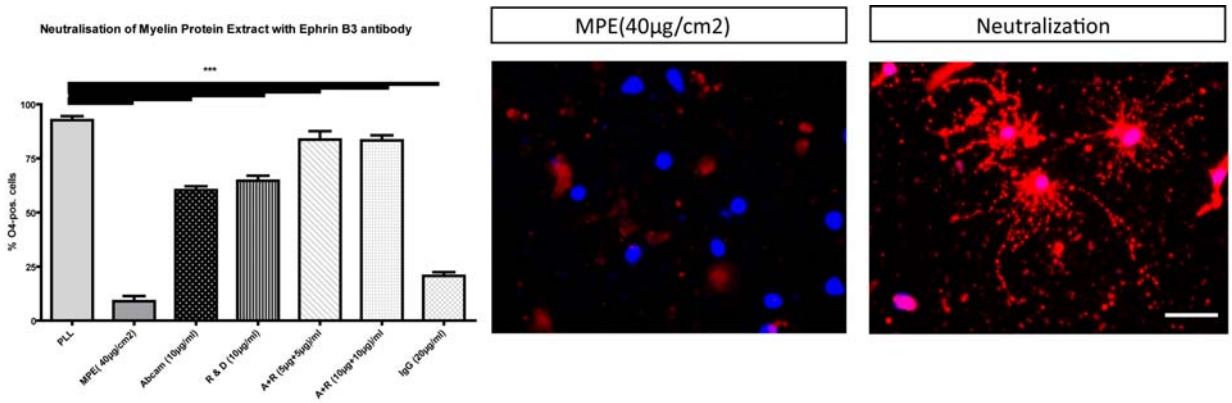


**Fig 23. Inhibitory effect of myelin protein extract (MPE) can be neutralized by masking MPE with ephrin B3 antibody.** Bar graph showing that the oligodendrocytes differentiate well when the myelin protein extract is masked by ephrin B3 anitbody. The photo showing that oligodendrocytes can overcome the inhibitory of myelin when substrate is neutralized with ephrin B3 antibody. scale bar 30µm

### 5.3.10 Ephrin B3 mediates its inhibitory effect via activation Rho A

Rho family GTPases regulate the polymerization of actin and thus control cellular cytoskeleton structure. It has been demonstrated that the expression of constitutively active RhoA inhibits process extension in oligodendrocyte lineage cells, whereas a dominant negative mutant of RhoA induced hyperextension of processes (Wolf et al., 2001). Furthermore, it was recently reported that myelin mediates its inhibitory effects on OPC differentiation via activation of RhoA and PKC (Baer et al., 2009). To assess whether ephrin B3 mediates inhibitory effect on OPC differentiation through the activation of RhoA a Rho pull down assay was conducted. For this purpose OPCs were cultured on MPE, ephrin B3, and control substrates for 24 h in differentiation medium and lysates were collected. Assessment of active RhoA demonstrates the presence of myelin inhibitors and ephrin B3 induces an increase of GTP bound RhoA.

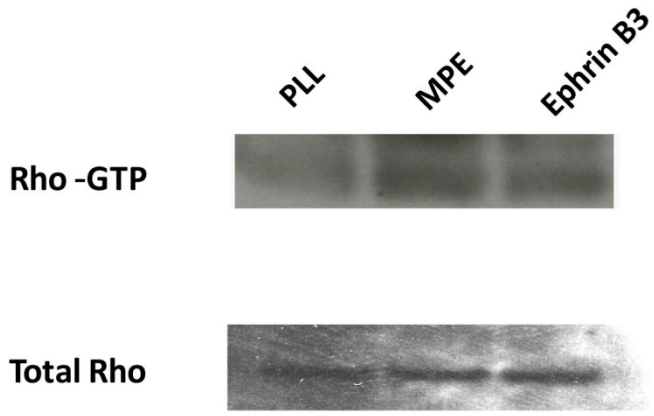


**Figure 24. Autoradiograph of Rho assay**

### 5.3.11 Ephrin B3 does not induce activation of PKC

As mentioned previously, myelin associated inhibitors not only activate RhoA signaling but also induce activation of PKC. Assessing PKC is technically challenging. However, recent studies have demonstrated that as a result of PKC activation in the presence of MAI the re-distribution of myristoylated alanine rich C kinase substrate (MARCKS) from the cytoplasm to the plasmamembrane which forms part of the normal differentiation program in OPCs was inhibited (Baer et al., 2009). To assess whether ephrin B3 also induces PKC activation, immunocytochemistry for MARCKS was conducted and the pattern of expression was analysed laser scanning microscopy. In contrast to my expectatins MARCKS was localized at the cell membrane indicating that ephrin B3 does not induce PKC activation.

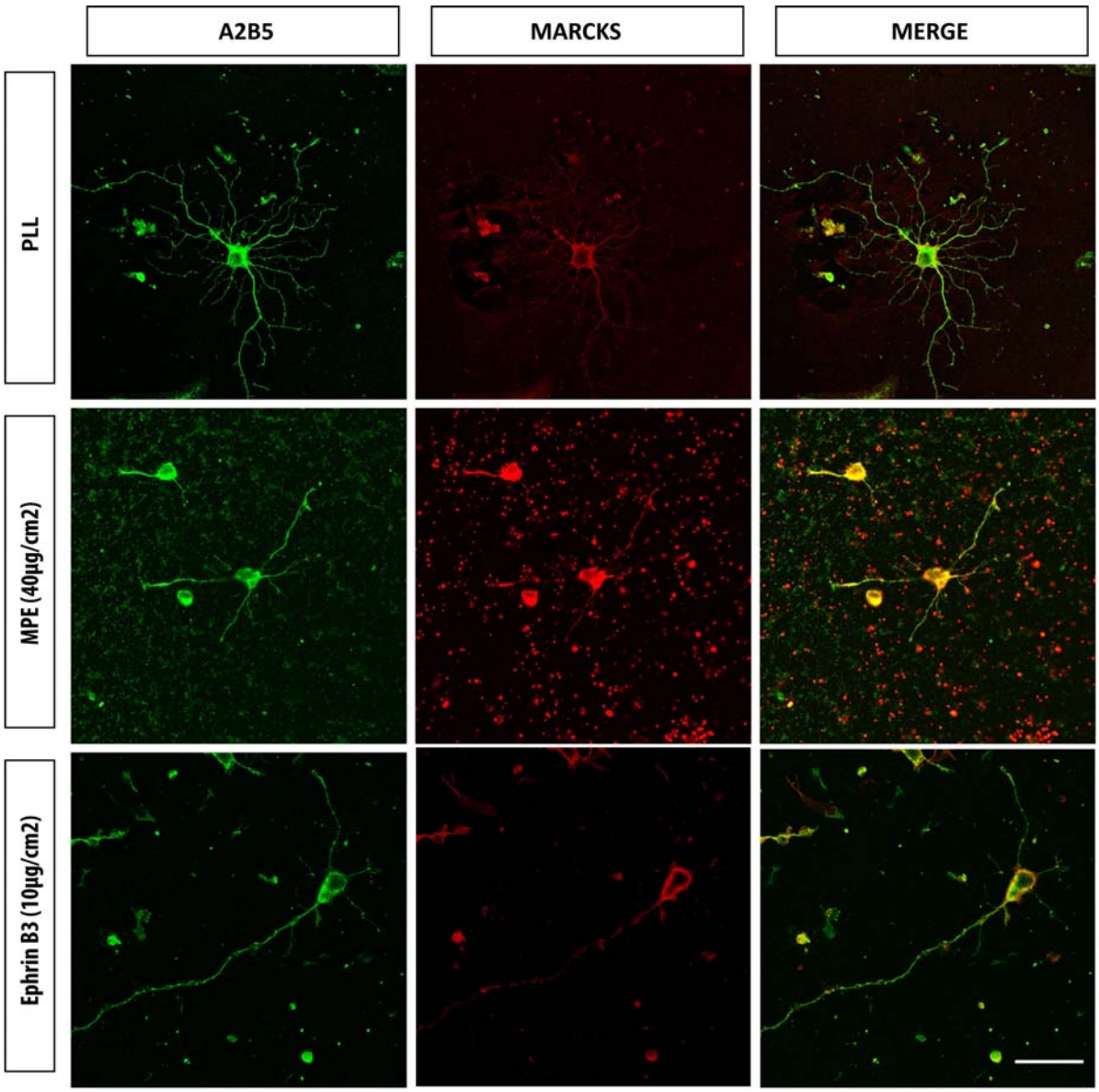


Fig 25. Oligodendrocytes double-labeled with antibodies against A2B5 (green) and MARCKS (red). Myristoylated alanin-rich C kinase substrate (MARCKS) cross-links filamentous actin (F-actin) and regulates its reorganization. This activity is reduced either by PKC induced MARCKS phosphorylation (PKC pathway) or by its direct binding to calmodulin (CaM; CaM pathway), both inducing MARCKS translocation and F-actin reorganization. In control cells (PLL) and cells plated on ephrin B3 MARCKS expression is more associated with the cell membrane, in presence of myelin inhibitors it lead to a cytoplasmatic MARCKS presence. Scale bar 30µm

## 5.4 Discussion

The experimental data presented here verify ephrin-B3 expression in oligodendrocyte lineage cells and demonstrate a dynamic expression pattern as the cells differentiate. Furthermore, in vivo ephrin B3 expression was found to be located in myelin sheaths. Apart from being a recognized axon guidance cue providing a midline barrier during development (Kullander et al., 2001), Ephrin B3 is able to inhibit neurite outgrowth (Benson et al., 2005), thus possibly contributing to the failure of axon regeneration following spinal cord injury. The present series of experiments demonstrated that ephrin B3 is also a potent inhibitor of OPC differentiation. Although the physiological function of ephrin B3 in oligodendrocyte lineage

cells remains unknown it is a plausible hypothesis that ephrin B3 expressed on mature oligodendrocytes provides a feed-back inhibition for early (A2B5+) precursor cells.

The experiments in which ephrin B3 epitopes were masked in myelin protein resulting in neutralization of the inhibitory effects of myelin on OPC differentiation demonstrate an important role of ephrin B3 for the myelin mediated differentiation block. Complete reversal of the inhibitory effects by antibody-mediated epitope masking even lead to suggest that the inhibitory effects of myelin rely on the presence of ephrin B3. However, more work is needed to demonstrate that ephrin B3 is necessary and not only sufficient to account for the inhibition of myelin on OPC differentiation. For example, testing the effects of myelin prepared from ephrin B3 KO mice would be an instructive experiment. However, finding that ephrin B3 does not induce PKC signaling in OPCs points to the possibility that other components in myelin exist which play an additional role in mediating inhibitory effects of myelin to OPC differentiation.

The intracellular domains of the transmembrane Eph family ligands show a strikingly high degree of homology. In particular, 31 of the last 34 amino acids of ephrin-B3 are identical to the comparable residues of ephrin-B1 and ephrin-B2 and the homology between human and mouse ephrin-B3 is >96% (Bergemann et al., 1998). This very high level of intracellular conservation among the transmembrane ephrin B ligands suggests a significant functional role for the cytoplasmic domains of these proteins. The expression of all the three ephin B ligands in oligodendrocytes suggests a role for ephrin B–mediated reverse signaling in OPCs.

Ephrin B3 binds to 5 different receptors. However the ligand receptor binding studies reveal that ephrin B3 has a high affinity with only one of them, EphB3 ($K_D$=1.5nm). The next best fit that was found was EphA4 (Bergemann et al., 1998). Both receptors are also expressed in OPCs on mRNA level. Hence, it is very likely that biologically significant receptor for ephrin-B3 is EphB3 and EphA4. However, a number of experiments are needed in order to confirm expression and functionality including RNAi based knock down experiments in OPCs.

One of the most fascinating features of Ephs and ephrins is their remarkable ability to induce bidirectional signaling. The results demonstrate that the ephrin mediated inhibition of OPC differentiation follow the RhoA activation. RhoA activation downstream of EphB receptors has not received much attention so far. Based on what has been so far reported, potential connections between EphB receptors and RhoA include singalling through Dishevelled, a cytoplasmic adaptor protein involved in Wnt signaling (Rothbacher et al., 1995) and dysregulation of the canonical Wnt pathway, which has shown to contributes towards failure of myelin repair (Fancy et al., 2009). The ability of EphA4 and other EphA receptors to activate RhoA may depend on the presence of exchange factors such as Ephexin and Vms-RhoGEF, since EphA4 overexpression does not substantially activate RhoA in 293 human embryonal kidney cells unless Vms-RhoGEF is also over expressed (Ogita et al., 2003). If RhoA is activated by signaling through EphA receptor in OPCs then the role of Ephexin/Vms-RhoGEF family signaling needs to elucidated.

# Chapter 6

# Ephrin B3 inhibits CNS remyelination

## 6.1 Introduction

Demyelination is the primary morphological hallmark of a number of neurological diseases including multiple sclerosis (MS) (Lassmann, 2007) and spinal cord injury (Guest et al., 2005), leading to axonal loss and neurological impairments. Remyelination can be a highly efficient process resulting in complete healing in both experimental models and clinical demyelinating diseases, including multiple sclerosis (Patrikios et al., 2006; Woodruff and Franklin, 1999). Remyelination requires the recruitment of oligodendrocyte precursor cells (OPCs) by proliferation and migration and further their differentiation into mature myelinating oligodendrocytes (Franklin, 2002a). However, in MS remyelination often fails although areas of demyelination contain cells of the oligodendrocate lineage which have become arrested at a premyelinating state (Chang et al., 2000; Chang et al., 2002; Kuhlmann et al., 2008b; Wolswijk, 1998, 2002). Assuming that the recruited OPC are naive and no defect in myelin gene expression, the failure of differentiation could be attributed to an inhibitory environment in MS lseions. Several potential inhibitors have been described including axonal expressed PSA-NCAM (Charles et al., 2002) astrocytic hyaluronan (Back et al., 2005), notch-jagged (John et al., 2002), LINGO-1 (Mi et al., 2005) and myelin debris (Kotter et al., 2006).

Chapter 5 described a series of experiments on the basis of which ephrin B3 was identified as a prominent factor in the differtiation block mediated by myelin in OPCs. Signaling by EphB/ephrinB in the context of CNS injury is becoming increasingly recognized and recent studies have demonstrated that EphB regulates astrocyte gliosis and formation of the glial scar (Du et al., 2007). B-class Ephs and ephrins have also been implicated in the astrocytes mediated phagocytosis of axonal debris following hippocampal injury and an up-regulation of ephrin-B1 and EphB receptors on astrocytes has been detected (Wang et al., 2005b). ephrinB-EphB receptor signaling has been implicated in synaptic plasticity and pain processing in the matured nervous system (Kobayashi et al., 2007; Song et al., 2008).Ephrin B3, expressed by myelinating oligodendrocytes have shown to induce neurite growth cone collapse (Benson et al., 2005).

In this chapter the hypothesis that ephrin B3 inhibits CNS remyelination was tested. For this purpose, a highly reproducible model of CNS remyelination was used, in which focal demyelination is induced in the white matter of the caudal cerebellar peduncles (CCP) of adult rats by stereotactic injection of ethidium bromide (EB) (Woodruff and Franklin, 1999). Subsequently ephrin B3 was delivered into the lesions using an osmotic pump connected to a stereotactically placed infusion cannula.

## 6.2 Materials and Methods

Full details of the materials and methods used in this chapter are provided in chapter 2.

### 6.2.1 Experimental design

All studies were performed in accordance with the German animal protection laws and approved by the responsible governmental authority (Nidersächsisches Lanesamt für

Verbraucherschutz und Lebensmittelsichherheit, animal license number RKO_033/2008) and Institutional (MaxPlanck institute for Experimental Medicine, Göttingen) guidelines.

Local areas of demyelination were created in the caudal cerebellar peduncle (CCP) of adult female Sprague Dawley (SD) rats by stereotaxic injection (stereotactic coordinates were 10.4mm caudal, ±2.6mm lateral and 7.07mm ventral to bregma) of 0.01% ethidium bromide (EB) as previously described (Woodruff and Franklin, 1999). For continuous local delivery of proteins into the demyelinated lesions, a 30 gauge modified mouse osmotic pump connector cannula with dummy wire was stereotactically placed in same surgical session. EphrinB3 (ephrin B3+Fc-IgG, 200µg/ml), was administered by an osmotic pump (0.5 µl/h, Alzet Osmotic Pumps, 2002, ALZA Corporation, USA), that was implanted and connected at 10 days after induction of demyelination. Control animals received Fc-IgG (20µg/ml). Infusion lasted for 14 days. As shown on Fig 23 animals were sacrificed 28 days after lesion induction. A group of animals was also sacrificed at 10 days. These served as a base line for the present experiment and those described in chapter 7.

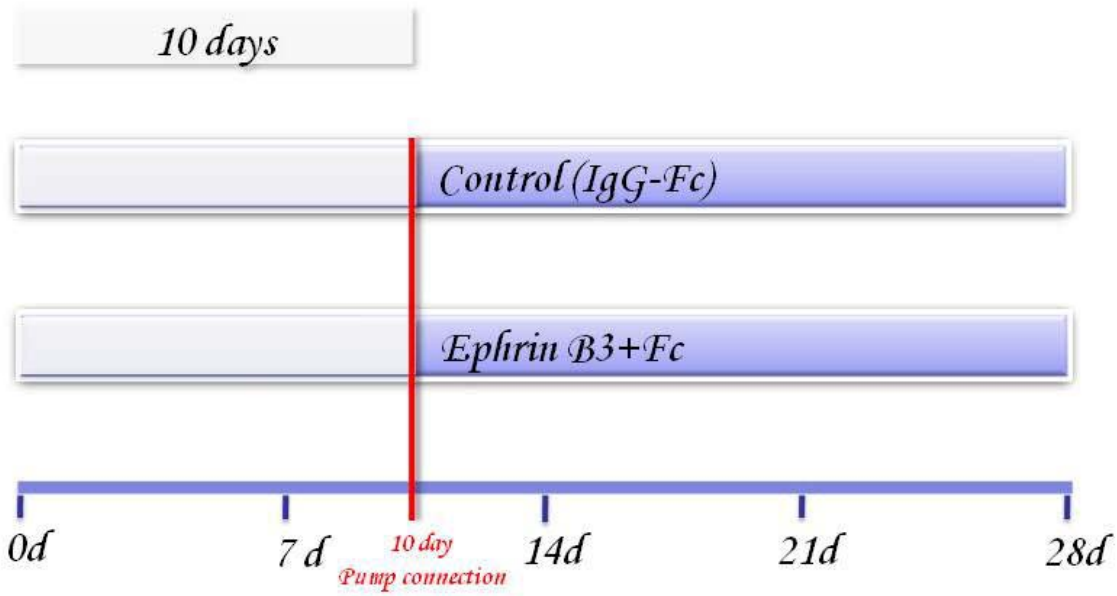


**Fig 26. Schematic diagram of experimental design for the *in vivo* experiment to test the effect of ephrin B3 in remyelination**

### 6.2.2 Histological analysis of remyelination

The rats were perfused through the heart first with HBSS and then with a fixative solution containing 4% phosphate buffered glutaraldehyde and the brains were post-fixed overnight. Tissue blocks encompassing the CCP were cut and the blocks processed through osmium tetroxide, dehydrated and embedded in TAAB resin. Semi-thin sections (1 µm) were cut and stained with methylene blue and azur-II.

The extent of remyelination between ephrin B3 infused and Fc-IgG infused groups was assessed on resin sections in a blind fold manner with the best remyelinated lesion receiving the highest rank value. The mean scores and SEM were calculated for each group of animals, and statistical analysis was performed using Mann–Whitney test.

### 6.2.3 Celluar analysis of remyelination

To examine molecular events of remyelination, in situ hybridization was conducted on animal scarified at 10 days, and at 28 days in the ephrin B3 infused and in the PBS infused groups. For this purpose animals were perfused with 4% paraformaldehyde in PBS, and 15µm tissue sections were prepared for *in situ* hybridisation as described previously (Kotter et al., 2006; Sim et al., 2000b). Following *in situ* hybridisation, RNA hybrids were visualised by a standard technique as described previously (Fruttiger *et al.* 1999). Lesions were identified on digital images of solochrome cyanine-stained sections, and the lesion area determined using a public domain program (Image J 1.43c; free download on http://rsb.info.nih.gov/ij/). The same program was used to determine the number of PDGFR-α+, Nkx2.2+, MsrB+, PLP+ and MOG+ cells within the lesions on digitised adjacent sections. Only lesions with a size > 0.4mm$^2$ were included in the analysis. OPC density was calculated as the ratio of cell numbers per lesion area. . All statistical calculations were done using GraphPad Prism (GraphPad software).

### 6.2.4 Electron microscopic analysis of remyelination

Ultrathin sections (50 nm) were cut using a Leica Ultracut S ultramicrotome (Leica, Vienna, Austria) from the lesion site and stained with an aqueous solution of 2% uranyl acetate (Merck) followed by lead citrate (Reynolds, 1963). The sections were viewed in a LEO EM 912AB electron microscope (Zeiss, Oberkochen, Germany), and pictures were taken with an on-axis 2048 x 2048 CCD camera (Proscan, Scheuring, Germany).

## 6.3 Results

### 6.3.1 Ephrin B3 inhibits CNS remyelination in experimental demyelination

Histological appearance of the resin section from the control animals, which received infusions of Fc-IgG, was characterized by thin myelin sheaths throughout. On the contrary lesions of the ephrin B3 infused group revealed a presence of nude axons throughout the lesion. The axons irrespective of their diameter remained demyelinated. Comparision between the treatment and control group was conducted on the basis of a blinded rank analysis. The results demonstrated a significant impairment of remyelination in ephrin B3 infused animals (Fig 27, Mann–Whitney *U* test, p = 0.0078).

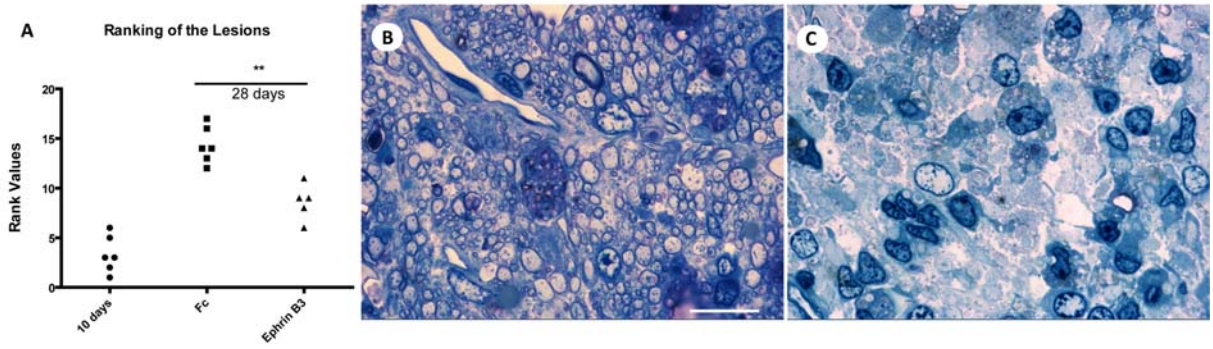


Fig 27. Ephrin B3 inhibits CNS remyelination A) Ranking analysis following EB-induced demyelination in ephrin-B3 infused animals versus Fc IgG infused animals. The 10 day group served as internal control B) Light microscopy on semi-thin resin sections of Fc IgG infused animals revealed successful remyelination following 4 weeks of induction of remyelination. Scale bar 30µm C) Transverse sections from ephrin B3 infused lesion, showing demyelinated axons after four weeks of induction of demyelination

### 6.3.2 Ephrin B3 doesn't alter the lesion size

In order to determine if ephrin B3 has any influence on the size of lesion in the CCP, cryostat sections of tissue was prepared for in situ hybridization carrying the largest lesion area was stained with the eriochrome cyanine stain, which specifically stains myelin sheaths blue. Measurement of the lesion areas using ImageJ showed no significant differences in size between the groups (Figure 28 A). The average area of lesions in 10 day group was 0.6088 ± 0.02614 $mm^2$, N=44; Fc-IgG infused controls 0.5523 ± 0.03579 $mm^2$ N=37 and ephrin B3-infused animals 0.5669 ± 0.02031$mm^2$ N=52. (Fig 28; p= 0, 3208; one way ANOVA).

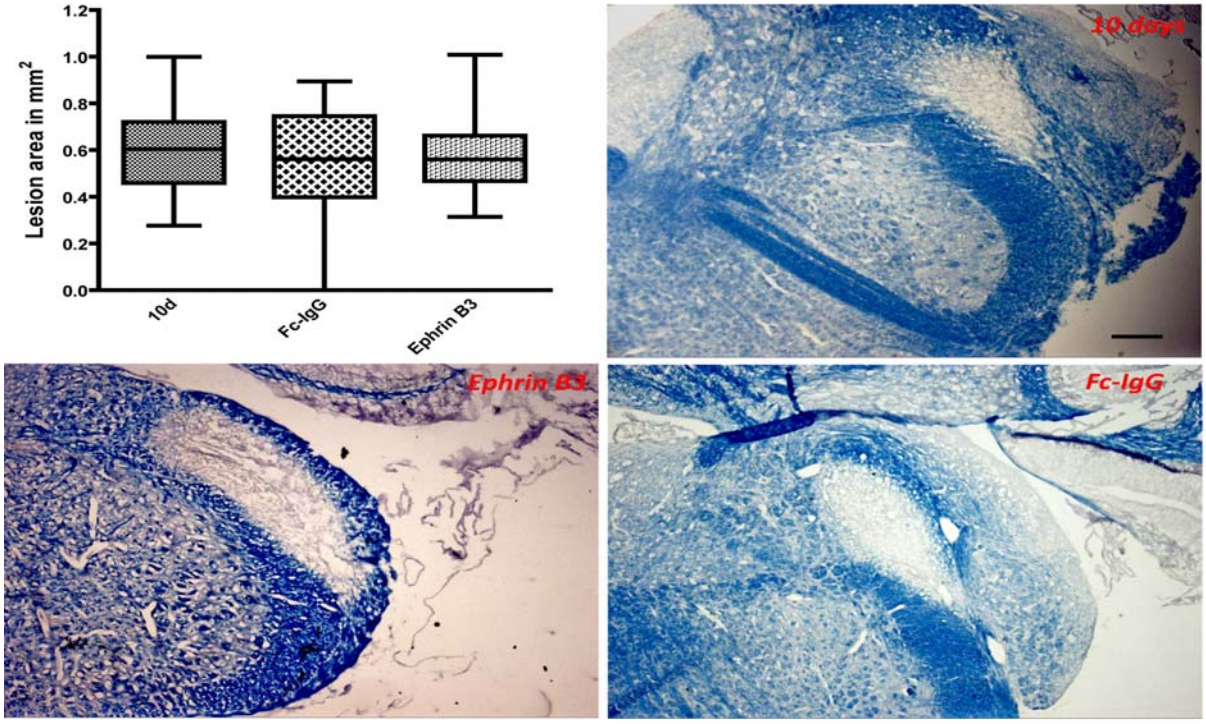


**Fig 28. EphrinB3 doesn't alter the lesion size.** The graph showing the average lesion area among different groups. The transverse section of resin section from 10 days, Fc-IgG and ephrin B3 infused lesison stained with eriochrome cyanine. Erichrome cyanine stains the myelin blue. The demyelinated area remains colourless. Scale bar 30µm

### 6.3.3 Ephrin B3 has no effect on the presence of OPC's

The presence of OPCs was estimated by the expression of PDGFR-α+ cell. Folowing the analysis I could detect no difference between the numbers of PDGFaR mRNA-expressing OPCs in the area of lesion among 10 day, ephrin infused and Fc-IgG Infused group. This observation suggests that the presence of OPCs is unaffected following infusion of ephrin B3. The average count for the PDGFRα-positive cells for 10day group was 143.1 ± 20.80 cells / $mm^2$; Fc-IgG: 133.4 ± 21.81 cells / $mm^2$ and ephrin B3:134.0 ± 12.12 cells / $mm^2$) (Fig 29; p= 0,9104, one way ANOVA).

The number of activated OPCs in this model peaks at day 10 and then gradually declines (Fancy et al., 2004). In the present experiment a significant difference between the number of activated OPC in the 10 days group as compared to that of the ephrin B3 and Fc-IgG infused group was detected (Nkx2.2, positive cells per area ± SEM, 10d: 268.8 ± 14.82 cells / $mm^2$; Fc-IgG : 178.1 ± 30.78 cells / $mm^2$; ephrinB3: 186.5 ± 22.44 cells / $mm^2$). (Fig 29; p= 0, 0275, one way ANOVA).

### 6.3.4 Ephrin B3 doesn't alter the PLP/MOG expression in experimental demyelination

To assess lineage progression of the OPC population within the lesions *in situ* hybridization for PLP/dm-20 was conducted. To my surprise, although infusion of ephrin B3 clearly resulted in an impairment of remyelination no differences were detectable with respect to PLP expression between the 10 day group, the ephrin B3 and the Fc-IgG infused group. (PLP positive cells per area ± SEM, 10d: 506.4 ± 75.40 cells / $mm^2$; Fc-IgG: 541.0 ± 125.0 cells / $mm^2$; ephrin B3: 759.4 ± 100.2 cells / $mm^2$) (Fig 29; p= 0,1418, one way ANOVA).

Myelin oligodendrocyte glycoprotein (MOG) is often considered as a marker for mature oligodendrocytes (Wolswijk, 2000). However, other studies suggested that PDGFRα expressing OPC are also able to express MOG (Li et al., 2002). In situ hybridization for MOG showed no differences among the groups (MOG positive cells per area ± SEM, 10d: 213.1 ± 25.84 cells / $mm^2$; Fc-IgG: 202.6 ± 27.71 cells / $mm^2$; ephrin B3: 312.8 ± 52.70 cells / $mm^2$) (Fig 29; p= 0,1458, one way ANOVA). It thus seems that OPCs in remyelinating lesions express MOG early and before initiation of the formation of myelin sheaths.

### 6.3.5 Immune response is unaffected in presence of ephrin B3

Macrophage scavenger receptor type B (MsrB) is a marker used as a means of quantification of the inflammatory response. Apart from OPCs, macrophages are key players in the process of myelin regeneration (Kotter et al., 2001). No difference was observed between the experimental groups which suggests that the infusion of ephrin B3 does not alter the immune response (MsrB positive cells per area ± SEM, 10d: 128.7 ± 25.91 cells / $mm^2$; Fc: 200.4 ± 45.63 cells / $mm^2$; ephrin B3: 154.6 ± 17.21 cells / $mm^2$). (Fig 29; p= 0,2488, one way ANOVA).

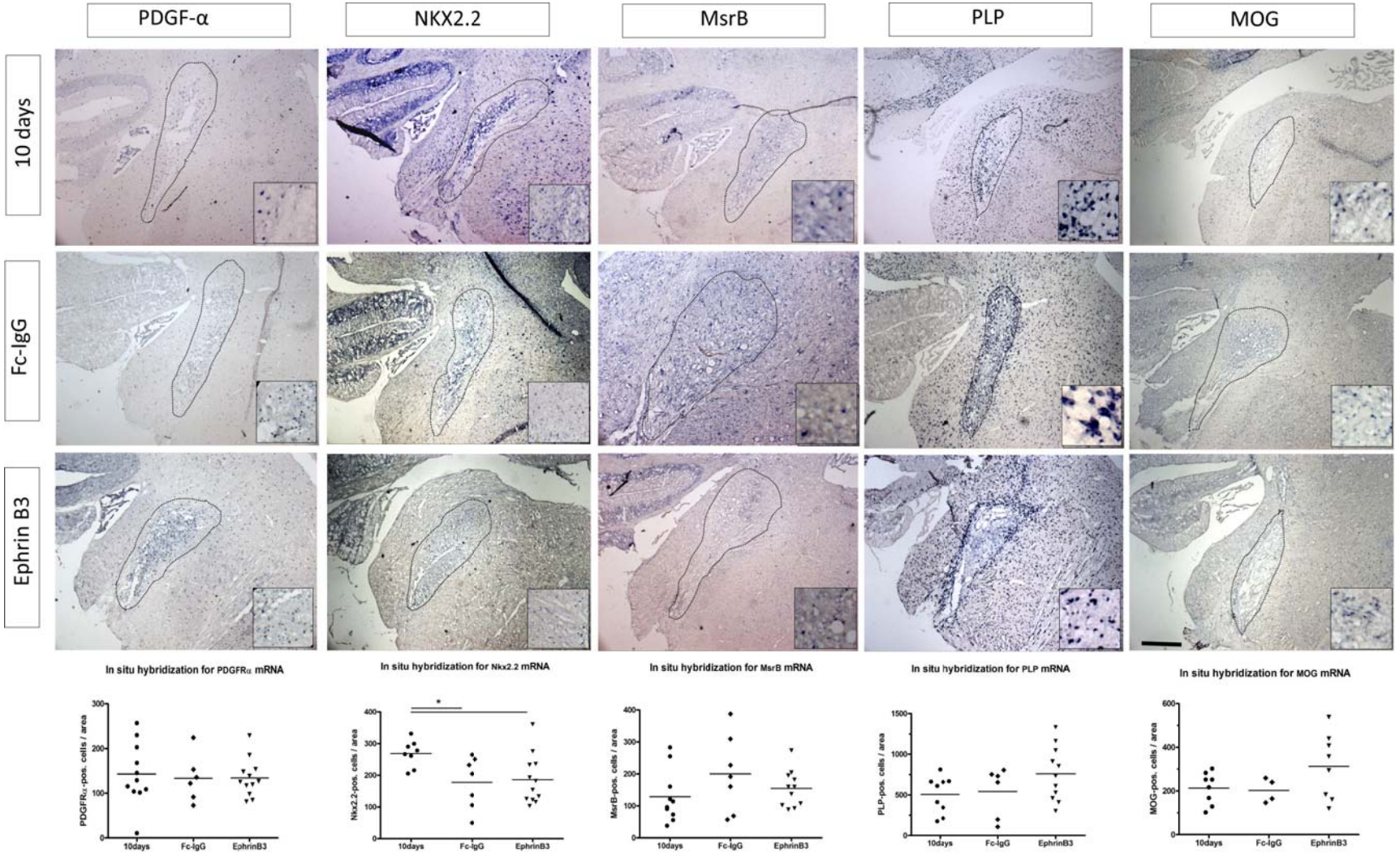


**Fig 29. Digoxigenin-labeled in situ hybridization on the demyelinating lesion from different groups for various different probes. Lower panel on the right hand side of the figure shows the positive cells from the lesion area at higher magnification.Scale Bar 50µm**

### 6.3.6 Differentiation of oligodendrocyte is arrested at premyelinating stage in presence of Ephrin B3

To confirm the findings obtained by light-microscopical analysis of resin embedded species, ultra-structural analysis of lesion was conducted. Electron micrographs showed that axons in lesions that received ephrin B3 infusions were healthy and showed no signs of stress (*no* axonal and mitochondrial swelling, number of mitochondria per axon was 4-8). Often axons were contacted by processes that seemed to be of oligodendrocyte origin. However, these failed to form myelin sheaths indicating an arrest of OLCs at a premyelinating stage (fig 30 c). Some of the OLCs arrived at forming a number of wraps around the axons; however, it is the formation of compact myelin was impaireds. These findings resemble the findings described in the context of the experiments in which myelin membrane preparations were infused into demyelinated lesions (Kotter et al., 2006).

Control lesions which were infused with Fc-IgG showed all the characteristics of remyelinated lesion (fig 30 A). Nearby all axons were surrounded by thin myelin sheaths that have been described in the context of remyelination (Blakemore, 1974).

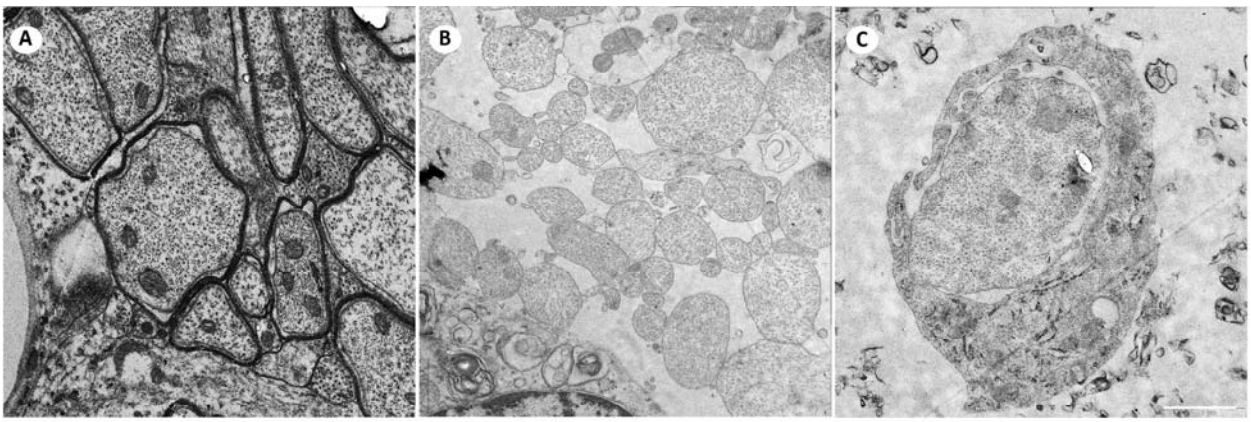


**Fig 30. Electron microscopic analysis of remyelination.** A) electron microscopic image of remyelinated axons-from control (Fc-IgG) infused lesions. The axons are remyelinated and reinvested with thin myelin sheaths. B) Electron photographs of lesion which got ephrin B3 infusion showing naked axons. No myelin debries were found C) The oligo-dendrocyte wrap the axons but fails to forms the myelin sheath in the presence of ephrin B3 and the differentiation arrest occurs in premyelinating state. Scale bar 1µm

### 6.3.7 Is Ephrin B3 a key player mediating myelin assembly?

Critical evaluation of the electron micrographs of ephrin B3 infused lesions indicated the presence of dense, myelin ball like structure in the cytoplasm of OLCs and their processes (fig31 A). These appeared like cholesterol-enriched vesicles. To form myelin sheaths, oligodendrocytes must deliver large amounts of myelin membrane to the axons (Baumann and Pham-Dinh, 2001; Kramer et al., 2001). A failure of the transport can result in the intracellular accumulation of membrane components and this could potentially provide an explanation for the failure of myelin sheath formation in ephrin B3 treated animals. Trajkovic *et al* provided evidence that during myelin biogenesis, at least a portion of proteolipid protein trafficking occurs via endosomes (Trajkovic et al., 2006). It is possible that the myelin ball like structures resemble endosomes carrying plp protein, which would be indicative of a failure of myelin assembly/transport in the presence of ephrin B3. However, further experiments

including rigorous quantification at electron microscopic level as well as in vitro studies are necessary to validate this hypothesis.

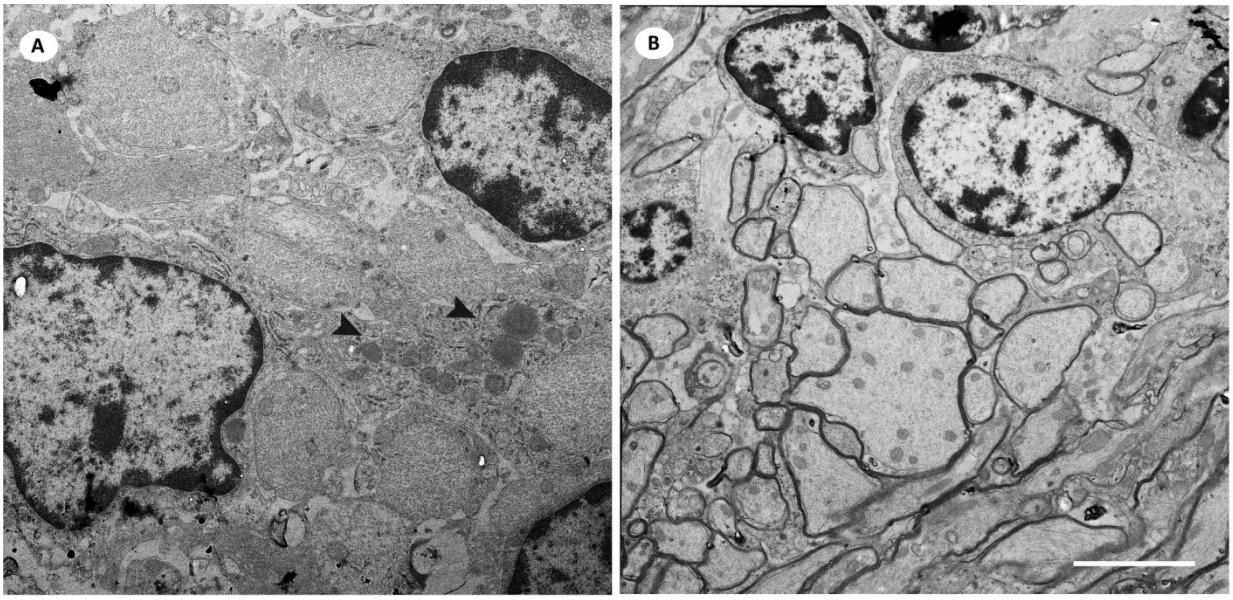


**Fig 31. Ephrin B3, a key player in myelin assembly ?** A) Trasverse section from CCP of animal infused with ephrin B3. After four weeks of demyelination the oligodendrocytes wrap around the axon but fail to produce the myelin sheeths. However there is presence of the myelin ball like structure (arrow) around the denuded axons, may be due failure of myelin protein trasport/assembly B) In control animals which were infused with Fc-IgG most axons were reinvested with myelin sheaths formed by remyelinating oligodendrocytes. No ball like structure are found. Scale bar 2µm

## 6.4 Discussion

In the present experiment the in vitro results described in chapter 5 were translated into an in vivo model of remyelination. The results provide clear evidence that ephrin B3 is a potent inhibitor of CNS remyelination. The results of the ISH for PLP and MOG are difficult to interpret, especially as hybridization was repeated and conducted in parallel with hybridization of tissue from the experiments described in chapter 7, which yielded the expected results with respect to PLP mRNA expression. On this basis technical issues can be ruled out. Strikingly, PLP levels were low in animals that received Fc-IgG and comparable to rats sacrificed at day 10 although remyelination as assessed on resin-embedded sections was for the most part complete. Inter-experimental comparison demonstrated significant differences between IgG and PBS control animals, which both reached fully remyelinated stages. In summary, PLP mRNA expression does not always correlate with OPC differentiation. Future studies using protein-detecting techniques will shed light on these contradictory findings. However, these were beyond the scope of the present thesis.

A potential explanation about the the lack of differences in PLP mRNA expression between treatment and control groups may be found in the experimental design. Day 10 following demyelination was chosen for the start of ephrin B3 infusion. At this stage most of the recruited OPCs have reached a Nkx2.2 state ready to differentiate. Day 10 is also the start of remyelination at the lesion border (Woodruff and Franklin, 1999). When ephrin B3 was added to the cultures at late stages after OPCs showed robust O4 expression associatd with an impaired expression of MBP. From this it was concluded that Ephrin B3 is able to inhibit OPC

differentiation at different stages of the lineage. Another explanation lies in the possibility that membrane transport was disrupted, a process that might be independent of transcriptional changes. This is supported by the finding of structures resembling “myelin balls” in the cytoplasm of cells that showed features of a dense cytoplasm commonly associated with OLCs. Similarly, in vitro data in chapter 5 demonstrated that ephrin B3 interferes with processs formation. The inability to form myelin sheaths may thus result from an inhibitory mechanism that acts at the level of process and myelin sheath formation.

Although Myelin oligodendrocyte glycoprotein (MOG), is often considered as marker for mature oligodendrocytes (Wolswijk, 2000) studies have demonstrated that in the dorsal funiculi of adult rats PDGFRα and NG2 expressing cells are able to co-express MOG supporting the notion that OPCs in the adult CNS express a marker that has been thought to be restricted to mature oligodendrocytes (Li et al., 2002). Moreover, in situ hybridization only detects expression on mRNA level and that often transcriptional expression is not translated into protein level. Therefore immunohistochemical analysis for mature markers of oligodendrocytes is necessary and will be conducted. However, due to limitations in time these experiments were not included in the present thesis

Ephrin B3 is synthesized at all stages of the oligodendrocyte lineage and reaches its maximum expression at the myelinating stage. A potential function of ephrin B3 expressed on mature OLCs may be an inhibitory feedback signal to immature OPCs preventing other cells to engage in the specific stretch of the axon that has already been myelinated. Furthermore, by inhibiting OPC differentiation it may contribute to maintaining the balance of the number OPCs the CNS. Further studies are necessary to determine the function of ephrin B3 in OLCs.

Following demyelination, degenerated myelin accumulates within lesions. In experimental lesions in young-adult animals this is efficiently cleared by macrophages of microglial and monocytic origin (Kotter et al., 2001; Kotter et al., 2005; Ousman and David, 2000). Whether MS lesions contain myelin debris has not yet been rigorously studied, however some recent electron microscopic investigations were able to demonstrate the presence of myelin debris like structures in chronic active lesions (unpublished data). It is conceivable that if the clearance of myelin debris is disturbed by alterations of the inflammatory response the presence of myelin debris can persist and thus for a prolonged period inhibit myelin regeneration. The result presented in chapter 5 demonstrated that ephrin B3 is an integral part of myelin membranes and that masking of ephrin B3 epitopes leads to robust differentiation of OPCs plated on myelin extracts. It is therefore likely that the inhibitory effect of myelin debris on OPC differentiation is due to the presence of ephrin B3.

It has been hypothesized that non-remyelinating chronic lesions could result from dysregulation of multiple steps in the remyelination process, resulting in a failure of the normal coordinated repair response (Franklin and Ffrench-Constant, 2008). However, it is also possible that the remyelination fails due to a persistent presence of only one or two key inhibitors of which could act as “master regulators” of this process. A number of differentiation inhibitors of remyelination have been proposed including PSA-NCAM (Charles

et al., 2002), hyaluronan (Back et al., 2005), and LINGO-1 (Mi et al., 2005). The present experiment establishes ephrin b3 as another potent inhibitor of OPC differentiation whose presence inhibits CNS remyelination. The data of the current study pave the way for subsequent studies which aim at promoting CNS remyelination by neutralising the inhibitory effects of ephrin B3. If successful strategies were found these could be translated into a clinical settings.

# Chapter 7

# Semaphorin 3A impairs CNS remyelination by inhibiting OPC differentiation

## 7.1 Introduction

Multiple sclerosis (MS) is the most common chronic inflammatory, demyelinating disease of the CNS in humans and is characterized by neurological deficits including sensory deficits, motor weakness, tremor, and ataxia. Remyelination failure during the course of multiple sclerosis contributes to the relentless progression of this disease (Franklin, 2002a). Large populations of immature oligodendrocytes can be found in fresh lesions of MS, which have potential to remyelinate (Chang et al., 2000; Maeda et al., 2001; Prineas et al., 1989; Raine et al., 1981). However the recruited progenitor cells often fail to differentiate into myelin forming cells, resulting in limited remyelination as observed in many of chronic multiple sclerosis lesions (Chang et al., 2002; Kuhlmann et al., 2008b) and impaired function (Andreasen et al., 2009). One possible explanation for the failure of remyelination is the persistence of differentiation inhibitors in chronic lesions. A number of such differentiation inhibitors have been found in MS lesions failure (Back et al., 2005; Charles et al., 2002; John et al., 2002; Mi et al., 2005).

Class 3 semaphorins are secreted proteins of about 120 kDa (Yu and Kolodkin, 1999). Semaphorin-3A (sema 3A) acts as a repellent for growth cones of DRG neurons (Luo et al., 1993), sensory neurons from the cranial nerve ganglia V and VII (Kobayashi et al., 1997), olfactory sensory neurons (Kobayashi et al., 1997), cortical neurons (Bagnard et al., 1998), and hippocampal neurons (Chedotal et al., 1998). Sema3A expression in the glial scar is detectable 1 week after axotomy and persists for at least up to 2 months after injury (Pasterkamp et al., 1999). The importance of Sema 3A in this context is highlighted by a recent study, which demonstrated that the selective inhibitor of Sema3A, SM-216289 is able to increase the regenerative response and functional recovery following transection of the spinal cord (Kaneko et al., 2006). Furthermore, migrating OPC have shown to express Sema 3A receptors and Sema 3A exerts chemorepulsive effect on migrating embryonic OPC's in the optic nerve (Spassky et al., 2002). Sema3A, through its binding to neuropilin1, induces a dramatic reduction of oligodendrocytes process extension in vitro (Ricard et al., 2001). Recently, a post-mortem study of active MS lesions showed an up-regulation of Sema 3A transcripts (Williams et al., 2007). The study also showed that astrocytes and microglia are the cellular source for the upregaultion of sema 3A although it is also expressed by cells expressing olig2 belonging to the oligodendroglial lineage (Williams et al., 2007).

The findings in the candidate approach that was used to identify potential inhibitors in chapter 3 suggested that Sema 3A is a potent inhibitor of OPC differentiation in vitro. In this chapter this has been confirmed in vitro and the hypothesis was tested that Sema 3A inhibits CNS remyelination. For this purpose, 10 days following *ethidium bromide*-induced demyelination, Sema 3A or control vehicle was stereotactically infused into the lesions. Subsequently the extent of remyelination as well as the OPC response was analyzed.

## 7.2 Materials and Methods

Full details of the materials and methods used in this chapter are provided in chapter 2

### 7.2.1 Experimental design

All studies were performed in accordance with the German animal protection laws and approved by the responsible governmental authority (Nidersächsisches Lanesamt für Verbraucherschutz und Lebensmittelsichherheit, animal license number RKO_033/2008) and Institutional (MaxPlanck institute for Experimental Medicine, Göttingen) guidelines.

Local areas of demyelination were created in the caudal cerebellar peduncle (CCP) of young adult female Sprague Dawley (SD) rats by stereotaxic injection (stereotaxic coordinates were 10.4mm caudal, ±2.6mm lateral and 7.07mm ventral to bregma) of 0.01% ethidium bromide (EB) as previously described (Kotter et al., 2006; Woodruff and Franklin, 1999). For continuous local delivery of proteins into the demyelinated lesion, a 30 gauge modified mouse osmotic pump connector cannula with dummy wire was stereotactically placed in same surgical session. Sema 3A (50µg/ml), was administered by an osmotic pump (0.5 µl/h, Alzet Osmotic Pumps, 2002, ALZA Corporation, USA), that was implanted and connected at 10 days after induction of demyelination. Control animals received PBS. Infusion lasted for 14 days. As shown on Fig 32, animals were sacrificed at 10 days and 28 days after lesion induction.

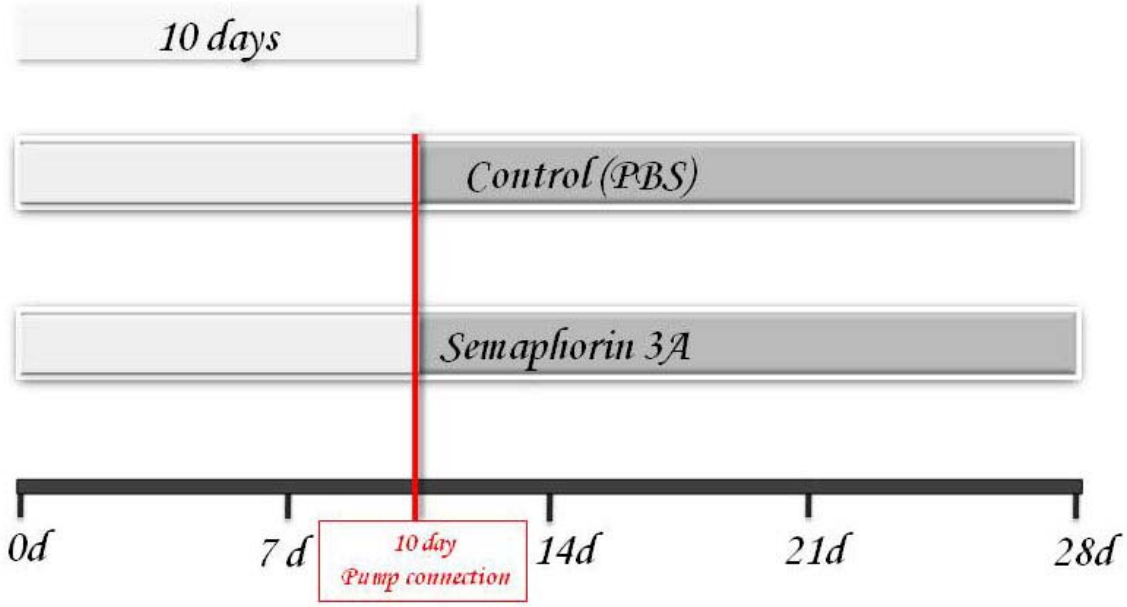


Fig 32. Experimental design to test the effect of semaphorin 3A on remyelination

### 7.2.2 Histological analysis of remyelination

The rats were perfused through the heart first with HBSS and then with a fixative solution containing 4% phosphate buffered glutaraldehyde and the brains were post-fixed overnight. Tissue blocks encompassing the CCP were cut and the blocks processed through osmium tetroxide, dehydrated and embedded in TAAB resin. Semi-thin sections (1 µm) were cut and stained with methylene blue and azur- II.

The extent of remyelination in Sema 3A infused and PBS infused animals was assessed by rank analysis with the investigator blinded with respect to the treatment group. The best remyelinated lesion received the highest rank value. Statistical analysis was performed using a non-parametric Mann–Whitney test.

### 7.2.3 Analysis of the OPC response

To examine profile the OPC response, in situ hybridization was conducted on animal scarified at 10 days, and at 28 days in the Sema 3A infused and in the PBS infused groups. For this purpose animals were perfused with 4% paraformaldehyde in PBS, and 15µm tissue sections were prepared for *in situ* hybridization as described previously (Kotter et al., 2006; Sim et al., 2000a). Following *in situ* hybridization, RNA hybrids were visualized by a standard technique as described previously (Fruttiger et al., 1999). Lesions were identified on digital images of eriochrome cyanine-stained sections, and the lesion area was determined using a public domain program (Image J 1.43c; free download on http://rsb.info.nih.gov/ij/). The same program was used to determine the number of PDGFR-α+, Nkx2.2+, MsrB+, PLP+ and MOG+ cells within the lesions on digitised adjacent sections. Only lesions with a size > 0.4mm$^2$ were included in the analysis. OPC density was calculated as the ratio of cell numbers per lesion area. All statistical calculations were done using Graph Pad Prism (Graph Pad software).

### 7.2.4 *Ultra structural* analysis of remyelination

Ultrathin sections (50 nm) were cut using a Leica Ultracut S ultramicrotome (Leica, Vienna, Austria) from the lesion site and stained with an aqueous solution of 4% uranyl acetate (Merck) followed by lead citrate (Reynolds, 1963). The sections were viewed in a LEO EM 912AB electron microscope (Zeiss, Oberkochen, Germany), and pictures were taken with an on-axis 2048 x 2048 CCD camera (Proscan, Scheuring, Germany).

## 7.3 Result

### 7.3.1 Sema 3A inhibits OPC differentiation

The experiments described in chapter 3 indicated that OPCs down-regulate O4 expression in the presence of Sema 3A. This was confirmed by three repeat experiments in which OPCs were plated on recombinant Sema 3A cultured in differentiation medium for 2 days followed by assessment of immunoreactivity for O4. The results demonstrate a significantly decreased O4 expression in presence of Sema 3A (Fig. 33; $p \leq 0.001$, one-way ANOVA; Dunnet multiple comparison test; PLL vs Sema 3A {(2.5µg/5µg/10µg)/cm$^2$} $P<0.05$).

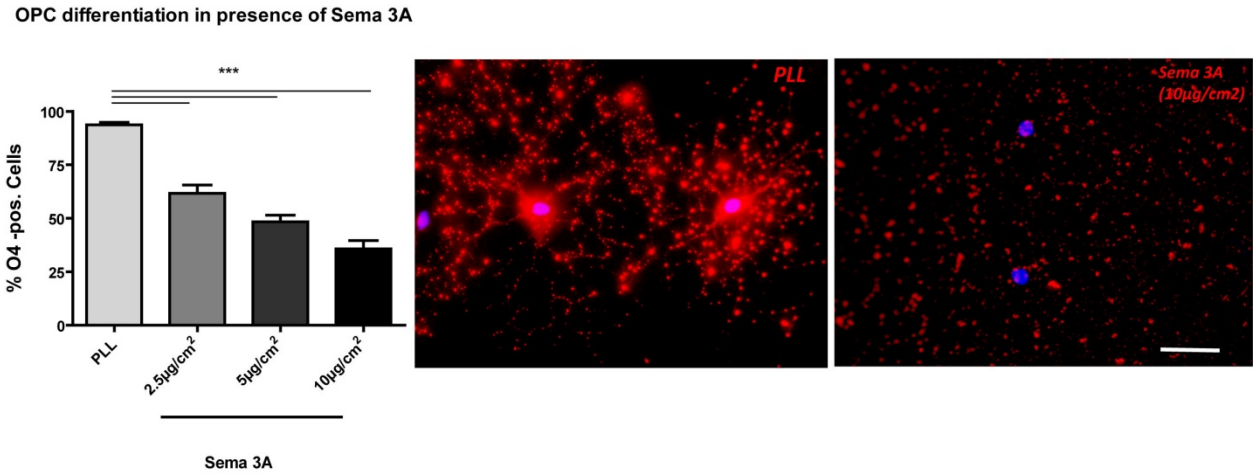


**Fig 33. Semaphorin Inhibit OPC differentiation in vitro.** Bar graph showing concentration dependent differentiation block mediated by Sema 3A. The OPC differentiate into oligodendrocytes when plated on Poly-L-Lysine. However, on Sema 3A they fail to differentiate.

### 7.3.2 Inhibitory effect of Sema 3A is selective

To rule out that the down-regulation of O4 in the presence of sema 3A was not a result of apoptosis of cells a tunnel assay was carried out. Although Sema3A has shown to induce apoptosis in monocyte-derived macrophages (Ji et al., 2009), no significant differences were observed in our experimental set up (Fig 34; $p > 0.05$, one-way ANOVA). Sema 3A therefore selectively affects OPC differentiation.

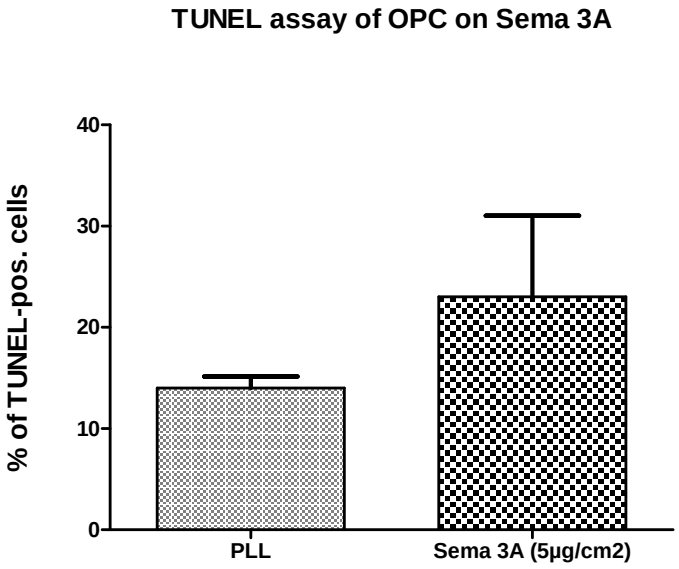


**Fig 34. The bar graph indicates that differentiation block mediated by the Sema 3A is selective**

### 7.3.3 Sema 3A inhibits CNS remyelination in gliotoxin model of remyelination

In a next step the hypothesis was tested that Sema 3A is an inhibitor of remyelination. For this purpose demyelinating lesions were induced in the caudal cerebellar peduncle of young-

adult female Sprague-Dawley rats by stereotactic infusion of ethidium bromide. During surgery a pair of infusion cannulae was also stereotactically placed at the same coordinates. 10 days later the cannulae were connected to a pair of subcutaneously placed osmotic minipumps (Alzet, 2002 model, US) delivering Sema 3A at a pumping rate of 0.5µl/hr or vehicle (PBS) into the demyelinated lesion. Animals were sacrificed at experimental day 28 and the tissue processed for light and electron microscopy or for in situ hybridization.

In Sema 3A infused lesions most axons remained demyelinated, and remyelination, where it occurred, was restricted to the border of the lesion. In sharp contrast, most axons in control animals were surrounded by thin hypodense rings with the prototypic appearance of remyelinated myelin sheaths (Blakemore, 1974).

A blinded scoring system was adopted to assess the extent of remyelination following digitalization of resin sections (Woodruff and Franklin, 1999). The results showed a significant difference between control and Sema 3A infused animals at 28 days (Fig 35; p =0.0005, Mann-Whitney U).

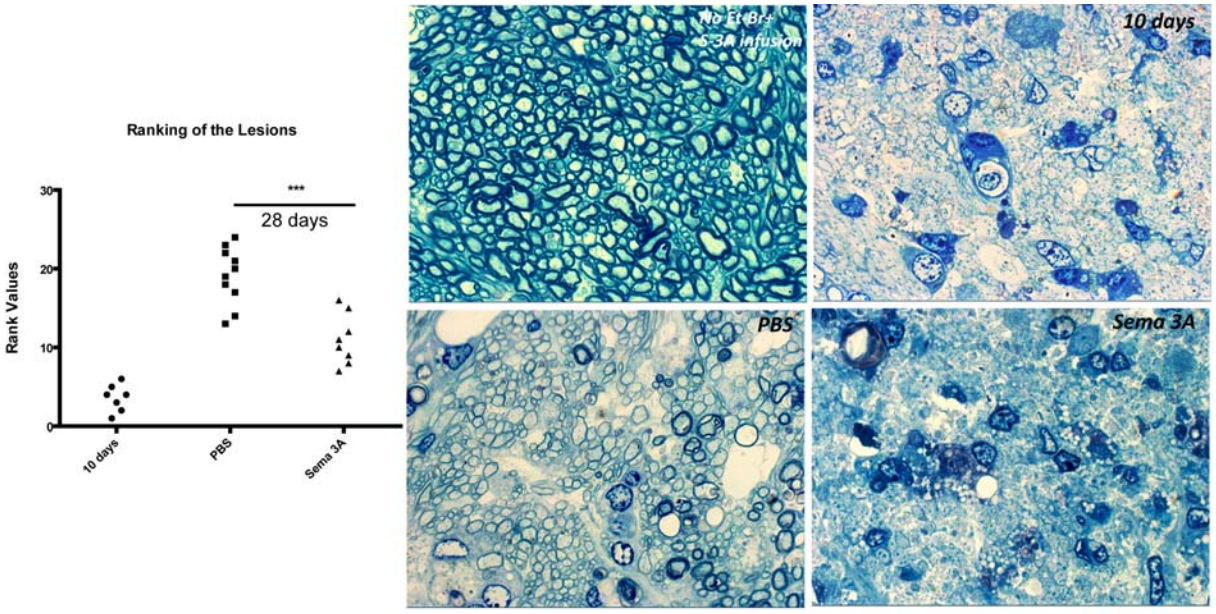


**Fig 35. Histological analysis of remyelination.** Ranking analysis showing a significant decrease in remyelination in animals which got Sema 3A infusion following demyelination. Transverse section of normal CCP which got the infusion of sema 3A showed no change in morphology of axons. On the 10 day of demyelination the axons had no myelin sheath. On the 28 day the control animals which got PBS infusion had the axons with thin rim of myelin sheath around them. In Sema 3A treated lesions the axons had no mylein sheath signifying impairment of myelin repair

### 7.3.4 Sema 3A infusion did not alter the lesion size

To visualize the demyelinated areas in the CCP and determine the sections carrying the largest lesion area, the tissue was stained with eriochrome cyanine staining on every 11$^{th}$ slide (each slide containing three sections). Eriochrome cyanine stains myelin sheaths, which appear blue on sections (Rabchevsky et al., 2001), whereas non-myelinated areas remain unstained. There was no significant difference between the average lesion areas is in all groups. The 10 day group had lesion with an average area of 0.6088 mm$^2$; Fc-IgG- 0.5680 mm$^2$ and ephrin B3- 0.6348mm$^2$. (Fig 36;p= 0,3280; one way ANOVA).

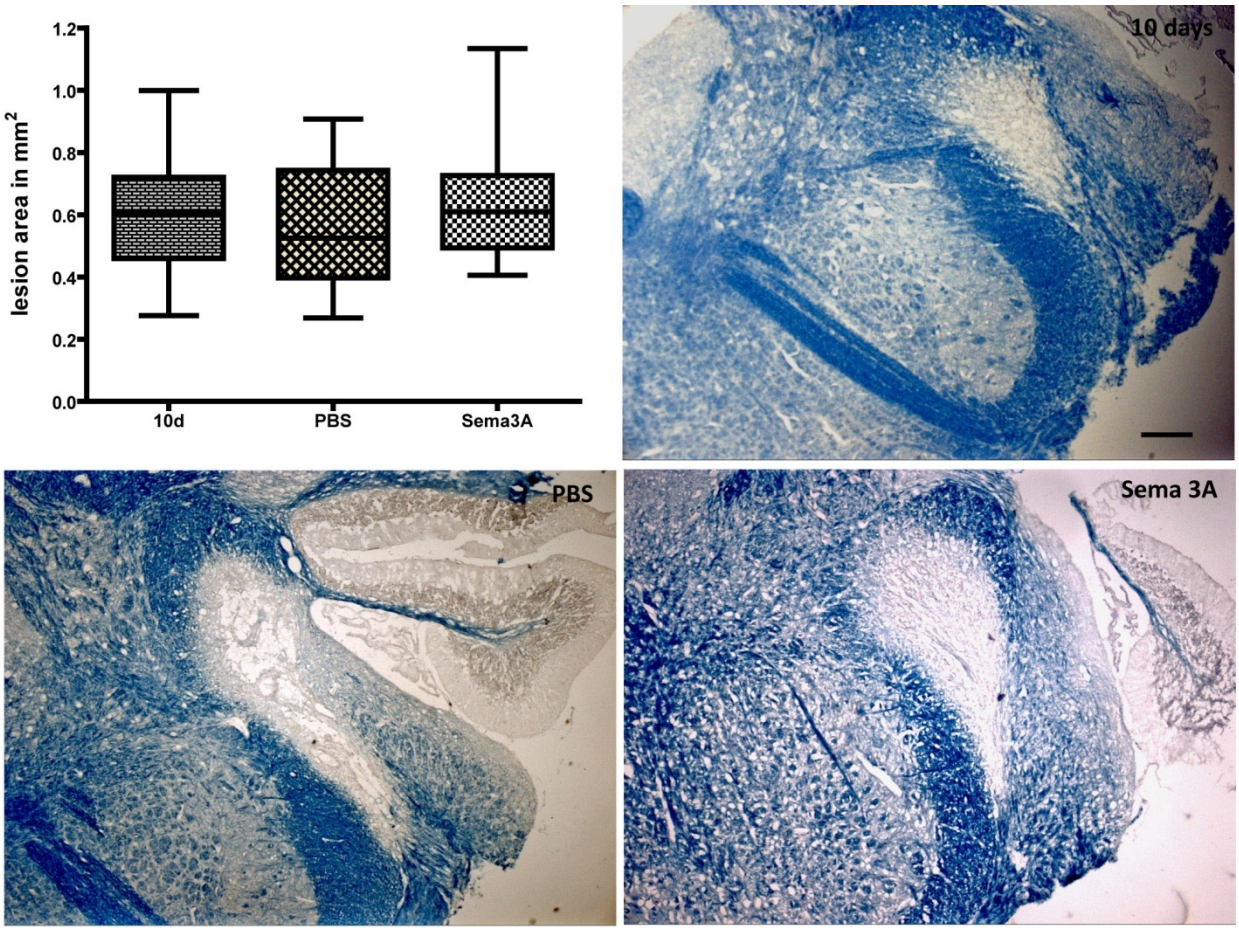


**Fig 36. Lesion size is unaffected in presence of Sema 3A.** The graph showing the average lesion area among different groups. The transverse section of resin section from 10 days, Fc-IgG and ephrin B3 infused lesison stained with eriochrome cyanine. Scale bar 30µm

### 7.3.5 Sema 3A doesn't affect the presence of the OPCs in the lesions

In order to determine the response of OPC in the lesion *in situ* hybridization was performed. Serial sections containing the centre of the lesion as determined on EC stained tissue were used for *in situ* hybridizations. In situ hybridization for PDGFRα mRNA+ cells within areas of demyelination has been successfully used to estimate the presence of OPCs (Kotter et al., 2006). Assessment of the number of PDGFRα-positive cells showed no differences between Sema3A-infused lesions (155.8 ± 10.10 cells / $mm^2$, N=7) 10 days (143.1 ± 20.80 cells / $mm^2$, N=11) and PBS-treated controls (155.0 ± 19.09 cells / $mm^2$, N=8) (Fig 37; p=0, 8542; one way ANOVA).

### 7.3.6 Sema 3A does n't affect the activation of OPCs in lesion

In situ hybridization for Nkx2.2 has been used to assess activated OPCs in remyelinating lesions (Fancy et al., 2004; Qi et al., 2001). In adult human CNS matter low levels of the Nkx2.2 are found in mature oligodendrocytes as compared to late progenitor cells(Kuhlmann et al., 2008b) . Assessment of Nkx2.2 revelaed a higher OPC density in 10 day group (268.8 ± 14.82 cells / $mm^2$, N=8, P = 0.0032) than controls 28 days post-lesion induction (PBS: 159.1 ± 28.84 cells / $mm^{2,}$ N=5). Interestingly, infusion of Sema3A was associated with a similar density of Nkx2.2-positive OPCs (176.5 ± 19.44 cells / $mm^2$, N=7, P = 0.6125) as

found in PBS controls. Similarly as with controls compared to 10 days samples, the amount of activated Nkx2.2-positive OPCs was markedly decreased in Sema3A-infused animals (Fig 37; p= 0.0021; one way ANOVA).

### 7.3.7 Sema 3A inhibits OPC lineage progression

To assess lineage progression of the OPC population within the lesions *in situ* hybridization for PLP/dm-20 was conducted. Sema3A infusion significantly decreased the density of PLP-positive cells in the lesion site (497.3 ± 127.9 cells / $mm^2$, N=7, p=0.0317) compared to PBS infused controls (911.0 ± 112.3 cells / $mm^2$, N=7). Levels of PLP-positive OLC following infusion of Sema3A infusion were comparable to those found in 10 days controls (506.4 ± 75.40 cells / $mm^2$, N=9), a time point at which lesions display minimal amounts of remyelination, whereas in 28 days PBS-controls had a significantly higher number of PLP-pos. OLs. (Fig 37; p=0, 0109; one way ANOVA; Dunnet post test; 10 days vs PBS and Sema 3A; P<0.05).

### 7.3.8 Sema 3A dosen't alter the presence of MOG-positive cells

As outlined in chapter 6, some studies suggested that MOG is a late marker of OPC differentiation (Wolswijk, 2002), whereas others reported contradictory findings (Li et al., 2002). Following in situ hybridization for MOG no differences between the Sema 3A /PBS infused and 10 days groups were (Fig 37; p=0,8442; one way ANOVA). The average number of MOG+ counts for 10 day was 213.1 ± 25.84 cells / $mm^2$, N=8; Sema 3A 259.9 ± 59.18 cells / $mm^2$ ,N=6 and PBS 271.9 ± 22.71 cells / $mm^2$ N=7). These findings support the notion that in remyelinating lesions a MOG-positive OPC population exists that change little as during the later stages of remyelination.

### 7.3.9 Sema 3A infusion does not alter the immune response

To assess whether Sema 3A infusion altered the presence of macrophages within the lesion *in situ* hybridizations on the macrophage scavenger receptor type B (MsrB) was conducted. The results showed that Sema3A had no impact on the macrophage response (167.7 ± 21.33 cells / $mm_2$, N=7) compared to PBS infused control lesions (135.3 ± 27.13 cells / $mm_2$, N=6) and levels were similar to that found in animals 10 days post-lesion induction (128.7 ± 25.91 cells / $mm_2$, N=10) (Fig 37; p=0, 8817; unpaired t test).

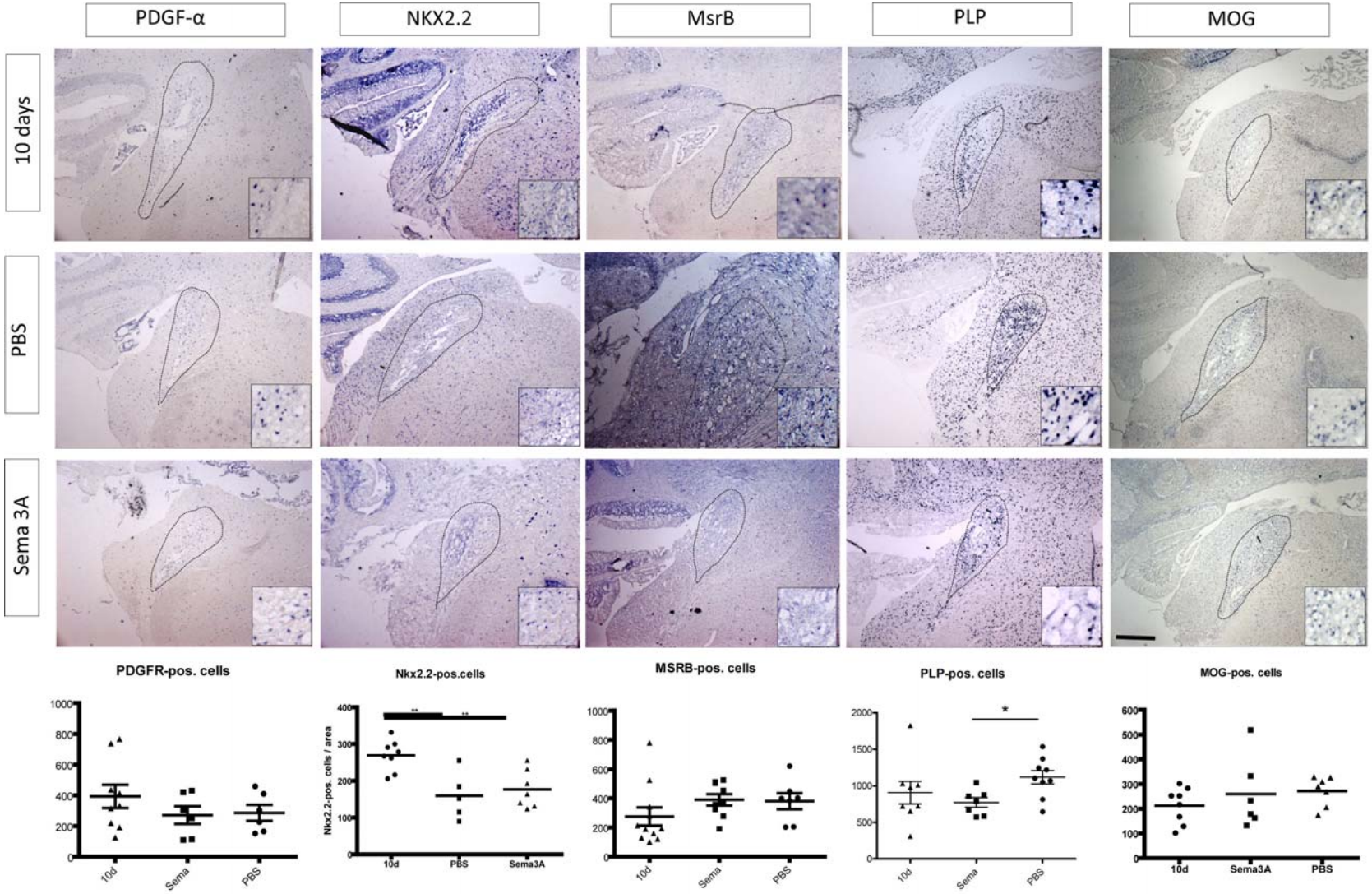


**Fig 37. Digoxigenin-labeled in situ hybridization on the demyelinating lesion from different groups for various different probes. Lower panel on the right hand side of the figure shows the positive cells from lesion area at higher magnification.Scale Bar 50µm**

### 7.3.10 Ultra structural analysis of the lesions

In a final step microscopy studies were conducted to confirm the light microscopic observations and for further descriptive analysis. This confirmed that the majority of the axons in Sema 3A infused animals remained naked. Some of the axons were contacted by cellular processes, resembling those of oligodendrocytes, which failed to form new myelin sheaths. Most of the axons had a healthy appearance and showed no sign of distress like axonal and mitochondrial swellings. As only occasionally reminiscent myelin debris was found, the bulk of myelin debris seemed to have been cleared by macrophages. In PBS infused lesions, the axons were surrounded by thin myelin sheaths, which are characteristic of remyelination. Schwann cell mediated remyelination was occasionally observed and the lesions did not show signs of myelin debris.

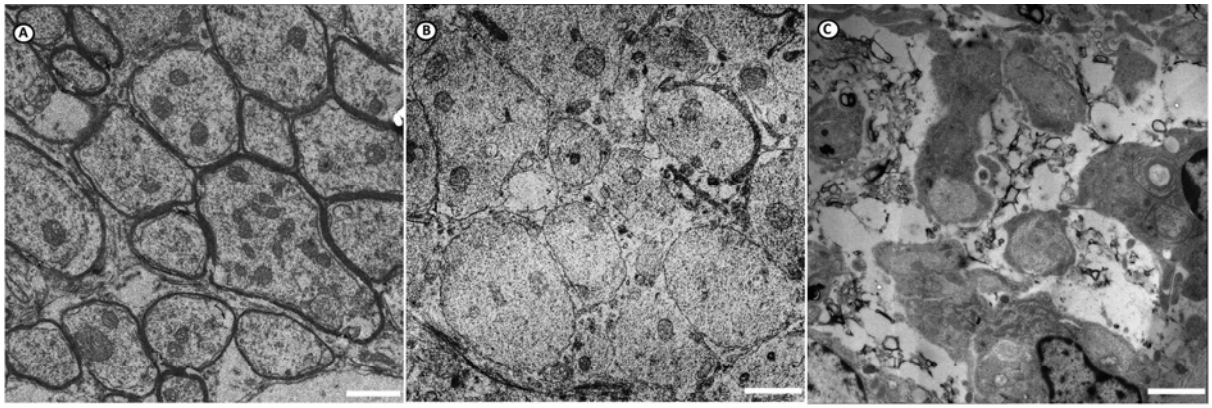


**Fig 38. Electron microscopic analysis of remyelination** A) Transverse section of PBS infused lesion. The axons have thin rim of myelin sheaths without any myelin debris. Scale bar 1µm B) Transverse section of the Sem 3A infused lesion. Majority of axons are demyelinated with few of them having one or two wraps of sheaths. Scale bar 1µm C) Oligodendrocyte process engaging axons but fail to form myelin membrane in Sema 3A treated lesion. Scale bar 2µm.

## 7.4 Discussion

Expression of Sema 3A has previously been associated with remyelination failure due to its inhibitory effects on OPC migration. Thus it was concluded that Sema3A could contribute to remyelination failure in cases where inefficient OPC recruitment occurred. However, an experimental proof has been lacking (Williams et al., 2007). On the other hand, a number of studies have demonstrated the presence of OLCs in chronic demyelinating MS lesions (Chang et al., 2002; Kuhlmann et al., 2008b). Thus it is thought that remyelination failure is more often associated with a failure of OPC differentiation than a failure of OPC recruitment. In this study Sema 3A was identified as a potent and selective inhibitor of OPC differentiation in vitro. Subsequently, these findings were translated into an in vivo model of remyelination. The results demonstrated a clear impairment of remyelination without disturbance in the presence of OLCs.

Thus the present findings imply another important remyelination-inhibiting effect of Sema3A in lesions in which OPCs were successfully recruited. Williams and colleagues have reported that following experimental demyelination and active MS lesion leads to an increase in semaphorin expression. Astrocytes and microglia are the main source of this semaphorin

expression, beside a small percentage is contributed by oligodendrocytes and neurons too. Futhermore, in both human and murine tissue, a subset of Olig2-positive oligodendroglial cells expresses the semaphorin receptors *NP1* and *NP2* around white matter demyelinating lesions (Williams et al., 2007). These results taken together suggest that the upregualtion of the semaphorin expression following demyelination has no effect on OPC recruitment; however it may inhibit OPC differentiation process. The results in the present chapter provide evidence that OPCs fail to differentiate into myelin forming oligodendrocytes in the presence of Sema 3A and hence the process of myelin repair fails.

The mechanisms of the Sema 3A induced OPC differentiation block have not yet been investigated. One of the first cytosolic proteins shown to link semaphorin receptor complexes to the actin cytoskeleton is collapsin response mediator protein (CRMP)-2, a member of a small family of cytosolic phosphoproteins (Goshima et al., 1995; Wang and Strittmatter, 1996). Sema 3A induced process retraction in oligodendrocyte progenitors, and oligodendrocytes and is mediated by CRMP-2 and CRMP-5 (Ricard et al., 2001; Ricard et al., 2000). Whether CRMPs are involved in mediating semaphorin-induced differentiation block on oligodendrocyte progenitors is unknown and needs to be elucidated. As inhibition Sema3A signalling has appeared as a prime target for promoting OPC differentiation, it will be essential to investigate the mechanisms of the Sema3A induced OPC differentiation block in future studies.

# Chapter 8
# Summary and Final conclusions

## Summary and Final conclusions

The main aim of thesis was to identify the molecular substrate of myelin which mediates inhibitory effect on OPC differentiation. Myelin is a complex structure with an unusual protein lipid ratio. By employing a protein purification approach, it was established that the inhibitory component in myelin is associated with the protein compartment. In a next step, to identify inhibitory proteins two approaches were applied. Firstly, a candidate protein approach was used, in which myelin proteins known to exert inhibitory effect on axon regeneration were tested. In this screen Ephrin B3 and Semaphorin 3A proved to exert inhibitory effects on OPC differentiation.

Second, a biochemical separation approach was employed to enrich the myelin inhibitory protein followed by mass spectrometric peptide identification. For this purpose MPE was subjected to a weak cationic CM column. Subsequently, pooled inhibitory fractions from several runs were subjected to a weak anionic High Q column. The proteins after two step purification were separated using 3D/Blue native PAGE. The separated proteins were identified using nano-HPLC-ESI-QTOF mass spectrometer. Out of 137 identified proteins only 19 had been previously identified in other myelin proteomic studies. The future investigation will focus on testing the identified proteins with respect to mediating inhibitory effects on OPC differentiation process.

Ephrin B3 emerged as the inhibitory protein on OPC differentiation process in the candidate protein approach. Its presence in OLCs in vitro as well as in in vivo, specifically in CNS myelin was established. Ephrin B3 is dynamically regulated in OLCs and increases as the cells differentiate which may suggest that it plays a role in the oligodendrocyte differentiation. In a next step it was confirmed that ephrin B3 exerts selective inhibitory effects on OPC differentiation in vitro. The presence of ephrin B3 not only induces a reduction of O4 expression but also a reduction in the complexity of OPC processes as well as down regulation of Nkx2.2, an important transcription factor necessary for oligodendrocyte differentiation. Ephrin/eph signaling invitro relies very much on the formation of clusters. The presence of pre-clustered ephrin B3+Fc-IgG in differentiation medium induced an increased inhibitory response on the OPC differentiation process. Furthermore, when pre-clustered Ephrin B3+Fc-IgG were presented to oligodendrocytes at a later stage it caused a reduction of process complexity and down regulation of MBP expression, although O4 expression remained unaffected.

It was then demonstrated that the inhibitory effect of ephrin B3 was reversed by antibody-mediated epitope masking. Interestingly, the inhibitory effect of MPE could also be reversed by masking MPE with ephrin B3 antibody; although further experiments indicated that at least one other inhibitory molecule is present in myelin. The mechanism by which ephrin B3 mediates its effects was examined by investigating RhoA and PKC signaling, both of which play a role in mediating inhibitory effects of myelin on OPC differentiation. Whereas ephrin B3 induced an activation of Rho A, no involvement of PKC signaling was detected. From this it was concluded that another molecule must exist in myelin exerting inhibitory effects on

OPCs via activation of PKC. Future work is required to identify this inhibitor as well as to identify the receptors and down-stream signaling partners mediating the effect of ephrin B3 in OPCs and OLCs.

The hypothesis that ephrin B3 inhibits CNS remyelination was explored by induction of focal demyelination in the caudal cerebellar peduncle in female young-adult Sprague-Dawley rats. Subsequently ephrin B3 or control vehicle was stereotactically infused into the lesion. Remyelination is complete by four weeks in this model. Light microscopic analysis showed significantly reduced remyelination in ephrin B3 infused lesions while cellular analysis on the basis of insitu hybridization showed no differences in the expression of immature or mature OLC markers in mRNA level. Analysis on an ultrastructural level confirmed that remyelination had failed in ephrin B3 treated animals meanwhile many axons were engaged with the oligodendrocyte like processes which failed to form myelin sheaths. An important study that was beyond the reach of this thesis will be to examine non-myelinating MS lesions for the presence of Ephrin B3.

Finally, the effects of Semaphorin 3A, another candidate protein which emerged from the candidate protein approach, on OPC differentiation and CNS remyelination were studied. The selectivity of Sema 3A induced OPC differentiation inhibition was confirmed. Subsequently, the hypothesis tested that Sema 3A inhibits remyelination. For this purpose a similar experimental design as in the ephrin B3 in vivio experiment was adopted relying on inducing of focal demyelination in the CCP and subsequent stereotactic infusion of Sema 3A. Histological analysis showed a significant impairment of remyelination in Sema 3A infused as compared to controls; the cellular analysis demonstrated that the presence of Sema 3A inhibits oligodendrocyte lineage progression as the number of PLP-positive cells was significantly reduced. Finally, electron microscopic analysis confirmed failed remyelination in Sema 3A treated animals. Future studies will be required to unravel the receptor and intracellular signaling mechanisms that mediate the inhibition of Sema 3A on OPC differentiation. Furthermore, the importance of Sema 3A needs to be addressed, e.g. using a specific inhibitor of Sema 3A.

# Chapter 9
# References

## References


Unified nomenclature for the semaphorins/collapsins. Semaphorin Nomenclature Committee. Cell, 1999; 97: 551-2.

Agresti C, D'Urso D, Levi G. Reversible inhibitory effects of interferon-gamma and tumour necrosis factor-alpha on oligodendroglial lineage cell proliferation and differentiation in vitro. Eur J Neurosci, 1996; 8: 1106-16.

Aguirre A, Dupree JL, Mangin JM, Gallo V. A functional role for EGFR signaling in myelination and remyelination. Nat Neurosci, 2007; 10: 990-1002.

Alcantara S, Ruiz M, De Castro F, Soriano E, Sotelo C. Netrin 1 acts as an attractive or as a repulsive cue for distinct migrating neurons during the development of the cerebellar system. Development, 2000; 127: 1359-72.

Amor S, Groome N, Linington C, Morris MM, Dornmair K, Gardinier MV, Matthieu JM, Baker D. Identification of epitopes of myelin oligodendrocyte glycoprotein for the induction of experimental allergic encephalomyelitis in SJL and Biozzi AB/H mice. J Immunol, 1994; 153: 4349-56.

An WF, Bowlby MR, Betty M, Cao J, Ling HP, Mendoza G, Hinson JW, Mattsson KI, Strassle BW, Trimmer JS, Rhodes KJ. Modulation of A-type potassium channels by a family of calcium sensors. Nature, 2000; 403: 553-6.

Andreasen A, Jakobsen J, Petersen T, Andersen H. Fatigued patients with multiple sclerosis have impaired central muscle activation. Mult Scler, 2009; 15: 818-27.

Apel ED, Litchfield DW, Clark RH, Krebs EG, Storm DR. Phosphorylation of neuromodulin (GAP-43) by casein kinase II. Identification of phosphorylation sites and regulation by calmodulin. J Biol Chem, 1991; 266: 10544-51.

Armstrong RC, Le TQ, Flint NC, Vana AC, Zhou YX. Endogenous cell repair of chronic demyelination. J Neuropathol Exp Neurol, 2006; 65: 245-56.

Armstrong RC, Le TQ, Frost EE, Borke RC, Vana AC. Absence of fibroblast growth factor 2 promotes oligodendroglial repopulation of demyelinated white matter. J Neurosci, 2002; 22: 8574-85.

Arnett HA, Mason J, Marino M, Suzuki K, Matsushima GK, Ting JP. TNF alpha promotes proliferation of oligodendrocyte progenitors and remyelination. Nat.Neurosci., 2001; 4: 1116-22.

Arnett HA, Wang Y, Matsushima GK, Suzuki K, Ting JP. Functional genomic analysis of remyelination reveals importance of inflammation in oligodendrocyte regeneration. J.Neurosci., 2003; 23: 9824-32.

Aveldano MI, Diaz RS, Regueiro P, Monreal J. Solubilization of myelin membranes by detergents. J Neurochem, 1991; 57: 250-7.

Back SA, Tuohy TM, Chen H, Wallingford N, Craig A, Struve J, Luo NL, Banine F, Liu Y, Chang A, Trapp BD, Bebo BF, Rao MS, Sherman LS. Hyaluronan accumulates in demyelinated lesions and inhibits oligodendrocyte progenitor maturation. Nat.Med., 2005.

Baer AS, Syed YA, Kang SU, Mitteregger D, Vig R, Ffrench-Constant C, Franklin RJ, Altmann F, Lubec G, Kotter MR. Myelin-mediated inhibition of oligodendrocyte precursor differentiation can be overcome by pharmacological modulation of Fyn-RhoA and protein kinase C signalling. Brain, 2009; 132: 465-81.

Bagnard D, Lohrum M, Uziel D, Puschel AW, Bolz J. Semaphorins act as attractive and repulsive guidance signals during the development of cortical projections. Development, 1998; 125: 5043-53.

Bansal R, Kumar M, Murray K, Morrison RS, Pfeiffer SE. Regulation of FGF receptors in the oligodendrocyte lineage. Mol Cell Neurosci, 1996; 7: 263-75.

Barbin G, Aigrot MS, Charles P, Foucher A, Grumet M, Schachner M, Zalc B, Lubetzki C. Axonal cell-adhesion molecule L1 in CNS myelination. Neuron Glia Biol, 2004; 1: 65-72.

Baron W, Shattil SJ, ffrench-Constant C. The oligodendrocyte precursor mitogen PDGF stimulates proliferation by activation of alpha(v)beta3 integrins. EMBO J, 2002; 21: 1957-66.

Barres BA, Hart IK, Coles HS, Burne JF, Voyvodic JT, Richardson WD, Raff MC. Cell death and control of cell survival in the oligodendrocyte lineage. Cell, 1992; 70: 31-46.

Barres BA, Lazar MA, Raff MC. A novel role for thyroid hormone, glucocorticoids and retinoic acid in timing oligodendrocyte development. Development, 1994; 120: 1097-108.

Barres BA, Schmid R, Sendnter M, Raff MC. Multiple extracellular signals are required for long-term oligodendrocyte survival. Development, 1993; 118: 283-95.

Batlle E, Henderson JT, Beghtel H, van den Born MM, Sancho E, Huls G, Meeldijk J, Robertson J, van de Wetering M, Pawson T, Clevers H. Beta-catenin and TCF mediate cell positioning in the intestinal epithelium by controlling the expression of EphB/ephrinB. Cell, 2002; 111: 251-63.

Battaglia AA, Sehayek K, Grist J, McMahon SB, Gavazzi I. EphB receptors and ephrin-B ligands regulate spinal sensory connectivity and modulate pain processing. Nat Neurosci, 2003; 6: 339-40.

Baumann N, Pham-Dinh D. Biology of oligodendrocyte and myelin in the mammalian central nervous system. Physiol Rev, 2001; 81: 871-927.

Bechmann I, Nitsch R. Identification of phagocytic glial cells after lesion-induced anterograde degeneration using double-fluorescence labeling: combination of axonal tracing and lectin or immunostaining. Histochem Cell Biol, 1997; 107: 391-7.

Behar O, Golden JA, Mashimo H, Schoen FJ, Fishman MC. Semaphorin III is needed for normal patterning and growth of nerves, bones and heart. Nature, 1996; 383: 525-8.

Behlke J, Labudde D, Ristau O. Self-association studies on the EphB2 receptor SAM domain using analytical ultracentrifugation. Eur Biophys J, 2001; 30: 411-5.

Bennett MK, Garcia-Arraras JE, Elferink LA, Peterson K, Fleming AM, Hazuka CD, Scheller RH. The syntaxin family of vesicular transport receptors. Cell, 1993; 74: 863-73.

Benowitz LI, Routtenberg A. GAP-43: an intrinsic determinant of neuronal development and plasticity. Trends Neurosci, 1997; 20: 84-91.

Benson MD, Romero MI, Lush ME, Lu QR, Henkemeyer M, Parada LF. Ephrin-B3 is a myelin-based inhibitor of neurite outgrowth. Proc Natl Acad Sci U S A, 2005; 102: 10694-9.

Bergemann AD, Zhang L, Chiang MK, Brambilla R, Klein R, Flanagan JG. Ephrin-B3, a ligand for the receptor EphB3, expressed at the midline of the developing neural tube. Oncogene, 1998; 16: 471-80.

Bieber AJ, Kerr S, Rodriguez M. Efficient central nervous system remyelination requires T cells. Ann.Neurol, 2003; 53: 680-4.

Bieber AJ, Warrington A, Asakura K, Ciric B, Kaveri SV, Pease LR, Rodriguez M. Human antibodies accelerate the rate of remyelination following lysolecithin-induced demyelination in mice. Glia, 2002; 37: 241-9.

Billard C, Delaire S, Raffoux E, Bensussan A, Boumsell L. Switch in the protein tyrosine phosphatase associated with human CD100 semaphorin at terminal B-cell differentiation stage. Blood, 2000; 95: 965-72.

Birgbauer E, Cowan CA, Sretavan DW, Henkemeyer M. Kinase independent function of EphB receptors in retinal axon pathfinding to the optic disc from dorsal but not ventral retina. Development, 2000; 127: 1231-41.

Blakemore WF. Pattern of remyelination in the CNS. Nature, 1974; 249: 577-8.

Blakemore WF, Crang AJ. The relationship between type-1 astrocytes, Schwann cells and oligodendrocytes following transplantation of glial cell cultures into demyelinating lesions in the adult rat spinal cord. J Neurocytol, 1989; 18: 519-28.

Blakemore WF, Gilson JM, Crang AJ. The presence of astrocytes in areas of demyelination influences remyelination following transplantation of oligodendrocyte progenitors. Exp Neurol, 2003; 184: 955-63.

Boguski MS, McIntosh MW. Biomedical informatics for proteomics. Nature, 2003; 422: 233-7.

Bondurand N, Girard M, Pingault V, Lemort N, Dubourg O, Goossens M. Human Connexin 32, a gap junction protein altered in the X-linked form of Charcot-Marie-Tooth disease, is directly regulated by the transcription factor SOX10. Hum Mol Genet, 2001; 10: 2783-95.

Braisted JE, McLaughlin T, Wang HU, Friedman GC, Anderson DJ, O'Leary D D. Graded and lamina-specific distributions of ligands of EphB receptor tyrosine kinases in the developing retinotectal system. Dev Biol, 1997; 191: 14-28.

Braunewell KH, Gundelfinger ED. Intracellular neuronal calcium sensor proteins: a family of EF-hand calcium-binding proteins in search of a function. Cell Tissue Res, 1999; 295: 1-12.

Brinkmann BG, Agarwal A, Sereda MW, Garratt AN, Muller T, Wende H, Stassart RM, Nawaz S, Humml C, Velanac V, Radyushkin K, Goebbels S, Fischer TM, Franklin RJ, Lai C,

Ehrenreich H, Birchmeier C, Schwab MH, Nave KA. Neuregulin-1/ErbB signaling serves distinct functions in myelination of the peripheral and central nervous system. Neuron, 2008; 59: 581-95.

Briscoe J, Pierani A, Jessell TM, Ericson J. A homeodomain protein code specifies progenitor cell identity and neuronal fate in the ventral neural tube. Cell, 2000; 101: 435-45.

Brosnan CF, Raine CS. Mechanisms of immune injury in multiple sclerosis. Brain Pathol, 1996; 6: 243-57.

Bruckner K, Pasquale EB, Klein R. Tyrosine Phosphorylation of Transmembrane Ligands for Eph Receptors. Science, 1997; 275: 1640-3.

Bundesen LQ, Scheel TA, Bregman BS, Kromer LF. Ephrin-B2 and EphB2 regulation of astrocyte-meningeal fibroblast interactions in response to spinal cord lesions in adult rats. J Neurosci, 2003; 23: 7789-800.

Cai D, Deng K, Mellado W, Lee J, Ratan RR, Filbin MT. Arginase I and polyamines act downstream from cyclic AMP in overcoming inhibition of axonal growth MAG and myelin in vitro. Neuron, 2002; 35: 711-9.

Carrion AM, Link WA, Ledo F, Mellstrom B, Naranjo JR. DREAM is a Ca2+-regulated transcriptional repressor. Nature, 1999; 398: 80-4.

Carroll WM, Jennings AR, Mastaglia FL. Experimental demyelinating optic neuropathy induced by intra-neural injection of galactocerebroside antiserum. J Neurol Sci, 1984; 65: 125-35.

Cattaneo E, Zuccato C, Tartari M. Normal huntingtin function: an alternative approach to Huntington's disease. Nat Rev Neurosci, 2005; 6: 919-30.

Cerghet M, Skoff RP, Bessert D, Zhang Z, Mullins C, Ghandour MS. Proliferation and death of oligodendrocytes and myelin proteins are differentially regulated in male and female rodents. J Neurosci, 2006; 26: 1439-47.

Chang A, Nishiyama A, Peterson J, Prineas J, Trapp BD. NG2-positive oligodendrocyte progenitor cells in adult human brain and multiple sclerosis lesions. J Neurosci, 2000; 20: 6404-12.

Chang A, Tourtellotte WW, Rudick R, Trapp BD. Premyelinating oligodendrocytes in chronic lesions of multiple sclerosis. N Engl J Med, 2002; 346: 165-73.

Charles P, Hernandez MP, Stankoff B, Aigrot MS, Colin C, Rougon G, Zalc B, Lubetzki C. Negative regulation of central nervous system myelination by polysialylated-neural cell adhesion molecule. Proc Natl Acad Sci U S A, 2000; 97: 7585-90.

Charles P, Reynolds R, Seilhean D, Rougon G, Aigrot MS, Niezgoda A, Zalc B, Lubetzki C. Re-expression of PSA-NCAM by demyelinated axons: an inhibitor of remyelination in multiple sclerosis? Brain, 2002; 125: 1972-9.

Chedotal A, Del Rio JA, Ruiz M, He Z, Borrell V, de Castro F, Ezan F, Goodman CS, Tessier-Lavigne M, Sotelo C, Soriano E. Semaphorins III and IV repel hippocampal axons via two distinct receptors. Development, 1998; 125: 4313-23.

Chen MS, Huber AB, van der Haar ME, Frank M, Schnell L, Spillmann AA, Christ F, Schwab ME. Nogo-A is a myelin-associated neurite outgrowth inhibitor and an antigen for monoclonal antibody IN-1. Nature, 2000; 403: 434-9.

Cheng HJ, Bagri A, Yaron A, Stein E, Pleasure SJ, Tessier-Lavigne M. Plexin-A3 mediates semaphorin signaling and regulates the development of hippocampal axonal projections. Neuron, 2001; 32: 249-63.

Chisholm A, Tessier-Lavigne M. Conservation and divergence of axon guidance mechanisms. Curr Opin Neurobiol, 1999; 9: 603-15.

Colman DR, Kreibich G, Frey AB, Sabatini DD. Synthesis and incorporation of myelin polypeptides into CNS myelin. J Cell Biol, 1982; 95: 598-608.

Connor RJ, Menzel P, Pasquale EB. Expression and tyrosine phosphorylation of Eph receptors suggest multiple mechanisms in patterning of the visual system. Dev Biol, 1998; 193: 21-35.

Cowan CA, Henkemeyer M. The SH2/SH3 adaptor Grb4 transduces B-ephrin reverse signals. Nature, 2001; 413: 174-9.

Cowan CA, Yokoyama N, Saxena A, Chumley MJ, Silvany RE, Baker LA, Srivastava D, Henkemeyer M. Ephrin-B2 reverse signaling is required for axon pathfinding and cardiac valve formation but not early vascular development. Dev Biol, 2004; 271: 263-71.

Curtin KD, Meinertzhagen IA, Wyman RJ. Basigin (EMMPRIN/CD147) interacts with integrin to affect cellular architecture. J Cell Sci, 2005; 118: 2649-60.

D'Souza B, Miyamoto A, Weinmaster G. The many facets of Notch ligands. Oncogene, 2008; 27: 5148-67.

Davis S, Gale NW, Aldrich TH, Maisonpierre PC, Lhotak V, Pawson T, Goldfarb M, Yancopoulos GD. Ligands for EPH-related receptor tyrosine kinases that require membrane attachment or clustering for activity. Science, 1994; 266: 816-9.

Davy A, Gale NW, Murray EW, Klinghoffer RA, Soriano P, Feuerstein C, Robbins SM. Compartmentalized signaling by GPI-anchored ephrin-A5 requires the Fyn tyrosine kinase to regulate cellular adhesion. Genes Dev, 1999; 13: 3125-35.

Dawson J, Miltz W, Mir AK, Wiessner C. Targeting monocyte chemoattractant protein-1 signalling in disease. Expert Opin Ther Targets, 2003; 7: 35-48.

Dawson MR, Levine JM, Reynolds R. NG2-expressing cells in the central nervous system: are they oligodendroglial progenitors? J Neurosci Res, 2000; 61: 471-9.

de Wit J, Verhaagen J. Role of semaphorins in the adult nervous system. Prog Neurobiol, 2003; 71: 249-67.

Domeniconi M, Cao Z, Spencer T, Sivasankaran R, Wang K, Nikulina E, Kimura N, Cai H, Deng K, Gao Y, He Z, Filbin M. Myelin-associated glycoprotein interacts with the Nogo66 receptor to inhibit neurite outgrowth. Neuron, 2002; 35: 283-90.

Don RH, Cox PT, Wainwright BJ, Baker K, Mattick JS. 'Touchdown' PCR to circumvent spurious priming during gene amplification. Nucleic Acids Res, 1991; 19: 4008.

Dottori M, Hartley L, Galea M, Paxinos G, Polizzotto M, Kilpatrick T, Bartlett PF, Murphy M, Kontgen F, Boyd AW. EphA4 (Sek1) receptor tyrosine kinase is required for the development of the corticospinal tract. Proc Natl Acad Sci U S A, 1998; 95: 13248-53.

Du J, Tran T, Fu C, Sretavan DW. Upregulation of EphB2 and ephrin-B2 at the optic nerve head of DBA/2J glaucomatous mice coincides with axon loss. Invest Ophthalmol Vis Sci, 2007; 48: 5567-81.

Du Y, Fischer TZ, Lee LN, Lercher LD, Dreyfus CF. Regionally specific effects of BDNF on oligodendrocytes. Dev Neurosci, 2003; 25: 116-26.

Duchala CS, Asotra K, Macklin WB. Expression of cell surface markers and myelin proteins in cultured oligodendrocytes from neonatal brain of rat and mouse: a comparative study. Dev Neurosci, 1995; 17: 70-80.

Duncan ID, Brower A, Kondo Y, Curlee JF, Jr., Schultz RD. Extensive remyelination of the CNS leads to functional recovery. Proc Natl Acad Sci U S A, 2009; 106: 6832-6.

Eastwood SL, Law AJ, Everall IP, Harrison PJ. The axonal chemorepellant semaphorin 3A is increased in the cerebellum in schizophrenia and may contribute to its synaptic pathology. Mol Psychiatry, 2003; 8: 148-55.

Eckhardt F, Behar O, Calautti E, Yonezawa K, Nishimoto I, Fishman MC. A novel transmembrane semaphorin can bind c-src. Mol Cell Neurosci, 1997; 9: 409-19.

Edgar JM, McLaughlin M, Yool D, Zhang SC, Fowler JH, Montague P, Barrie JA, McCulloch MC, Duncan ID, Garbern J, Nave KA, Griffiths IR. Oligodendroglial modulation of fast axonal transport in a mouse model of hereditary spastic paraplegia. J.Cell Biol., 2004; 166: 121-31.

Ellison JA, Scully SA, de Vellis J. Evidence for neuronal regulation of oligodendrocyte development: cellular localization of platelet-derived growth factor alpha receptor and A-chain mRNA during cerebral cortex development in the rat. J Neurosci Res, 1996; 45: 28-39.

Emery B, Agalliu D, Cahoy JD, Watkins TA, Dugas JC, Mulinyawe SB, Ibrahim A, Ligon KL, Rowitch DH, Barres BA. Myelin gene regulatory factor is a critical transcriptional regulator required for CNS myelination. Cell, 2009; 138: 172-85.

Fadool JM, Linser PJ. 5A11 antigen is a cell recognition molecule which is involved in neuronal-glial interactions in avian neural retina. Dev Dyn, 1993; 196: 252-62.

Fancy SP, Baranzini SE, Zhao C, Yuk DI, Irvine KA, Kaing S, Sanai N, Franklin RJ, Rowitch DH. Dysregulation of the Wnt pathway inhibits timely myelination and remyelination in the mammalian CNS. Genes Dev, 2009; 23: 1571-85.

Fancy SP, Zhao C, Franklin RJM. Increased expression of Nkx2.2 and Olig2 identifies reactive oligodendrocyte progenitor cells responding to demyelination in the adult CNS. Mol.Cell Neurosci., 2004; 27: 247-54.

Feiner L, Webber AL, Brown CB, Lu MM, Jia L, Feinstein P, Mombaerts P, Epstein JA, Raper JA. Targeted disruption of semaphorin 3C leads to persistent truncus arteriosus and aortic arch interruption. Development, 2001; 128: 3061-70.

Ferguson B, Matyszak MK, Esiri MM, Perry VH. Axonal damage in acute multiple sclerosis lesions. Brain, 1997; 120 ( Pt 3): 393-9.

Filbin MT. Myelin-associated inhibitors of axonal regeneration in the adult mammalian CNS. Nat.Rev Neurosci., 2003; 4: 703-13.

Fok-Seang J, Miller RH. Distribution and differentiation of A2B5+ glial precursors in the developing rat spinal cord. J Neurosci Res, 1994; 37: 219-35.

Foote AK, Blakemore WF. Inflammation stimulates remyelination in areas of chronic demyelination. Brain, 2005; 128: 528-39.

Fournier AE, GrandPre T, Strittmatter SM. Identification of a receptor mediating Nogo-66 inhibition of axonal regeneration. Nature, 2001; 409: 341-6.

Franklin RJ. Why does remyelination fail in multiple sclerosis? Nat Rev Neurosci, 2002a; 3: 705-14.

Franklin RJ, Ffrench-Constant C. Remyelination in the CNS: from biology to therapy. Nat Rev Neurosci, 2008; 9: 839-55.

Franklin RJM. Why does remyelination fail in multiple sclerosis? Nat.Rev.Neurosci., 2002b; 3: 705-14.

Franklin RJM, Barnett SC. The electron microscopic appearance of the beta-galactosidase reaction product. Acta Neuropathol (Berl), 1991; 81: 686-7.

Franklin RJM, Blakemore WF. Transplanting oligodendrocyte progenitors into the adult CNS. J Anat, 1997; 190 ( Pt 1): 23-33.

Franklin RJM, Gilson JM. Remyelination in the CNS of the hypothyroid rat. Neuroreport, 1996; 7: 1526-30.

Fruttiger M, Karlsson L, Hall AC, Abramsson A, Calver AR, Bostrom H, Willetts K, Bertold CH, Heath JK, Betsholtz C, Richardson WD. Defective oligodendrocyte development and severe hypomyelination in PDGF-A knockout mice. Development, 1999; 126: 457-67.

Gao PP, Yue Y, Zhang JH, Cerretti DP, Levitt P, Zhou R. Regulation of thalamic neurite outgrowth by the Eph ligand ephrin-A5: implications in the development of thalamocortical projections. Proc Natl Acad Sci U S A, 1998; 95: 5329-34.

Genain CP, Cannella B, Hauser SL, Raine CS. Identification of autoantibodies associated with myelin damage in multiple sclerosis. Nat.Med., 1999; 5: 170-5.

Gherardi E, Love CA, Esnouf RM, Jones EY. The sema domain. Curr Opin Struct Biol, 2004; 14: 669-78.

Gilson J, Blakemore WF. Failure of remyelination in areas of demyelination produced in the spinal cord of old rats. Neuropathol Appl Neurobiol, 1993; 19: 173-81.

Goldberg JL, Vargas ME, Wang JT, Mandemakers W, Oster SF, Sretavan DW, Barres BA. An oligodendrocyte lineage-specific semaphorin, Sema5A, inhibits axon growth by retinal ganglion cells. J Neurosci., 2004; 24: 4989-99.

Goldshmit Y, Galea MP, Wise G, Bartlett PF, Turnley AM. Axonal regeneration and lack of astrocytic gliosis in EphA4-deficient mice. J Neurosci, 2004; 24: 10064-73.

Gomes WA, Mehler MF, Kessler JA. Transgenic overexpression of BMP4 increases astroglial and decreases oligodendroglial lineage commitment. Dev Biol, 2003; 255: 164-77.

Goshima Y, Nakamura F, Strittmatter P, Strittmatter SM. Collapsin-induced growth cone collapse mediated by an intracellular protein related to UNC-33. Nature, 1995; 376: 509-14.

Gregg C, Shikar V, Larsen P, Mak G, Chojnacki A, Yong VW, Weiss S. White matter plasticity and enhanced remyelination in the maternal CNS. J Neurosci, 2007; 27: 1812-23.

Guest JD, Hiester ED, Bunge RP. Demyelination and Schwann cell responses adjacent to injury epicenter cavities following chronic human spinal cord injury. Exp Neurol, 2005; 192: 384-93.

Guo H, Zucker S, Gordon MK, Toole BP, Biswas C. Stimulation of matrix metalloproteinase production by recombinant extracellular matrix metalloproteinase inducer from transfected Chinese hamster ovary cells. J Biol Chem, 1997; 272: 24-7.

Hamasaki T, Goto S, Nishikawa S, Ushio Y. A role of netrin-1 in the formation of the subcortical structure striatum: repulsive action on the migration of late-born striatal neurons. J Neurosci, 2001; 21: 4272-80.

Hashimoto M, Ino H, Koda M, Murakami M, Yoshinaga K, Yamazaki M, Moriya H. Regulation of semaphorin 3A expression in neurons of the rat spinal cord and cerebral cortex after transection injury. Acta Neuropathol, 2004; 107: 250-6.

Hattori M, Osterfield M, Flanagan JG. Regulated cleavage of a contact-mediated axon repellent. Science, 2000; 289: 1360-5.

Hauser SL. Multiple sclerosis: tip of the iceberg? Ann Neurol, 2006; 59: 11A-2A.

Hauser SL, Oksenberg JR. The neurobiology of multiple sclerosis: genes, inflammation, and neurodegeneration. Neuron, 2006; 52: 61-76.

He Y, Dupree J, Wang J, Sandoval J, Li J, Liu H, Shi Y, Nave KA, Casaccia-Bonnefil P. The transcription factor Yin Yang 1 is essential for oligodendrocyte progenitor differentiation. Neuron, 2007; 55: 217-30.

Hemler ME. Tetraspanin functions and associated microdomains. Nat Rev Mol Cell Biol, 2005; 6: 801-11.

Hendricks KB, Wang BQ, Schnieders EA, Thorner J. Yeast homologue of neuronal frequenin is a regulator of phosphatidylinositol-4-OH kinase. Nat Cell Biol, 1999; 1: 234-41.

Henkemeyer M, Orioli D, Henderson JT, Saxton TM, Roder J, Pawson T, Klein R. Nuk controls pathfinding of commissural axons in the mammalian central nervous system. Cell, 1996; 86: 35-46.

Himanen JP, Chumley MJ, Lackmann M, Li C, Barton WA, Jeffrey PD, Vearing C, Geleick D, Feldheim DA, Boyd AW, Henkemeyer M, Nikolov DB. Repelling class discrimination: ephrin-A5 binds to and activates EphB2 receptor signaling. Nat Neurosci, 2004; 7: 501-9.

Himanen JP, Nikolov DB. Eph receptors and ephrins. Int J Biochem Cell Biol, 2003; 35: 130-4.

Himanen JP, Rajashankar KR, Lackmann M, Cowan CA, Henkemeyer M, Nikolov DB. Crystal structure of an Eph receptor-ephrin complex. Nature, 2001; 414: 933-8.

Hindges R, McLaughlin T, Genoud N, Henkemeyer M, O'Leary DD. EphB forward signaling controls directional branch extension and arborization required for dorsal-ventral retinotopic mapping. Neuron, 2002; 35: 475-87.

Hinks GL, Franklin RJM. Delayed changes in growth factor gene expression during slow remyelination in the CNS of aged rats. Mol.Cell Neurosci., 2000; 16: 542-56.

Hirsch E, Hu LJ, Prigent A, Constantin B, Agid Y, Drabkin H, Roche J. Distribution of semaphorin IV in adult human brain. Brain Res, 1999; 823: 67-79.

Holland SJ, Gale NW, Mbamalu G, Yancopoulos GD, Henkemeyer M, Pawson T. Bidirectional signalling through the EPH-family receptor Nuk and its transmembrane ligands. Nature, 1996; 383: 722-5.

Holmberg J, Armulik A, Senti KA, Edoff K, Spalding K, Momma S, Cassidy R, Flanagan JG, Frisen J. Ephrin-A2 reverse signaling negatively regulates neural progenitor proliferation and neurogenesis. Genes Dev, 2005; 19: 462-71.

Horner PJ, Power AE, Kempermann G, Kuhn HG, Palmer TD, Winkler J, Thal LJ, Gage FH. Proliferation and differentiation of progenitor cells throughout the intact adult rat spinal cord. J.Neurosci., 2000; 20: 2218-28.

Hou ST, Keklikian A, Slinn J, O'Hare M, Jiang SX, Aylsworth A. Sustained up-regulation of semaphorin 3A, Neuropilin1, and doublecortin expression in ischemic mouse brain during long-term recovery. Biochem Biophys Res Commun, 2008; 367: 109-15.

Huang JK, Phillips GR, Roth AD, Pedraza L, Shan W, Belkaid W, Mi S, Fex-Svenningsen A, Florens L, Yates JR, 3rd, Colman DR. Glial membranes at the node of Ranvier prevent neurite outgrowth. Science, 2005; 310: 1813-7.

Hubbard SR, Till JH. Protein tyrosine kinase structure and function. Annu Rev Biochem, 2000; 69: 373-98.

Huynh-Do U, Stein E, Lane AA, Liu H, Cerretti DP, Daniel TO. Surface densities of ephrin-B1 determine EphB1-coupled activation of cell attachment through alphavbeta3 and alpha5beta1 integrins. EMBO J, 1999; 18: 2165-73.

Imamoto K, Paterson JA, Leblond CP. Radioautographic investigation of gliogenesis in the corpus callosum of young rats. I. Sequential changes in oligodendrocytes. J Comp Neurol, 1978; 180: 115-28, 32-7.

Imondi R, Wideman C, Kaprielian Z. Complementary expression of transmembrane ephrins and their receptors in the mouse spinal cord: a possible role in constraining the orientation of longitudinally projecting axons. Development, 2000; 127: 1397-410.

Irie F, Yamaguchi Y. EphB receptors regulate dendritic spine development via intersectin, Cdc42 and N-WASP. Nat Neurosci, 2002; 5: 1117-8.

Ishibashi T, Ding L, Ikenaka K, Inoue Y, Miyado K, Mekada E, Baba H. Tetraspanin protein CD9 is a novel paranodal component regulating paranodal junctional formation. J Neurosci, 2004; 24: 96-102.

Ivanova A, Nakahira E, Kagawa T, Oba A, Wada T, Takebayashi H, Spassky N, Levine J, Zalc B, Ikenaka K. Evidence for a second wave of oligodendrogenesis in the postnatal cerebral cortex of the mouse. J.Neurosci.Res., 2003; 73: 581-92.

Jeffery ND, Blakemore WF. Locomotor deficits induced by experimental spinal cord demyelination are abolished by spontaneous remyelination. Brain, 1997; 120 ( Pt 1): 27-37.

Ji B, Li M, Wu WT, Yick LW, Lee X, Shao Z, Wang J, So KF, McCoy JM, Pepinsky RB, Mi S, Relton JK. LINGO-1 antagonist promotes functional recovery and axonal sprouting after spinal cord injury. Mol Cell Neurosci, 2006; 33: 311-20.

Ji JD, Park-Min KH, Ivashkiv LB. Expression and function of semaphorin 3A and its receptors in human monocyte-derived macrophages. Hum Immunol, 2009; 70: 211-7.

Jin Z, Strittmatter SM. Rac1 mediates collapsin-1-induced growth cone collapse. J Neurosci, 1997; 17: 6256-63.

John GR, Shankar SL, Shafit-Zagardo B, Massimi A, Lee SC, Raine CS, Brosnan CF. Multiple sclerosis: re-expression of a developmental pathway that restricts oligodendrocyte maturation. Nat.Med., 2002; 8: 1115-21.

Kadi L, Selvaraju R, de Lys P, Proudfoot AE, Wells TN, Boschert U. Differential effects of chemokines on oligodendrocyte precursor proliferation and myelin formation in vitro. J Neuroimmunol, 2006; 174: 133-46.

Kaneko S, Iwanami A, Nakamura M, Kishino A, Kikuchi K, Shibata S, Okano HJ, Ikegami T, Moriya A, Konishi O, Nakayama C, Kumagai K, Kimura T, Sato Y, Goshima Y, Taniguchi M, Ito M, He Z, Toyama Y, Okano H. A selective Sema3A inhibitor enhances regenerative responses and functional recovery of the injured spinal cord. Nat Med, 2006; 12: 1380-9.

Kang SU, Fuchs K, Sieghart W, Lubec G. Gel-based mass spectrometric analysis of recombinant GABA(A) receptor subunits representing strongly hydrophobic transmembrane proteins. J Proteome Res, 2008; 7: 3498-506.

Kappler J, Franken S, Junghans U, Hoffmann R, Linke T, Muller HW, Koch KW. Glycosaminoglycan-binding properties and secondary structure of the C-terminus of netrin-1. Biochem Biophys Res Commun, 2000; 271: 287-91.

Keirstead HS, Levine JM, Blakemore WF. Response of the oligodendrocyte progenitor cell population (defined by NG2 labelling) to demyelination of the adult spinal cord. Glia, 1998; 22: 161-70.

Kessaris N, Fogarty M, Iannarelli P, Grist M, Wegner M, Richardson WD. Competing waves of oligodendrocytes in the forebrain and postnatal elimination of an embryonic lineage. Nat Neurosci, 2006; 9: 173-9.

Kirk P, Wilson MC, Heddle C, Brown MH, Barclay AN, Halestrap AP. CD147 is tightly associated with lactate transporters MCT1 and MCT4 and facilitates their cell surface expression. EMBO J, 2000; 19: 3896-904.

Kobayashi H, Kitamura T, Sekiguchi M, Homma MK, Kabuyama Y, Konno S, Kikuchi S, Homma Y. Involvement of EphB1 receptor/EphrinB2 ligand in neuropathic pain. Spine (Phila Pa 1976), 2007; 32: 1592-8.

Kobayashi H, Koppel AM, Luo Y, Raper JA. A role for collapsin-1 in olfactory and cranial sensory axon guidance. J Neurosci, 1997; 17: 8339-52.

Kolodkin AL, Levengood DV, Rowe EG, Tai YT, Giger RJ, Ginty DD. Neuropilin is a semaphorin III receptor. Cell, 1997; 90: 753-62.

Komitova M, Perfilieva E, Mattsson B, Eriksson PS, Johansson BB. Enriched environment after focal cortical ischemia enhances the generation of astroglia and NG2 positive polydendrocytes in adult rat neocortex. Exp Neurol, 2006; 199: 113-21.

Kotter MR, Li WW, Zhao C, Franklin RJM. Myelin Impairs CNS Remyelination by Inhibiting Oligodendrocyte Precursor Cell Differentiation. Journal of Neuroscience, 2006; 26: 328-32.

Kotter MR, Setzu A, Sim FJ, Van Rooijen N, Franklin RJM. Macrophage depletion impairs oligodendrocyte remyelination following lysolecithin-induced demyelination. Glia, 2001; 35: 204-12.

Kotter MR, Zhao C, Van Rooijen N, Franklin RJM. Macrophage-depletion induced impairment of experimental CNS remyelination is associated with a reduced oligodendrocyte progenitor cell response and altered growth factor expression. Neurobiol.Dis., 2005; 18: 166-75.

Kottis V, Thibault P, Mikol D, Xiao ZC, Zhang R, Dergham P, Braun PE. Oligodendrocyte-myelin glycoprotein (OMgp) is an inhibitor of neurite outgrowth. J Neurochem, 2002; 82: 1566-9.

Kramer EM, Schardt A, Nave KA. Membrane traffic in myelinating oligodendrocytes. Microsc Res Tech, 2001; 52: 656-71.

Kruger RP, Aurandt J, Guan KL. Semaphorins command cells to move. Nat Rev Mol Cell Biol, 2005; 6: 789-800.

Krull CE, Lansford R, Gale NW, Collazo A, Marcelle C, Yancopoulos GD, Fraser SE, Bronner-Fraser M. Interactions of Eph-related receptors and ligands confer rostrocaudal pattern to trunk neural crest migration. Curr Biol, 1997; 7: 571-80.

Kuhlmann T, Gutenberg A, Schulten HJ, Paulus W, Rohde V, Bruck W. Nogo-a expression in glial CNS tumors: a tool to differentiate between oligodendrogliomas and other gliomas? Am J Surg Pathol, 2008a; 32: 1444-53.

Kuhlmann T, Miron V, Cuo Q, Wegner C, Antel J, Bruck W. Differentiation block of oligodendroglial progenitor cells as a cause for remyelination failure in chronic multiple sclerosis. Brain, 2008b; 131: 1749-58.

Kuhn TB, Brown MD, Wilcox CL, Raper JA, Bamburg JR. Myelin and collapsin-1 induce motor neuron growth cone collapse through different pathways: inhibition of collapse by opposing mutants of rac1. J Neurosci, 1999; 19: 1965-75.

Kullander K, Croll SD, Zimmer M, Pan L, McClain J, Hughes V, Zabski S, DeChiara TM, Klein R, Yancopoulos GD, Gale NW. Ephrin-B3 is the midline barrier that prevents corticospinal tract axons from recrossing, allowing for unilateral motor control. Genes Dev, 2001; 15: 877-88.

Kumanogoh A, Kikutani H. Roles of the semaphorin family in immune regulation. Adv Immunol, 2003; 81: 173-98.

Lackmann M, Mann RJ, Kravets L, Smith FM, Bucci TA, Maxwell KF, Howlett GJ, Olsson JE, Vanden Bos T, Cerretti DP, Boyd AW. Ligand for EPH-related kinase (LERK) 7 is the preferred high affinity ligand for the HEK receptor. J Biol Chem, 1997; 272: 16521-30.

Lackmann M, Oates AC, Dottori M, Smith FM, Do C, Power M, Kravets L, Boyd AW. Distinct subdomains of the EphA3 receptor mediate ligand binding and receptor dimerization. J Biol Chem, 1998; 273: 20228-37.

Lai KO, Chen Y, Po HM, Lok KC, Gong K, Ip NY. Identification of the Jak/Stat proteins as novel downstream targets of EphA4 signaling in muscle: implications in the regulation of acetylcholinesterase expression. J Biol Chem, 2004; 279: 13383-92.

Lappe-Siefke C, Goebbels S, Gravel M, Nicksch E, Lee J, Braun PE, Griffiths IR, Nave KA. Disruption of Cnp1 uncouples oligodendroglial functions in axonal support and myelination. Nat.Genet., 2003; 33: 366-74.

Larocca JN, Norton WT. Isolation of myelin. Curr Protoc Cell Biol, 2007; Chapter 3: Unit3 25.

Larsen PH, Wells JE, Stallcup WB, Opdenakker G, Yong VW. Matrix metalloproteinase-9 facilitates remyelination in part by processing the inhibitory NG2 proteoglycan. J Neurosci, 2003; 23: 11127-35.

Lassmann H. Multiple sclerosis: is there neurodegeneration independent from inflammation? J Neurol Sci, 2007; 259: 3-6.

Lawrenson ID, Wimmer-Kleikamp SH, Lock P, Schoenwaelder SM, Down M, Boyd AW, Alewood PF, Lackmann M. Ephrin-A5 induces rounding, blebbing and de-adhesion of EphA3-expressing 293T and melanoma cells by CrkII and Rho-mediated signalling. J Cell Sci, 2002; 115: 1059-72.

Lebar R, Lubetzki C, Vincent C, Lombrail P, Boutry JM. The M2 autoantigen of central nervous system myelin, a glycoprotein present in oligodendrocyte membrane. Clin Exp Immunol, 1986; 66: 423-34.

Lee X, Yang Z, Shao Z, Rosenberg SS, Levesque M, Pepinsky RB, Qiu M, Miller RH, Chan JR, Mi S. NGF regulates the expression of axonal LINGO-1 to inhibit oligodendrocyte differentiation and myelination. J Neurosci, 2007; 27: 220-5.

Li G, Crang AJ, Rundle JL, Blakemore WF. Oligodendrocyte progenitor cells in the adult rat CNS express myelin oligodendrocyte glycoprotein (MOG). Brain Pathol, 2002; 12: 463-71.

Li WW, Penderis J, Zhao C, Schumacher M, Franklin RJ. Females remyelinate more efficiently than males following demyelination in the aged but not young adult CNS. Exp Neurol, 2006; 202: 250-4.

Lin W, Kemper A, Dupree JL, Harding HP, Ron D, Popko B. Interferon-gamma inhibits central nervous system remyelination through a process modulated by endoplasmic reticulum stress. Brain, 2006; 129: 1306-18.

Linington C, Engelhardt B, Kapocs G, Lassman H. Induction of persistently demyelinated lesions in the rat following the repeated adoptive transfer of encephalitogenic T cells and demyelinating antibody. J Neuroimmunol, 1992; 40: 219-24.

Liu Y, Wu Y, Lee JC, Xue H, Pevny LH, Kaprielian Z, Rao MS. Oligodendrocyte and astrocyte development in rodents: an in situ and immunohistological analysis during embryonic development. Glia, 2002; 40: 25-43.

Lu Q, Sun EE, Klein RS, Flanagan JG. Ephrin-B Reverse Signaling Is Mediated by a Novel PDZ-RGS Protein and Selectively Inhibits G Protein-Coupled Chemoattraction. Cell, 2001; 105: 69-79.

Lu QR, Sun T, Zhu Z, Ma N, Garcia M, Stiles CD, Rowitch DH. Common developmental requirement for Olig function indicates a motor neuron/oligodendrocyte connection. Cell, 2002; 109: 75-86.

Lu QR, Yuk D, Alberta JA, Zhu Z, Pawlitzky I, Chan J, McMahon AP, Stiles CD, Rowitch DH. Sonic hedgehog--regulated oligodendrocyte lineage genes encoding bHLH proteins in the mammalian central nervous system. Neuron, 2000; 25: 317-29.

Ludwin SK. Central nervous system demyelination and remyelination in the mouse: an ultrastructural study of cuprizone toxicity. Lab Invest, 1978; 39: 597-612.

Luo Y, Raible D, Raper JA. Collapsin: a protein in brain that induces the collapse and paralysis of neuronal growth cones. Cell, 1993; 75: 217-27.

Mabie PC, Mehler MF, Marmur R, Papavasiliou A, Song Q, Kessler JA. Bone morphogenetic proteins induce astroglial differentiation of oligodendroglial-astroglial progenitor cells. J Neurosci, 1997; 17: 4112-20.

Mabuchi T, Kitagawa K, Ohtsuki T, Kuwabara K, Yagita Y, Yanagihara T, Hori M, Matsumoto M. Contribution of microglia/macrophages to expansion of infarction and response of oligodendrocytes after focal cerebral ischemia in rats. Stroke, 2000; 31: 1735-43.

Madison RD, Zomorodi A, Robinson GA. Netrin-1 and peripheral nerve regeneration in the adult rat. Exp Neurol, 2000; 161: 563-70.

Maeda Y, Solanky M, Menonna J, Chapin J, Li W, Dowling P. Platelet-derived growth factor-alpha receptor-positive oligodendroglia are frequent in multiple sclerosis lesions. Ann Neurol, 2001; 49: 776-85.

Mandai K, Matsumoto M, Kitagawa K, Matsushita K, Ohtsuki T, Mabuchi T, Colman DR, Kamada T, Yanagihara T. Ischemic damage and subsequent proliferation of oligodendrocytes in focal cerebral ischemia. Neuroscience, 1997; 77: 849-61.

Marmur R, Kessler JA, Zhu G, Gokhan S, Mehler MF. Differentiation of oligodendroglial progenitors derived from cortical multipotent cells requires extrinsic signals including activation of gp130/LIFbeta receptors. J Neurosci, 1998; 18: 9800-11.

Martone ME, Holash JA, Bayardo A, Pasquale EB, Ellisman MH. Immunolocalization of the receptor tyrosine kinase EphA4 in the adult rat central nervous system. Brain Res, 1997; 771: 238-50.

Mason JL, Suzuki K, Chaplin DD, Matsushima GK. Interleukin-1beta promotes repair of the CNS. J.Neurosci., 2001; 21: 7046-52.

Matsushima GK, Morell P. The neurotoxicant, cuprizone, as a model to study demyelination and remyelination in the central nervous system. Brain Pathol, 2001; 11: 107-16.

McCarthy KD, de Vellis J. Preparation of separate astroglial and oligodendroglial cell cultures from rat cerebral tissue. The Journal of Cell Biology, 1980; 85: 890-902.

McFarland HF, Martin R. Multiple sclerosis: a complicated picture of autoimmunity. Nat Immunol, 2007; 8: 913-9.

McKay JS, Blakemore WF, Franklin RJM. Trapidil-mediated inhibition of CNS remyelination results from reduced numbers and impaired differentiation of oligodendrocytes. Neuropathol Appl Neurobiol, 1998; 24: 498-506.

McKerracher L, David S, Jackson DL, Kottis V, Dunn RJ, Braun PE. Identification of myelin-associated glycoprotein as a major myelin-derived inhibitor of neurite growth. Neuron, 1994; 13: 805-11.

McMorris FA, Dubois-Dalcq M. Insulin-like growth factor I promotes cell proliferation and oligodendroglial commitment in rat glial progenitor cells developing in vitro. J Neurosci Res, 1988; 21: 199-209.

Menn B, Garcia-Verdugo JM, Yaschine C, Gonzalez-Perez O, Rowitch D, Alvarez-Buylla A. Origin of oligodendrocytes in the subventricular zone of the adult brain. J Neurosci, 2006; 26: 7907-18.

Mi S, Hu B, Hahm K, Luo Y, Kam Hui ES, Yuan Q, Wong WM, Wang L, Su H, Chu TH, Guo J, Zhang W, So KF, Pepinsky B, Shao Z, Graff C, Garber E, Jung V, Wu EX, Wu W. LINGO-1 antagonist promotes spinal cord remyelination and axonal integrity in MOG-induced experimental autoimmune encephalomyelitis. Nat Med, 2007; 13: 1228-33.

Mi S, Lee X, Shao Z, Thill G, Ji B, Relton J, Levesque M, Allaire N, Perrin S, Sands B, Crowell T, Cate RL, McCoy JM, Pepinsky RB. LINGO-1 is a component of the Nogo-66 receptor/p75 signaling complex. Nat.Neurosci., 2004; 7: 221-8.

Mi S, Miller RH, Lee X, Scott ML, Shulag-Morskaya S, Shao Z, Chang J, Thill G, Levesque M, Zhang M, Hession C, Sah D, Trapp B, He Z, Jung V, McCoy JM, Pepinsky RB. LINGO-1 negatively regulates myelination by oligodendrocytes. Nat.Neurosci., 2005; 8: 745-51.

Miao H, Burnett E, Kinch M, Simon E, Wang B. Activation of EphA2 kinase suppresses integrin function and causes focal-adhesion-kinase dephosphorylation. Nat Cell Biol, 2000; 2: 62-9.

Miao H, Li S, Hu YL, Yuan S, Zhao Y, Chen BP, Puzon-McLaughlin W, Tarui T, Shyy JY, Takada Y, Usami S, Chien S. Differential regulation of Rho GTPases by beta1 and beta3 integrins: the role of an extracellular domain of integrin in intracellular signaling. J Cell Sci, 2002; 115: 2199-206.

Miao H, Wei BR, Peehl DM, Li Q, Alexandrou T, Schelling JR, Rhim JS, Sedor JR, Burnett E, Wang B. Activation of EphA receptor tyrosine kinase inhibits the Ras/MAPK pathway. Nat Cell Biol, 2001; 3: 527-30.

Mikule K, Gatlin JC, de la Houssaye BA, Pfenninger KH. Growth cone collapse induced by semaphorin 3A requires 12/15-lipoxygenase. J Neurosci, 2002; 22: 4932-41.

Miranda JD, White LA, Marcillo AE, Willson CA, Jagid J, Whittemore SR. Induction of Eph B3 after Spinal Cord Injury. Experimental Neurology, 1999; 156: 218-22.

Monschau B, Kremoser C, Ohta K, Tanaka H, Kaneko T, Yamada T, Handwerker C, Hornberger MR, Loschinger J, Pasquale EB, Siever DA, Verderame MF, Muller BK, Bonhoeffer F, Drescher U. Shared and distinct functions of RAGS and ELF-1 in guiding retinal axons. EMBO J, 1997; 16: 1258-67.

Morell P, Jurevics H. Origin of cholesterol in myelin. Neurochem Res, 1996; 21: 463-70.

Mozell RL, McMorris FA. Insulin-like growth factor I stimulates oligodendrocyte development and myelination in rat brain aggregate cultures. J Neurosci Res, 1991; 30: 382-90.

Murai KK, Nguyen LN, Irie F, Yamaguchi Y, Pasquale EB. Control of hippocampal dendritic spine morphology through ephrin-A3/EphA4 signaling. Nat Neurosci, 2003; 6: 153-60.

Murai KK, Pasquale EB. Can Eph receptors stimulate the mind? Neuron, 2002; 33: 159-62.

Nait-Oumesmar B, Picard-Riera N, Kerninon C, Decker L, Seilhean D, Hoglinger GU, Hirsch EC, Reynolds R, Baron-Van Evercooren A. Activation of the subventricular zone in multiple sclerosis: evidence for early glial progenitors. Proc Natl Acad Sci U S A, 2007; 104: 4694-9.

Nasir J, Floresco SB, O'Kusky JR, Diewert VM, Richman JM, Zeisler J, Borowski A, Marth JD, Phillips AG, Hayden MR. Targeted disruption of the Huntington's disease gene results in embryonic lethality and behavioral and morphological changes in heterozygotes. Cell, 1995; 81: 811-23.

Nicolay DJ, Doucette JR, Nazarali AJ. Transcriptional control of oligodendrogenesis. Glia, 2007; 55: 1287-99.

Niederost BP, Zimmermann DR, Schwab ME, Bandtlow CE. Bovine CNS myelin contains neurite growth-inhibitory activity associated with chondroitin sulfate proteoglycans. J Neurosci, 1999; 19: 8979-89.

Nielsen JA, Berndt JA, Hudson LD, Armstrong RC. Myelin transcription factor 1 (Myt1) modulates the proliferation and differentiation of oligodendrocyte lineage cells. Mol Cell Neurosci, 2004; 25: 111-23.

Noble M, Murray K, Stroobant P, Waterfield MD, Riddle P. Platelet-derived growth factor promotes division and motility and inhibits premature differentiation of the oligodendrocyte/type-2 astrocyte progenitor cell. Nature, 1988; 333: 560-2.

Norton WT, Poduslo SE. Myelination in rat brain: method of myelin isolation. J.Neurochem., 1973; 21: 749-57.

Oertle T, van der Haar ME, Bandtlow CE, Robeva A, Burfeind P, Buss A, Huber AB, Simonen M, Schnell L, Brosamle C, Kaupmann K, Vallon R, Schwab ME. Nogo-A inhibits neurite outgrowth and cell spreading with three discrete regions. J Neurosci, 2003; 23: 5393-406.

Oestreicher AB, De Graan PN, Gispen WH, Verhaagen J, Schrama LH. B-50, the growth associated protein-43: modulation of cell morphology and communication in the nervous system. Prog Neurobiol, 1997; 53: 627-86.

Ogita H, Kunimoto S, Kamioka Y, Sawa H, Masuda M, Mochizuki N. EphA4-mediated Rho activation via Vsm-RhoGEF expressed specifically in vascular smooth muscle cells. Circ Res, 2003; 93: 23-31.

Oleszak EL, Chang JR, Friedman H, Katsetos CD, Platsoucas CD. Theiler's virus infection: a model for multiple sclerosis. Clin Microbiol Rev, 2004; 17: 174-207.

Olivieri G, Miescher GC. Immunohistochemical localization of EphA5 in the adult human central nervous system. J Histochem Cytochem, 1999; 47: 855-61.

Orioli D, Henkemeyer M, Lemke G, Klein R, Pawson T. Sek4 and Nuk receptors cooperate in guidance of commissural axons and in palate formation. EMBO J, 1996; 15: 6035-49.

Ousman SS, David S. Lysophosphatidylcholine induces rapid recruitment and activation of macrophages in the adult mouse spinal cord. Glia, 2000; 30: 92-104.

Papastefanaki F, Chen J, Lavdas AA, Thomaidou D, Schachner M, Matsas R. Grafts of Schwann cells engineered to express PSA-NCAM promote functional recovery after spinal cord injury. Brain, 2007; 130: 2159-74.

Park HC, Appel B. Delta-Notch signaling regulates oligodendrocyte specification. Development, 2003; 130: 3747-55.

Park SK, Solomon D, Vartanian T. Growth factor control of CNS myelination. Dev Neurosci, 2001; 23: 327-37.

Pasterkamp RJ, Anderson PN, Verhaagen J. Peripheral nerve injury fails to induce growth of lesioned ascending dorsal column axons into spinal cord scar tissue expressing the axon repellent Semaphorin3A. Eur J Neurosci, 2001; 13: 457-71.

Pasterkamp RJ, Giger RJ, Ruitenberg MJ, Holtmaat AJ, De Wit J, De Winter F, Verhaagen J. Expression of the gene encoding the chemorepellent semaphorin III is induced in the fibroblast component of neural scar tissue formed following injuries of adult but not neonatal CNS. Mol Cell Neurosci, 1999; 13: 143-66.

Pasterkamp RJ, Peschon JJ, Spriggs MK, Kolodkin AL. Semaphorin 7A promotes axon outgrowth through integrins and MAPKs. Nature, 2003; 424: 398-405.

Pasterkamp RJ, Verhaagen J. Emerging roles for semaphorins in neural regeneration. Brain Res Brain Res Rev, 2001; 35: 36-54.

Pasterkamp RJ, Verhaagen J. Semaphorins in axon regeneration: developmental guidance molecules gone wrong? Philos Trans R Soc Lond B Biol Sci, 2006; 361: 1499-511.

Patrikios P, Stadelmann C, Kutzelnigg A, Rauschka H, Schmidbauer M, Laursen H, Sorensen PS, Bruck W, Lucchinetti C, Lassmann H. Remyelination is extensive in a subset of multiple sclerosis patients. Brain, 2006; 129: 3165-72.

Payne HR, Lemmon V. Glial cells of the O-2A lineage bind preferentially to N-cadherin and develop distinct morphologies. Dev Biol, 1993; 159: 595-607.

Penderis J, Shields SA, Franklin RJM. Impaired remyelination and depletion of oligodendrocyte progenitors does not occur following repeated episodes of focal demyelination in the rat central nervous system. Brain, 2003; 126: 1382-91.

Penzes P, Beeser A, Chernoff J, Schiller MR, Eipper BA, Mains RE, Huganir RL. Rapid induction of dendritic spine morphogenesis by trans-synaptic ephrinB-EphB receptor activation of the Rho-GEF kalirin. Neuron, 2003; 37: 263-74.

Peters A, Sethares C. Oligodendrocytes, their progenitors and other neuroglial cells in the aging primate cerebral cortex. Cereb Cortex, 2004; 14: 995-1007.

Petratos S, Gonzales MF, Azari MF, Marriott M, Minichiello RA, Shipham KA, Profyris C, Nicolaou A, Boyle K, Cheema SS, Kilpatrick TJ. Expression of the low-affinity neurotrophin receptor, p75(NTR), is upregulated by oligodendroglial progenitors adjacent to the subventricular zone in response to demyelination. Glia, 2004; 48: 64-75.

Pirko I, Ciric B, Gamez J, Bieber AJ, Warrington AE, Johnson AJ, Hanson DP, Pease LR, Macura SI, Rodriguez M. A human antibody that promotes remyelination enters the CNS and decreases lesion load as detected by T2-weighted spinal cord MRI in a virus-induced murine model of MS. FASEB J, 2004; 18: 1577-9.

Ponomarev ED, Shriver LP, Maresz K, Dittel BN. Microglial cell activation and proliferation precedes the onset of CNS autoimmunity. J Neurosci Res, 2005; 81: 374-89.

Ponta H, Sherman L, Herrlich PA. CD44: from adhesion molecules to signalling regulators. Nat Rev Mol Cell Biol, 2003; 4: 33-45.

Popko B. Notch signaling: a rheostat regulating oligodendrocyte differentiation? Dev Cell, 2003; 5: 668-9.

Pozas E, Pascual M, Nguyen Ba-Charvet KT, Guijarro P, Sotelo C, Chedotal A, Del Rio JA, Soriano E. Age-dependent effects of secreted Semaphorins 3A, 3F, and 3E on developing hippocampal axons: in vitro effects and phenotype of Semaphorin 3A (-/-) mice. Mol Cell Neurosci, 2001; 18: 26-43.

Prestoz L, Chatzopoulou E, Lemkine G, Spassky N, Lebras B, Kagawa T, Ikenaka K, Zalc B, Thomas JL. Control of axonophilic migration of oligodendrocyte precursor cells by Eph-ephrin interaction. Neuron Glia Biol, 2004; 1: 73-83.

Prineas JW, Kwon EE, Goldenberg PZ, Ilyas AA, Quarles RH, Benjamins JA, Sprinkle TJ. Multiple sclerosis. Oligodendrocyte proliferation and differentiation in fresh lesions. Lab Invest, 1989; 61: 489-503.

Qi Y, Cai J, Wu Y, Wu R, Lee J, Fu H, Rao M, Sussel L, Rubenstein J, Qiu M. Control of oligodendrocyte differentiation by the Nkx2.2 homeodomain transcription factor. Development, 2001; 128: 2723-33.

Qian X, Davis AA, Goderie SK, Temple S. FGF2 concentration regulates the generation of neurons and glia from multipotent cortical stem cells. Neuron, 1997; 18: 81-93.

Quaglia X, Beggah AT, Seidenbecher C, Zurn AD. Delayed priming promotes CNS regeneration post-rhizotomy in Neurocan and Brevican-deficient mice. Brain, 2008; 131: 240-9.

Rabchevsky AG, Fugaccia I, Sullivan PG, Scheff SW. Cyclosporin A treatment following spinal cord injury to the rat: behavioral effects and stereological assessment of tissue sparing. J Neurotrauma, 2001; 18: 513-22.

Raine CS, Scheinberg L, Waltz JM. Multiple sclerosis. Oligodendrocyte survival and proliferation in an active established lesion. Lab Invest, 1981; 45: 534-46.

Rajebhosale M, Greenwood S, Vidugiriene J, Jeromin A, Hilfiker S. Phosphatidylinositol 4-OH kinase is a downstream target of neuronal calcium sensor-1 in enhancing exocytosis in neuroendocrine cells. J Biol Chem, 2003; 278: 6075-84.

Ramalho-Santos M, Yoon S, Matsuzaki Y, Mulligan RC, Melton DA. "Stemness": transcriptional profiling of embryonic and adult stem cells. Science, 2002; 298: 597-600.

Reynolds BA, Weiss S. Central nervous system growth and differentiation factors: clinical horizons--truth or dare? Curr Opin Biotechnol, 1993; 4: 734-8.

Reynolds ES. The use of lead citrate at high pH as an electron-opaque stain in electron microscopy. J Cell Biol, 1963; 17: 208-12.

Ricard D, Rogemond V, Charrier E, Aguera M, Bagnard D, Belin MF, Thomasset N, Honnorat J. Isolation and expression pattern of human Unc-33-like phosphoprotein 6/collapsin response mediator protein 5 (Ulip6/CRMP5): coexistence with Ulip2/CRMP2 in Sema3a- sensitive oligodendrocytes. J Neurosci, 2001; 21: 7203-14.

Ricard D, Stankoff B, Bagnard D, Aguera M, Rogemond V, Antoine JC, Spassky N, Zalc B, Lubetzki C, Belin MF, Honnorat J. Differential expression of collapsin response mediator proteins (CRMP/ULIP) in subsets of oligodendrocytes in the postnatal rodent brain. Mol Cell Neurosci, 2000; 16: 324-37.

Ricard J, Salinas J, Garcia L, Liebl DJ. EphrinB3 regulates cell proliferation and survival in adult neurogenesis. Molecular and Cellular Neuroscience, 2006; 31: 713-22.

Ridet JL, Malhotra SK, Privat A, Gage FH. Reactive astrocytes: cellular and molecular cues to biological function. Trends Neurosci, 1997; 20: 570-7.

Robinson S, Miller RH. Contact with central nervous system myelin inhibits oligodendrocyte progenitor maturation. Dev.Biol., 1999; 216: 359-68.

Rogister B, Ben-Hur T, Dubois-Dalcq M. From neural stem cells to myelinating oligodendrocytes. Mol Cell Neurosci, 1999; 14: 287-300.

Roth AD, Leisewitz AV, Jung JE, Cassina P, Barbeito L, Inestrosa NC, Bronfman M. PPAR gamma activators induce growth arrest and process extension in B12 oligodendrocyte-like cells and terminal differentiation of cultured oligodendrocytes. J Neurosci Res, 2003; 72: 425-35.

Rothbacher U, Laurent MN, Blitz IL, Watabe T, Marsh JL, Cho KW. Functional conservation of the Wnt signaling pathway revealed by ectopic expression of Drosophila dishevelled in Xenopus. Dev Biol, 1995; 170: 717-21.

Roy K, Murtie JC, El-Khodor BF, Edgar N, Sardi SP, Hooks BM, Benoit-Marand M, Chen C, Moore H, O'Donnell P, Brunner D, Corfas G. Loss of erbB signaling in oligodendrocytes alters myelin and dopaminergic function, a potential mechanism for neuropsychiatric disorders. Proc Natl Acad Sci U S A, 2007; 104: 8131-6.

Satoh J, Tabunoki H, Yamamura T, Arima K, Konno H. TROY and LINGO-1 expression in astrocytes and macrophages/microglia in multiple sclerosis lesions. Neuropathol Appl Neurobiol, 2007; 33: 99-107.

Schlierf B, Werner T, Glaser G, Wegner M. Expression of connexin47 in oligodendrocytes is regulated by the Sox10 transcription factor. J Mol Biol, 2006; 361: 11-21.

Schmucker J, Ader M, Brockschnieder D, Brodarac A, Bartsch U, Riethmacher D. erbB3 is dispensable for oligodendrocyte development in vitro and in vivo. Glia, 2003; 44: 67-75.

Schwarting GA, Kostek C, Ahmad N, Dibble C, Pays L, Puschel AW. Semaphorin 3A is required for guidance of olfactory axons in mice. J Neurosci, 2000; 20: 7691-7.

Schweigreiter R, Walmsley AR, Niederost B, Zimmermann DR, Oertle T, Casademunt E, Frentzel S, Dechant G, Mir A, Bandtlow CE. Versican V2 and the central inhibitory domain of Nogo-A inhibit neurite growth via p75NTR/NgR-independent pathways that converge at RhoA. Mol Cell Neurosci, 2004; 27: 163-74.

Seidenbecher CI, Gundelfinger ED, Bockers TM, Trotter J, Kreutz MR. Transcripts for secreted and GPI-anchored brevican are differentially distributed in rat brain. Eur J Neurosci, 1998; 10: 1621-30.

Seidenbecher CI, Richter K, Rauch U, Fassler R, Garner CC, Gundelfinger ED. Brevican, a chondroitin sulfate proteoglycan of rat brain, occurs as secreted and cell surface glycosylphosphatidylinositol-anchored isoforms. J Biol Chem, 1995; 270: 27206-12.

Serafini T, Kennedy TE, Galko MJ, Mirzayan C, Jessell TM, Tessier-Lavigne M. The netrins define a family of axon outgrowth-promoting proteins homologous to C. elegans UNC-6. Cell, 1994; 78: 409-24.

Setzu A, Lathia JD, Zhao C, Wells K, Rao MS, Ffrench-Constant C, Franklin RJ. Inflammation stimulates myelination by transplanted oligodendrocyte precursor cells. Glia, 2006; 54: 297-303.

Shamah SM, Lin MZ, Goldberg JL, Estrach S, Sahin M, Hu L, Bazalakova M, Neve RL, Corfas G, Debant A, Greenberg ME. EphA receptors regulate growth cone dynamics through the novel guanine nucleotide exchange factor ephexin. Cell, 2001; 105: 233-44.

Shen S, Sandoval J, Swiss VA, Li J, Dupree J, Franklin RJ, Casaccia-Bonnefil P. Age-dependent epigenetic control of differentiation inhibitors is critical for remyelination efficiency. Nat Neurosci, 2008; 11: 1024-34.

Sherman LS, Back SA. A 'GAG' reflex prevents repair of the damaged CNS. Trends Neurosci, 2008; 31: 44-52.

Shi W, Kumanogoh A, Watanabe C, Uchida J, Wang X, Yasui T, Yukawa K, Ikawa M, Okabe M, Parnes JR, Yoshida K, Kikutani H. The class IV semaphorin CD100 plays nonredundant roles in the immune system: defective B and T cell activation in CD100-deficient mice. Immunity, 2000; 13: 633-42.

Sim FJ, Hinks GL, Franklin RJ. The re-expression of the homeodomain transcription factor Gtx during remyelination of experimentally induced demyelinating lesions in young and old rat brain. Neuroscience, 2000a; 100: 131-9.

Sim FJ, Hinks GL, Franklin RJM. The re-expression of the homeodomain transcription factor Gtx during remyelination of experimentally induced demyelinating lesions in young and old rat brain. Neuroscience, 2000b; 100: 131-9.

Sim FJ, Zhao C, Li WW, Lakatos A, Franklin RJM. Expression of the POU-domain transcription factors SCIP/Oct-6 and Brn-2 is associated with Schwann cell but not oligodendrocyte remyelination of the CNS. Mol Cell Neurosci, 2002a; 20: 669-82.

Sim FJ, Zhao C, Penderis J, Franklin RJM. The age-related decrease in CNS remyelination efficiency is attributable to an impairment of both oligodendrocyte progenitor recruitment and differentiation. J.Neurosci., 2002b; 22: 2451-9.

Skene JH. Axonal growth-associated proteins. Annu Rev Neurosci, 1989; 12: 127-56.

Sobel RA. Ephrin A receptors and ligands in lesions and normal-appearing white matter in multiple sclerosis. Brain Pathol, 2005; 15: 35-45.

Song XJ, Zheng JH, Cao JL, Liu WT, Song XS, Huang ZJ. EphrinB-EphB receptor signaling contributes to neuropathic pain by regulating neural excitability and spinal synaptic plasticity in rats. Pain, 2008; 139: 168-80.

Sorensen O, Perry D, Dales S. In vivo and in vitro models of demyelinating diseases. III. JHM virus infection of rats. Arch Neurol, 1980; 37: 478-84.

Southwood C, He C, Garbern J, Kamholz J, Arroyo E, Gow A. CNS myelin paranodes require Nkx6-2 homeoprotein transcriptional activity for normal structure. J Neurosci, 2004; 24: 11215-25.

Spassky N, de Castro F, Le Bras B, Heydon K, Queraud-LeSaux F, Bloch-Gallego E, Chedotal A, Zalc B, Thomas JL. Directional guidance of oligodendroglial migration by class 3 semaphorins and netrin-1. J Neurosci., 2002; 22: 5992-6004.

Spencer SA, Schuh SM, Liu WS, Willard MB. GAP-43, a protein associated with axon growth, is phosphorylated at three sites in cultured neurons and rat brain. J Biol Chem, 1992; 267: 9059-64.

Stapleton D, Balan I, Pawson T, Sicheri F. The crystal structure of an Eph receptor SAM domain reveals a mechanism for modular dimerization. Nat Struct Biol, 1999; 6: 44-9.

Stein E, Lane AA, Cerretti DP, Schoecklmann HO, Schroff AD, Van Etten RL, Daniel TO. Eph receptors discriminate specific ligand oligomers to determine alternative signaling complexes, attachment, and assembly responses. Genes Dev, 1998; 12: 667-78.

Steinman L. Multiple approaches to multiple sclerosis. Nat Med, 2000; 6: 15-6.

Stolt CC, Rehberg S, Ader M, Lommes P, Riethmacher D, Schachner M, Bartsch U, Wegner M. Terminal differentiation of myelin-forming oligodendrocytes depends on the transcription factor Sox10. Genes Dev, 2002; 16: 165-70.

Stolt CC, Schlierf A, Lommes P, Hillgartner S, Werner T, Kosian T, Sock E, Kessaris N, Richardson WD, Lefebvre V, Wegner M. SoxD proteins influence multiple stages of oligodendrocyte development and modulate SoxE protein function. Dev Cell, 2006; 11: 697-709.

Stone LA, Albert PS, Smith ME, DeCarli C, Armstrong MR, McFarlin DE, Frank JA, McFarland HF. Changes in the amount of diseased white matter over time in patients with relapsing-remitting multiple sclerosis. Neurology, 1995; 45: 1808-14.

Sussman CR, Vartanian T, Miller RH. The ErbB4 neuregulin receptor mediates suppression of oligodendrocyte maturation. J Neurosci, 2005; 25: 5757-62.

Suto F, Ito K, Uemura M, Shimizu M, Shinkawa Y, Sanbo M, Shinoda T, Tsuboi M, Takashima S, Yagi T, Fujisawa H. Plexin-a4 mediates axon-repulsive activities of both secreted and transmembrane semaphorins and plays roles in nerve fiber guidance. J Neurosci, 2005; 25: 3628-37.

Swiercz JM, Kuner R, Behrens J, Offermanns S. Plexin-B1 directly interacts with PDZ-RhoGEF/LARG to regulate RhoA and growth cone morphology. Neuron, 2002; 35: 51-63.

Syed YA, Baer AS, Lubec G, Hoeger H, Widhalm G, Kotter MR. Inhibition of oligodendrocyte precursor cell differentiation by myelin-associated proteins. Neurosurg Focus, 2008; 24: E5.

Takahashi T, Fournier A, Nakamura F, Wang LH, Murakami Y, Kalb RG, Fujisawa H, Strittmatter SM. Plexin-neuropilin-1 complexes form functional semaphorin-3A receptors. Cell, 1999; 99: 59-69.

Takasu MA, Dalva MB, Zigmond RE, Greenberg ME. Modulation of NMDA receptor-dependent calcium influx and gene expression through EphB receptors. Science, 2002; 295: 491-5.

Takemoto M, Fukuda T, Sonoda R, Murakami F, Tanaka H, Yamamoto N. Ephrin-B3-EphA4 interactions regulate the growth of specific thalamocortical axon populations in vitro. Eur J Neurosci, 2002; 16: 1168-72.

Tamagnone L, Artigiani S, Chen H, He Z, Ming GI, Song H, Chedotal A, Winberg ML, Goodman CS, Poo M, Tessier-Lavigne M, Comoglio PM. Plexins are a large family of receptors for transmembrane, secreted, and GPI-anchored semaphorins in vertebrates. Cell, 1999; 99: 71-80.

Tamagnone L, Comoglio PM. Signalling by semaphorin receptors: cell guidance and beyond. Trends Cell Biol, 2000; 10: 377-83.

Tang Y, Nakada MT, Rafferty P, Laraio J, McCabe FL, Millar H, Cunningham M, Snyder LA, Bugelski P, Yan L. Regulation of vascular endothelial growth factor expression by EMMPRIN via the PI3K-Akt signaling pathway. Mol Cancer Res, 2006; 4: 371-7.

Taveggia C, Thaker P, Petrylak A, Caporaso GL, Toews A, Falls DL, Einheber S, Salzer JL. Type III neuregulin-1 promotes oligodendrocyte myelination. Glia, 2008; 56: 284-93.

Taylor CM, Marta CB, Claycomb RJ, Han DK, Rasband MN, Coetzee T, Pfeiffer SE. Proteomic mapping provides powerful insights into functional myelin biology. Proceedings of the National Academy of Sciences, 2004; 101: 4643-8.

Timsit S, Martinez S, Allinquant B, Peyron F, Puelles L, Zalc B. Oligodendrocytes originate in a restricted zone of the embryonic ventral neural tube defined by DM-20 mRNA expression. J Neurosci, 1995; 15: 1012-24.

Torres R, Firestein BL, Dong H, Staudinger J, Olson EN, Huganir RL, Bredt DS, Gale NW, Yancopoulos GD. PDZ proteins bind, cluster, and synaptically colocalize with Eph receptors and their ephrin ligands. Neuron, 1998; 21: 1453-63.

Toth J, Cutforth T, Gelinas AD, Bethoney KA, Bard J, Harrison CJ. Crystal structure of an ephrin ectodomain. Dev Cell, 2001; 1: 83-92.

Trajkovic K, Dhaunchak AS, Goncalves JT, Wenzel D, Schneider A, Bunt G, Nave KA, Simons M. Neuron to glia signaling triggers myelin membrane exocytosis from endosomal storage sites. J Cell Biol, 2006; 172: 937-48.

Trapp BD. Myelin-associated glycoprotein. Location and potential functions. Ann N Y Acad Sci, 1990; 605: 29-43.

Tsai HH, Tessier-Lavigne M, Miller RH. Netrin 1 mediates spinal cord oligodendrocyte precursor dispersal. Development, 2003; 130: 2095-105.

Tsunoda I, Fujinami RS. Two models for multiple sclerosis: experimental allergic encephalomyelitis and Theiler's murine encephalomyelitis virus. J Neuropathol Exp Neurol, 1996; 55: 673-86.

Tumbar T, Guasch G, Greco V, Blanpain C, Lowry WE, Rendl M, Fuchs E. Defining the epithelial stem cell niche in skin. Science, 2004; 303: 359-63.

Vana AC, Flint NC, Harwood NE, Le TQ, Fruttiger M, Armstrong RC. Platelet-derived growth factor promotes repair of chronically demyelinated white matter. J Neuropathol Exp Neurol, 2007; 66: 975-88.

Vanrobaeys F, VanCoster R, Dhondt G, Devreese B, VanBeeumen J. Profiling of Myelin Proteins by 2D-Gel Electrophoresis and Multidimensional Liquid Chromatography Coupled to MALDI TOF-TOF Mass Spectrometry. Journal of Proteome Research, 2005; 4: 2283-93.

Vartanian T, Corfas G, Li Y, Fischbach GD, Stefansson K. A role for the acetylcholine receptor-inducing protein ARIA in oligodendrocyte development. Proc Natl Acad Sci U S A, 1994; 91: 11626-30.

Viehover A, Miller RH, Park SK, Fischbach G, Vartanian T. Neuregulin: an oligodendrocyte growth factor absent in active multiple sclerosis lesions. Dev Neurosci, 2001; 23: 377-86.

Vikis HG, Li W, He Z, Guan KL. The semaphorin receptor plexin-B1 specifically interacts with active Rac in a ligand-dependent manner. Proc Natl Acad Sci U S A, 2000; 97: 12457-62.

Wahl S, Barth H, Ciossek T, Aktories K, Mueller BK. Ephrin-A5 induces collapse of growth cones by activating Rho and Rho kinase. J Cell Biol, 2000; 149: 263-70.

Wang HU, Anderson DJ. Eph family transmembrane ligands can mediate repulsive guidance of trunk neural crest migration and motor axon outgrowth. Neuron, 1997; 18: 383-96.

Wang KC, Kim JA, Sivasankaran R, Segal R, He Z. P75 interacts with the Nogo receptor as a co-receptor for Nogo, MAG and OMgp. Nature, 2002a; 420: 74-8.

Wang KC, Koprivica V, Kim JA, Sivasankaran R, Guo Y, Neve RL, He Z. Oligodendrocyte-myelin glycoprotein is a Nogo receptor ligand that inhibits neurite outgrowth. Nature, 2002b; 417: 941-4.

Wang LH, Strittmatter SM. A family of rat CRMP genes is differentially expressed in the nervous system. J Neurosci, 1996; 16: 6197-207.

Wang S, Sdrulla AD, diSibio G, Bush G, Nofziger D, Hicks C, Weinmaster G, Barres BA. Notch receptor activation inhibits oligodendrocyte differentiation. Neuron, 1998; 21: 63-75.

Wang SZ, Dulin J, Wu H, Hurlock E, Lee SE, Jansson K, Lu QR. An oligodendrocyte-specific zinc-finger transcription regulator cooperates with Olig2 to promote oligodendrocyte differentiation. Development, 2006; 133: 3389-98.

Wang Y, Ni ZM, Zhou CF. Denervation-induced spatiotemporal upregulation of ephrin-A2 in the mouse hippocampus after transections of the perforant path. FEBS Lett, 2005a; 579: 1055-60.

Wang Y, Ying G, Liu X, Zhou C. Semi-quantitative expression analysis of ephrin mRNAs in the deafferented hippocampus. Brain Res Mol Brain Res, 2003; 120: 79-83.

Wang Y, Ying GX, Liu X, Wang WY, Dong JH, Ni ZM, Zhou CF. Induction of ephrin-B1 and EphB receptors during denervation-induced plasticity in the adult mouse hippocampus. Eur J Neurosci, 2005b; 21: 2336-46.

Wang Z, Colognato H, Ffrench-Constant C. Contrasting effects of mitogenic growth factors on myelination in neuron-oligodendrocyte co-cultures. Glia, 2007; 55: 537-45.

Watanabe M, Toyama Y, Nishiyama A. Differentiation of proliferated NG2-positive glial progenitor cells in a remyelinating lesion. J Neurosci Res, 2002; 69: 826-36.

Williams A, Piaton G, Aigrot MS, Belhadi A, Theaudin M, Petermann F, Thomas JL, Zalc B, Lubetzki C. Semaphorin 3A and 3F: key players in myelin repair in multiple sclerosis? Brain, 2007; 130: 2554-65.

Willson CA, Irizarry-Ramirez M, Gaskins HE, Cruz-Orengo L, Figueroa JD, Whittemore SR, Miranda JD. Upregulation of EphA receptor expression in the injured adult rat spinal cord. Cell Transplant, 2002; 11: 229-39.

Willson CA, Miranda JD, Foster RD, Onifer SM, Whittemore SR. Transection of the adult rat spinal cord upregulates EphB3 receptor and ligand expression. Cell Transplant, 2003; 12: 279-90.

Wilson HC, Onischke C, Raine CS. Human oligodendrocyte precursor cells in vitro: phenotypic analysis and differential response to growth factors. Glia, 2003; 44: 153-65.

Wolf RM, Wilkes JJ, Chao MV, Resh MD. Tyrosine phosphorylation of p190 RhoGAP by Fyn regulates oligodendrocyte differentiation. J.Neurobiol., 2001; 49: 62-78.

Wolswijk G. Chronic stage multiple sclerosis lesions contain a relatively quiescent population of oligodendrocyte precursor cells. J.Neurosci., 1998; 18: 601-9.

Wolswijk G. Oligodendrocyte precursor cells in the demyelinated multiple sclerosis spinal cord. Brain, 2002; 125: 338-49.

Wolswijk G. Oligodendrocyte survival, loss and birth in lesions of chronic-stage multiple sclerosis. Brain, 2000; 123 ( Pt 1): 105-15.

Wong ST, Henley JR, Kanning KC, Huang KH, Bothwell M, Poo MM. A p75(NTR) and Nogo receptor complex mediates repulsive signaling by myelin-associated glycoprotein. Nat.Neurosci., 2002; 5: 1302-8.

Woodruff RH, Franklin RJM. Demyelination and remyelination of the caudal cerebellar peduncle of adult rats following stereotaxic injections of lysolecithin, ethidium bromide, and complement/anti-galactocerebroside: a comparative study. Glia, 1999; 25: 216-28.

Woodruff RH, Fruttiger M, Richardson WD, Franklin RJ. Platelet-derived growth factor regulates oligodendrocyte progenitor numbers in adult CNS and their response following CNS demyelination. Mol Cell Neurosci, 2004; 25: 252-62.

Woyciechowska JL, Trapp BD, Patrick DH, Shekarchi IC, Leinikki PO, Sever JL, Holmes KV. Acute and subacute demyelination induced by mouse hepatitis virus strain A59 in C3H mice. J Exp Pathol, 1984; 1: 295-306.

Xin M, Yue T, Ma Z, Wu FF, Gow A, Lu QR. Myelinogenesis and axonal recognition by oligodendrocytes in brain are uncoupled in Olig1-null mice. J Neurosci, 2005; 25: 1354-65.

Xu Q, Alldus G, Holder N, Wilkinson DG. Expression of truncated Sek-1 receptor tyrosine kinase disrupts the segmental restriction of gene expression in the Xenopus and zebrafish hindbrain. Development, 1995; 121: 4005-16.

Xu Q, Wilkinson DG. Eph-related receptors and their ligands: mediators of contact dependent cell interactions. J Mol Med, 1997; 75: 576-86.

Yamada H, Fredette B, Shitara K, Hagihara K, Miura R, Ranscht B, Stallcup WB, Yamaguchi Y. The brain chondroitin sulfate proteoglycan brevican associates with astrocytes ensheathing cerebellar glomeruli and inhibits neurite outgrowth from granule neurons. J Neurosci, 1997; 17: 7784-95.

Yamaguchi Y. Lecticans: organizers of the brain extracellular matrix. Cell Mol Life Sci, 2000; 57: 276-89.

Yan H, Wood PM. NT-3 weakly stimulates proliferation of adult rat O1(-)O4(+) oligodendrocyte-lineage cells and increases oligodendrocyte myelination in vitro. J Neurosci Res, 2000; 62: 329-35.

Yaron A, Huang PH, Cheng HJ, Tessier-Lavigne M. Differential requirement for Plexin-A3 and -A4 in mediating responses of sensory and sympathetic neurons to distinct class 3 Semaphorins. Neuron, 2005; 45: 513-23.

Yazdani U, Terman JR. The semaphorins. Genome Biol, 2006; 7: 211.

Ye P, Li L, Richards RG, DiAugustine RP, D'Ercole AJ. Myelination is altered in insulin-like growth factor-I null mutant mice. J Neurosci, 2002; 22: 6041-51.

Yokoyama N, Romero MI, Cowan CA, Galvan P, Helmbacher F, Charnay P, Parada LF, Henkemeyer M. Forward Signaling Mediated by Ephrin-B3 Prevents Contralateral Corticospinal Axons from Recrossing the Spinal Cord Midline. Neuron, 2001; 29: 85-97.

Yong VW, Chabot S, Stuve O, Williams G. Interferon beta in the treatment of multiple sclerosis: mechanisms of action. Neurology, 1998; 51: 682-9.

Yoo S, Wrathall JR. Mixed primary culture and clonal analysis provide evidence that NG2 proteoglycan-expressing cells after spinal cord injury are glial progenitors. Dev Neurobiol, 2007; 67: 860-74.

Yoshida Y, Han B, Mendelsohn M, Jessell TM. PlexinA1 signaling directs the segregation of proprioceptive sensory axons in the developing spinal cord. Neuron, 2006; 52: 775-88.

Yu HH, Kolodkin AL. Semaphorin signaling: a little less per-plexin. Neuron, 1999; 22: 11-4.

Yue Y, Su J, Cerretti DP, Fox GM, Jing S, Zhou R. Selective inhibition of spinal cord neurite outgrowth and cell survival by the Eph family ligand ephrin-A5. J Neurosci, 1999; 19: 10026-35.

Yung SY, Gokhan S, Jurcsak J, Molero AE, Abrajano JJ, Mehler MF. Differential modulation of BMP signaling promotes the elaboration of cerebral cortical GABAergic neurons or oligodendrocytes from a common sonic hedgehog-responsive ventral forebrain progenitor species. Proc Natl Acad Sci U S A, 2002; 99: 16273-8.

Zanata SM, Hovatta I, Rohm B, Puschel AW. Antagonistic effects of Rnd1 and RhoD GTPases regulate receptor activity in Semaphorin 3A-induced cytoskeletal collapse. J Neurosci, 2002; 22: 471-7.

Zhao C, Li WW, Franklin RJ. Differences in the early inflammatory responses to toxin-induced demyelination are associated with the age-related decline in CNS remyelination. Neurobiol Aging, 2006; 27: 1298-307.

Zhao C, Zawadzka M, Roulois AJ, Bruce CC, Franklin RJ. Promoting remyelination in multiple sclerosis by endogenous adult neural stem/precursor cells: defining cellular targets. J Neurol Sci, 2008; 265: 12-6.

Zhou YX, Flint NC, Murtie JC, Le TQ, Armstrong RC. Retroviral lineage analysis of fibroblast growth factor receptor signaling in FGF2 inhibition of oligodendrocyte progenitor differentiation. Glia, 2006; 54: 578-90.

Zou Y, Komuro I, Yamazaki T, Aikawa R, Kudoh S, Shiojima I, Hiroi Y, Mizuno T, Yazaki Y. Protein kinase C, but not tyrosine kinases or Ras, plays a critical role in angiotensin II-induced activation of Raf-1 kinase and extracellular signal-regulated protein kinases in cardiac myocytes. J Biol Chem, 1996; 271: 33592-7.

Zuccato C, Ciammola A, Rigamonti D, Leavitt BR, Goffredo D, Conti L, MacDonald ME, Friedlander RM, Silani V, Hayden MR, Timmusk T, Sipione S, Cattaneo E. Loss of huntingtin-mediated BDNF gene transcription in Huntington's disease. Science, 2001; 293: 493-8.

# Chapter 10
# Appendix

## 10.1 Chemicals and Antibodies

| | |
|---|---|
| Acetic Acid | SIGMA-ALDRICH |
| Agarose | Biozym |
| Aprotinin | SIGMA-ALDRICH |
| Auqa poly mount | Polyscience ltd. |
| b-FGF (Basic Fibroblast Growth Factor) | Peprotech |
| Brevican | Novus Biologicals |
| BSA (Bovine Serum Albumin Fraction V) | SIGMA-ALDRICH |
| BrdU *In-Situ* Detection Kit | BD Biosciences |
| Bromphenol blue | SIGMA-ALDRICH |
| mercaptoethanol | SIGMA-ALDRICH |
| Complete EDTA-free, Protease inhibitor cocktail Tablets | Roche |
| Commassie brilliant blue R-250 | SIGMA-ALDRICH |
| Dead EndTM Colorimetric TUNEL System | Promega |
| DEPC (DiethylenePyrocarbonate) | SIGMA-ALDRICH |
| DNAseI Type IV | SIGMA-ALDRICH |
| DAPI | Roche |
| DMEM (Dulbecco's Modified Eagle Medium) | SIGMA-ALDRICH |
| DTT (Dithiothreitol) | SIGMA-ALDRICH |
| ECL Western Blotting Detection Kit | Amersham Biosciences |
| EDTA | SIGMA-ALDRICH |
| Ethanol | MERCK |
| *Ephrin-B3/Fc Chimera* | R&D |
| Eriochrome cyanine | Fluka |
| Ethidium Bromide | Fluka |
| Eukitt | Kindler GmbH |
| FBS (Fetal Bovine Serum) | SIGMA-ALDRICH |
| FGF (Basic Fibroblast Growth Factor) | SIGMA-ALDRICH |
| Formamide deionised | SIGMA-ALDRICH |
| Formaldehyde | Merck |
| Formamide | Fluka |
| Glycerophosphate | SIGMA-ALDRICH |
| HCl 37% | SIGMA-ALDRICH |
| Hoechst Solution | SIGMA-ALDRICH |
| Human Holo-Transferrin | SIGMA-ALDRICH |
| Human IgG Fc-fragment | Chemicon |
| Insuline | SIGMA-ALDRICH |
| Iron(III)chloride | SIGMA |
| Isoproponal | Merck |
| Leupeptin | SIGMA-ALDRICH |
| L-Cysteine Hydrochloride | SIGMA-ALDRICH |
| L-Glutamine | SIGMA-ALDRICH |
| Glycerin | SIGMA-ALDRICH |

| | |
|---|---|
| MAG | SIGMA-ALDRICH |
| Magnesiumchlorid-Hexahydrat | SIGMA-ALDRICH |
| Maleic acid | SIGMA-ALDRICH |
| MEM (Modified Eagle Medium) | SIGMA-ALDRICH |
| Methanol | MERCK |
| Milk powder | SIGMA-ALDRICH |
| n-Pentane | Merck |
| Netrin-1 | R&D |
| Normal Goat Serum | SIGMA-ALDRICH |
| Normal Sheep Serum | SIGMA-ALDRICH |
| NP-40 | SIGMA-ALDRICH |
| OMgP | Novus Biologicals |
| Octyl-β-D-Glucopyranoside | FLUKA |
| Page RulerTM Prestained Protein Ladder Plus | Fermentas |
| 10xPBS (Phosphate Buffered Saline) | Invitrogen |
| Papain | Worthington |
| PDGF-AA (Platelet Derived Growth Factor) | Peprotech |
| PDGF (Platelet-Derived Growth Factor) | SIGMA-ALDRICH |
| Penstrep (Penicillin-Streptomycin) | GIBCO |
| PFA (Paraformaldehyde) | SIGMA-ALDRICH |
| PMSF (Phenylmethylsulfonylfluorid) | SIGMA-ALDRICH |
| Protease Inhibitor Mix (PIM) | Roche |
| Poly-L-Lysine-Hydrobromide | SIGMA-ALDRICH |
| Poly vinyl alcohol | Apllichem |
| Progesterone | SIGMA-ALDRICH |
| Protein A-sepharose | Santa cruz |
| Putrescine (1,4- Diaminobutane) | SIGMA-ALDRICH |
| SDS | SIGMA-ALDRICH |
| SDS-Page 12.5% | Invitrogen |
| *Rho* Activation Assay *Kit* | Millipore |
| *Semaphorin 3A Fc. Chimera.* | R&D |
| Sodiumchloride | SIGMA-ALDRICH |
| Sodiumfluoride | SIGMA-ALDRICH |
| Sodium Hydroxide | SIGMA-ALDRICH |
| Sodium Selenite Anhydrous | SIGMA-ALDRICH |
| Sodium orthovanadate | SIGMA-ALDRICH |
| Sucrose | SIGMA-ALDRICH |
| T3 (3,3′,5-Triiodo-L-thyronine sodium salt) | SIGMA-ALDRICH |
| T4 (L-Thyroxine) | SIGMA-ALDRICH |
| Tris | SIGMA-ALDRICH |
| Triton X-100 | SIGMA-ALDRICH |
| Trypan Blue Solution | SIGMA-ALDRICH |
| Tween 20 | SIGMA-ALDRICH |
| VECTASHIELD Mounting Medium | Vectorlabs |
| Xylol | Merck |

**Antibodies**

| | |
|---|---|
| A2B5 | Chemicon |
| MBP | Chemicon |
| O4 | Chemicon |
| Ephrin B3 | R&D;Abcam |
| Sema 3A | R&D |

## 10.2 Media, solutions and buffer

## A Cell culture media for primary oligodendrocytes.

**DMEM:**

| | |
|---|---|
| DMEM | 500ml |
| L-glutamine | 4mM |
| Penstrep | 5000U/ml |
| heat inactivated FCS | 10% |

**MEM:**

| | |
|---|---|
| MEM | 500ml |
| L-glutamine | 4mM |
| Penstrep | 5000U/ml |

**Sato's Medium:**

| | |
|---|---|
| DMEM | 500ml |
| L-glutamine | 4mM |
| Penstrep | 5000U/ml |
| Bovine insulin | 5µg/ml |
| Human transferrin | 50µg/ml |
| Bovine serum albumin (BSA) fraction V | 100µg/ml |
| Progesterone | 6,2ng/ml |
| Putrescine | 16µg/ml |
| Sodium selenite | 5ng/ml |
| T3 | 400ng/ml |
| T4 | 400ng/ml |

**Differentiation medium:**

Sato's Medium plus 0.5% heat inactivated FCS

**Digestion Solution:**

| | |
|---|---|
| MEM | 500ml |
| Papain | 30U/ml |
| Cysteine | 0,24mg/ml |
| DNAse I type IV | 40µg/ml |

## B Buffer and Solutions

**Fixation solution for Immunocytochemistry:**
4% PFA in 1xPBS

**Solution A:**

| | |
|---|---|
| PBS | 1x |
| Triton-X | 30% |
| NGS | 10% |

**Solution B:**

| | |
|---|---|
| PBS | 1x |
| Triton-X | 30% |
| NGS | 2% |

**SDS-Gel loading buffer, 2X**

| | |
|---|---|
| Tris/HCl 0.5M, pH 6.8 | 125mM |
| Glycerol | 10% |
| SDS | 10% (w/v) |
| DTT | 130mM |
| Bromphenol blue | 0.006% (w/v) |

**SDS-Gel running buffer, 10X**

| | |
|---|---|
| Tris base | 30.3 g |
| Glycine | 144 g |
| SDS | 10 g |

make to 1L with dH2O

**Tris Buffered Saline (TBS)**

| | |
|---|---|
| Tris-base | 20mM |
| NaCl | 0.9% |

adjust pH to 7.4 with HCl

**TBS-T**
TBS plus 0.1% Tween 20

**Transfer Buffer**

| | |
|---|---|
| Tris base | 2.4g |
| Glycine | 14.2g |
| Methanol | 200ml |
| 10%SDS | 1ml |
| dH2O | up to 1000ml |

**Blocking Buffer**

| | |
|---|---|
| TBS | 100ml |
| BSA | 5g |
| Tween 20 | 0.1ml |

**Stripping Solution**

| | |
|---|---|
| Tris-HCl 6.8 | 62.5mM |
| β-Mercaptoethanol | 100mM |
| SDS | 2% |

**Comassie stain (for SDS Gels)**

| | |
|---|---|
| Comassies brilliant blue R250 | 0.1% (w/v) |
| Methanol | 40% (v/v) |
| dH2O | 50% |

**Comassie destain (for SDS Gels)**

| | |
|---|---|
| Acetic Acid | 10% (v/v) |
| Methanol | 40% (v/v) |
| dH2O | 50% |

**Mg2+ Lysis/Wash Buffer 5x (5xMLB)**

| | |
|---|---|
| Hepes | 25mM |
| NaCl | 750mM |
| Igepal CA-630 | 5% (v/v) |
| MgCl2 | 50mM |
| EDTA | 5mM |
| Glycerol | 10% (v/v) |
| Aprotinin | 10µg/ml |
| Leupeptin | 10µg/ml |
| NaF | 25mM |
| Na3VO4 | 1mM |

**NP-40 Buffer**

| | |
|---|---|
| NaCl | 150mM |
| NP-40 | 1% (v/v) |
| Tris pH 8 | 50mM |
| PMSF | 1mM |
| Glycerophosphate | 10mM |
| NaF | 1mM |
| Na3VO4 | 1mM |
| Protease Inhibitor Mix (PIM) | 1x |

## C Solutions for routine histology and in situ hybridisation

### Perfusion Buffer

### 4% paraformaldehyde in PBS

For 1 litre:

Heat up 1L of phosphate buffer to approximately 50°C in a fume hood, add 40g of paraformaldehyde and continue heating and stirring up to approx. 60°C. Just below 60°C, turn of the heat and add approx. 10 drops of 40% sodium hydroxide. Leave for 5-10 minutes whilst stirring, and check whether solution has cleared. If solution still seems cloudy, add 1-2 drops more sodium hydroxide. Adjust pH to 7.4 with concentrated hydrochloric acid.

### Millonig's osmium tetroxide solution

Add an ampoule containing 2g osmium tetroxide (Oxkem Ltd. Oxford) to 100ml phosphate buffer.

### Toluidine blue for staining sections for light microscopy

Mix equal parts of 1% toluidine blue with 1% borax. Filter before use.

### Eriochrome Cyanine Stain (stain for myelin sheath (Rabchevsky et al., 2001)

*Solution A (10% $FeCl_3$):*

10 g $FeCl_3$ q.s. to 10 ml 3 ml HCl in 97 ml $H_2O$ 10% $FeCl_3$ = 10 ml 100% $FeCl_3$ + 90 ml 3% aq HCl

*Solution B:*

2.5 ml $H_2SO_4$ + 497.5 ml $dH_2O$, 1 g eriochrome cyanine RC (Sigma) in 500 ml 0.5% $H_2SO_4$ Boil for 5 min. No need to filter

*Solution C (prepared fresh for each use):*

Aqueous $NH_4OH$ = 2.15 ml 29.1% $NH_4OH$ in 247.85 ml $dH_2O$

*Staining solution:* 10 ml Solution A + 200 ml Solution B. Adjust volume to 250 ml with $dH_2O$.

### Embedding resin (all solutions from TAAB Laboratories equipment, Ltd.)

| | |
|---|---|
| TAAB embedding resin | 50ml |
| Dodecenyl succinic anhydride (DDSA) | 34ml |
| Methyl nadic anhydride (plasticiser: MNA) | 16ml |

Mix for 5 minutes, and then add 2ml of 2-4-6 tri-dimethylaminoethylphenol activator (DMP30) and mix for further 5min.

**Methylene Blue-Azur II stain for resin sections**

| | |
|---|---|
| Methyele blue (100ml) | |
| Sodium tetraborate | 1g |
| Methylene blue | 1g |

| | |
|---|---|
| Azur-II(100ml) | |
| $dH_2O$ | 100ml |
| Azur-II | 1g |

Mix methylene blue and azur-II in 1:1 ratio. Filter the solution.The solution is stable for one day.

**Uranylacetate**

4 g uranyl acetate in 100ml of 25% ethanol.

**D Solutions for *in situ* hybridization**

**DEPC treated H2O**

| | |
|---|---|
| DEPC | 1ml |
| dH2O | 999ml |

Shake well, leave over night then autoclave.

**Saline sodium citrate (SSC) buffer, 20 x**

| | |
|---|---|
| NaCl | 350.6g |
| Na3Citrate 2H2O | 176.4g |
| DEPC treated H2O | up to 2000ml |

Adjust pH to 7.0 (with 1M HCL), add further water to total of 2l. Treat with DEPC (0.1% final concentration) for at least 2-hours and sterilise by autoclaving.

**10 x "Salts" for *in situ* hybridization buffer**

| | |
|---|---|
| NaCl | 11.7g |
| EDTA (0.5M, pH 8.0) | 10ml |
| Tris-HCl (1M, pH 7.5) | 10ml |
| NaH2PO4 | 0.6g |
| Na2HPO4 | 0.71g |
| DEPC-treated H2O | 60ml |

Mix and adjust pH to 7.5 with HCl. Make up to 100ml with DEPC-treated water and sterile filter.

**RNA-based *in situ* hybridization buffer**

| | |
|---|---|
| 10x “Salts” | 5ml |
| Formamide | 25ml |
| Baker’s yeast tRNA (10mg/ml*;* Boehringer) | 0.5ml |
| Dextran sulphate | 5g |
| 50x Denhardt’s solution | 5ml |

Make up to 50ml, aliquot 5ml into separate tubes and store frozen at -20°C.

**MABT, 5x**

| | |
|---|---|
| Maleic acid | 69.1g |
| NaCl | 43.8g |
| Tween-20 | 5ml |
| dH2O | to1000ml |

Dissolve the maleic acid first, then adjust pH to 7.5 with NaOH and add the remaining components.

**Blocking solution**

| | |
|---|---|
| 5x MABT | 2ml |
| 10% Blocking reagent (Roche) | 2ml |
| Heat-inactivated sheep serum (SIGMA ALDRICH) | 2ml |
| dH2O | 4ml |

**Prestaining buffer**

| | |
|---|---|
| Tris-HCl | 6.1g |
| NaCl | 2.9g |

dH2O 450ml

To avoid precipitation, make up without MgCl2 and add this freshly every time using a 1M stock (25ml of MgCl2 per 500ml prestaining buffer). Mix and adjust pH to 9 with HCl and make up volume to 500ml.

**Staining buffer**

| | |
|---|---|
| Tris-HCl | 6.1g |
| NaCl | 2.9g |
| MgCl2 (1M) | 25ml |
| Polyvinyl alcohol (PVA*;* average MW 70-100kDa) | 25g |
| dH2O | 450ml |

To dissolve the PVA, warm the mixture in water bath. Adjust pH to 9 with HCl, make up volume with dH2O and store at 4°C. Immediately before use, add 350µl BCIP/NBT stock solution (Roche) to 30ml staining buffer in a glass coplin jar.

## 10.3 Staining of sections

***1) Methele blue-Azur II staining for light microscopy***

1. Dry sections by heating on a heating bench at $60^{O}$.
2. Cover sections with methylene blue-azur II and heat on heating bench for 1 min/ $60^{O}$C
3. Wash in distilled water followed by warm running water

4. Mount with Eukitt

.

***2) Solochrome cyanine and van Gieson's staining for light microscopy***

1. Air dry section and take the section through Hemo De ( 15 min) 90% {Alternatively fix in ice cold acetone for 5 min}, EtOH(3min),70%EtOH,50%EtOH,dH2O(2min)
2. Stain for 10 min in staining medium.
3. Wash in $dH_2O$ to remove excess stain.
4. Place section in Solution C. Start checking differentiation at 45 sec. gray matter has to be clear; white matter should be deep blue.
5. Stop Differentiation by holding it in running tap water.
6. Dehydrate for 30 sec in EtOH for 30 Sec.
7. Dry it overnight and mount it with Eukitt

# Table of figures

# Curriculum Vitae

**Personal data**

| | |
|---|---|
| Name | Syed Yasir Ahmed |
| Date of Birth | 25 March 1981 |
| Nationality | Indian |
| Marital status | Single |
| University | University of Natural Resources and Applied Life Sciences Vienna |

**Education**

| | |
|---|---|
| PhD | University of Natural Resources and Applied Life Sciences, Vienna, Austria /MaxPlanck institute for experimental medicine, Gottingen, Germany |
| MSc | University of Mysore, India |
| BSc | University of Mysore, India |

**Research experience**

| | |
|---|---|
| Vienna, Austria/Gottingen, Germany | Myelin protein mediated inhibition of CNS remyelination, MUW Vienna, & Max Planck Institute of experimental Medicine, Gottingen, Dr. Mark Kotter |
| Vienna, Austria | Wlds mediated protection after spinal cord injury,MUW Vienna, & Max Planck Institute of experimental Medicine, Gottingen, Dr. Mark Kotter |
| Kentucky ,USA | Mitochondrial differences in different strain of mouse after spinal cord injury, 2005, University of Kentucky, USA, Prof. Stephan Scheff |
| Bangalore, India | Identification of Putative AP-2α genes by promoter sequence analysis, Indian Institute of Sciences, Prof. Kumaravel Somasundaram |
| Lucknow, India | Study of profile of proteins in resting and activated neutrophil's, Central Drug Research Institute, Prof. Madhu Dkshit |

**Publications**

Baer AS, **Syed YA**, Kang SU (contributing authors), Mitteregger D, Vig R, Ffrench-Constant C, Franklin RJ, Altmann F, Lubec G, Kotter MR. Myelin-mediated inhibition of oligodendrocyte precursor differentiation can be overcome by pharmacological modulation of Fyn-RhoA and protein kinase C signalling. Brain, 2009; 132: 465-81.

**Syed YA**, Baer AS, Lubec G, Hoeger H, Widhalm G, Kotter MR. Inhibition of oligodendrocyte precursor cell differentiation by myelin-associated proteins. Neurosurg Focus, 2008; 24: E5.